

University of Nottingham  
Department of Chemical Engineering

# The Characterisation of Coals for Combustion

by

Edward Lester BSc.

Thesis submitted to the University of Nottingham

for the degree of Doctor of Philosophy

September 1994

## ACKNOWLEDGEMENTS

I would like to thank the following people;

Mike Cloke, my supervisor, for being helpful, generous with funds and straightforward with advice

Dave Clift for helping me with all things petrographic

Harold Smith for teaching me how to point count, and giving me an insight into the world of the petrologist.

Martin Allen, the fastest programmer in the world, who was very helpful during the development stage of the work

Andy Pickering for wading through this effort, attempting to proof read it

My Parents for helping me out financially

And Sarah, my wife, and Sam, my Dog

And all others, who with comments, criticism and general involvement, have made the past three years what they have been

**‘Necessity is the mother of invention’**

**Sixteenth Century Proverb**

# Table of Contents

## ABSTRACT

## CHAPTER 1 - COAL COMBUSTION

1.1 The Importance Of Efficient Burnout	1
1.2 Nomenclature	2
1.3 Pyrolysis Behaviour of Macerals	4
1.3.1 Individual Macerals	
<i>Vitrinite</i>	5
<i>Inertinite</i>	5
<i>Liptinite</i>	6
1.3.2 Microlithotypes	7
1.4 Char Burnout	8
1.5 Rank Effects	9
1.6 Particle Effects	10
1.6.1 Maceral Fractionation	10
1.6.2 Size Effects	10
1.7 Mineral Effects	11
1.8 Aims of the Project	12

## CHAPTER 2 - EXPERIMENTAL

2.1 Drop Tube Furnace	14
2.2 Alpine Jet Sieve	17
2.3 Thermogravimetric Analysis (TGA)	18
2.3.1 Sample Weights	18
2.3.2 Proximate Analysis of Coals	18
2.3.3 Proximate Analysis of Chars	19
2.3.4 Intrinsic Reactivity	20

2.4 Block preparation	21
2.4.1 Coal Block Preparation	21
2.4.2 Char Block Preparation	21
2.5 Polishing Procedures	21
2.6 The Microscope	22
2.7 The Image Analyser	22
2.8 Microscopic Analysis of Coal	23
2.8.1 Rank Measurements	23
2.8.2 Maceral Analysis	23
2.8.3 Char Analysis	24

## **CHAPTER 3 - IMAGE ANALYSIS AND COAL CHARACTERISATION**

3.1 Introduction	35
3.2 Analysis Of Coal	35
3.2.1 Manual Methods	36
<i>Advantages of Manual Methods</i>	36
<i>Disadvantages of Manual Methods</i>	37
3.2.2 Photomultiplier Systems	37
<i>Advantages of photomultiplier systems</i>	38
<i>Disadvantages of photomultiplier systems</i>	38
3.2.3 Image Analysis Systems	38
<i>Advantages of the Image Analysis System</i>	39
<i>Disadvantages of the Image Analysis System</i>	39
3.2.4 Summary of all Methods	39
3.3 Image Analysis	40
3.3.1 The system layout	40
3.3.2 Grey Scale Analysis Using Image Analysis	41
3.3.2.1 Image Capture	42
3.3.2.2 Image Digitisation	42
3.3.2.3 Image Manipulation	42
3.3.2.4 Image Segmentation	43
3.3.2.5 Image Quantification	43
3.4 Programs Developments	43

3.4.1 Morphology Program	44
3.4.2 Reflectance/Fluorescence Method	45
3.4.3 Reactivity Program	47
3.4.4 Semi Automated Maceral Analysis	48
3.4.5 Microlithotype Analysis	48
3.4.6 Char Analysis	49
3.4.6.1 Semi-Automated Analysis	49
<i>Evaluation of the method</i>	50
3.4.6.2 Automated Dilation Erosion Program	50
<i>Evaluation of the method</i>	51
3.4.6.3 Automated Distance Transform Program	51
<i>Experiment 1</i>	52
<i>Experiment 2</i>	52
<i>Experiment 3</i>	53
<i>Evaluation of the method</i>	53
3.5 Conclusions Of Chapter 3	53
<b>CHAPTER 4 - DROP TUBE FURNACE EXPERIMENTS</b>	
4.1 Initial Drop Tube Experiments	69
4.1.1 Purpose of Initial Experiments	69
4.1.2 Coal Specification	69
4.1.3 Drop Tube Conditions	70
4.1.4 Collection Efficiency	71
4.1.5 The R factor	71
4.2 Results from the Initial Experiments	72
4.2.1 TGA Analysis of the Point of Ayr Chars	72
4.2.2 Conclusions	73
4.3 Further Drop Tube Experiments	74
4.3.1 Aims Of The Experiments	74
4.3.2 The Coals Used In The Experiments	74
4.3.3 The Size Ranges	75
4.4 Results of Part Two	76
4.4.1 Proximate Analysis	76
4.4.1.1 Particle Size	76
4.4.1.2 Temperature Effects	76
4.4.1.3 Oxygen Content	77
4.4.1.4 R factor	77
4.4.2 Manual Char Type	79
4.4.2.1 Tenui-Chars %	80

4.4.2.2 Spheres %	81
4.4.2.3 Solids %	83
4.4.3 Automated Char Analysis	84
4.4.3.1 Temperature Effects	84
4.4.3.2 Particle Size Effects	85
4.4.3.3 Oxygen Content Effects	86
4.5 Conclusions For Chapter Four	87
4.5.1 Temperature Effects	87
4.5.2 Particle Size Effects	88
4.5.3 A Comparison of Manual Char Analysis and Automated Char Analysis (ACA)	88
4.5.4 Drop Tube Furnace Operating Conditions	89
<b>CHAPTER 5 CHARACTERISATION OF COALS FOR COMBUSTION</b>	
5.1 Introduction	112
5.2 Drop Tube Furnace Conditions	112
5.3 Analysis of the 11 Coals	113
5.3.1 Proximate Analysis of Sized Coal Fractions	113
5.3.2 Maceral and Rank (Vitrinite Reflectance) Analysis	114
5.2.3 Image Analysis Of The Coal Samples	114
5.4 Char Results	115
5.4.1 Volatile Release	115
5.4.1.1 Proximate Volatile Content	115
5.4.1.2 Collection Efficiency	115
5.4.1.3 R factor	116
5.4.2 Manual Char Analysis Results	117
5.4.2.1 Tenui-Chars %	117
5.4.2.2 Spheres %	118
5.4.2.3 Solids %	119
5.4.3 Automated Char Analysis (ACA)	120
5.4.4 TGA Intrinsic reactivity Measurements	121
5.4.4.1 Peak Temperature	121
5.4.4.2 Burnout Temperature	122
5.5 Prediction Systems	122
5.5.1 Reactive Macerals with Rank	123
5.5.2 Reactive Macerals with Reactive Number	124

5.5.3	Reactive Macerals with Average Reactive Number	124
5.5.4	Reactive Macerals with Fuel Ratio	124
5.5.5	Rank with Reactive Number	124
5.5.6	Rank with Average Reactive Number	125
5.5.7	Rank with Fuel Ratio	125
5.5.8	Reactive Number with Fuel Ratio	125
5.5.9	Reactive Number with Average Reactive Number	125
5.5.10	Average Reactive Number with Fuel Ratio	125
<b>5.6</b>	<b>Prediction Comparison</b>	<b>126</b>
5.6.1	Reactive Number	127
5.6.2	Reactive Macerals	129
5.6.3	Rank	129
5.6.4	Average Reactive Number	129
5.6.5	Fuel Ratio	130
5.6.6	Tenui-Chars%	130
5.6.7	Spheres %	130
5.6.8	Solids %	130
5.6.9	{3} ACA Values	131
5.6.10	{5} ACA Values	131
5.6.11	95% ACA Values	131
5.6.12	Peak Temperature	131
5.6.13	General Conclusions For The Correlation Data.	131
5.6.14	Prediction Parameter Conclusions	132
<b>5.7</b>	<b>Coals Below 1% Reflectance</b>	<b>133</b>
5.7.1	Reactive Number	133
5.7.2	Reactive Macerals	135
5.7.3	Rank	135
5.7.4	Average Reactive Number	135
5.7.5	Fuel Ratio	135
5.7.6	Tenui-Chars %	136
5.7.7	Spheres %	136
5.7.8	Solids %	136
5.7.9	{3} ACA values	137
5.7.10	{5} ACA values	137
5.7.11	95% ACA values	137
5.7.12	Peak Temperature	137
<b>5.8</b>	<b>Overall Conclusions On The Prediction Parameters</b>	<b>137</b>

## **CHAPTER 6 CONCLUSIONS AND RECOMMENDATIONS FOR FURTHER WORK**

<b>6.1</b>	<b>Particle Size</b>	<b>170</b>
------------	----------------------	------------

6.2	Intrinsic Reactivity	171
6.3	Prediction Systems	171
6.3.1	Rank	171
6.3.2	Reactive Macerals	172
6.3.3	Fuel Ratio	172
6.3.4	Average Reactive Number	173
6.3.5	Reactive Number	173
6.4	Image Analysis in Industry	174
6.5	Directions for Future Research	174
6.5.1	Intrinsic Reactivity	174
6.5.2	Combustion Macro	175
6.5.3	1 MW Furnace	176
6.5.4	Interpretation of the Reactivity Results	176
6.5.5	Artificial Intelligence	177
6.5.6	Single Particle Analysis	177

References	179
------------	-----

Glossary	198
----------	-----

## Appendices

<b>A</b>	- Char Nomenclature Photographs
<b>B</b>	- Proximate Analysis Results for the Point of Ayr Chars
<b>C</b>	- Proximate Analysis Results for Kromdraai, Tower and Kellingley Chars
<b>D</b>	- Manual Char Analysis Results for Kromdraai, Tower and Kellingley Chars.
<b>E</b>	- Proximate Analysis Results for the 11 coals used in Chapter 5.
<b>F</b>	- Maceral Analysis Results for the 11 coals used in Chapter 5.
<b>G</b>	- Reflectance/Fluorescence Plots for the 11 Coals used in Chapter 5.
<b>H</b>	- Proximate Analysis Results for the chars produced in Chapter 5.
<b>I</b>	- Manual Char Analysis Results for the chars produced in Chapter 5.

# List of Figures

## Chapter 2

Figure 2.1.1	A photograph of the main working area of the Drop Tube Furnace	25
Figure 2.1.2	A schematic diagram of the Drop Tube Furnace	26
Figure 2.1.3	A photograph of the Feeder device	25
Figure 2.1.4	A photograph of the Feeder positioned above the Drop Tube Furnace	27
Figure 2.1.5	A typical temperature profile from the Drop Tube Furnace	28
Figure 2.1.6	A photograph of the gas filter arrangement	27
Figure 2.2.1	A schematic of the Alpine Jet Sieve	29
Figure 2.2.2	A photograph of the Alpine Jet Sieve	30
Figure 2.3.2	A schematic of the program used to perform proximate analysis in the TGA	31
Figure 2.3.4	A typical profile from the Intrinsic Reactivity test	32
Figure 2.4.1	A photograph of the Presi Mecapress C	33
Figure 2.5.1	A photograph of the Struers Pedamet Rotapol polisher	33
Figure 2.6.1	A photograph of the Leitz Ortholux Microscope	34
Figure 2.7.1	A photograph of the Kontron Image Analyser	34

## Chapter 3

Figure 3.3.1	The layout of the Kontron Image Analyser	55
Figure 3.3.2	A typical reflectance histogram of coal	56
Figure 3.4.2	A flowchart showing the reflectance/fluorescence method	57
Figure 3.4.5	A flowchart showing the microlithotype logic tree	58
Figure 3.4.6.1	The correlation between char voids % and char type	59
Figure 3.4.6.2	A graph of the maximum/minimum diameters of different chars	60-I
Figure 3.4.6.3	The sequence of processes used to close a char particle	60-II
Figure 3.4.6.4	The correlation between Manual and Automated Voids %	61
Figure 3.4.6.5	The distance transform mapping process	62
Figure 3.4.6.6	Idealised char types	63
Figure 3.4.6.7	The distance transform results for the idealised char types	64
Figure 3.4.6.8	A graph showing the effects of particle size on the distance transform method	65
Figure 3.4.6.9	The distance transform results for several real char particles	66

## Chapter 4

Figure 4.1.1	The Point of Ayr reflectance histogram	91
--------------	--	----

Figure 4.1.2	A graph showing the repeatability of the Point of Ayr chars, in terms of their volatile content	92
Figure 4.4.1	Particle Size Effects: The volatile content of Kellingley chars	93
Figure 4.4.2	Particle Size Effects: The volatile content of Kromdraai chars	94
Figure 4.4.3	Particle Size Effects: The volatile content of Tower chars	95
Figure 4.4.4	Temperature Effects: The volatile content of Kellingley chars	96
Figure 4.4.5	Temperature Effects: The volatile content of Kromdraai chars	97
Figure 4.4.6	Temperature Effects: The volatile content of Tower chars	98
Figure 4.4.7	The effect of temperature on the R factor values of Kromdraai chars	99
Figure 4.4.8	The effect of particle size on the R factor values of Kromdraai chars	100

## Chapter 5

Figure 5.4.1	Particle Size Effects: The volatile content of the chars from the 11 coals	140
Figure 5.4.2	Particle Size Effects: ACA {3} values for the 11 coals	141
Figure 5.4.3	Particle Size Effects: ACA {5} values for the 11 coals	142
Figure 5.4.4	Particle Size Effects: ACA {95%} values for the 11 coals	143
Figure 5.5.1	The correlation of Reactive Macerals with Rank	144
Figure 5.5.2	The correlation of Reactive Macerals with Reactive Number	144
Figure 5.5.3	The correlation of Reactive Macerals with Average Reactive Number	145
Figure 5.5.4	The correlation of Reactive Macerals with Fuel Ratio	145
Figure 5.5.5	The correlation of Rank with Reactive Number	146
Figure 5.5.6	The correlation of Rank with Average Reactive Number	146
Figure 5.5.7	The correlation of Rank with Fuel Ratio	147
Figure 5.5.8	The correlation of Reactive Number with Fuel Ratio	147
Figure 5.5.9	The correlation of Reactive Number with Average Reactive Number	148
Figure 5.5.10	The correlation of Average Reactive Number with Fuel Ratio	148
Figure 5.6.1	The correlation of Reactive Number and ACA {3}	149
Figure 5.6.2	The correlation of Reactive Number and ACA {5}	150
Figure 5.6.3	The correlation of Reactive Number and ACA {95%}	151
Figure 5.7.1	9 Coals: The correlation of Reactive Number and ACA {3}	152
Figure 5.7.2	9 Coals: The correlation of Reactive Number and ACA {5}	153
Figure 5.7.3	9 Coals: The correlation of Reactive Number and ACA {95%}	154

# List of Tables

## Chapter 3

Table 3.2.2	The comparison of analysis techniques from the Kojima Paper	67
Table 3.4.2	The fluorescent characteristics of the different maceral species taken from Stachs' textbook	68

## Chapter 4

Table 4.1.1	The Proximate Analysis of Point of Ayr coal	101
Table 4.1.2	The maceral analysis results for the 53-75 fraction of the Point of Ayr coal	102
Table 4.1.3	The Ultimate Analyses of the Point of Ayr coal	103
Table 4.2.1	The R Factor and Collection Efficiency results for the Point of Ayr Chars	104
Table 4.3.1	The Proximate Analyses of Kromdraai, Kellingley and Tower	105
Table 4.4.1	The R Factor and Collection Efficiency results for the Kromdraai, Kellingley and Tower chars	106
Table 4.4.2	Manual Char Analysis: Tenui-Chars % results	107
Table 4.4.3	Manual Char Analysis: Spheres % results	108
Table 4.4.4	Manual Char Analysis: Solids % results	109
Table 4.4.5	Automated Char Analysis: 3 % oxygen results	110
Table 4.4.6	Automated Char Analysis: 0% oxygen results	111

## Chapter 5

Table 5.3.1	The Rank results for the 11 coals	155
Table 5.3.2	A brief description of the petrographic nature of the 11 coals used in Chapter 5	156
Table 5.3.3	The maceral analyses from the image analysis reflectance/fluorescence method	157
Table 5.4.1	The collection efficiency results for all the chars	158
Table 5.4.2	The R factor results from all the chars	159
Table 5.4.3	The Tenui-Char % results	160
Table 5.4.4	The Spheres % results	160
Table 5.4.5	The Solids % results	160
Table 5.4.6	The Automated Char Analysis results	161
Table 5.4.7	The Intrinsic Reactivity results	162
Table 5.5.1	The Prediction Parameter results	163
Table 5.6.1	The correlation data between all Prediction Parameters and Char Analysis results for the 53-75 micron chars	164
Table 5.6.2	The correlation data between all Prediction Parameters	

	and Char Analysis results for the 106-125 micron chars	165
Table 5.6.3	The correlation data between all Prediction Parameters and Char Analysis results for the 180-212 micron chars	166
Table 5.7.1	9 Coals: The correlation data between all Prediction Parameters and Char Analysis results for the 53-75 micron chars	167
Table 5.7.2	9 Coals: The correlation data between all Prediction Parameters and Char Analysis results for the 106-125 micron chars	168
Table 5.7.3	9 Coals: The correlation data between all Prediction Parameters and Char Analysis results for the 180-212 micron chars	169

# List of Publications

**Lester, E., Cloke, M., and Miles, N.,**

*Coal Characterisation for combustion*

Proc. IChemE Research Event 1993, 299

**Cloke, M., and Lester, E.,**

*Characterisation of coals for combustion using petrographic analysis*

Fuel 73, 315

**Lester, E., Cloke, M., Miles, N.,**

*The effect of operating conditions on char produced in a drop-tube furnace*

Fuel Processing Technology 1993, 36, 101

**Lester, E., Allen, M., Cloke, M. and Miles, N.J.,**

*Image Analysis techniques for petrographic analysis*

Fuel Processing Technology 1993, 36, 17

**Lester, E., Cloke, M., Gibb, W.H. and Miles, N.J.,**

*Coal characterisation for combustion by drop-tube furnace and image analysis*

Proc. Int. Conf. Coal Science, Banff, Canada, 1993, II-117

**Lester, E., Cloke, M., Allen, M. and Miles, N.J.,**

*The use of image analysis in the modelling of coal combustion*

Proc. IChemE Research Event 1994, 667

**Lester, E., Allen, M., Cloke, M. and Miles N.J.,**

*Maceral analysis by automated image analysis techniques*

12th International Coal Preparation Congress, 1994, 531. Poland.

## Papers Awaiting Publication

**Lester, E., Allen, M., Cloke, M., Miles, N.J.,**

*An automated image-analysis system for major maceral group analysis in coals*

accepted for publication by Fuel

**Cloke, M., Lester, E., Allen, M. and Miles, N.J.,**

*Automated maceral analysis using fluorescence microscopy and image analysis*

accepted for publication by Fuel

**Cloke, M., Lester, E., Allen, M. and Miles N.J.,**

*Repeatability of maceral analysis using image analysis systems*

accepted for publication by Fuel

**Lester, E., Atkin, B., Cloke, M., Allen, M. and Miles, N.J.,**

*Automated microlithotype and maceral analysis of a solid coal block using image analysis techniques*

International Conference on Coalbed Methane and Coal Geology, 1994. 12-16th September, 1994. Cardiff, Wales.

**Lester, E., Cloke, M., Allen, M.,**

*The reaction kinetics of char particle burnout using thermogravimetric analysis and computer imaging techniques*

Proc. IChemE Research Event 1995

## ABSTRACT

The use of coal in the production of energy, will continue around the world into the next century, and onwards. From an environmental perspective, as well as a financial one, man has attempted to increase the efficiency of energy production from initial raw materials. Environmentally, the poor conversion of coal to energy means a waste of earth's resources, as well as the production of more waste. From a financial viewpoint, poor combustion means less energy per tonne of coal, hence less profit. Poor combustion will also mean higher levels of carbon in ash. Increased carbon levels will change the physical properties of the ash, and therefore reduce the possible number of outlets for its disposal.

It is essential, from a coal buyer's point of view that he makes an 'informed' choice, as to the type of coal he is buying, especially if coals in question are imported. There is sufficient evidence to suggest that most techniques that currently exist are unable to characterise world coals successfully. The reason for this has been linked to the unusual petrographic nature of various world coals. It seems logical therefore, that an analytical technique based on the petrography of a coal, would be capable of providing a better characteristic assessment of any given coal type.

The use of image analysis in providing petrographic information has been investigated, along with several different techniques for the characterisation of char and coal particles. Char production itself has been studied, mainly concerned with the production of representative char samples. A range of different operating conditions were used, including temperature ranges of 1000°C to 1400°C, oxygen contents of 0 to 3%, and residence times of 100 to 200 milliseconds.

From the experiments carried out, it was possible to correlate char structure to the initial coal using a reflectance/fluorescence program, specially designed for the measurement of a coal's 'reactivity'. Other prediction systems, such as Rank, Fuel Ratio and Reactive Macerals did not correlate as well to the combustion products from the Drop Tube Furnace.

# CHAPTER 1 - COAL COMBUSTION

## 1.1 The Importance Of Efficient Burnout

Pulverised fuel combustion is used widely in power plant for the generation of electricity. Selection and testing of coals is vital to the efficient operation of these plants and many different tests are carried out for this purpose. Where coals are to be obtained from many different sources, especially from different parts of the world, this process can become difficult. As with all supplies that are delivered in bulk, coal quality may vary significantly over time despite originating from the same source, and these variations in quality can effect the burnout performance of the plant. When proximate analysis is used to characterise a coal, it is not without its problems, especially when dealing with coals from abroad (Bengtsson, 1987). Any electricity company buying coals from different countries will need to know how the coal will burn and if and when the supply changes. Carbon in ash levels are important, not only because it indicates combustion efficiency, but also because it affects the sale and use of the pulverised fuel ash (PFA) afterwards. An example of this would be the use of PFA in plasterboard. Standards govern the level of combustible material which can be present in the plasterboard for fire protection purposes.

Coal type and organic constituents within the coal will depend on factors such as area and time of deposition and degree of coalification. Monitoring coal supplies for these constituents can be carried out using maceral analysis. The type and quantity of each maceral, as well as their degree of coalification, can be used to predict the coals origin. The analysis can also give an indication of the coals behaviour in various fields of utilisation (Lee and Whaley, 1983).

The following sections of chapter 1 take an in-depth look at the factors that have been linked with coal combustion.

## 1.2 Nomenclature

Inertinites are not all inert and vitrinites were not all reactive, hence maceral nomenclature is ambiguous (Chao et al, 1982). However, it is the extent to which this is true which is in some doubt (Diessel & Wolff-Fischer, 1987b). Gondwala coals can contain a high proportion of inertinite (Stach et al, 1982), hence there must be some explanation as to why these coals can and are burned lucratively without resulting in low burnout. Australian coals can often burn more efficiently than vitrinite rich coals from the Northern Hemisphere (Shibaoka, 1986).

One must define reactivity if one wishes to rectify the situation. For a maceral to be classed as *reactive*, it must exhibit thermoplasticity during pyrolysis and char formation, hence when classifying 'inerts' as reactive, a worker must be confident that some degree of structural alteration has occurred. Reactive macerals are those which will become fluid and form isotropic or anisotropic units, and this will include some inertinite (Diessel & Wolff-Fischer, 1987b). In recent years attempts have been made to study the behaviour of the 'inert' fractions of the reactive macerals and the 'reactive' fractions of the inert macerals.

When dealing with coal combustion systems, Tate et al. (1987) separated a coal into two fractions called reactive and less reactive, acknowledging the change in reactivity of maceral groups and submacerals within them. C. Zhang (1986) introduces a group called the semi vitrinites within his coal analysis, which comes under the active organic fraction. Other workers have been known to use this grouping for the higher reflectance vitrinite (Kosina & Hrcir, 1983), but discount the majority of it as unreactive, even suggesting that it be renamed semi-inertinite. The variations in the performance observed in each group show that no one group is reactive, but macerals will lie on some kind of scale between reactive and unreactive. One cannot, therefore, successfully predict the way that a coal may behave with only the three basic maceral groups; vitrinite, inertinite and liptinite.

### *Discrepancy in the Vitrinite Group*

Vitrinite is chemically reactive and contains more oxygen than the other macerals (Stach et al., 1982). Depending on the Rank of the vitrinite in the coal, it can be easily pyrolysed or oxidised (Carpenter, 1988). Oxidized vitrinite has been acknowledged as behaving differently with respect to most other types of vitrinite (Kaegi 1985, Benedict 1968, Nandi et al,1977). Pseudovitrinite is a type of vitrinite, but a petrologist involved in combustion science would probably label this sub-macerals as inert. Pseudovitrinite and vitrinite do not have similar properties (Crelling et al.. 1988), hence intramaceral group variations do exist. For these reasons vitrinite combustion ranges from 'good' to 'very poor', dependant on both Rank and speciation (Oka, 1987). It is also possible for some inertinites to be more reactive than some vitrinites (Thomas et al, 1989b, Phong-Anant, 1989 , Shibaoka et al, 1985a , Suarez-Ruiz et al, 1991.)

### *Discrepancy in the Inertinite Group*

A certain fraction of inertinite will be reactive, although this fraction is generally estimated as a minority (Bengtsson, 1986). Figures offered range from 10% (Kosina & Hrnecir, 1983) to 30% (Schapiro & Gray, 1961, Furimsky, 1990) up to 90% (Thomas et al., 1991a). Hence it is an area of disagreement at present (Diessel & Wolff-Fischer, 1987b). An index for the reactive fraction of the inertinite group has been developed called the Relative Reactive Index (RRI) (Thomas et al., 1991a). The reason why the RRI varies so much is due to the nature of inertinite i.e. the majority of inertinite macerals in Australia have a low reflectance, whereas European coals contain a greater overall quantity of high reflectance inertinite (Shibaoka et al, 1989c). High figures for reactive inerts have been found by workers using microlithotype analysis to characterize coals (Rentel, 1987).

Although low reflectance inertinite is the most likely sub-macerals in which one would see plasticity during combustion (Thomas et al., 1991b), medium reflectance inertinite can also undergo some

degree of deformation. The varying reactivity of inertinite could well be more effected more greatly by speciation within a maceral group, than by Rank differences (Phong-Anant, 1989).

Micrinite is another example of a type of inertinite which could probably be considered to be reactive during combustion. This is because micrinite has a small surface area and is usually enclosed inside a vitrinite particle, thus as the vitrinite vesiculates, the micrinite will either be exposed and burnt or incorporated into the char walls. The micrinite will then burnt along with the vitrinitic char (Diessel & Wolff-Fischer, 1987.; Lee & Whaley, 1983). Micrinite also has a close association with liptinite (Taylor & Liu, 1989), particularly alginite (Taylor et al, 1989) and so will contain a lot more hydrogen than the other inertinite sub-macerals, yielding more volatiles during combustion.

### Summary

Many workers have attempted to define the point at which reactive becomes unreactive, generally linking the reflectance of each maceral type with its degree of reactivity Thomas et el., (1991a), Thomas et el., 1989b), Jones et al., (1985b), Steyn & Smith (1977), Speight (1983), Bailey et al., (1990), Diessel & Wolff-Fischer (1987), Kosina & Hrnecir, (1983), Gransden et al., (1991), Coin & Hall (1989), Kuili et al (1988).

### 1.3 Pyrolysis Behaviour Of Macerals

As mentioned earlier, coal pyrolysis is the first part of coal combustion. The coal will begin to combust at any point above 300°C (Stanmore, 1989), and this is marked by the evolution of gaseous products. The gases form a cloud around the particle called a flame front. These gases are then burnt leaving behind a char particle.

The type of char formed, and combustion in general, can depend on the macerals present (Tsai, 1985) and their associations (Rentel, 1987), the Rank of the coal, the particle size and temperature

of char formation (Jones et al., 1985a). Heating rates also effect the weight loss during pyrolysis (Ciuryla et al., 1979; Gibbins et al., 1991)

### 1.3.1 Individual Macerals

#### *Vitrinite*

This maceral is the most influenced by Rank changes (Shibaoka, 1987, Neill et al., 1987), and so can produce a number of different char 'types' (Bend et al., 1992). Phong-Anant (1989) recognized that vitrinite combustion can vary greatly.

Vitrinite can give tenuispheres (Bailey et al., 1990) with thin walls and high porosity (Lightman & Street, 1968, Gromulski & Sieurin, 1983, Ward, 1984) but higher Ranked coals can give crassinetworks and crassispheres (Oka et al., 1987). Cenospheres, in general, are predominantly from vitrinites (Skorupska et al., 1987, Thomas et al., 1989b & 1989c, Goodarzi & Murchison, 1978).

Networks from vitrinites tend to be prevalent in lower Ranked coals (Kleesattel, 1987), rather than in higher Ranks (Oka et al., 1987). The formation of networks and spheres is related to a macerals aromaticity within the particle, as is anisotropy.

#### *Inertinite*

Inertinite macerals have the highest reflectance levels, the highest carbon ratio, the lowest hydrogen and volatile yield, and have the highest degree of aromaticity. Despite this, inertinite can be capable of swelling during combustion (Thomas et al., 1989b), but manages to retain its original structure for longer than the other macerals (Bengtsson, 1984). However, high Rank inertinite is much less likely to be effected during pyrolysis due to its structural 'inertness' and low quantities of volatile matter. It is also less likely to form anisotropic chars due to its lack of fluidity (Skorupska & Marsh, 1989). Low reflectance semi-fusinite, however, can give highly porous chars because of its

fluidity during combustion (Thomas et al., 1989b). High reflectance semi-fusinite has a lower porosity compared with lower Ranked inertinite (Vleeskens & Nandi, 1986), and so is less able to fluidize, even under high heating rates.

Recent work involving the heating of a single maceral with a laser revealed that low reflectance semi-fusinite did vesiculate forming relatively porous chars (Shibaoka et al., 1989a). This technique of particle combustion with a laser beam is especially valuable because it positively identifies the kind of char that can be produced by a particular maceral. Oka (1987) also distinguished between the char type formed by inertinite in low Rank coals, which are generally microdisrupted, skeleton type in medium Rank, and unfused in higher Ranks.

Hence, during pyrolysis, inertinite can form open char types with rounded vacuoles (Goodarzi & Murchison, 1979, Young et al., 1987), anisotropic crassispheres (Tsai, 1985) or solids with low porosity (Jones et al., 1985b), dependant on the reflectance of the inertinite species (Diessel & Wolff Fischer 1987, Phong Anant, 1989).

### *Liptinite*

Liptinite is generally a minor component in bituminous coals but has the highest hydrogen content and volatile yield, the lowest reflectance and contains more aliphatic groups than the other maceral groups. There is only a small amount of doubt concerning the nature of liptinite (Crelling, 1992), and so liptinite is generally accepted as useful in obtaining flame stability (Shibaoka, 1969, Lee & Whaley, 1983, Ottaway, 1982).

Devolatilization of liptinite will be over, leaving no remains, within 200 milliseconds (Bengtsson, 1984). The gases produced can 'blow' holes in the plasticizing vitrinite which will then continue to burn for much longer (Bengtsson, 1986). Higher temperatures and heating rates ( $10^5$  °C/sec) will cause a more rapid weight loss, and subsequently a lower combustion time in liptinite rich coals, (Tsai, 1985). Lower heating rates of around  $10^2$  °C/min see less marked change with high liptinite coals (Ciuryla et al., 1979).

The presence of liptinite will enhance ignitability and weight loss in a particle, although the larger the particle the lower the effect. Liptinites even in non-swelling coals i.e. those with fusinitic groundmass, can undergo extensive devolatilization whereas in swelling coals liptinites can form coalescing fluidized tubular masses (White et al., 1989), allowing rapid combustion.

### 1.3.2 Microlithotypes

Microlithotypes are acknowledged to alter the combustion efficiency of the individual macerals (Skorupska et al., 1987). Vitrites and Clarites have been found to give tenuispheres and tenuinetworks, or fragments which are probably made from broken-up tenuispheres (Bailey et al., 1990, White et al., 1989, Street et al., 1969). These vitrinite rich structure are the most likely to produce low density chars which subsequently reduce combustion times. They will also alter the percentage of highly porous chars that will be found in the sample (Bend et al., 1989). Vitrite is thought to have good burnout (Jones et al., 1985b), but can give poorer combustion properties when in association with larger inertinite fragments (Nandi et al., 1977, Young & Smith, 1986). This may be the result of inertinite restricting the vesiculation of the vitrinite (Bengtsson, 1987, Bailey 1990). A similar effect was observed in a Canadian coal in which vitrinite was constricted by layers of semi-fusinite and fusinite, thus retarding the pyrolysis and eventual combustion of the coal (Nandi et al. 1977). This is obviously when inertinite is present as macrinite or fusinite rather than micrinite, which would not be able to impede the vesiculation of a particle with a high vitrinite content. Hence particles which are made up of macerals which can freely swell, without the restriction of non-swelling macerals, are much more likely to form chars which have a high surface area with large surface pores. Duroclarites, vitrinertite-I and clarodurites, being lower in vitrinite, give thicker walled or mixed porous type chars. Durites tend to give inertoid, mixed dense solids and fusinoids (Bailey et al., 1989c)

## 1.4 Char Burnout

Most workers agree that char reactivity as well as char type can be related back to coal type (Cuiryla et al., 1979, Tate et al., 1987), whereas some do not (Young et al., 1987). Some workers have concluded that inertinite char burns slower than vitrinite char (Jones et al., 1985b, Crelling 1992, Morgan et al., 1986), whilst acknowledging that other features may be more significant than the initial maceral composition.

An explanation for inertinite coals taking longer to burn than vitrinite may be due to delayed pyrolysis before the formation of char (Shibaoka et al., 1985a). But this would appear to contradict Crelling et al. (1992) who found that even though semifusinite ignited before vitrinite, vitrinite had the greater combustion rate and so burned faster. Certain workers (Young et al., 1989, Shibaoka et al. 1985a, Thomas et al. 1989a) have found that inertinite char can burn as fast, if not faster (Phong Anant, 1989) than vitrinite char, although solids and open solids can be the exception (Shibaoka et al., 1989c).

It would appear that cenospheres and networks have generally similar reactivities whether formed from inertinites or vitrinites. Tenuispheres and networks will burn more readily due to their increased surface area and poorly ordered textures (isotropic). Not only the texture of the char walls but the size of pores, formed during pyrolysis, is important. Pores greater than 2  $\mu\text{m}$  can play a key role in char combustion (C. Zhang, 1986) in that they appear to be a critical size allowing sufficient 'ventilation' for  $\text{O}_2$  adsorption to be possible on the surfaces of the char. The size of these pores formed in vitrite char is more subject to variation with Rank than inertite char. Inertites exhibit little variation in the pore size with increasing Rank (Jones et al., 1985b). The knowledge of the external and internal pores can be used to explain the nature of char burnout (Oka et al., 1987; Bailey et al., 1990; Skorupska et al., 1987).

## 1.5 Rank Effects

Rank, or vitrinite reflectance, can be particularly influential in deciding coal combustion (Allen & Gehring, 1989; Kopp & Harris, 1984; Essenhigh, 1981, Stanmore, 1989). It is also difficult to mention Rank without discussing macerals, because maceral behaviour, to some extent, is dependant on Rank values as mentioned in section 1.3 . Both will be important factors in determining combustion efficiency.

Liptinite, vitrinite and inertinite can all be 'reactive' during combustion, if one considers their thermoplastic behaviour (Shibaoka et al., 1987). Reactivity can also be directly related to Rank (Steller et al., 1991), and in this way vitrinite reflectance or Rank is proportional to burnout properties. Rank is, at present, the most likely parameter to accurately predict a coal's combustion behaviour (Skorupska & Marsh, 1989, Young et al., 1987 & 1989, Bailey et al., 1990, Bengtsson, 1986, Morgan & Roberts, 1987, Haley et al., 1991), although the relationship of Rank with char type has been shown to be non-linear (Young & Smith 1986, Crelling, 1988). From subbituminous through to anthracitic coals, the percentage of tenuouspheres and cenospheres will decrease to make way for increasing amounts of crassi-walled or solid chars with anisotropic textures (Bend et al., 1992). Fluidity/fusibility has been shown to decrease with an increasing Rank (Sakurovs et al., 1991).

An increase in Rank will also mean a decrease in liptinite present, and also a decrease in the reactivity of the vitrinite. Hence, for many reasons, Rank is an integral part of any attempt to predict combustion behaviour.

## 1.6 Particle Effects

### 1.6.1 Maceral Fractionation

Before coal combustion, the raw coal is ground down to what is called pulverized fuel, of which 70-80% is below 75 micron. Grinding a coal, however, can cause macerals to concentrate into certain size fractions (Carpenter, 1988, Jones et al., 1985a, Bustin, 1991).

Street et al. (1969) found that the finest fractions were rich in inertinite, whereas the coarser harder fractions were more likely to contain a higher proportion of liptinite and vitrinite. Lee and Whaley (1983) did not encounter this kind of partitioning in their suite of coals but acknowledged that it could occur. Pseudovitrinite was found to be concentrated in the smaller size fractions due to its brittle and friable nature (Bengtsson, 1987).

Liptinites are relatively tough 'leathery' macerals (Bouska, 1981), and by their very nature will hold coal particles together. Coals with a high proportion of liptinite are often found to have a low Hardgrove Index value (Bustin et al. 1983, Hower et al., 1990, Stach et al., 1982), and this can explain why liptinite is enriched in larger sized particles (Tsai and Scaroni, 1987).

Therefore for various physicochemical reasons, one can expect to find macerals being concentrated in a particular size fraction. Inertinites like semi-fusinite will peak at the smaller end of the size range, and high reflectance fusinite, will tend to fracture and break up during grinding because of its brittle nature. Fusinite is therefore most concentrated in the fines (Pratt, 1989).

### 1.6.2 Size Effects

Despite the fact that larger sized particles ( $> 10^2$  mm) are more likely to fragment during combustion (Young et al., 1989, Fujiwara et al., 1989), they correlate well to high carbon in ash values (Shibaoka, 1986, 1989c, 1985, Williamson et al., 1991). Hence the size of a particle affects burnout in a number of ways. Analysis of fly ash products revealed that vitrinite probably contributes towards some of the unburnt carbon. This was done by relating initial and final

proportions of inertinite present (Bailey et al., 1990). Recent reports have also shown that vitrinite is slow to ignite (Crelling, 1992), this delay in ignition could perhaps explain why some vitrinite particles only partially combust.

## 1.7 Mineral Effects

A coal will be partially demineralised before it is ready for combustion but a proportion of the original mineral matter remains in the coal and is 'fired' along with the coal, hence if mineral matter does effect combustion, then one must understand what effects the different minerals have (Mahajan & Walker, 1979, Wall et al., 1989a). Mineral matter is not necessarily an inert diluent of the coal (Carpenter, 1988, Wall, 1985). Flame stability and char burnout can be partially dictated by the presence or absence of certain minerals (Jones et al., 1987, Patrick & Shaw, 1972).

The presence of certain types of mineral matter can obscure the effect that macerals have on char speciation (Skorupska et al., 1987, Vleeskens & Nandi, 1986). As well as affecting the chemisorption on the surface of the coal particles occurring during pyrolysis (Crelling et al., 1992, Radovic et al., 1983), cations can strongly influence char morphology in both lignitic and subbituminous coals (Kleesattel et al., 1987). The addition of sodium, potassium and calcium ions made a 'dramatic' decrease in the formation of cenospheric char, and an increase in mesospheres (or thicker walled networks). Removal of  $\text{Na}^+$ ,  $\text{K}^+$  and  $\text{Ca}^{2+}$  cations can increase the percentage of cenospheric and mesospheric chars with the loss of honeycomb and inertospheric types. Sodium Carbonate has been proved to reduce the fluidity of coals, and this explains why thicker walled chars and networks result from the presence of mineral matter (Jenkins et al., 1973). The presence of  $\text{Na}^+$  is also known to cause fouling when  $\text{Na}_2\text{O}$  reaches 8-10% in ash (Schobert, 1983).

The larger the particle, the greater the quantity of mineral matter that will be present (Littlejohn, 1966). For this reason it is possible that larger particles like durains and clarains will be increasingly effected by cations present in the minerals, and hence will form thicker walled, less combustible chars. Hence if one is attempting to characterize coals and perhaps predict combustion behaviour,

one must take into account any mineral matter in the feed coal which may well have a deleterious effect on the combustion behaviour of the coal.

## 1.8 Aims of the Project

As mentioned in section 1.1, many of the standard techniques used to characterise coals are limited or slow. The main limitation has always been the range of coals that can be successfully analysed. British coals tend to obey certain rules as regards maceral composition and general utilisation behaviour. Many Gondwala coals, however, do not obey these rules, hence the main area of interest with this project will be to investigate new methods of providing a rapid characterisation of coals from around the world, with regard to combustion.

The Drop Tube furnace is a useful means of achieving conditions which are reasonably representative of a real boiler. Unfortunately, little work has been published which discusses realistic operating conditions which could simulate pyrolysis or combustion. Therefore, as part of the project, investigations will be made into the effects of the operating conditions of the Drop Tube on various coals. Variable conditions include residence time, oxygen content and operating temperature.

Thermogravimetric analysis (TGA) is well known to many workers in coal combustion, and will be used to analyse all coals and char samples generated during the project. Since the TGA is capable of controlled ramp rates and oxygen levels, any particular sample can be tested for its intrinsic reactivity (Unsworth et al., 1991), as well as its proximate analysis (British Standard, 1977).

The use of an image analyser to perform automated maceral analysis has been <sup>established</sup> for some time (Riepe & Steller, 1984, Kojima, 1976). Despite this, problems still remain in distinguishing liptinite from the background resin, and therefore some investigations will be made into potential methods for complete, automated maceral analysis using image analysis.

The rapid characterisation of coal based on its petrographic constituents is virtually unknown by the Electricity Industry, despite its potential when considering the combustion performance of different coal types. Therefore, the eventual aim of the project is to identify any correlation between a coal's combustion behaviour and its petrographic composition. This petrographic composition will be determined by both automated and manual methods.

# CHAPTER 2 - EXPERIMENTAL

This chapter gives details of the equipment used in the course of the thesis work, and the developments made to that equipment. The procedures for each analytical test are also included.

## 2.1 Drop Tube Furnace

A Drop Tube Furnace system was developed at PowerGen plc. to provide a means of producing reasonable quantities of char sample at similar conditions to those of a commercial pulverised fuel boiler at a power station. This would mean the simulation of heating rates of the order of  $10^4$  °C /sec to  $10^5$  °C/sec, and low oxygen levels (0-10%) when simulating the first few hundred milliseconds inside a boiler. The Drop Tube Furnace is similar to several others in use in the UK and was designed by Severn Furnaces Ltd. Figure 2.1.1 is a photograph of the main working area of the rig. The system has essentially 5 main working areas

1. Gas supply and flow regulators
2. Sample feeder system
3. Reaction or Work Tube, probes and collection cyclone
4. Heating controls
5. Gas filter

Figure 2.1.2 is a schematic of the essential parts of the Drop Tube Furnace

### *Gas supply*

The gas cylinders were supplied by Air Products Ltd and used standard gas regulator valves. The flow rates of air and nitrogen were used to control the residence time in the Drop Tube

Furnace as well as the oxygen levels inside the reaction tube. Fine tuning to the required oxygen level was achieved using an oxygen meter which sampled a small proportion of the gas supply throughout each experiment, in order to monitor any changes that may occur during the experiment.

### *Feeder system*

This was specially designed for the project and made in the Chemical Engineering workshop at Nottingham University. Figure 2.1.3 shows the side profile of the finished feeder. Figure 2.1.4 shows the feeder as it sits ready to begin a series of runs. It was necessary to develop a feeder system which did not require the operator's attention throughout the experiment, as keeping the filter system unblocked was felt to be more important. Previous devices involved trough and weir mechanisms which required vibrating throughout the experiment. These systems did not provide a steady flow rate and required some of the operators time to ensure smooth running. In order to provide a fluidised movement of the coal sample, two small motors with eccentric weights were attached to the ends of the feeder and powered by a small battery. This increased the feed rate of the sample and did not allow the sample to grip the edges of the internal hopper. Feed rates were in the range of 6 to 11 grams per hour, dependant on the particle size of the sample. Smaller sized samples required longer to pass through the screw feeder system.

### *Heating system and controls*

From figure 2.1.2 it can be seen that there are 3 separate heaters in the system. Firstly a PREHEATER which heats the gases as they enter the top of the Drop Tube Furnace. This heater is essentially a coiled carbon graphite plate wrapped round the feeder probe. The second heater is the MAIN HEATER which consists of four carbon graphite rods at each corner of the Drop Tube Furnace. Finally the TRIM HEATER compensates for the effect of the large water cooled collector probe, which causes a drop in temperature near the bottom of

the Drop Tube Furnace. Each heater control is connected to two Pt/Rh (13%) thermocouples, positioned at right angles to the reaction tube at the appropriate position.

It was acknowledged that there would be a difference between the temperature as measured by the thermocouples on the outside of the work tube and the temperature inside. In order to calculate the temperature settings necessary on the controllers to achieve the required temperatures inside the reaction tube, a series of experiments were performed using a specially made thermocouple which could be placed inside the Drop Tube Furnace whilst in a working condition. The thermocouple was approximately 1.5 metres long and made of thin ceramic segments each 15 centimetres long. Two holes in the centre of each ceramic rodlet allowed a Pt wire and a Pt/Rh (13%) to run parallel to the end of the thermocouple where they were welded together. The thermocouple was placed inside the furnace and readings were taken at set distances at four different temperatures and three different residence times. This allowed an average temperature to be obtained for the distance between the feeder and collector probes. An example of these profiles is given in figure 2.1.5.

It was also acknowledged that in order to achieve the required temperatures over the complete distance, the temperature of the work tube between the probes exceeds the required temperature. The shorter the distance between feeder and collector probes, the higher this peak is. The difference between recorded and required operating temperatures will increase with increasing average temperature.

### *The Work tube and Probes*

The Work Tube is a 2 metre ceramic tube with an internal diameter of 50mm, and 5mm thick walls. The maximum operating temperature of the system was around 1600°C.

Both collector and feeder probes are made of stainless steel hence need water cooling to operate at temperatures exceeding 600°C. The cooling system is an internal closed circuit 50 gallon unit which flows through both probes before running into a main tank outside the

Rigby building at PowerGen. A heat exchanger and fan, positioned above the main water tank, are used to keep the water temperatures as low as possible. A biocide called Fernox was added at regular intervals in order to minimise the amount of organic activity in the system. This was done to avoid any build up of material on the internal filters, which could lead to an emergency shut down of the system. Water flow rates are between 2-3 litres a minute and on average the water temperature is raised 10-20°C after passing through the two probes.

### *Gas filter*

The system for filtering the gases leaving the reaction tube was designed and made to improve the ease of use and effectiveness of the removal of tars and particulates before the gases exit into the fume cupboard. Figure 2.1.6 is a photo of the bottom section of the Drop Tube Furnace. The metal tube from the cyclone is connected to the filter section. The exit gas is pumped through one of the filters containing a filter paper and a wad of fibre glass on which the tar and particulates are deposited. Once the fibre glass inside the filter housing became blackened, the valves on the other side of the filter device were opened allowing the blackened fibre glass to be removed. The time required for a filter to become significantly blackened depended on the type of coal being passed through the system, and the oxygen content inside the reaction tube. Tower, a Welsh anthracite did not require any change of filter, whereas a coal like Bentinck required a filter change every 2 minutes.

## 2.2 Alpine Jet Sieve

With all coal samples 2-3 kilograms of pulverised sample was obtained. These samples were supplied originally in the form of doubles to PowerGen Sample Preparation Unit at Ratcliffe on Soar Power Station. 10 kilograms of doubles were quarter coned, one quarter being used for grindability tests, the rest for grinding.

In order to divide the pulverised fuel samples into tight size bands, an Alpine Jet Sieve was used. This device allows suction to be maintained on the under side of modified Endecott sieves whilst allowing a rotating finger to blow a thin jet of air back through the sieve. This thin jet of air releases coal particles stuck on the surface of the sieve, hence agitates the sieving process and decreases the time required for a required size range to be obtained. Figure 2.2.1 shows the side profile of the system and figure 2.2.2 is a photograph of the system along with pressure gauge, modified sieves and shortened brush to clean sieves. Fines (below 53 microns) were sieved off first, using the 53 micron sieve on its own. Then with two sieves together, the sample trapped between the two sieves after the required sieving time was considered to be within that size range.

## 2.3 Thermogravimetric Analysis (TGA)

A Stanton Redcroft STA 1000 thermogravimetric analyser was used for the proximate analysis experiments, with a single arm facility allowing up to 100 milligrams of sample to be loaded in the sample cup. Char reactivity experiments were performed with the dual cup TGA/DTA arm which allows a smaller cup taking between 10 and 12 milligrams to be referenced throughout the experiment to an identical cup containing an inert material, both in terms of mass changes but also thermodynamic differences.

### 2.3.1 Sample Weights

50 ±1mg of each sample was loaded onto the single arm of the TGA. This weight was found to give a repeatability of ±1% with ash content and less than ±1% with volatiles and moisture contents.

### 2.3.2 Proximate Analysis of Coals

A program was developed which simulated the general procedure for the Proximate test (British Standard 1016:3, 1965)

The coal sample is heated up through a sequence of ramps as follows.

- From 20°C to 120°C at 50°C/min
- Hold for 3 minutes
- From 120°C to 920°C at 50°C/min
- Hold for 1 minute
- From 920°C to 820°C at 50°C/min
- Change to Air supply from nitrogen
- Hold for 32 minutes

The thermogravimetric analyser is able to measure the temperature of the sample in the cup, and in general this was seen to be approximately 20 degrees below that of the furnace.

Figure 2.3.2. shows the sequence as represented by a ramp chart also showing the different stages in the decomposition of the coal sample.

### 2.3.3 Proximate Analysis of Chars

Similar to the proximate test for coal but the time for the carbon burnout is longer due to the higher levels of carbon present in the sample.

The char sample is heated up through a sequence of ramps as follows.

- From 20°C to 120°C at 50°C/min
- Hold for 3 minutes
- From 120°C to 920°C at 50°C/min
- Hold for 1 minute
- From 920°C to 820°C at 50°C/min

- Change to Air supply from nitrogen
- Hold for 40 minutes

#### 2.3.4 Intrinsic Reactivity

A modified program was written to allow the evaluation of the chars intrinsic reactivity (Unsworth et al., 1991). 10-12 mg of char was loaded into the sample cup on the dual arm of the TGA and the following program used.

- From 20°C to 300°C at 50°C/min
- Hold for 0 minutes
- From 300°C to 700°C at 10°C/min

The whole program runs with air as the resident gas. The reactivity analysis is based on the burnoff of char at a low temperature. This will allow oxygen to enter the interior of the chars and so burn-out from inside the char as well as on the external surface. The key indicator of the intrinsic reactivity of the char is the temperature at which the char begins to oxidise rapidly. This is indicated by the position of the DTA peak on the Weight/Temperature graph plotted during the experiment. Figure 2.3.4 shows a typical graph with the DTA, TGA plots against temperature. The value for the DTA peak is called the Peak Temperature. Another important temperature reading is the point at which the derivative TGA profile reaches a combustion rate of 1% per minute. This point is called the Burnout Temperature. The choice of 1 % per minute was chosen because it gave a definite point on the profile to take a value at the very tail end of the peak profile. The use of Peak Temperature and Burnout Temperature is documented by other workers (Unsworth et al., 1991).

## 2.4 Block preparation

### 2.4.1 Coal Block Preparation

A method for preparing coal and char samples was required which did not require a long time between the availability of the sample and the sample's analysis. Therefore a method was adopted from British Steel.

A powdered dental resin called Simplex Rapid is mixed with the coal sample in the proportions 2:5 respectively, by weight. The amount of coal used to make the block was generally dependant on the amount of sample available. Any amount between ten and two grams has been used although for other work less has been used. The mix is then 'wetted' with a small amount of methyl methacrylate. Using a Presi Mecapress C, shown in figure 2.4.1, the mixture is pressed at 150°C and 2.5 bar pressure for 20 minutes followed by a short cooling time. When the sample is in short supply the wetted sample is squashed down in a layer and pure resin used to form a back to the block.

### 2.4.2 Char Block Preparation

Again the mounting procedures for char depend on the availability of the sample. Generally at least 0.15 grams of char is mixed with roughly 0.15 grams of Simplex Rapid and then 'wetted' with several drops of methyl methacrylate. Conditions in the Mecapress C are altered from the coal settings to give 17 minutes at 120°C and 2 bar pressure.

## 2.5 Polishing Procedures

There are several stages in the polishing procedure, resulting in the block being 'relief free' as well as having minimal amounts of scratching on the surface of the vitrinite particles.

The blocks (up to 6 at one time) are polished using a Struers Pedemat Rotapol polisher. The whole polishing procedure takes about five minutes. The process has three parts, with the polishing media becoming finer each time. Each block has exactly 30N pressure exerted from an extendible arm above. The general polishing sequence is as follows:

- 500 grit for 1 minute
- 1200 grit for 1 minute
- 1 micron alumina solution on synthetic silk for 50 seconds

Figure 2.5.1 shows the Struers Pedamet polisher. The two basins are used with the different polishing solutions so as to avoid contamination which would cause poor quality blocks.

## 2.6 The Microscope

The microscope used is a Leitz Ortholux II POL-BK. Figure 2.6.1 shows the microscope with the fluorescent attachment on the left hand side. This attachment was added early on in the work, in order to allow mineral matter to be distinguished from the Liptinite maceral. Maceral analysis, manual char analysis and Image analysis of coal all use a 32x magnification oil-immersion lens and non-fluorescing oil from Leitz. The eyepiece of the microscope includes a 10x magnification lens

## 2.7 The Image Analyser

A Hammamatsu C2400-SIT black and white high resolution video camera was mounted on top of the microscope and was used to downput the image under the microscope to an IBAS 2000 IMAGE PROCESSING SYSTEM. The image system is a PC hosted, hardwired image processor manufactured by the Kontron Image Analyser Division. Figure 2.7.1 shows the system is essentially a large single unit comprising of two monitors, one for control and one

for the microscope image, along with a keyboard and technical mouse. The image analysis system is discussed in detail in Chapter 3.

## 2.8 Microscopic Analysis of Coal

### 2.8.1 Rank Measurements

A manual stage was attached to the microscope, allowing the operator to move to any position on the block. The block was then traversed right to left taking a measurement on any grain of vitrinite which fell under the cross hairs with a reasonably blemish free surface. 100 measurements were taken using a Leitz photometer which was also used with total maceral analysis. The photometer was standardised using a glass prism light standard from Leitz, with a value of 1.24%. The Welsh anthracite and high ranked American coal (Island Creek) used in Chapters 4 and 5, both had reflectance values above 1.24%, so a SiC standard was used for these samples. The SiC standard had a value of 7.51%, and so covered both coals adequately. Unfortunately a lower standard was not available and it is acknowledged that a reflectance standard with a reflectance of around 3% would have been much more accurate.

After each set of measurements the respective standard was placed back under the lens in order to check for variations in the reference line.

### 2.8.2 Maceral Analysis

The block was set on a semi-automatic stage connected to a Swift point counting device. The stage movements were set to 1/3mm which is the specified stepping distance in British Standard 6127:3 (1981). 500 points corresponding to the maceral under the cross hairs each time were recorded on the point counting device. Only the major maceral groups were identified with the exception of the inertinite group, which was split into semi-fusinite and fusinite.

### 2.8.3 Char Analysis

The char block was set on a semi-automatic stage connected to a Swift point counting device. 500 points corresponding to the char under the cross hairs each time were recorded on the point counting device. The types of char identified are featured in Appendix A. It was realised that there are numerous classification systems and so the most appropriate names and types have been collated into the system. The system takes the two factors of wall thickness and basic char structure as being the most important parameters. Four main char types were specifically identified, namely: spheres; networks; fused; solids. Distinctions were made between the thickness of the walls of spheres and networks i.e. walls under 5 microns thick were classed as tenui-, and those above were crassi-. A third category for networks was introduced to describe the main char type formed by a low ranked Indonesian coal. The char itself was a microfine network and was classed as a 'sponge'.



Figure 2.1.1 - The main working area of the Drop Tube Furnace

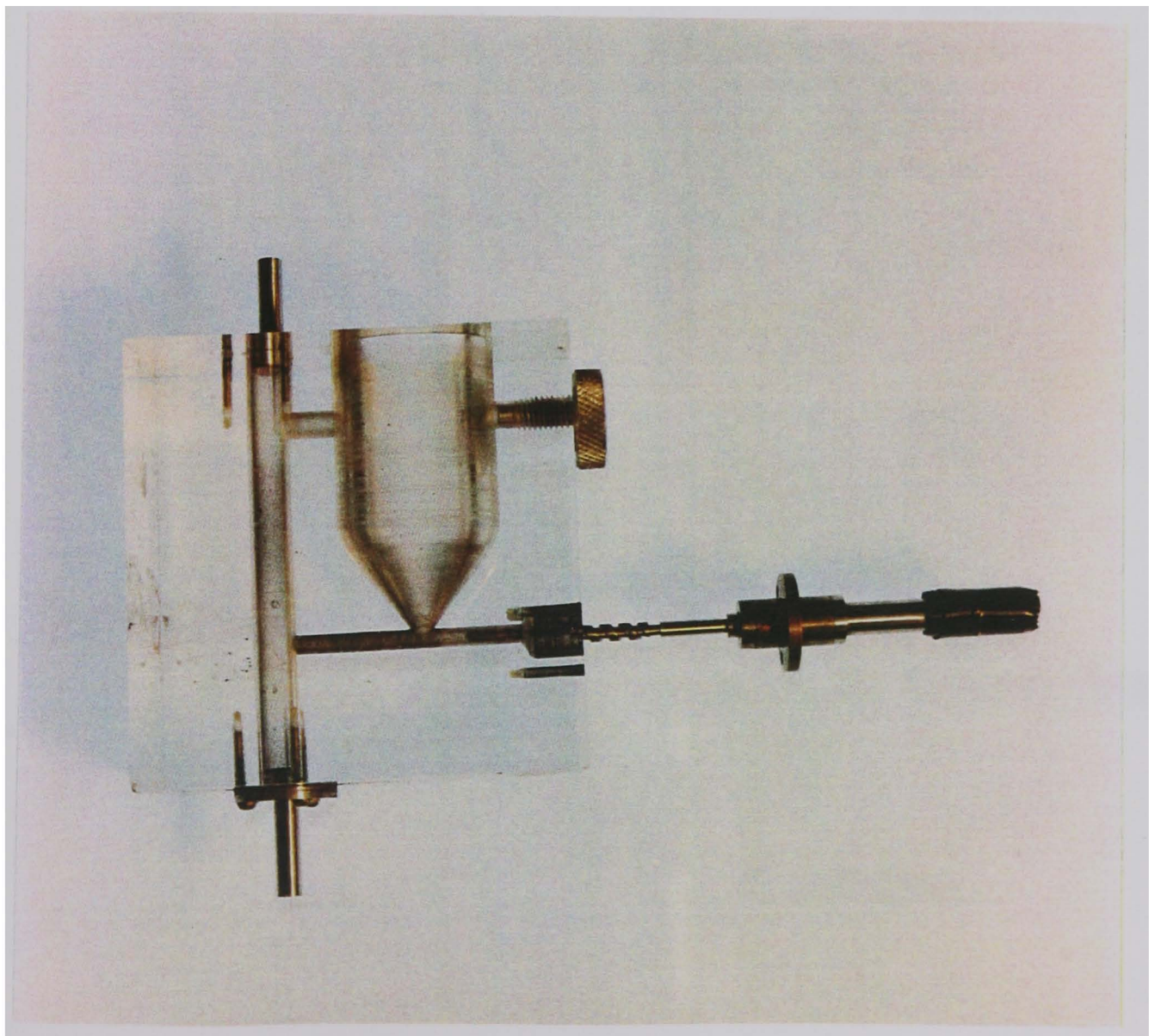
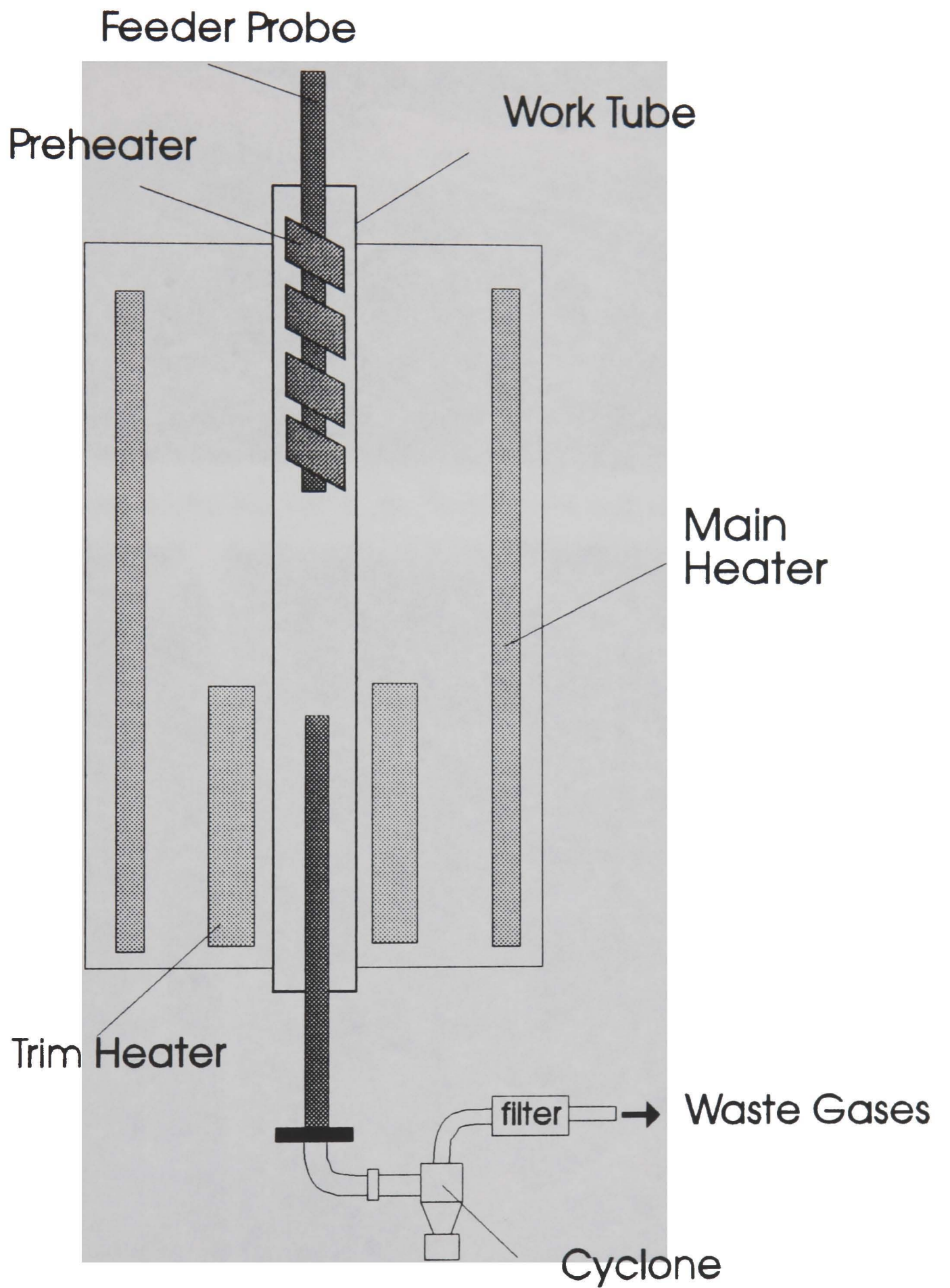


Figure 2.1.3 - The side profile of the screw feeder showing the thread of the screw

Figure 2.1.2 Schematic of the Drop Tube Furnace



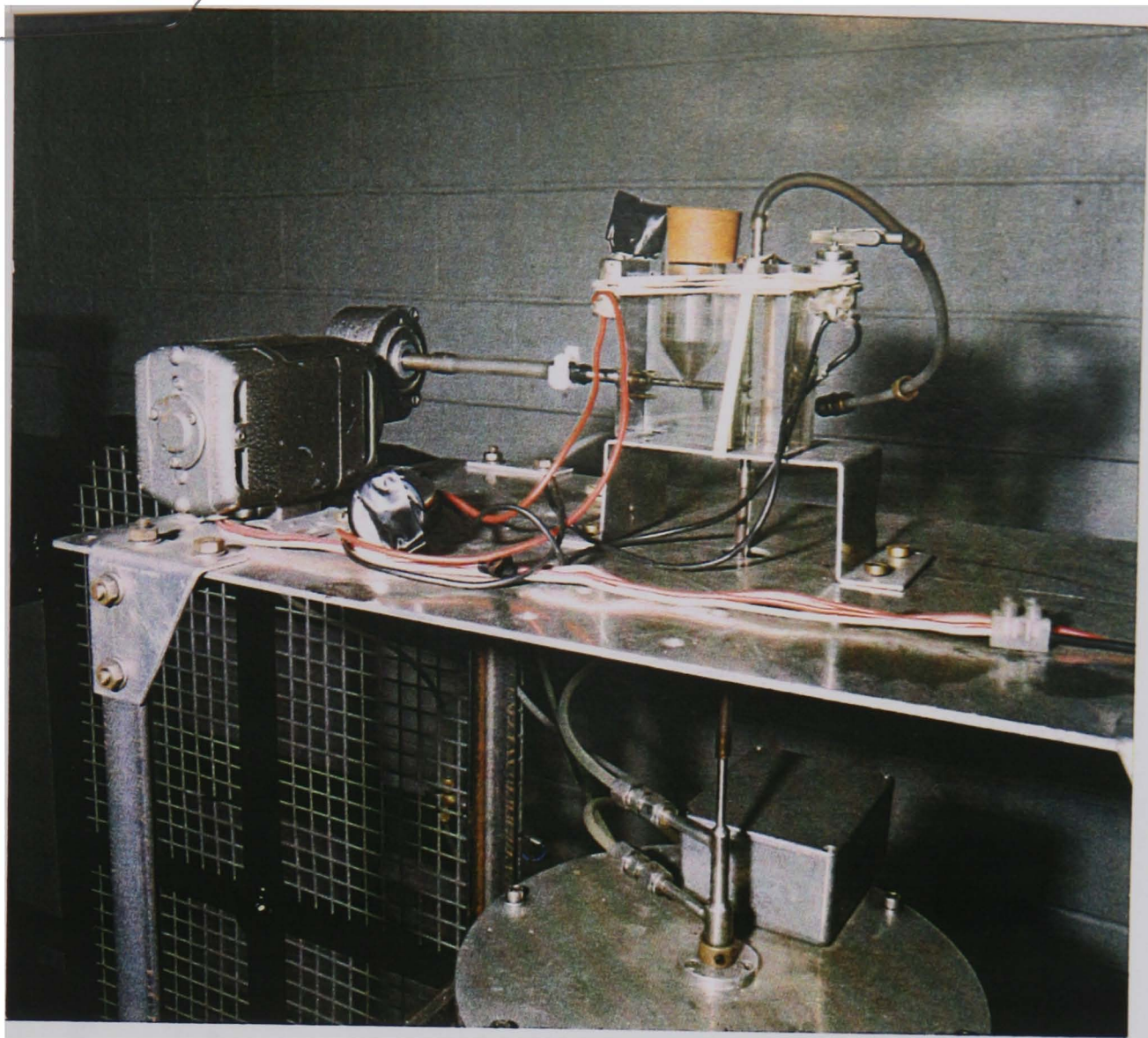


Figure 2.1.4 - The screw feeder attached to the feeder probe and variable speed motor.

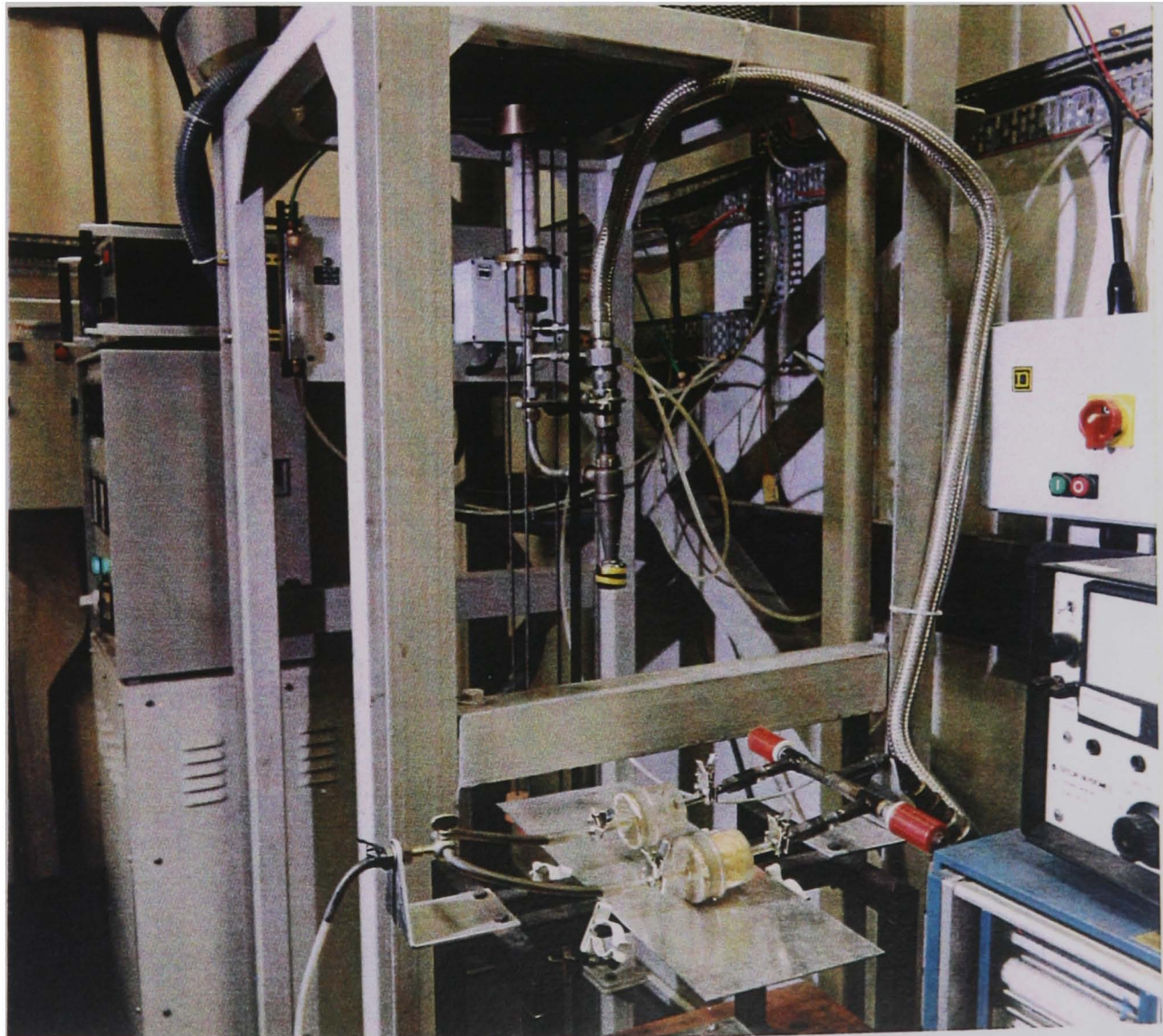


Figure 2.1.6 - The collector probe (with ceramic sleeves in view) connected to the exhaust pipe and filter rig. Note the tar build up around the T piece.

**Figure 2.1.5 A typical temperature profile from  
the Drop Tube Furnace**

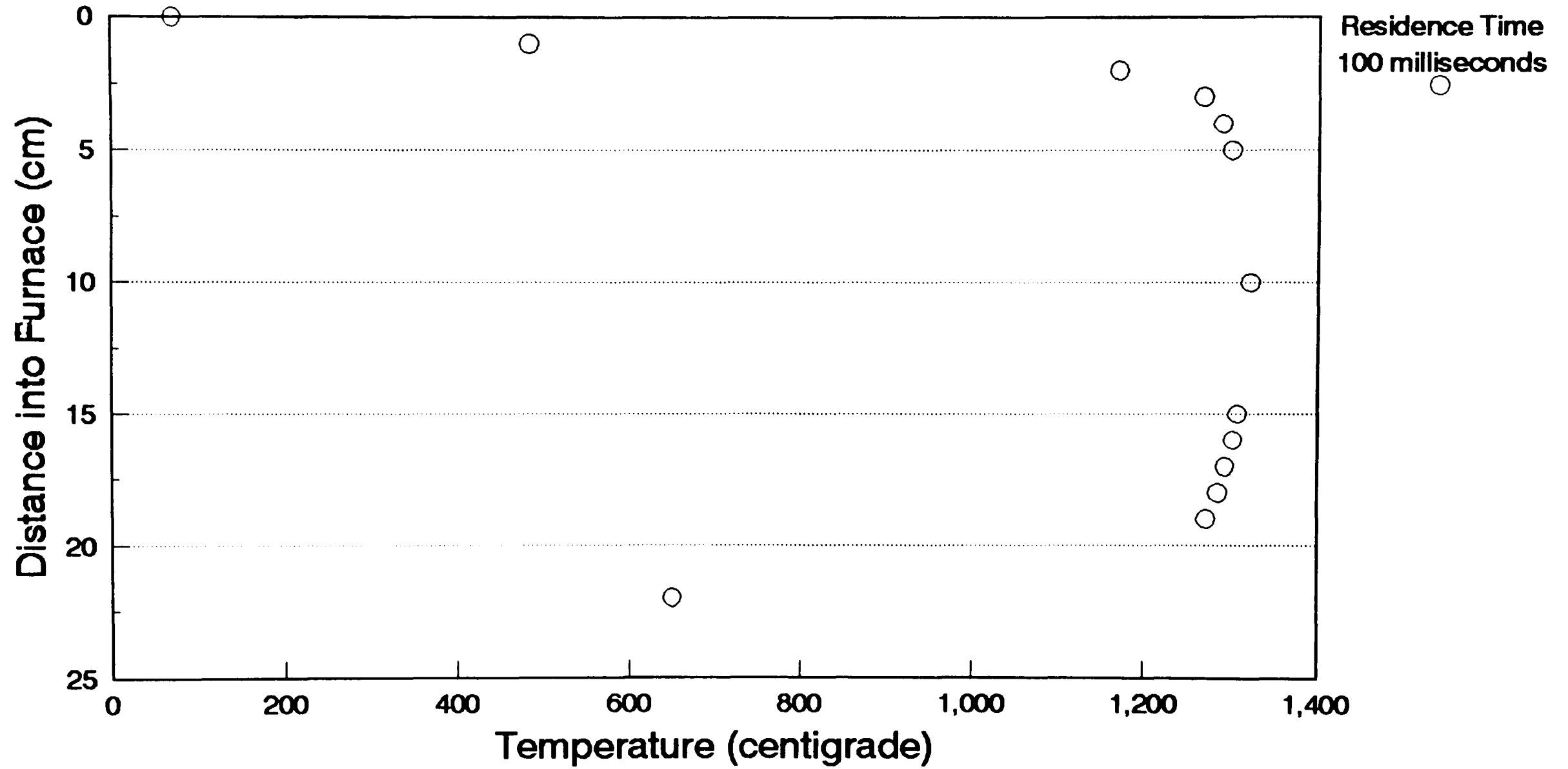
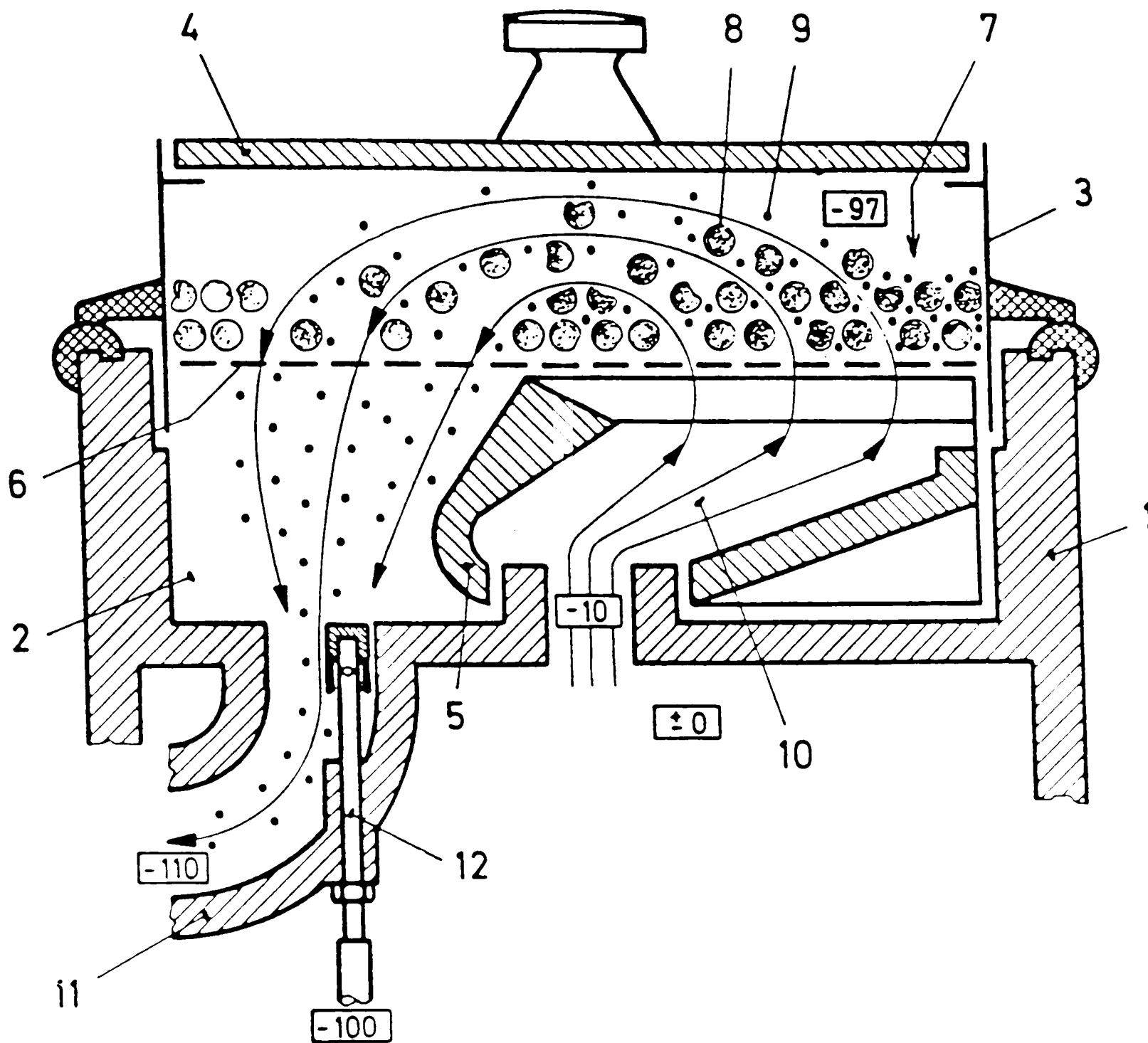


Figure 2.2.1 A Schematic of the Alpine Jet Sieve



- |               |  |
|---------------|--|
| 1 Housing     | 7 Layer of material                      |
| 2 Dish        | 8 Coarse material                        |
| 3 Sieve drum  | 9 Fine material                          |
| 4 Lid         | 10 Air jet                               |
| 5 Slit-nozzle | 11 Discharging socket                    |
| 6 Gauze       | 12 Pressure gauge socket, with dust hood |

$\boxed{-100}$  Air pressure in mm. WG

Figure 2.2.2 - The Alpine Jet Sieve, with sieves, pressure gauge and brush.



# Thermogravimetric Analysis of Coal

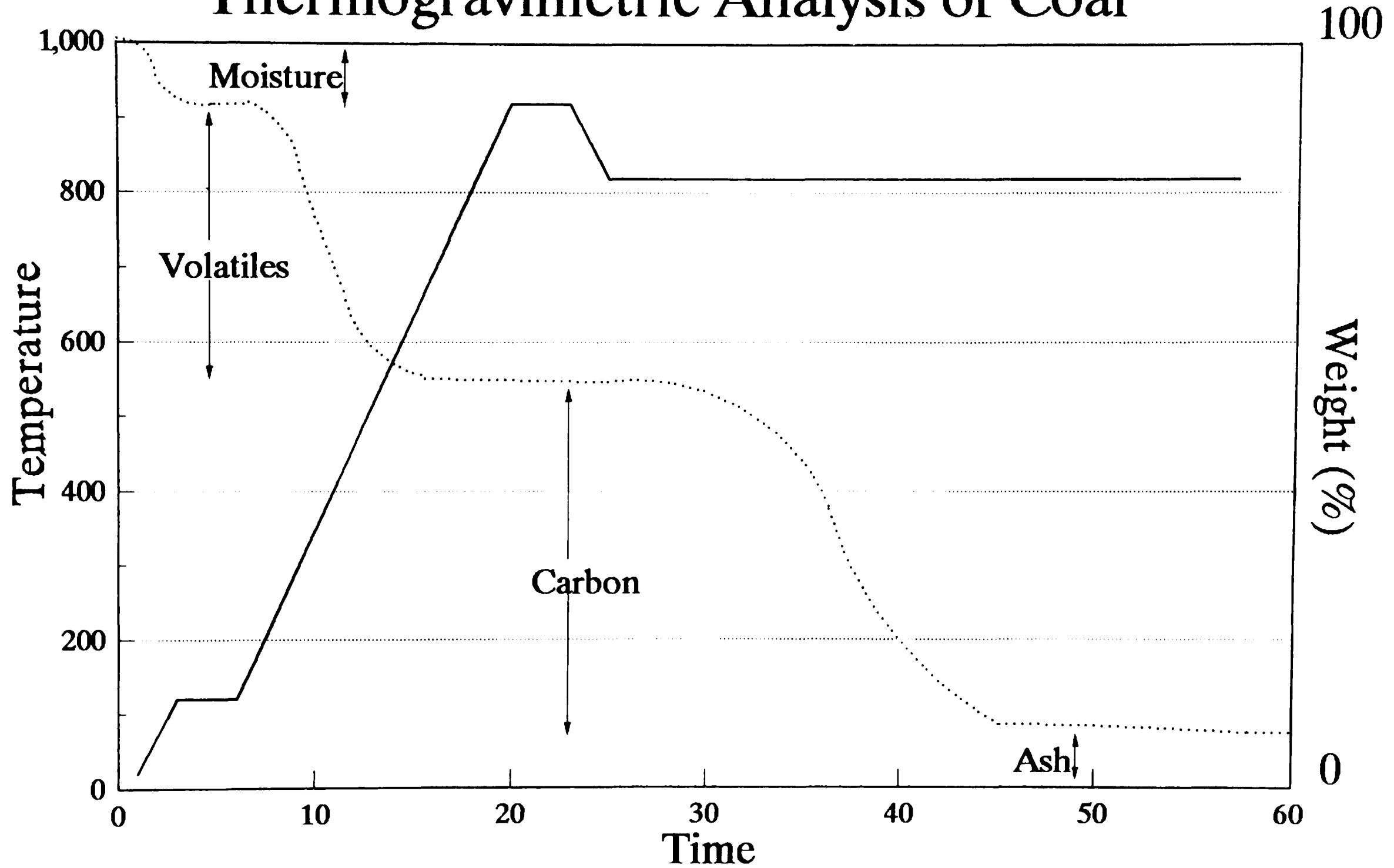
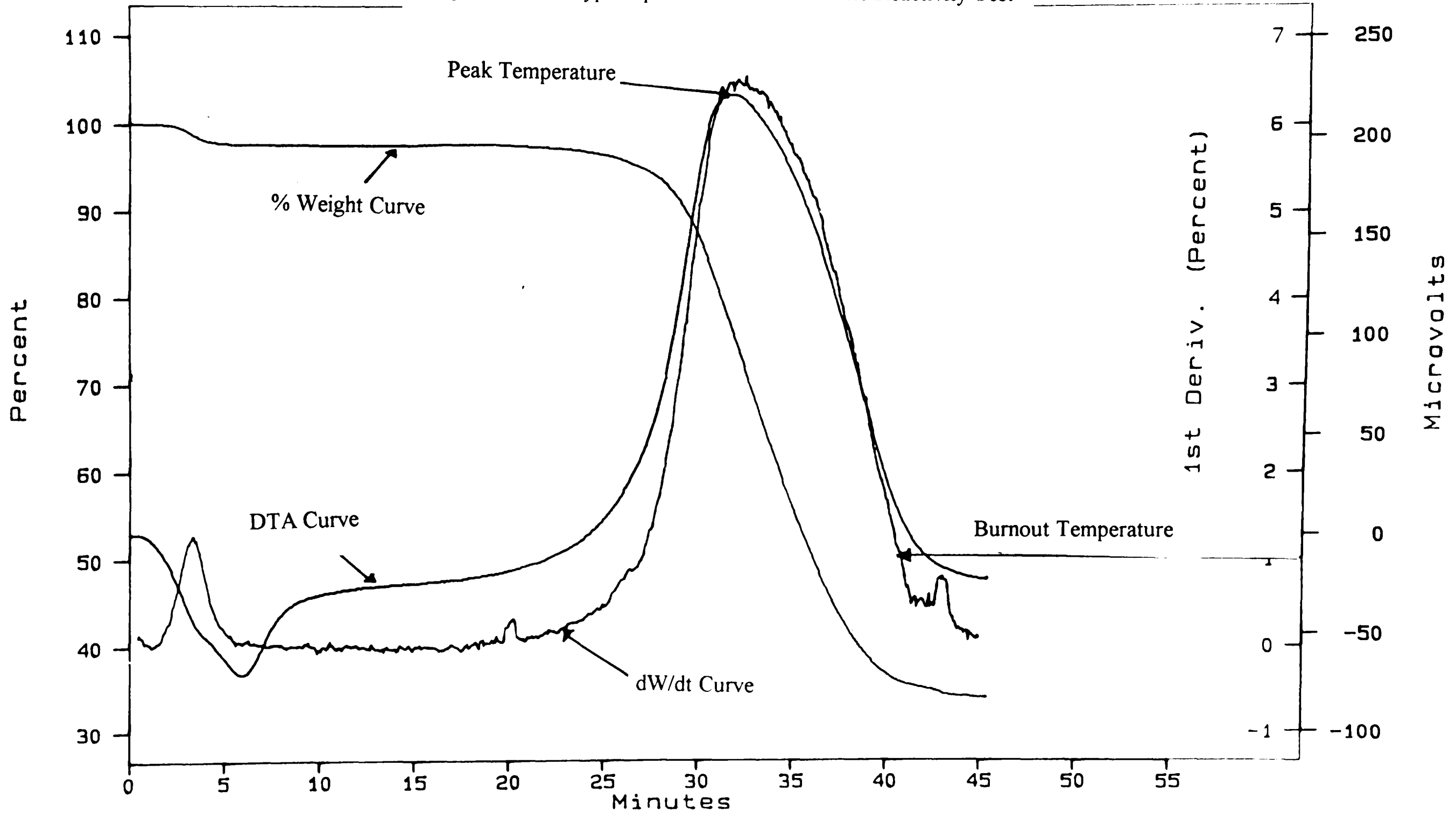


Figure 2.3.2 A Schematic of the program used to perform proximate analysis in the TGA

Figure 2.3.4 A typical profile from the Intrinsic Reactivity Test



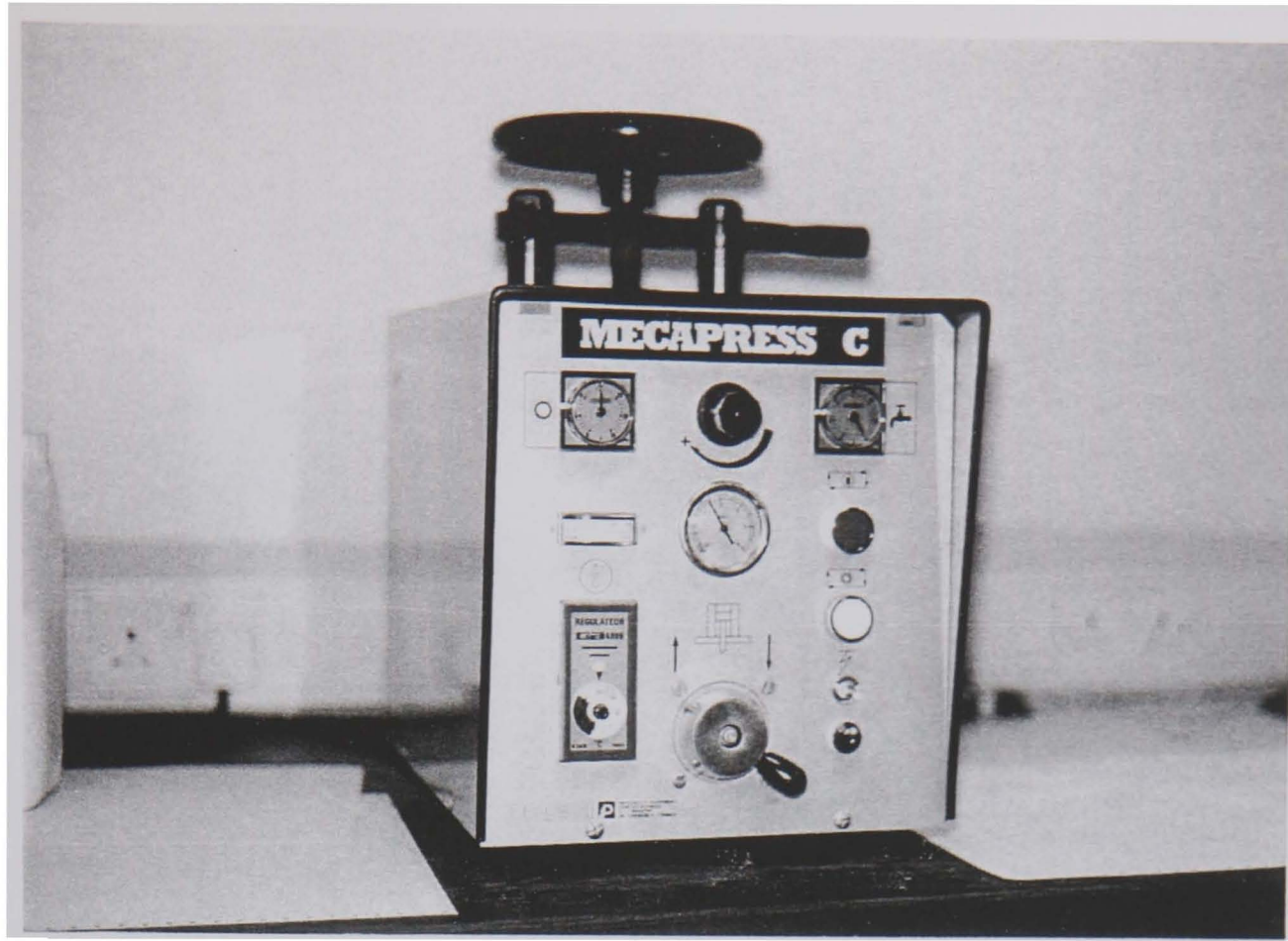


Figure 2.4.1 - Mecapress C block press with temperature and pressure controls in view.



Figure 2.5.1 - The Struers Pedamet Rotapol Polisher. Note the two separate trays for rough and fine polishing.

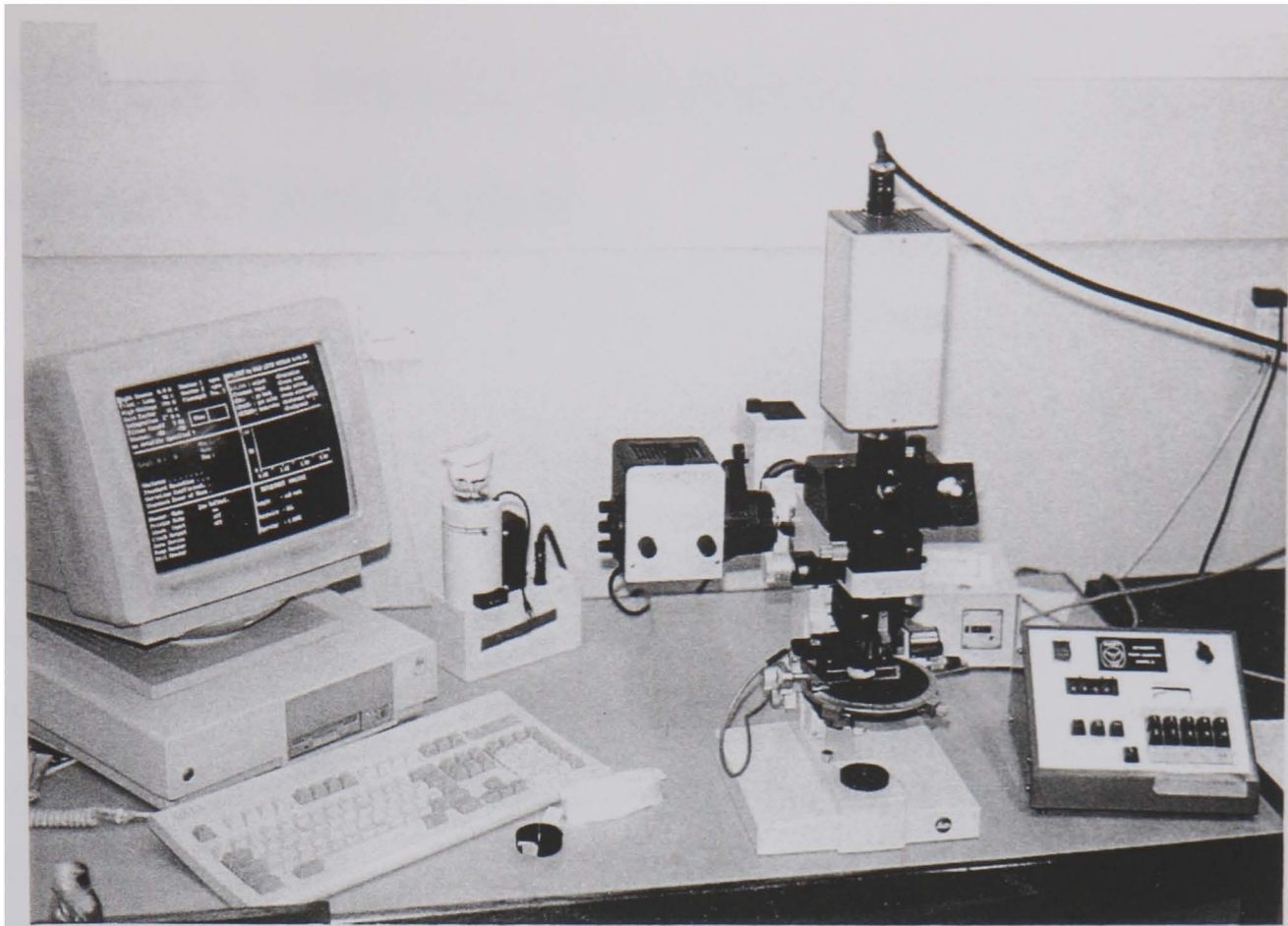


Figure 2.6.1 - The Leitz Ortholux II POL-BK microscope - including the Hammamatsu camera and Fluorescent attachment on the left hand side.

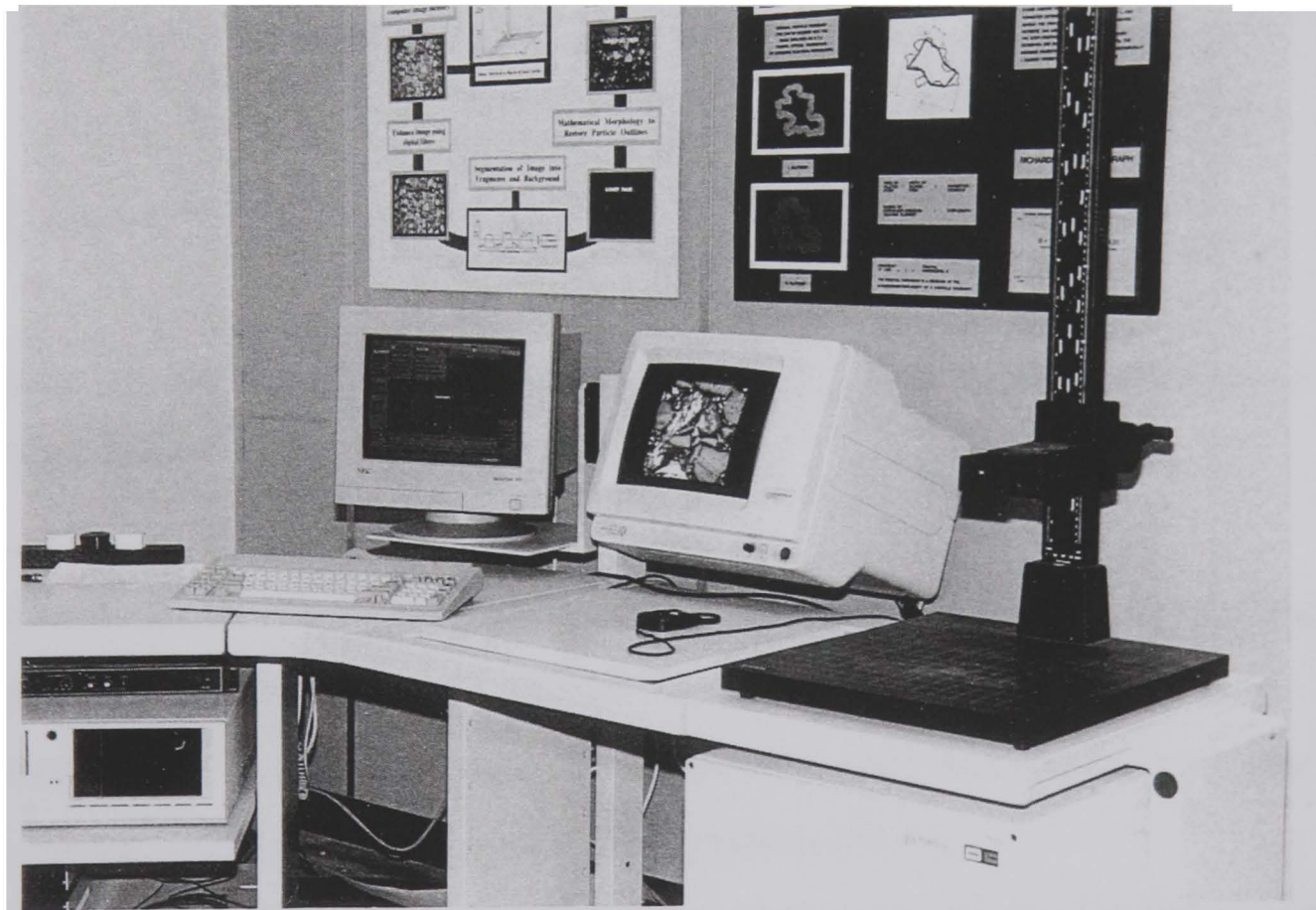


Figure 2.7.1 - The Kontron Image Analyser - showing the image monitor and the program menu monitor during the analysis of a particulate coal sample.

# CHAPTER 3 - IMAGE ANALYSIS AND COAL CHARACTERISATION

## 3.1 Introduction

A number of new image analysis techniques for the characterisation of coals and char have been developed and are featured in this chapter. All programs present either a new approach to an old problem or provide new methods for the analysis of coals or combustion products. The first section reviews the development of image analysis systems. The second section gives details of the new methods.

Manual point counting is a tedious process, and criticism also exists concerning the subjectivity involved with manual point counting. If a machine can increase objectivity and repeatability, then the whole process of geological coal analysis can be made a more precise art.

## 3.2 Analysis Of Coal

There are three existing methods for microscopic coal characterisation and these are listed in chronological order:

- *Manual Methods* - based on modal analysis, first applied to coal in 1934 by Glagolev, but originated by Delesse in the late 19th century.
- *Photomultiplier systems* - the flying spot microscope and photomultiplier system (Roberts and Young, 1952) was the beginning of automated systems.
- *Image Analysis Systems* - a progression in technology led to the replacement of the photomultiplier with a video camera. The image under the microscope is then fed to the image analysis system for analysis.

### 3.2.1 Manual Methods

There are two ways of performing manual analysis, both based upon modal analysis.

#### Lineal analysis

Lineal analysis uses an automated stage which moves the block under the eyepiece using a series of micrometer spindles (Krevelen, 1961, Galehouse, 1971). Each maceral type has its own spindle which is used to pass the cross hairs over the particle. At the end of the analysis, after sufficient traversing, the contribution of the total distance travelled made by each individual spindle is calculated, in order to give the total percentage of each maceral type.

#### Point Counting

An automatic point counter keeps a running total of the number of points out of 500 labelled for each maceral type. The movement of the stage is automated, and the distance moved each time is constant. Once the maceral identification has been made, the autostage moves on to the next field of view. Each point corresponds to the maceral deemed to lie under the cross hairs after each automated stage movement.

#### *Advantages of Manual Analysis*

Point counting still remains the most important and most frequently used petrographic technique, despite attempts to introduce automated systems. The main reason for this popularity is due to the reliability and precision that inevitably results from a well standardised method. Precision tends to be good for a particular group of analysts, especially when trained by the same petrologist.

The identification of macerals is not only based on colour and shade, but also the shapes of the macerals and their apparent associations. The process of decision making necessary to associate maceral types as well as shapes cannot be emulated by a computer, at least not without Expert Systems (Prado, 1992), and so the experienced manual operator still remains the most proficient at maceral analysis.

### *Disadvantages of Manual Analysis*

The disadvantages of point counting are related to the nature of the analysis. Point counting is labour intensive, time consuming and requires a skilled operator. All these factors together make point counting an expensive way to characterise coals. A second problem associated with manual analysis is the increasing difficulty that is encountered when the particle size in the coal block decreases. Standards for coal analysis dictate a maximum particle size of 1mm (British Standard 6127:2, 1981) or 850 microns (ISO Standard 7404:2, 1985), with the minimum of fines. Pulverised fuel (75% < 75 micron) can present problems to the manual operator (Fermont et al., 1989).

### 3.2.2 Photomultiplier Systems

One of the key features which can be used to distinguish maceral types is their visual brightness. This brightness is a function of the relative reflectances of the macerals and is generally characteristic for each maceral group. The human eye can detect small changes in shade and colour, but would struggle to quantify these changes. Using a photomultiplier will allow not only the determination of maceral content, but also rank (vitrinite reflectance) values.

### *Advantages of photomultiplier systems*

The introduction of automated systems will almost always see a decrease in the time required for analysis. Early systems could analyse  $10^6$  points in 20 minutes (Denton 1967). The system from the Nippon Steel company was developed ten years later and compromised speed for increased accuracy (Kojima., 1976). 20,000 points required 30 minutes and so it is still preferable to manual methods. Table 3.2.2. shows the published results of the Kojima paper.

### *Disadvantages of photomultiplier systems*

One potential disadvantage is the fact that only a three way maceral analysis is performed i.e. vitrinite, inertinite and liptinite. In some utilisation fields this would not be enough to use for behavioural characterisation, because the division of inertinite into semi-fusinite and fusinite has been shown to be important with certain coals (Thomas et al., 1991a).

The speed of analysis often compromises the sampling techniques. That is to say, only a small spacing between sampling points is possible (2-3 microns) when analysing points at such speed. Larger gaps would augment the analysis time because of the additional time required to move about the surface of the block. Small stepping distances between points mean that a very large number of points have to be sampled (Pitt and Dawson 1979).

### 3.2.3 Image Analysis Systems

Until very recently image analysis systems have, like photomultipliers, relied on the use of the characteristic reflectance of the macerals (Stach et al., 1982). Instead of using a photomultiplier to measure one part of the field of view, a video camera captures the entire image and sends it to the image analysis system. A captured image is digitised into an array or matrix of individual pixels. Each pixel is then ascribed a grey scale value dependant upon its reflectance. A captured image can contain any amount of pixels in it (up to 1,000,000), the

analysis of which requires less than a second. Image analysis systems are therefore favourable to other systems like photomultipliers, which take much longer to collate the same number of points.

### *Advantages of the Image Analysis System*

Image analysis systems are fast reliable and do not require a skilled operator to run on a day to day basis. Each captured image can be manipulated to correct 'halo effects' and uneven illumination. Other methods, like the photomultiplier, cannot correct this sort of problem.

Image analysis systems can perform the same functions as a photomultiplier, as well as being able to attempt microlithotype analysis (Chao et al., 1982a, Crelling, 1982) liberation analysis (Finch & Gomez, 1989) and association analysis (Vleeskens et al., 1984).

### *Disadvantages of the Image Analysis System*

The sensitivity of the video camera will dictate the value of the results. The extreme contrast in reflectance values for the macerals and the visual overlap of certain phases can overcome the system (Chapparro, 1987). An example of contrast would be a bituminous Northern Hemisphere coal where one would expect to find 5 to 10% liptinite content in the coal, probably in the form of dark spores. The inertinite present will generally have a high reflectance, hence in the same image one could expect to see both dark macerals and extremely bright macerals. This extreme contrast will adversely effect the video camera.

Another, more serious, problem is the overlap in reflectance of the liptinite species in the coal and the resin binder used to hold the coal block together. If the camera is to avoid burnout from over exposure to bright inertinite particles, then liptinite is virtually impossible to resolve from the resin, because the camera settings are so low.

A problem in the use of the image analysis system for the measurement of vitrinite reflectance, is that it requires the calibration of the camera using several standards. This takes time, and since the process must be repeated for each new sample, there is little difference in the time required for rank analysis with a photomultiplier and with an image analysis system.

### 3.2.4 Summary of all Methods

All three techniques as described, have advantages and disadvantages. Because point counting is the most subjective of the three techniques, more effort has been made to standardise it. Despite this, it still relies heavily on the interpretation of the operator. Therefore, manual analysis requires a trained operator, and takes a reasonable length of time to perform. For this reason, point counting is rather specialised.

Automated systems provide a more rudimentary set of results but are, on the whole, faster and do not require a high level of skill. Photomultipliers can provide a more accurate determination of rank (Kuili et al., 1988), whereas image analysis systems can provide specialised information on the associations and dissociations of maceral phases.

## 3.3 Image Analysis

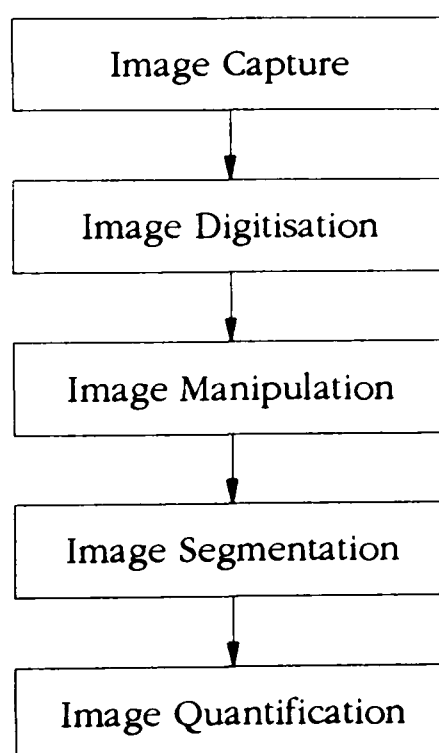
### 3.3.1 The system layout

Figure 3.3.1 shows the basic layout of the hardware in the image analysis system. The system is called an IBAS 2000 Image Analyser made by Kontron Image Associates. The system is centred around a 386 PC based host processor, connected to a hardwired image processor via a high speed link cable. The image processor captures images from a high resolution video camera via a camera control box. The on-line image from the camera is usually displayed on the RGB monitor. The software for the IBAS system allows the user to interact via a

keyboard, digitiser and a VGA monitor. Each image can be captured, stored, printed or loaded onto a floppy disc. An autostage connected to the IBAS allows a running program to move the stage automatically using the appropriate software command. Movements are only possible in two directions via the motor control processor (MCP).

### 3.3.2 Grey Scale Analysis Using Image Analysis

The next few sections describe how maceral analysis can be performed using simple grey scale techniques. Even though this method is not particularly useful or effective, it gives a basic background to the way a program works with image analysis systems. Until the programs described in the later sections of this chapter were written, grey scale analysis was generally accepted as the method for maceral analysis. The analysis procedure has 5 main parts and these are shown in the chart below.



### 3.3.2.1 Image Capture

The live image is effectively 'frozen' and loaded onto the RAM of the PC. From here the next stages of the analysis process are possible. The quantity of the image captured will determine the value of the results i.e. a poor image will generate poor results. Good illumination, fresh oil and scratch free surface will ensure that the image captured is fit for analysis.

### 3.3.2.2 Image Digitisation

Once the image has been captured, it is digitised. The image analyser divides up the image into individual pixels and assigns each one a grey scale value ranging between 0 (black) and 255 (white), dependant on the reflectance of the material in that pixel area. In experiments at Nottingham a field view of 512\*512 pixels was used.

### 3.3.2.3 Image Manipulation

Despite the stabilised light source used in the microscope, the digitised image has an uneven level of illumination. The centre of the image is brighter than the edges. The reason for this can be related to the optical set-up of the microscope, and is difficult to alter. However a captured image can be corrected for this effect. To correct the problem, the image must be manipulated using a 'light filter'. The light filter is a digital image that has been captured and quantifies the variation over the whole image, hence allowing the previous image to be corrected.

The light standard used to calibrate the camera control box also serves as the light filter. The light levels throughout the image should be the same, hence any variation in the values for each pixel on a homogenous surface, such as an optical standard, will be the result of uneven illumination.

#### 3.3.2.4 Image Segmentation

Each of the components, the macerals and the resin, present in the polished coal mounts have characteristic reflectances or levels of brightness, and hence can be segmented after digitisation. This means that vitrinite can be separated as a function of its grey scale to form a simple binary image i.e. vitrinite particles are present as white pixels on a totally black background.

Liptinite and the resin, as mentioned earlier have virtually indistinguishable grey scale values, but vitrinite has a grey scale value somewhat higher than liptinite, hence can be easily separated. Figure 3.3.2 shows a typical grey scale histogram along with the typical cut off points that would be expected.

#### 3.3.2.5 Image Quantification

The percentage area of a phase in relation to the image is calculated by creating a binary image and then dividing it by the total area of the screen image. By using the values determined during image segmentation, one can progress through each maceral phase, creating a binary image each time and calculating a percentage value for each maceral respectively.

### 3.4 Programs Developments

The most basic method for maceral analysis i.e. simple grey scale analysis has been described in detail in section 3.3. The most important point needing further emphasis is the problem that exists in the differentiation between the liptinite fraction and the resin. Figure 3.3.2 shows the problem well, where the difference in grey scale between liptinite and resin phase is too close to distinguish. The liptinite in this case is >10% hence its lack of detection is quite serious.

Several new programs were devised which were capable of recognition of all the maceral types, although in the final project only two were pursued at length. The first, called the *Morphology method*, the second *Fluorescence/Reflectance*. It was realised that the image analysis system could be used for more than just maceral analysis. Other programs could be used to characterise chars particles, from basic measurements of porosity, to providing profiles relating to the burnoff characteristics of each char.

As described in Chapter 1, maceral analysis is not enough to predict the burnout behaviour of coals, other parameters like rank are important too. Therefore a program which could give a relative characterisation of each coal based on the reflectance values of each maceral type would provide useful results. The association of the macerals is also of interest, but only a small amount of work in this area was performed on particulate materials. The main work in this area was done with solid coal blocks. The distribution of the macerals, in terms of size, was another area of interest and hence a further program was written to provide information on the size of each maceral type.

Some of the programs developed at Nottingham are reviewed in the following sections, although the results for each method have not been given heavy emphasis because they can be found in subsequent chapters or in the listed publications.

#### 3.4.1 Morphology Program

The method which has been developed is not intended to be used blindly on an unknown coal sample. It is particularly aimed at situations where a large number of samples of the same coal are to be processed. The program is based on the microlithotype associations of the macerals found in a coal block, and uses several processor tools on the IBAS system to manipulate each image.

Since the morphology program has not been used in subsequent chapters - the method is not discussed. A description of the program, along with the functions used to perform the analysis, are discussed in detail in a paper published in FUEL (Lester et al., 1994c).

### 3.4.2 Reflectance/Fluorescence Method

When illuminated by strong blue light various constituents of the polished coal mount will begin to fluoresce. In very low rank coals, macerals will fluoresce, with the exception of inertinite. Very high rank coals do not fluoresce, regardless of the maceral type. The details of the fluorescent nature of each maceral types can be seen in Table 3.4.2. Most commonly available resins used to mount coal also fluoresce to varying degrees. Attempts to find a non-fluorescing resin were unsuccessful. The components of the polished coal mounts that fluoresce, the strength of the fluorescence, and the wavelength of the emitted light depend upon the rank of the coal and the type of resin used to make the block.

For the hard coals typically analysed the liptinite fluoresces moderately to strongly with yellow, orange and brown colours. The Vitrinite and Inertinite do not fluoresce. The resin fluoresces moderately to strongly with a distinctive green colour. If Liptinite is consistently the strongest fluorescing maceral then one can carry out maceral analysis by using the method described below. A program has been developed which uses the reflectance and fluorescence of the macerals in both white and blue light respectively.

#### *Basis of Program*

For a complete maceral analysis to be performed, two separate analysis runs need to be made. Either can be used first. One is specially written for white light, the other is required when operating in blue light. Both perform the same number of tasks. These are as follows:

The first stage in the program is the *initialising*. The Image analyser checks that all functions including the auto staging equipment is operational. The operator is asked which objective is being used in the experiment. This enables the Analyser to calculate the appropriate stage movements so as not to overlap images, and also to calculate the size of each image, to indicate the total area analysed in microns. These details are then printed on the screen.

The next step is the *standardising* of the camera settings. A light standard, normally used for rank measurements, is placed under the microscope. The image is then captured by the Analyser and the average value for the grey scale intensity of the whole screen image is calculated. A standard deviation measurement is also made. The average value, or normalising value, is used for adjusting the camera settings to allow an identical analysis of all coals. The normalising value that is used will affect the spread of results in the analyses and hence a value was required which provided the greatest contrast between the various phases.

The light filter, created from the light standard, also allows each image to be corrected for light variations over the image field. The standard deviation value gives an indication of the how even the light level is over the whole image. Another reason for adopting a normalising value of around 120 was the effect that the normalising value had on the deviation in the image light levels. Once the required camera settings have been made the operator is required to input a value for the *auto-focussing*. The greater the severity, the longer the analysis time. No focussing will mean a 50 image analysis takes 5 minutes. With the most severe focussing on the same 50 images, the program will take over 8 minutes.

The operator must decide how many *images* are required for the analysis. The size of the particles in the block will effect the number of images necessary to achieve satisfactory repeatability. The information produced during the analysis is stored in a *data file* which is named by the operator at this point in the procedure.

The program then begins. Each image is digitising an array of 512\*512 'points' with 256 grey levels ranging from 0 to 255. The method is similar to that used by other workers (Riepe & Steller, 1984). Each image is analysed in the same way and include the image correction procedure using the light filter. Once the required number of analyses is produced, the autostage returns the block back to the starting position, ready for the next stage in the operation.

At this point, in order to evaluate the presence of liptinite, the lighting is changed to blue light. A blue excitation filter is placed between the light source switching box and the high pressure mercury bulb. A green-yellow suppression filter is positioned in the compensator slot, on the side of the nosepiece. A purple separation filter is positioned in the clear aperture of the rotating analyser, which is used to block out most of the green light emitted from the fluorescing resin but it does not interfere with the yellow light from the liptinite. 90 percent of the light reflected from the block is fed to the eyepieces. These filters and light arrangements are important in order to achieve a high level of fluorescence in only the Liptinite species and not the background resin media.

A slightly different program was designed when operating with a blue light source. The initialisation procedures are similar, although this time a light filter is not necessary because of the presence of only two distinct phases, liptinite (white) and the rest of the sample (black). Figure 3.4.2 is a flow chart of the analysis procedure. The figure shows how the various lighting is achieved and how the phases present are eliminated or enhanced.

A paper is awaiting publication in FUEL which discusses this method and includes investigation into the repeatability and reproducibility of the method (Allen et al., 1994).

### 3.4.3 Reactivity Program

This program is used to identify the fraction of the coal which is deemed to be 'reactive'. This method is virtually identical to 3.4.2 apart from the way in which the light standard is used to calibrate the system. With 3.4.2, the main purpose of the light filter is to correct uneven illumination, whereas with the Reactivity program, the light standard is necessary to ensure that all results are relative. In all work in the next two chapters, a sapphire standard was used to calibrate the field of view to 115 grey scale units. The captured image of the standard was also used as an illumination corrector or 'light filter' to even out the variations that exist on each image.

#### 3.4.4 Semi Automated Maceral Analysis

The program was devised as a halfway house between manual analysis and a fully automated image system. The program is controlled from a keyboard. All stage movements are automated, once the stepping distances are programmed in along with the number of points required for analysis (up to 1000). Similar to 3.4.1 this program was not used in the thesis work, and so is not discussed in any detail.

#### 3.4.5 Microlithotype Analysis

Two programs are required to produce a set of microlithotype analyses. The first program performs the analysis in terms of maceral content per screen image, and the second converts the maceral information into the various microlithotype categories. At this stage, only solid coal blocks have been analysed because of the liptinite grey level problem and so a program similar to that in section 3.3 is used. The manual method for microlithotype analysis requires 500 data points using a 50 micron wide Kotter graticule with at least 10 of the 20 points landing on coal material (British Standard 6127:4, 1990). For this program the usual image size of 512\*512 pixels was reduced down to approximately 100\*100 pixels. This corresponds to a 50 micron square with a 32X oil immersion lens. 10 rows of 50 images are analysed using the British standard measurements for the stepping distances. The analysis requires about 2 hours to analyse 500 images. Figure 3.4.5 shows the logic tree used in the second program to convert the maceral data into microlithotype information.

#### *General Evaluation of the Method*

There are two main conclusions concerning the program as it stands. Firstly, sampling a solid coal block presents a significant difficulty as far as repeatability is concerned. Because bedding planes exist in a 2 inch coal block, one cannot expect a scanning pattern which runs in a straight line to give reasonably accurate results. Secondly a Kotter graticule has 20 points on it, hence if any maceral lies beneath any one of them, it can be considered to be >5% of the total.

However, when 10000 pixels are taken into consideration, results for any one maceral type is accurate to .01%. Therefore if vitrinite is 92% of the screen image and inertinite and liptinite are both about 4%, then there is a nomenclature problem i.e. the results will fit no particular microlithotype group. The remedy for this problem has been to take the largest of the two minor group as >5% in order to give the closest microlithotype. If microlithotype analysis is to progress with image systems then this type of problem should be properly addressed. The disadvantage of the program is that the time for analysis is quite slow, although it is still faster than the time for manual analysis (>2.5 hours).

A more detailed paper has been accepted as part of the International Conference on Coal Geology and Coal Bed Methane at Cardiff in September 1994.

### 3.4.6 Char Analysis

Three different char programs were developed during the project, and each one was based on a particular processing tool on the Kontron Image Analyser, in order to characterise the different char types.

#### 3.4.6.1 Semi-Automated Analysis

This program requires the operator to perform a few tasks before the image analyser was able to make a series of measurements. The operator singles out one char particle at a time and then rebuilds it, depending on its physical condition. These actions are all performed with a mouse, making the whole procedure quite straightforward. Once the operator has restored the particle, and given it a char type - the image analyser makes a series of measurements including a maximum and minimum diameter, average wall thickness and char voids %. Char voids % relates the internal surface voids to the walls which surround the voids. All this data is presented in the form of a spread sheet, and from there can be manipulated into meaningful data for char burnout predictions.

The benefit of this method is that it provides a huge amount of information about each particle. All the data generated is of potential value when considering char burnout. The drawback of the system is the time required for the analysis. 100 particles required around 1 hour from the operator. Hence this technique is labour intensive.

Figure 3.4.6.1 is the correlation between % voids for each char type, as decided by the operator. It was important to know that the operator was not labelling a tenui-sphere a crassi-sphere in different samples. This figure would indicate that this was not the case because each char type from the eleven different coals had a characteristic value for voids %. Figure 3.4.6.2 shows the maximum/ minimum diameter sizing as calculated by the image analyser. Since these are the result of sized coal samples passing through a drop-tube furnace, one would expect bandings similar to those seen in this figure.

#### *Evaluation of the method*

The program provided a great deal of information concerning the structure of the chars. The only real drawback with this program was the time required to analyse sufficient amounts of chars to obtain repeatable results. This program, although relatively objective, is perhaps more labour intensive than manual maceral analysis.

#### 3.4.6.2 Automated Dilation Erosion Program

This program involves the manipulation of each screen image so that char particles are closed to form a perfectly whole char. This was necessary because most chars were not quite intact after polishing because of the fragile nature of the char walls. Figure 3.4.6.3 shows the process by which each char is closed. This process requires the use of the *close* function on the morphology software on the IBAS 2000. The char particles are then *filled* to provide solid objects. A simple calculation then allows char voids % to be calculated which is the ratio of the internal void space to the area of the char walls. This voids % can then be used to indicate

the openness of the particles. This sort of parameter may be of use if one could link high char voids % to good combustion characteristics.

### *Evaluation of the method*

Although the method was full automated, it became apparent that the program was not as successful as was hoped for, particularly with fragile chars. Figure 3.4.6.4 shows the correlation between manual voids % and those calculated by the image analyser. One can see that there is a poor correlation. Manual char voids % was determined from a combination of the manual char analyses and the % voids for each char type as determined by the method described in section 3.4.6.1. The reason for this is probably due to the close function not working with thin walled chars. This was partly due to the fragmentation that seemed to result during the mounting process. The close function closed fragments together which were not necessarily from one char particle and didn't successfully close all particles. Steps were taken to reduce this fragmentation by altering the block preparation procedure. The eventual changes made were to lower the block setting temperature and a reduction of the pressure put on the block. Even so, it was apparent that the program was not going to be accurate enough and so was not pursued much further.

### 3.4.6.3 Automated Distance Transform Program

This program used the *distance transform* function present with the IBAS software. Since the thickness of char material will probably affect burnout, a useful parameter to measure would be the thickness of the char material. A balloon-like char may burn at the same rate as a solid sphere of the same diameter - but it will require far less time to burn out due to the amount of material present.

The method is simple and is shown in Figure 3.4.6.5. The char particles are singled out into binary images. The edges of any particle (shown by a 0-256 grey scale gradient) are given the grey scale number 1. Any neighbouring white pixels are then called '2'. The row of pixels after

this are then '3'. Hence a particle is contoured until all the white pixels present after thresholding have been designated a contour number. To test the distance transform program a series of experiments were carried out using the program. This was done to test the programs validity and also to determine what the program was capable of.

### *Experiment 1*

A series of idealised chars were drawn up, which represent the main types of char seen under the microscope. Figure 3.4.6.6 show these char types. Each char was captured using a video camera attached to the image analyser. A normal photographic lens was attached to the camera. Once the image was captured, the whole screen was inverted making all black objects white and vice versa. Each char was then analysed using the distance transform technique. Figure 3.4.6.7 shows the results for the different char types. One can see that each type has its own distinctive trace.

### *Experiment 2*

The series of images shown in Figure 3.4.6.6 were enlarged and reduced by a known factor using a photocopier. The new images were captured and analysed in the same way as in experiment 1. The results for each type were then compared. Clearly the image analyser using the distance transform method is capable of distinguishing between changes in size without any difficulty, even if the char shape is exactly the same.

Figure 3.4.6.8 shows the point at which 95% of each char type is 'burnt out'. One can see that with the thin walled (tenui) particles - even a large change in size does not effect the burnout time. The thicker walled particles however has a much increased time for burnout e.g. the mixed porous char increases from 30 to 60 units for an increase from 65% to 141% in size.

### *Experiment 3*

Several real char particles were captured using the same program but with the video camera sitting on a microscope. Figure 3.4.6.9 shows the results for the different types of char. Again it is possible to see a clear distinction between the different types.

### *Evaluation of the method*

This method appeared to be the best out of the three attempted during the project, because it was able to run automatically whilst generating useful information as regards char structure. The dilation erosion program described in section 3.4.6.2 became inaccurate when analysing fragmented chars, but the results from distance transform program were unaffected by this, and hence this was a major advantage over the other two methods.

### 3.5 Conclusions of Chapter 3

The image analyser can be a powerful tool when looking at char and coal particles. In most cases an object can be dissected, structured or associated using one or several different tools available on the system. Problems with maceral analysis were overcome by taking a fresh approach to an old problem. In short most objects can be analysed or characterised by identifying any features unique to that object and finding a means for the image analysis system to detect that feature.

The time for analysis can be decreased with the use of image analysis. The need for a skilled operator is also decreased, although none of these systems are sufficiently developed to allow a non-skilled operator to run them (yet!).

Objectivity during analysis is paramount and hence, with an image analysis system, the theoretical accuracy/precision of the results is increased. In practice, increasing the number of scans and the number of images per scan will lead to an increase in repeatability (Allen et al.,

1994). The validity of the reactivity program and the automated distance transform program for chars is discussed in Chapter 5, in which different world coals are passed through a drop tube furnace and then re-analysed for the combustion products produced.

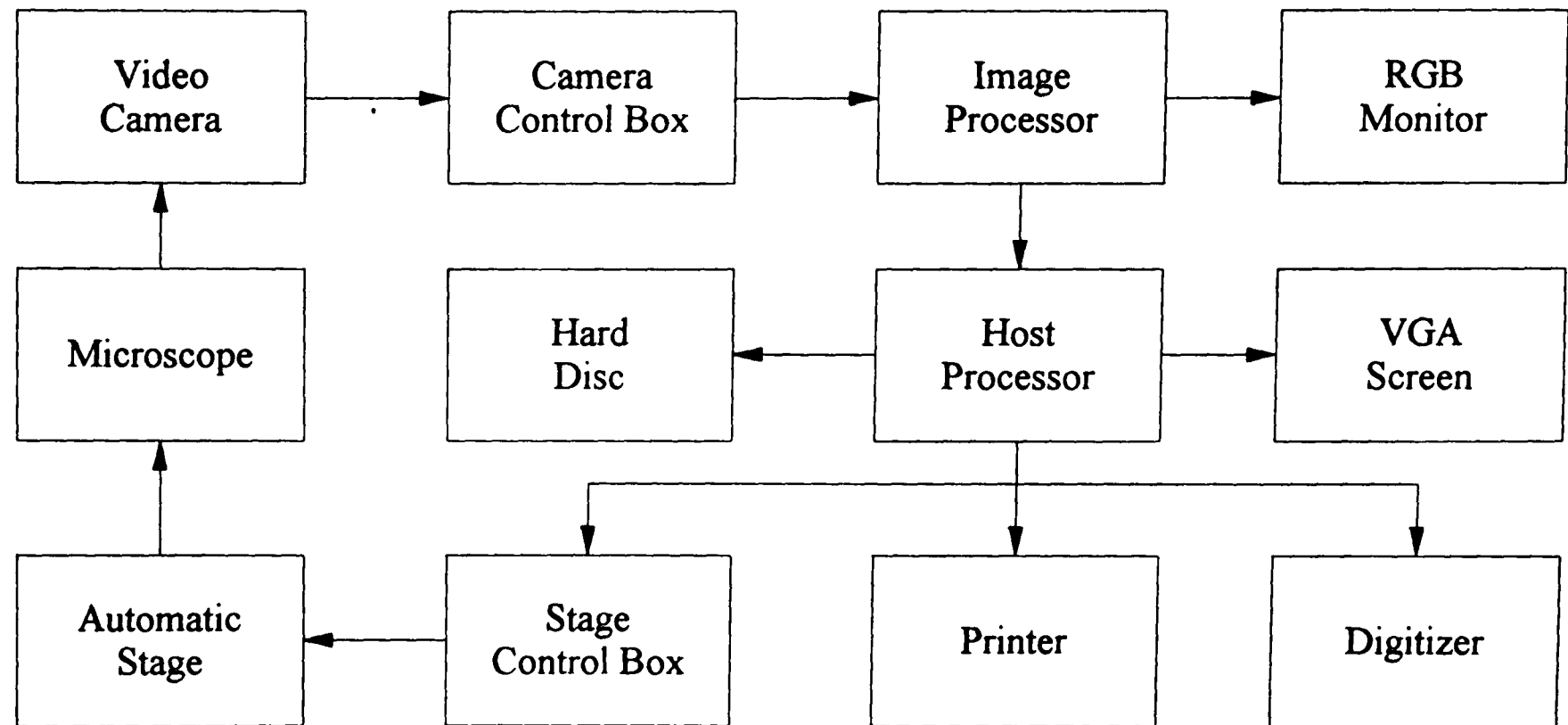
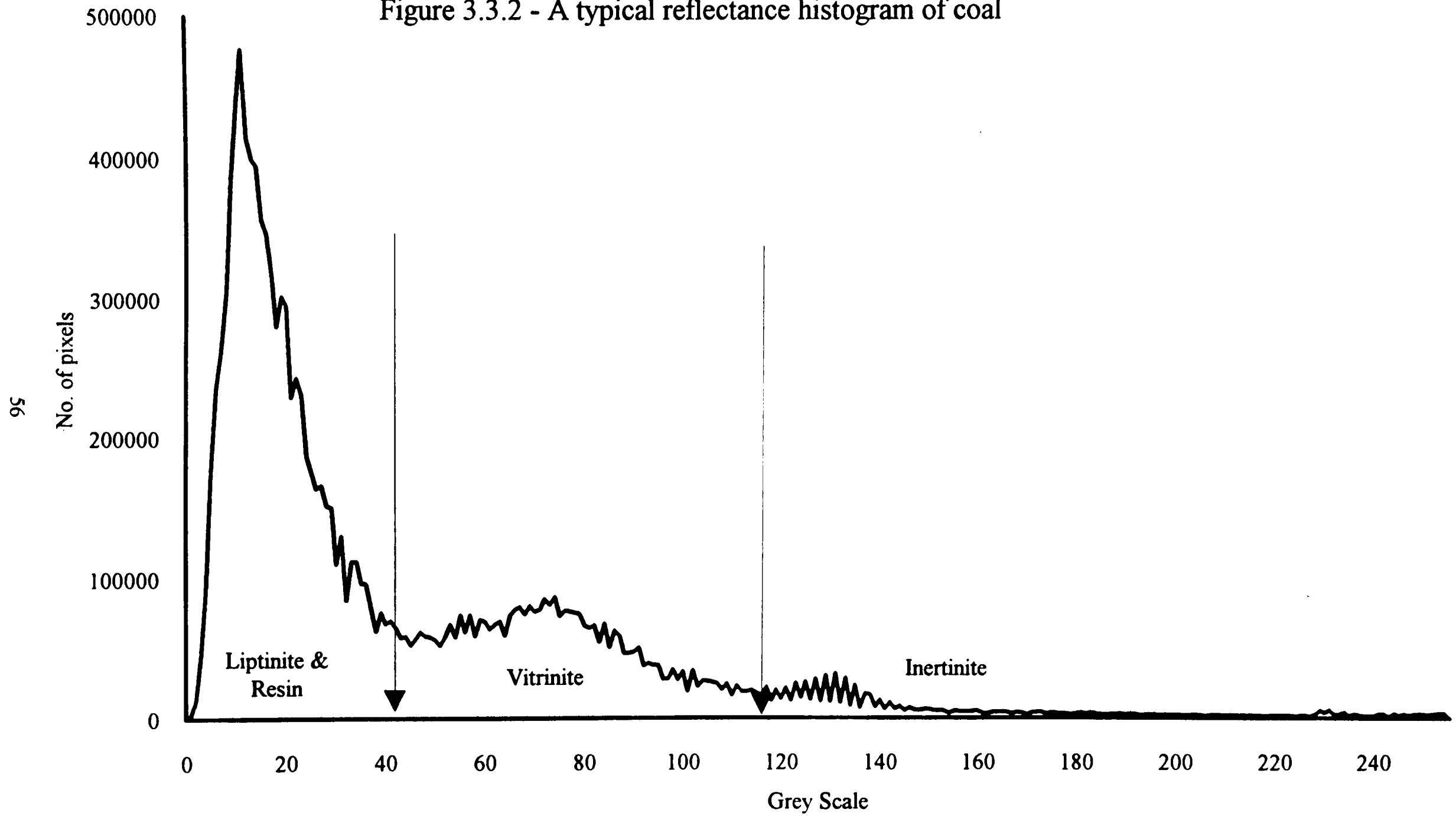


Figure 3.3.1 Layout of the Kontron Image Analyser

Figure 3.3.2 - A typical reflectance histogram of coal



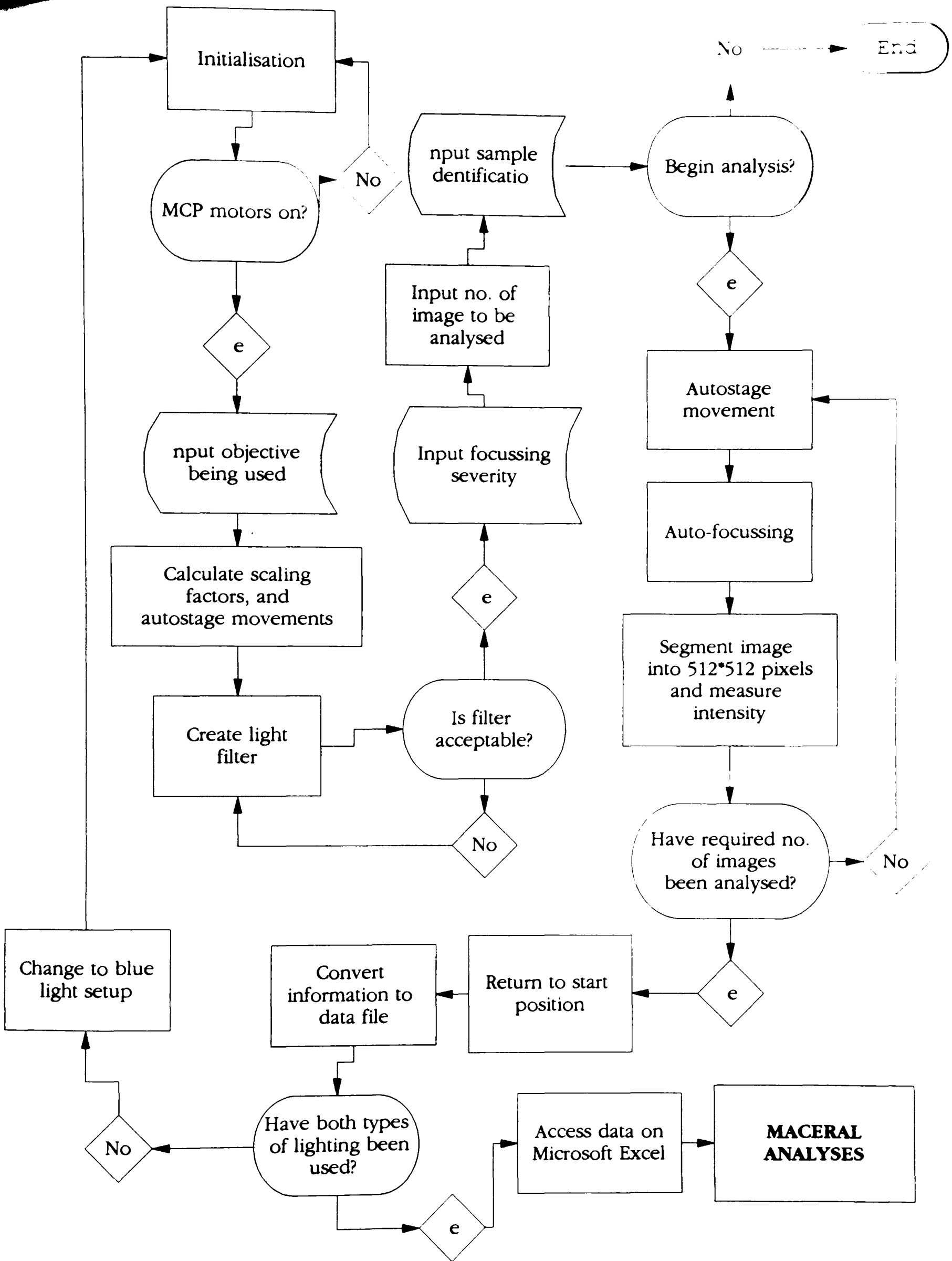


Figure 3.4.2 - a flowchart showing the reflectance/fluorescence method

Figure 3.4.5 - The microlithotype logic tree

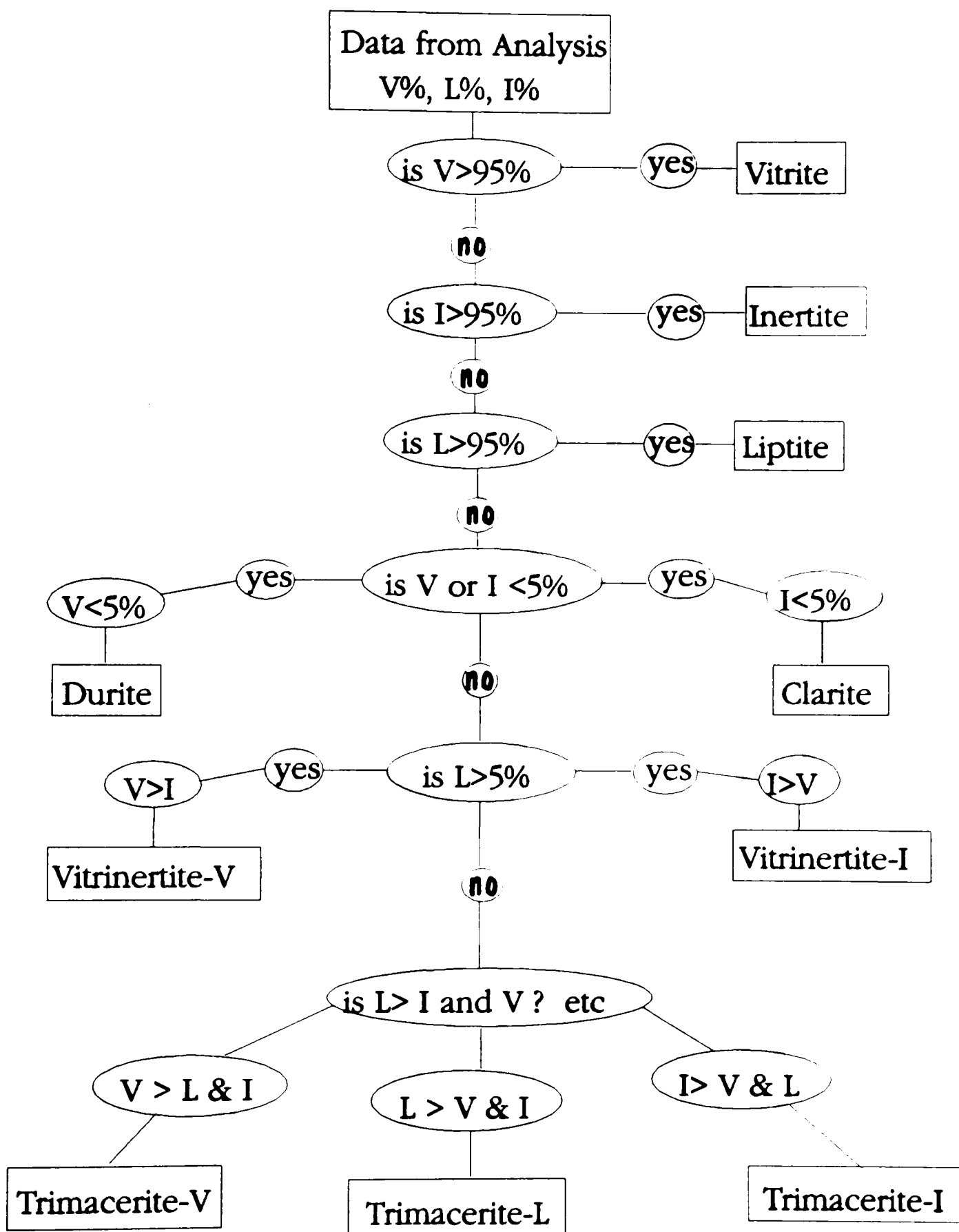


Figure 3.4.6.1 - The correlation between char voids % and char type

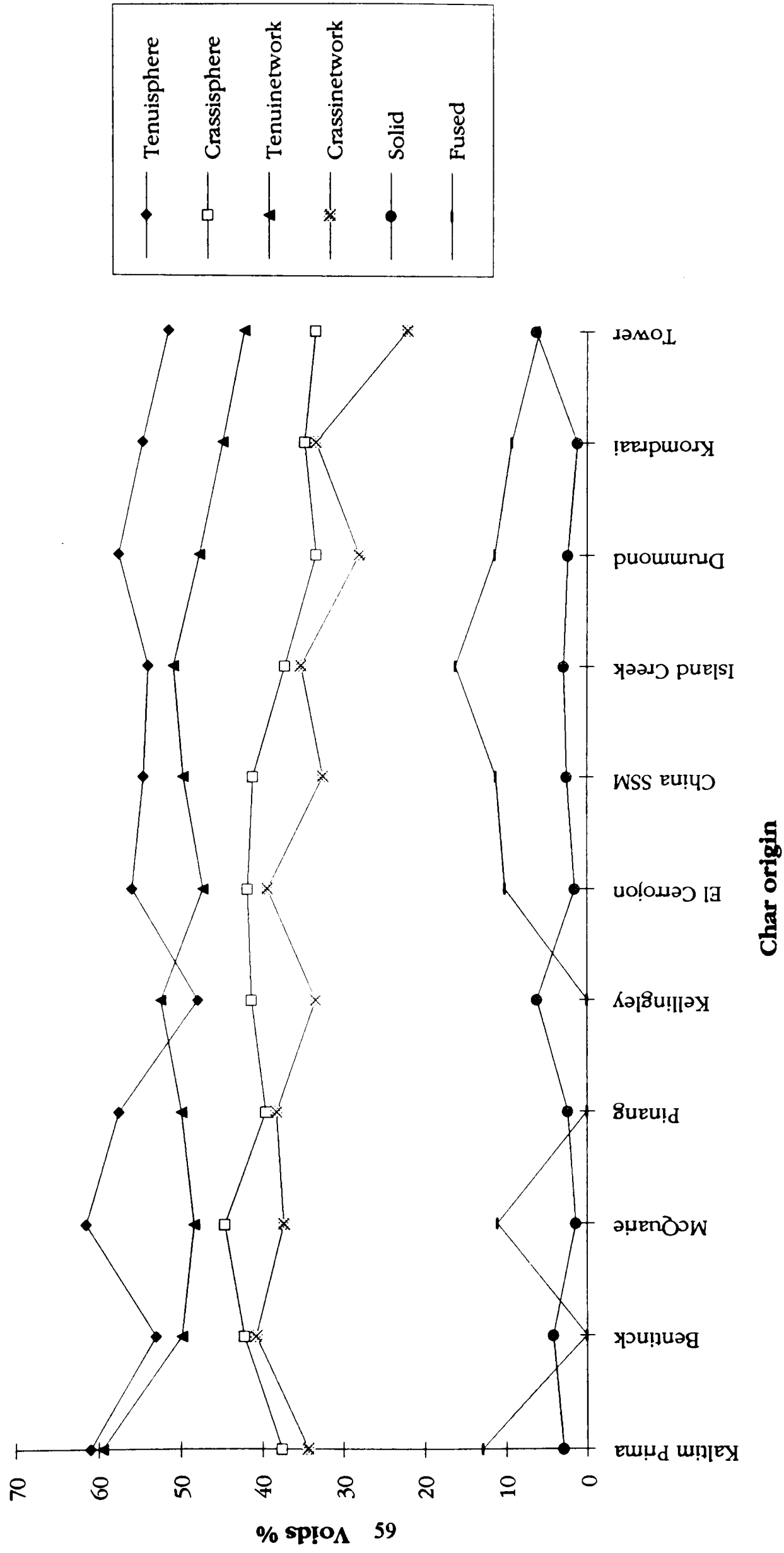


Figure 3.4.6.2 - A graph of the maximum/minimum diameters of different chars

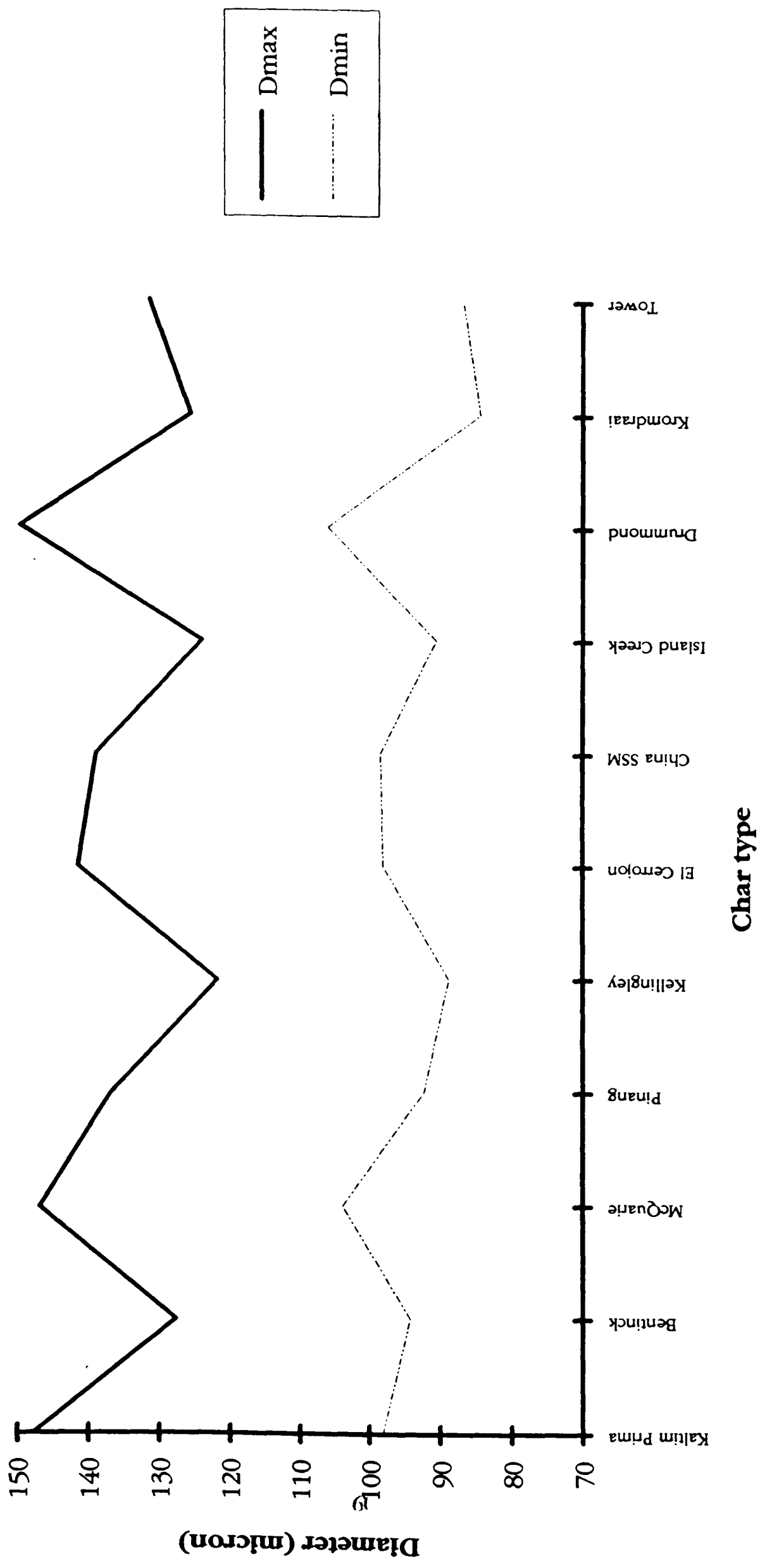


Figure 3.4.6.3 - The 'closing' sequence

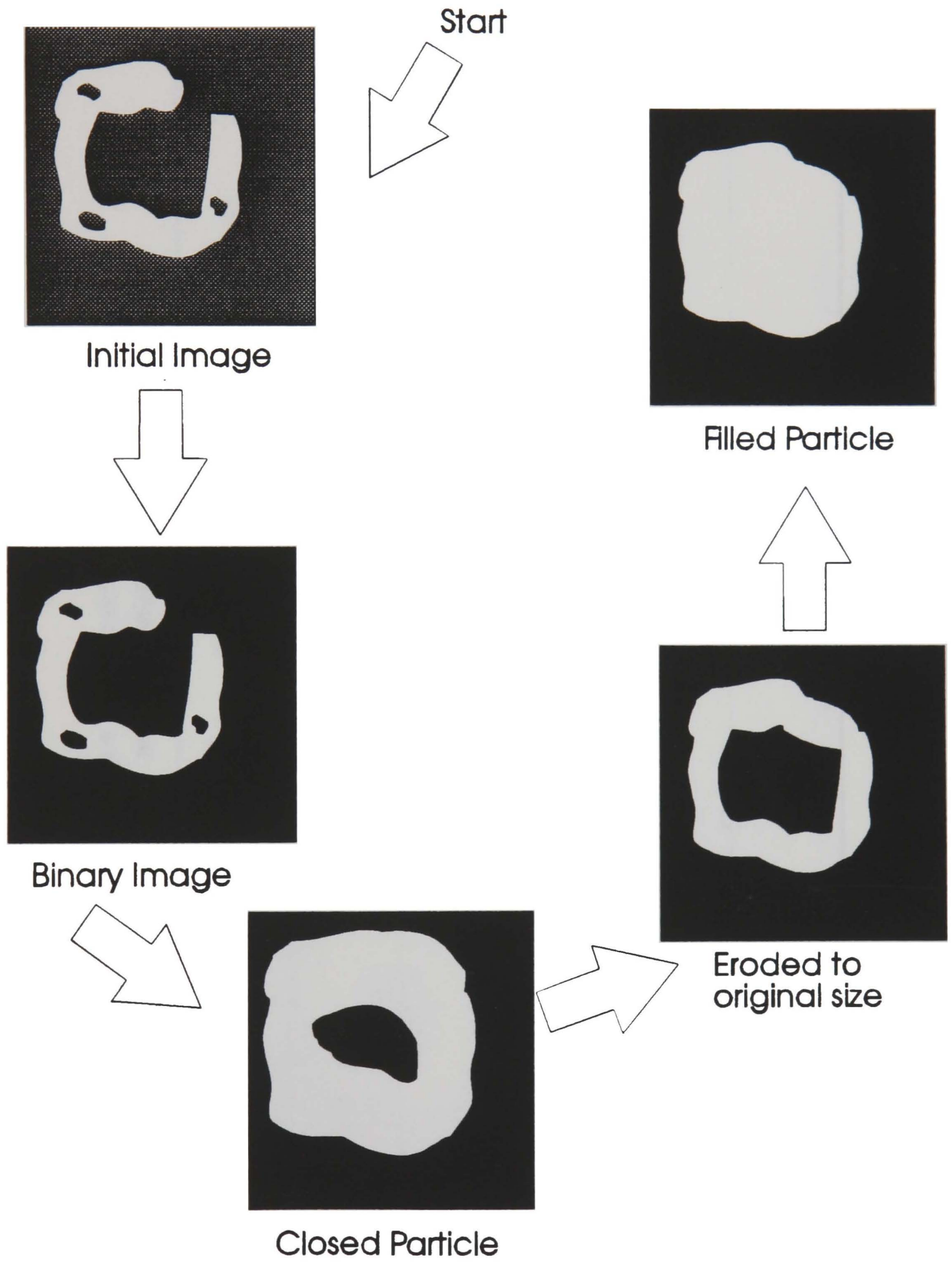
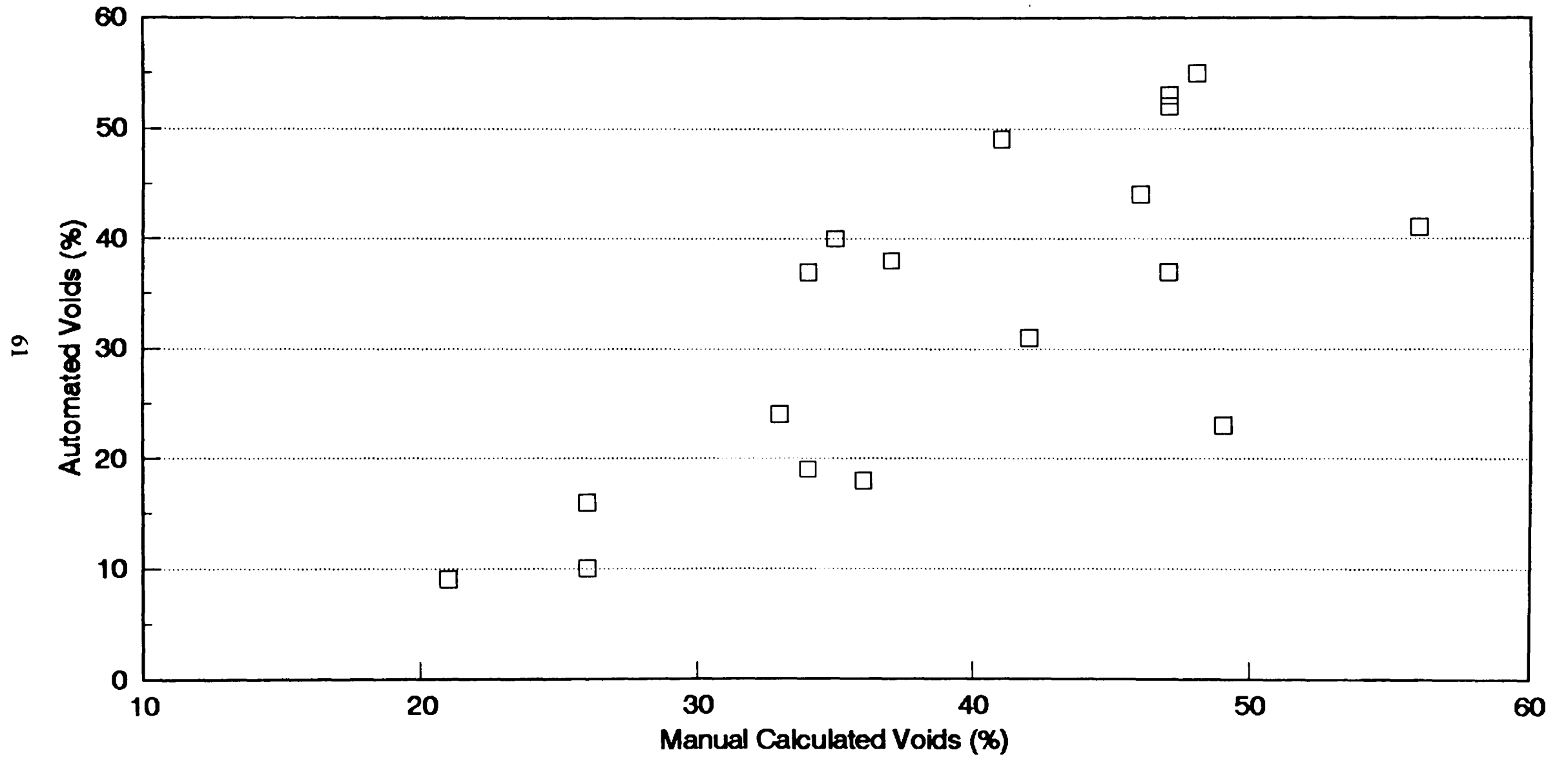


Figure 3.4.6.4 The correlation between Manual and Automated Voids %



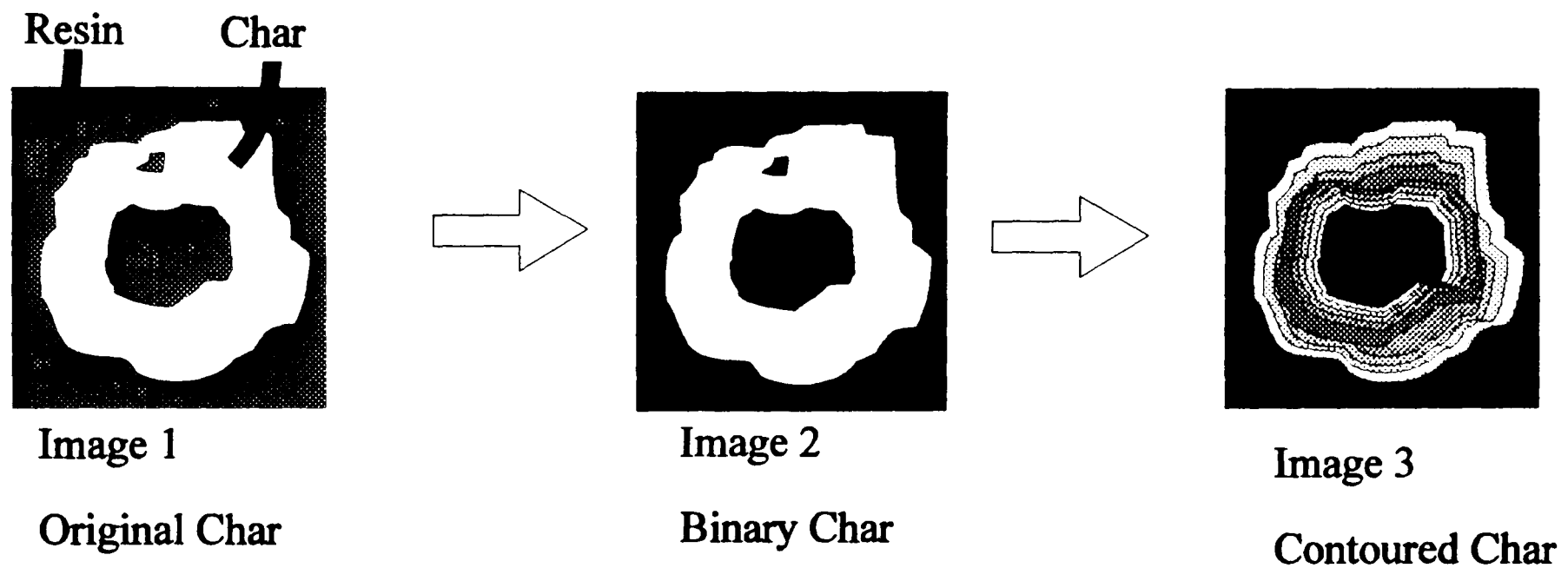


Figure 3.4.6.5 The distance transform mapping process

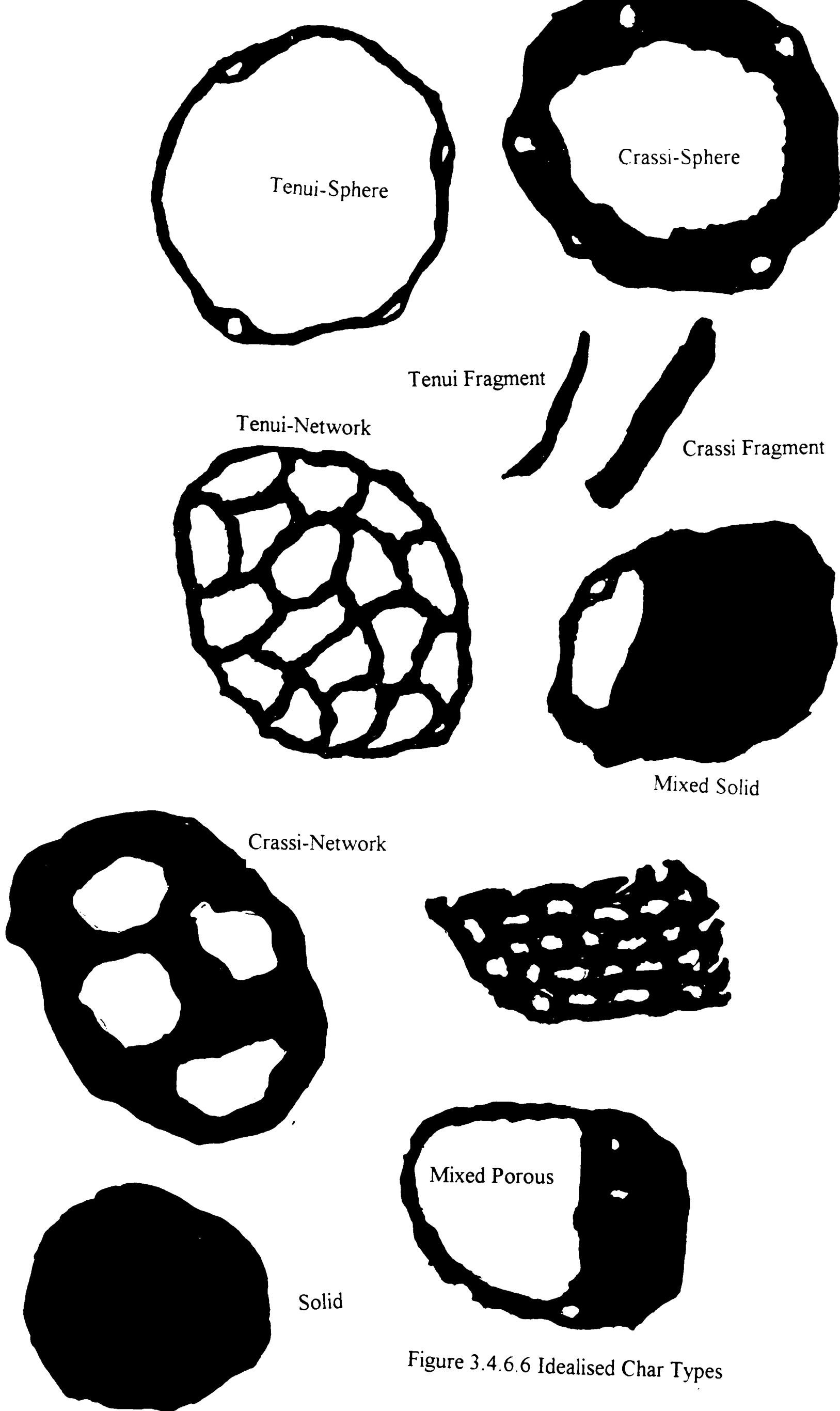


Figure 3.4.6.6 Idealised Char Types

Figure 3.4.6.7 - The distance transform results for the idealised char types

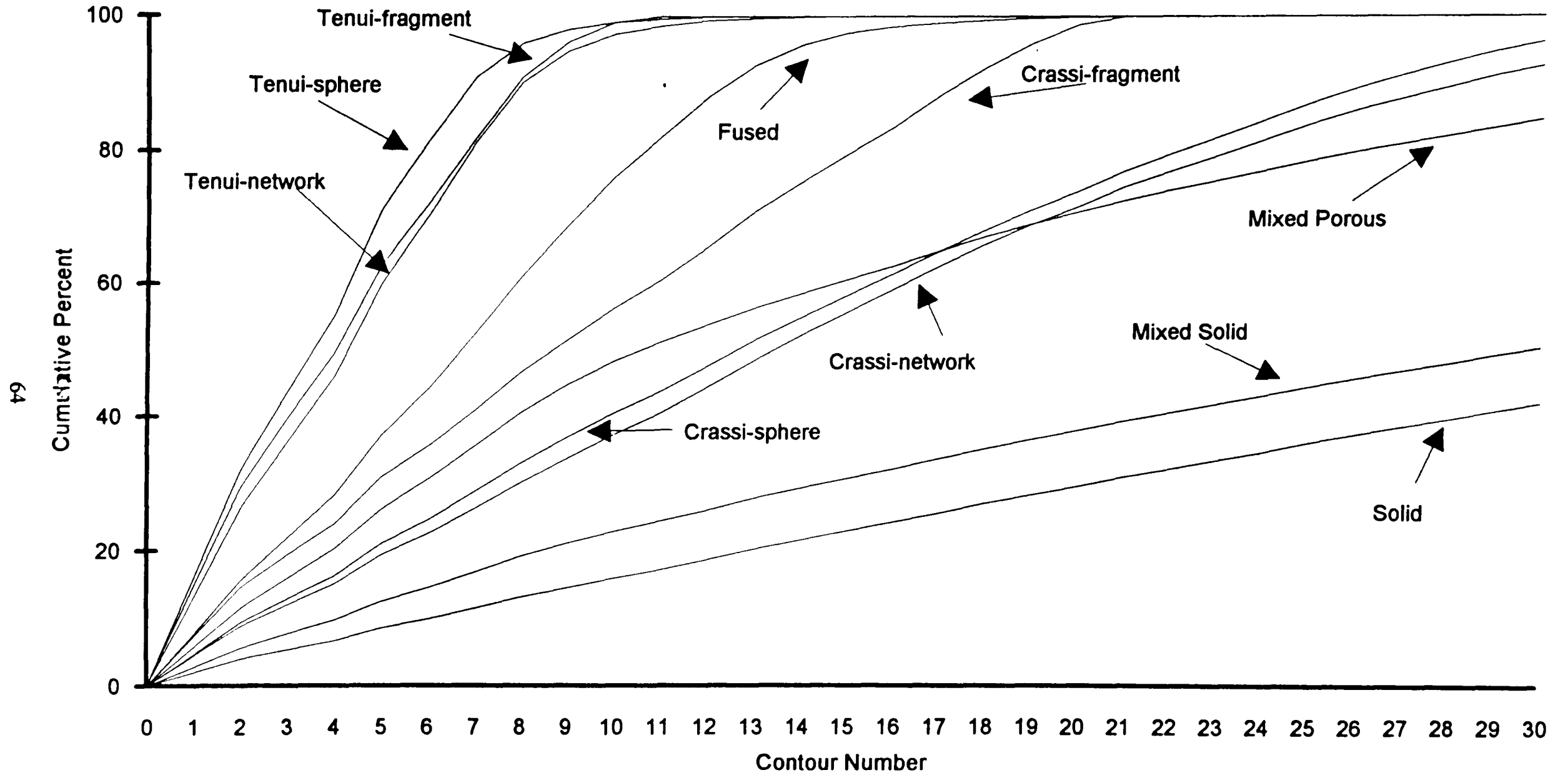


Figure 3.4.6.8 A graph showing the effects of particle size on the distance transform method

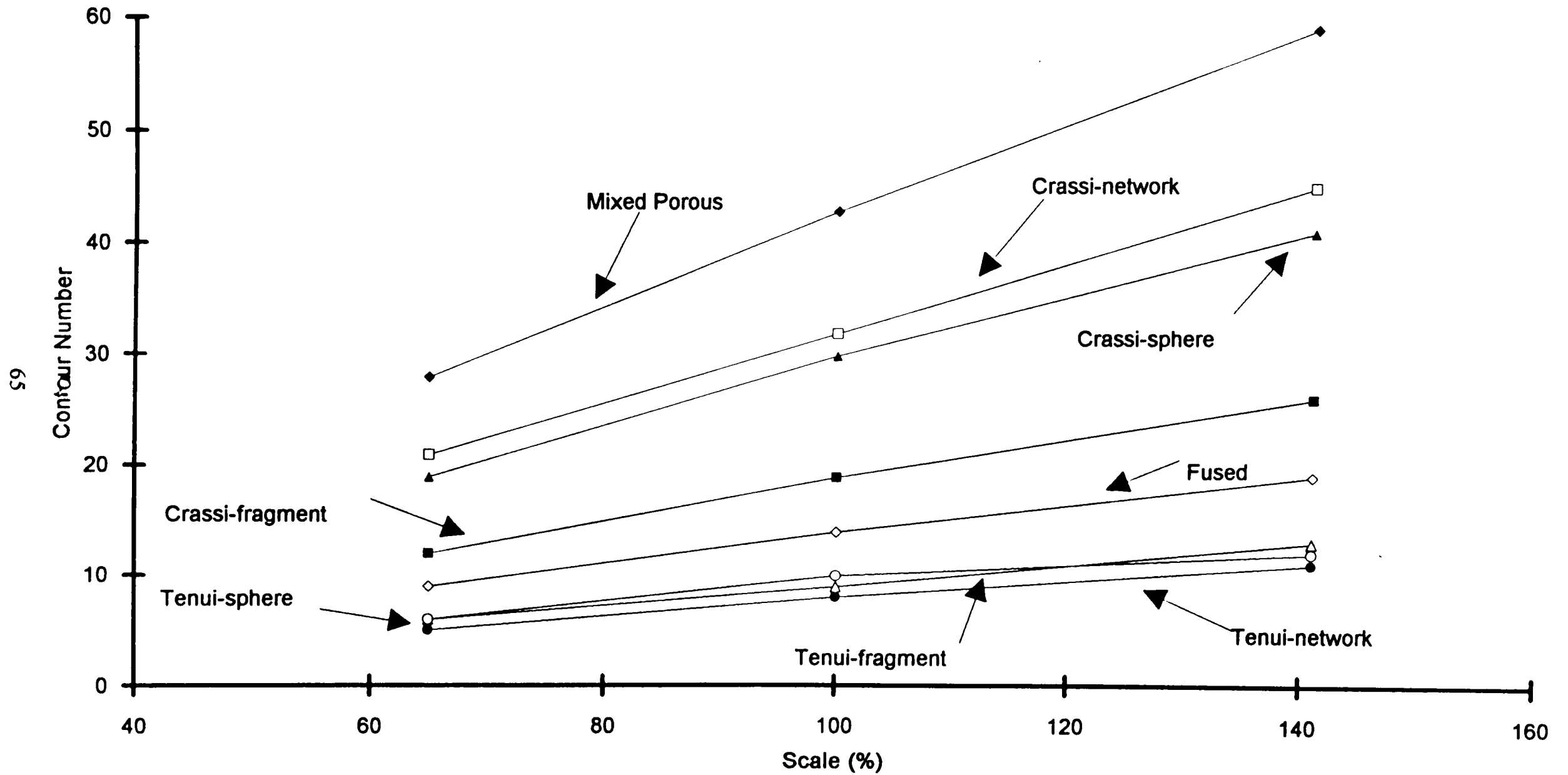


Figure 3.4.6.9 - The distance transform results for several real char particles

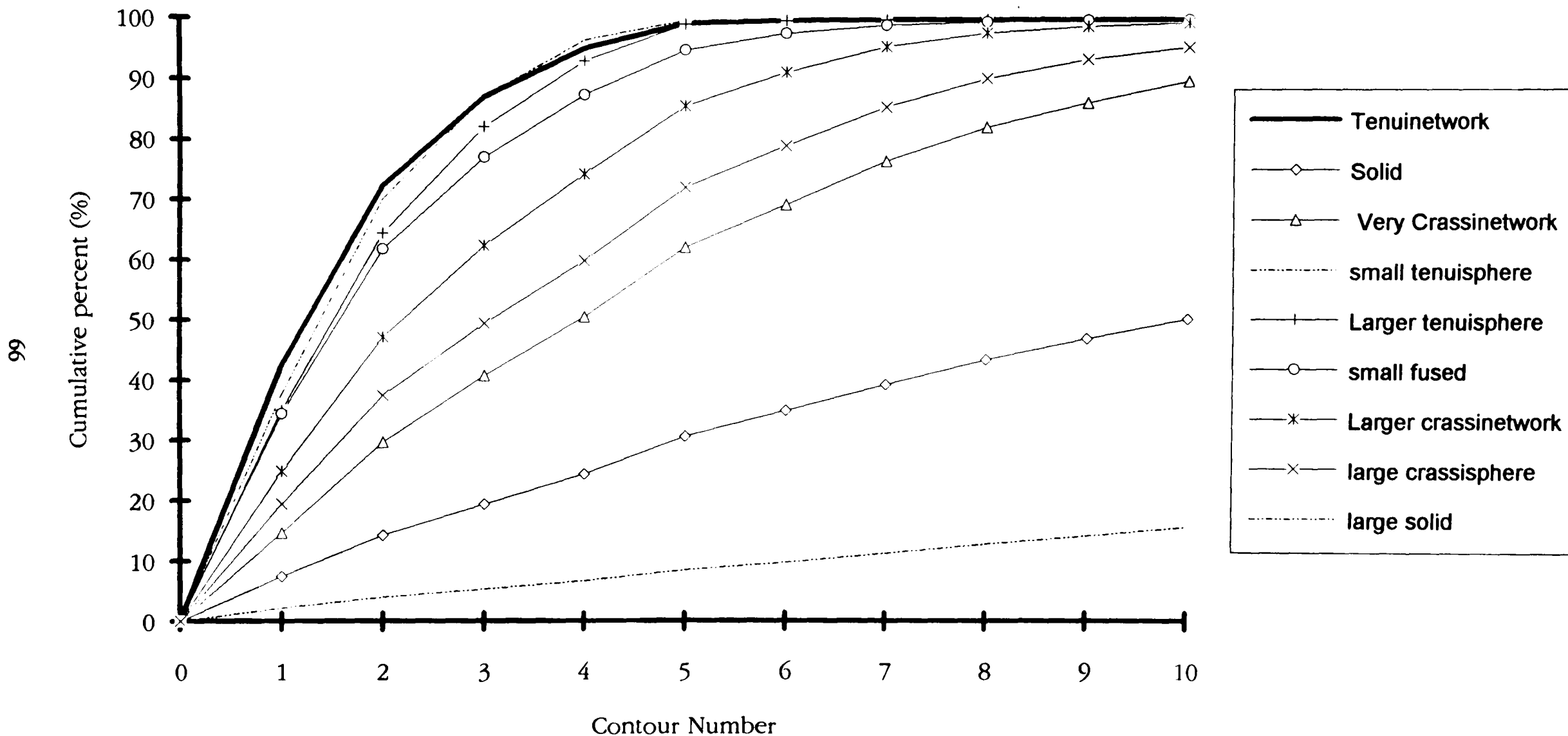


Table 3.2.2 - Aa comparison of analysis techniques from the Kojima paper (1976)

	Manual Analysis	Automated System
Capacity for Samples	4 per day	10 per day
Points Counted	500 per sample	20000 per sample
Accuracy	20-25%	2%
Operator Status	Skilled	Unskilled

**Table 3.4.2** Fluorescence colours and intensities for the different maceral groups at different coal ranks using blue light excitation (Stach et al., 1982).

Coal Rank	Liptinite	Vitrinite	Inertinite
Soft Brown Coal (Lignite)	Strong Green Yellow Orange Brown	Strong - Weak Yellow Brown OR None	None
Hard Brown Coal (Lignite)	Strong - Moderate Green Yellow Yellow Orange Brown	Very Weak Brown OR None	None
Low Rank Bituminous Coal	Strong - Weak Yellow Orange Brown	Very Weak Brown OR None	None
High Rank Coal	None	None	None

# **CHAPTER 4 - DROP TUBE FURNACE EXPERIMENTS**

## **4.1 Initial Drop Tube Experiments**

### **4.1.1 Purpose of Initial Experiments**

The first part of Chapter 4 presents the results from initial tests performed on the Drop Tube Furnace after some of the equipment had been revised or rebuilt (see Chapter 2). The tests were carried out in order to investigate the repeatability and reproducibility of the system by feeding identical coal samples through the Drop Tube Furnace, hereafter known as the DTF, under the same test conditions, one sample after another. Any char samples produced would be tested for variations in proximate analysis. The experiments were also to act as a preliminary investigation into the effect of oxygen content, the temperature setting of the DTF and residence time in the DTF. It was considered important that a suitable operating condition, which reflected full scale combustion conditions, was established to show that the chars produced from the DTF could be related to those actually produced in larger scale burners, as well as allowing samples to be produced on a small scale that are both reproducible and repeatable.

### **4.1.2 Coal Specification**

The coal chosen for these first experiments was a British bituminous coal from Point of Ayr, in North Wales. Its availability and reasonable combustion characteristics were both factors in its choice. The coal was also under investigation by other members of the Coal Technology Research Group for other utilisation purposes.

The coal was sieved into a 53-75 micron size range using an Alpine Jet Sieve. This narrow size range was used for two reasons. Firstly, pulverised fuel tends to block screw or weir feeders, when fines are present. Secondly, relating char types to the original feed material

would be complicated by the presence of a wide size range, since certain chars could be formed from the fragments of larger coal particles. The proximate analysis of the Point of Ayr sample is given in Table 4.1.1. The Fuel Ratio, which is the fixed carbon percentage (dafb) over the volatile content (dafb), was calculated to be 1.72, for this size fraction of Point of Ayr coal.

Point of Ayr was fairly typical of British coals in terms of its maceral analysis, which is shown in Table 4.1.2. Its mean random vitrinite reflectance, or Rank, was found to be 0.72%. The reflectance range can be seen in Figure 4.1.1. Unfortunately, results for the ultimate analysis of the 53-75 micron fraction were unavailable. However, Table 4.1.3 shows the results given in the Coal Research Establishments Coal Handbook (CRE, 1992) for Point of Ayr coal, which can be used to give a rough indication of the nature of the coal's ultimate matrix.

#### 4.1.3 Drop Tube Conditions

As mentioned in Section 4.1.1, one of the intentions of the project was to establish a suitable working condition which was similar to that in a full scale combustion rig. Temperature range between 1000°C and 1500°C, depending on the position in the flame, but temperatures in the Near Burner Zone hotter than 1000°C have been measured (Gibb, 1992). Unfortunately, due to operating constraints, many workers adopted 1000°C as a temperature representative of real combustion conditions (Skorupska, 1987, Tsai, 1985). Since this is not so, and temperature does affect char type (Bailey, 1990), a range of temperatures were used to study these effects. With this initial study, two temperatures were used - 1000°C and 1300°C. It was expected that basic differences between char samples would be observed over this range, hence indicating that temperature was important, worth further investigation.

Oxygen levels were known to be relatively low in the Near Burner Zone (Gibb, 1992), hence 0% and 3% levels were taken to be a reasonable range.

The residence time of coal particles in the Near Burner Zone is short, hence the two shortest obtainable residence times in the Drop Tube were used i.e. 100 and 200 milliseconds. 1 gram samples of the coal were passed through the DTF, in order to provide enough char sample to carry out all the required tests, and some for possible further testing.

#### 4.1.4. Collection Efficiency

A similar collection efficiency for each set of drop tube runs would tend to indicate that the DTF was functioning normally, giving repeatable results. For this reason, the collection efficiency was calculated for every sample. The collection efficiency was calculated from the formula given below which uses changes in ash content to calculate the theoretical weight of char that should collect in the cyclone after passing through the furnace.

$$\text{Collection Efficiency} = \frac{\text{Mass of Char collected} \times \text{Ash \% of Char (db)}}{\text{Mass of Sample Feed} \times \text{Ash \% of Sample Feed (db)}}$$

(Badzioch et al., 1968)

#### 4.1.5 The R factor

The R factor is a way of comparing the volatile loss actually incurred with the volatile loss that should theoretically occur. It has been observed (Badzioch et al., 1968, Gibbins et al., 1991) that certain coals appear to give more volatile matter than is measured in a normal proximate analysis. This is probably caused by the low temperature at which the proximate test is carried out. Proximate analysis reaches a maximum temperature of 900°C, above which no volatiles are assumed to be present. However if a coal is subject to higher temperatures and higher heating rates, then a coal may emit more volatiles than were originally measured using proximate analysis. Higher ranked coals in particular are seen to give high R factors. As with collection efficiency, a stable R factor value for a particular coal type would indicate repeatability within a system, as well as alluding to the volatile

nature of the coal itself. Therefore the R factor was calculated for every char sample produced. The R factor for a char can be calculated as follows.

$$R = \frac{\text{weight loss of coal (\% daf)}}{\text{prox. VM content of coal (\%daf)}}$$

(Badzioch et al., 1968)

## 4.2 Results from the Initial Experiments

### 4.2.1 TGA Analysis of the Point of Ayr Chars

The proximate analysis for the Point of Ayr chars can be found in Appendix B. The collection efficiency and R factors results for all the samples are shown in Table 4.2.1.

Ash repeatability between repeat runs, on a dry basis, were unpredictable i.e. at certain conditions, 4 out of 6 repeat samples gave close agreement, leaving two outliers. An example of this was with the 200 millisecond, 2% runs at 1000°C, where ash levels on average were around 18%, but one char gave 14.82% and another gave 22.02%. A range of 7.20% for ash levels when testing repeatability would appear to be unacceptable. One noticeable feature from Appendix B was the repeatability of the volatile content on a dry, ash free basis. The sum of the fixed carbon percentage plus the ash percentage, at each condition varied less than 1%, between samples, which indicated that variations in ash only produced variations in the carbon content.

There was a small difference in volatile and ash content between all the different conditions. As expected, a larger residence time produced lower levels of volatile matter. Increased oxygen content also lowered the volatile content, probably by allowing any residual tars to be burnt off in the mildly oxidising atmosphere. Residual volatile matter was also lower at the higher temperature setting.

The R factor and collection efficiency results, varied in accordance with changes in ash levels. This is to be expected since both parameters are calculated from the ash content of each individual char. As with the ash results, the R factor and collection efficiencies were close for 3 or 4 out of the 6 results in the set, but the occasional outlier questioned the repeatability of the technique.

#### 4.2.2 Conclusions

The poor ash repeatability observed was probably due to the size of sample used in the TGA. 10-15 milligrams of sample did not give a stable ash reading of chars or coals, although the fact that the volatile content of the repeat samples, on a dry basis, were so close (Figure 4.1.2) indicated that the samples themselves were probably quite similar. Therefore, it was possible that the errors were more likely to be a result of poor sampling.

The arm of the TGA was changed to allow more sample to be analysed. Instead of a dual cup arrangement - which measured DTA as well as TGA - a single arm, single cup attachment was fitted to allow samples of up to 100 milligrams to be analysed. With a sample weight of 50 milligrams, repeatability with the single pan was found to give a much improved repeatability on ash analysis, and this can be seen in Chapter 5.

If the outliers seen in Table 4.2.1 were taken as outliers, then the R factor can be seen to increase with increasing temperature. Although this is logical, and has been shown by other workers (Gibbins et al., 1991), it was a useful indication of the difference between the two conditions used in the experiments, as well as the ability of the DTF in achieving them.

## 4.3 Further Drop Tube Experiments

The second part of the study was a larger scale investigation using three different coals in order to further study the effects of the operating conditions in a Drop Tube Furnace and the behaviour of the different coals at each condition. The morphological nature of the chars produced was also investigated along with the residual volatile and ash content of the chars

### 4.3.1 Aims Of The Experiments

The initial Point of Ayr tests yielded interesting information concerning the operating conditions of the Drop Tube Furnace, including the effect of residence time, temperatures and oxygen content. The aim of this study was to extend these parameters further to investigate:-

- Additional temperature settings of 1150°C and 1400°C
- Particle size effects
- A slightly larger difference in the oxygen content in the Work Tube
- The effects of these DTF conditions on three different coals instead of one

### 4.3.2 The Coals Used In The Experiments

Three coals were selected for these trials on the basis of their distinctly different geological character.

***Kellingley*** - A British coal with standard characteristics of a British bituminous coal.

***Kromdraai*** - A South African coal with high levels of inertinite.

***Tower*** - a Welsh anthracite, made up of mainly high reflectance vitrinite

The proximate analysis for the coals can be found in Table 4.3.1

### 4.3.3 The Size Ranges

The coals were all sieved into three tight size ranges using the Alpine Jet Sieve. The sieving procedure can be found in Chapter 2. The size ranges used are as follows

*53-75 microns*

*106-125 microns*

*180-212 microns*

The 53-75 micron fraction was the smallest fraction possible with the available sieves for the Alpine Jet Sieve. The 180-212 fraction was the largest possible fraction collectable from a pulverised fuel sample, since all particles are theoretically below 212. The 106-125 fraction was chosen simply as a midway point between the smallest and the largest fractions.

## 4.4 Results of Further Tests

### 4.4.1 Proximate Analysis

The proximate data for the chars discussed in section 4.4 can be found in Appendix C

#### 4.4.1.1 Particle Size

Figures 4.4.1 to 4.4.3 show the effect of particle size on the residual volatile content after 100 milliseconds at each DTF condition. Most apparent is the large change in volatile content between the lower particles sizes to the largest 180-212 micron. This effect can be related to the increased volume of the largest sized particles i.e. theoretically the 180-212 sized particles have approximately 5 times more volume than the 106-125 size - which will in a DTF require more time to devolatilise, even with high heating rates and high temperatures. There is a delay before devolatilisation begins because of the increased volume of the larger particles. This is why there is a great difference between the size fractions at 1000°C and 0% oxygen condition than at 1300°C and 3% oxygen level. The reverse is seen in Tower fractions where a minimal amount of difference exists between the size fractions when temperatures are below 1150°C. This could be related to the minimal change that had occurred to the proximate nature of the coal. Little volatile matter was lost and even less carbon was lost, particularly in the 0% oxygen conditions. Therefore none of the different particle sizes show any great difference in volatile content until the DTF was heated to 1300°C and above. At these temperatures the smaller particles devolatilized more extensively - although one must remember that the coal sample did not have a great deal of volatile matter to begin with. This minimal change in the proximate content of the sample is one reason why odd values for the R factor can be seen in Table 4.4.1 .

#### 4.4.1.2 Temperature Effects

Figures 4.4.4 to 4.4.6 show the effect of the operating temperature of the DTF on the residual volatile content in the char. It is clear that a temperature below 1300°C only

partially devolatilised the largest size cut. However, only around 5% volatiles in the Kellingley and Kromdraai samples remained at temperatures of 1300°C or 1400°C. The absolute extinction of all volatiles was not seen as important since it is possible that residual volatiles are probably present during the combustion stage anyway (Jalmalludin, 1992). What was important, however, was the production of char particles with the minimum quantity of semi-pyrolysed coal particles which would make subsequent analyses difficult. This phenomenon was only seen in the 1000°C and 1150°C samples where liptinite megaspores were observed in the 180-212 micron fraction during char analysis, indicating that the degree of heating had not been sufficient to devolatilise large liptinite particles, which is thought to begin devolatilisation at around 300°C (Lee and Whaley, 1983). This further emphasises the effect of 180-212 micron fraction being much larger, in terms of volume, compared to the two size fractions. Therefore, with this size fraction, either a longer residence time in the DTF is required, or a temperature higher than 1150°C. No liptinite was observed in the 180-212 fraction from the 1300°C and 1400°C runs.

#### 4.4.1.3 Oxygen Content

Oxygen content appeared to make a minimal amount of difference between the residual volatile content of most of the char samples from one particular temperature condition. However, on a practical note, it was apparent from handling the sample after each run, that the presence of some oxygen allowed a cleaner, more 'fluid' sample to be produced. Some of the 180-212 micron samples of Kellingley below 1150°C with 0% oxygen were sticky with a degree of agglomeration, as a result of residual volatiles which had recondensed on the surface of the external walls, causing the particles to stick together.

#### 4.4.1.4 R Factor

The results for the R factor calculations of the 3 coal types are shown in Table 4.4.1. The first noticeable feature in the table is that most of the R factor results for the Tower coal are negative. This was because the ash percentage in the collected char sample was less than that of the initial coal feed sample, until 1400°C. Part of the explanation can be found in the percentage ash content of the initial Tower coal fractions. Ash tracers are known to

be highly inaccurate when the ash levels are below or around 5%, as in the case of Tower, because of the nature of the R factor calculation. A possible reason for the R factor, for Tower, reaching a positive number with the DTF at 1400°C could be due to the fact that until this temperature, the proximate constitution of the sample was not changing sufficiently to permit a significant change to the char samples ash content. The difference between the ash percentage of the Tower chars and the initial Tower samples was only small i.e. ±1-2%, hence the ash results generally fell within the area of experimental error for the TGA apparatus. When only a minimal change occurred in the char sample, it is understandable that a large R factor value was not produced.

Another reason why the collected char samples contained less ash than the original coal sample could be due to the fact that the collector probe inside the DTF did not collect 100% of the char produced. Lighter particles especially, may have been lost in the gas flow even though the flow was theoretically laminar. The gas flow is, in practice, unlikely to be have a perfect uniform downward flow.

A further explanation as to how the ash percentage could be lower than the coal sample may be related to the selective loss of particles inside the collector probe. As the particles in the gas flow experienced rapid thermal quenching, some of the unburned volatiles probably recondensed on the walls of the collector probe. Hence as the number of runs increased, so did the amount of tarry residue. Ash particles may have adhered more readily to this tarry surface. In order to reduce the chance of this occurring, the collector probe was cleaned after each day of operation.

Kromdraai gave the most accessible results for the R factor tests. Figure 4.4.7 compares the R factor results for the different temperatures in the DTF. It is apparent that the R factor value increases with increasing temperature. This would be expected, since the hotter a coal sample gets the greater the chance of residual volatiles being emitted. Figure 4.4.8 shows the effect of particle size on the R factor value. The difference between 106-125 and 53-75 is minimal, and in some cases, the 106-125 fraction has a higher value, indicating that 106-125 particles are more reluctant to emit volatiles at lower temperatures, or perhaps contain more volatiles undetected by proximate tests. The 180-

212 fraction in all cases had a lower R factor value, which indicates that the particles require longer in the DTF with higher temperatures before they will emit more volatiles than were detected in the proximate test. The 1400°C 3% line stands out at the top of the graph, as one would expect, as does the 1000°C 3% and 0% lines at the bottom.

The reason for the Kromdraai R factors being all positive may be related to the nature of the ash in the initial coal sample. As mentioned earlier, liberated ash particles could be lost inside the work tube, or on the inner face of the collector probe. Kromdraai ash may well be of a more inherent nature than Kellingley (D. White, 1994) - hence allowing a majority of ash to pass through the DTF process and remain in the char sample collected inside the cyclone. However, this is only speculative.

Despite the fact that Kellingley and Kromdraai are very different in their maceral constituents - no real difference is apparent from the proximate tests of the chars. The R factor values for the 106-125 and 180-212 micron samples are perhaps a little higher for Kromdraai, which may be a result of the inertinite particles devolatilising more readily at temperatures above 1000°C than during proximate tests, but it is not possible to say with any great certainty.

#### 4.4.2 Manual Char Type

The chars produced by each coal at all the DTF conditions were analysed for general morphological type according to the procedure described in Chapter 2, and are shown in Appendix D.

Since it is difficult to put all these results in graphical form and impractical to discuss from an appendix- 3 basic indices have been established.

- Tenui-Chars % which consists of thin walled chars, namely tenuinetworks and tenuispheres, both having wall thickness' of less than 5 microns. The results are given in Table 4.4.2 .

- Spheres %, which consists of all spheroidal chars whether thick or thin walled. The results are given in Table 4.4.3 .
- Solids %, is made up from all fusinoid or solids chars, which may be a cause of poor burnout in full scale burners. The results are given in Table 4.4.4 .

#### 4.4.2.1 Tenui-Chars %

##### *Temperature Effects*

With Kromdraai and Tower, the operating temperature affected the percentage of thin walled chars. The higher the temperature, the greater the quantity of thin walled char. Tower 180-212 micron feed produced 10% thin walled chars at 1000°C and 3% oxygen but with 1400°C and 3% oxygen produced about 40%.

Temperature effects were visible with Kellingley, but were not quite the same as with the two other coals because less tenuispheres were produced at higher temperatures in the presence of oxygen. This is in partial agreement with the findings of Bailey (1990), who also observed a reduction in Tenui-Chars between 1000°C and 1500°C. The reason for this is not clear although it is possible that the thin walled species may not have made it through the block preparation stage - despite attempts to moderate the mounting process.

##### *Oxygen Content Effects*

Nothing definite can be concluded from the char results as far as the effects of oxygen content is concerned, but as mentioned earlier, the presence of oxygen produced a cleaner sample, more suitable for block preparation.

##### *Size Effects*

The most visible effect from the char results was the effect of particle size on the quantity of thin walled chars. In most cases, the larger particles vesiculated more slowly and

produced thicker chars. This difference was less with the higher temperatures, but was still apparent to some degree.

e.g. Kellingley 180-212 gave 38% tenui-chars, and 53-75 gives 59% , when both are at 1300°C and 3% oxygen. At 1000°C and 3% oxygen 180-212 gives 25.2% and 53-75 gives 69.2%.

Kellingley was able to form large numbers of tenui-chars at most temperatures in both the 53-75 and 106-125 ranges, but the 180-212 fraction struggled to break the 5 micron crassi/tenui border.

#### 4.4.2.2 Spheres %

##### *Temperature Effects*

A reasonable trend for Kellingley can be seen from Table 4.4.3, which tended to form spheres in large quantities, whereas the other two coal types on the whole formed network like chars with several voids within the main walls.

The Tower sample displaying unusual characteristics by losing significant levels of spheres at 1300°C. Unfortunately the 1400°C 0% oxygen run was not performed because of mechanical difficulties - but would have perhaps clarified whether the sudden drop in Spheres % was more than just an anomaly. All the Tower size fractions tended to produce more network chars at the higher temperature levels.

Kromdraai did not show any interesting temperature effects, perhaps because the vitrinite in the sample, which is most likely to most form spheres, was of a low rank. This low rank vitrinite was able to vesiculate at 1000°C as well as 1400°C, since its aromaticity is low (Stach et al., 1982).

The problem with manual analysis, in general, is the difficulty experienced in distinguishing a true network from a true sphere, as well as determining the general thickness of char

walls above and below the 5 micron criteria. For this reason care must be taken when interpreting data of this kind, since char analysis can be potentially more subjective than maceral analysis (Lester et al., 1994b).

### *Oxygen Content Effects*

Table 4.4.3 shows a small trend in the numbers of spheres produced with temperature and oxygen variations, but nothing particularly significant can be seen.

### *Size Effects*

The Kromdraai results show that at the lowest temperature of 1000°C the 53-75 micron fraction was more able to form spheres - this changes gradually to the top temperature of 1400°C where all the three size cuts have a similar amounts of spheres.

The results for Kellingley were similar to Kromdraai in that the lower temperatures exaggerated the difference between the size fractions. At 1000°C the difference between the 53-75 and the 180-212 size fractions was 20% with 3% oxygen and 35% with 0%. This, difference decreased quickly as temperature increased to 1400°C- all three size fractions contained roughly the same amount of spheres.

The Tower chars showed the most significant difference between the size ranges e.g. the 180-212 micron fraction contained very few spheres at all the different temperatures and oxygen contents, whereas the 53-75 micron fraction, at 1150°C, contained 50%. The 1000°C, 0% values may be a result of particle mis-identification of open networks as spheres, since the difference between the two was often very subjective. The 53-75 fraction remained clearly the most able in forming spheres, unlike the other two coals, and contained up to 5 times the amount of spheres as the next size fraction at certain conditions.

#### 4.4.2.3 Solids %

##### *Temperature Effects*

A fairly definite trend of Solids % to temperature can be seen in Table 4.4.4, showing an increase in the solids produced with decreasing temperatures. It is worth noting that Solids % for Tower chars include all the coal particles which had not yet undergone any transformation. Since the reflectance of the initial anthracite coal was similar to the char produced, it was considered too subjective to try and distinguish between those particles that were really Solids, and coal particles that would eventually undergo some change, given further time.

##### *Oxygen Content Effects*

Kellingley was observed to contain more solids at any temperature without oxygen present but this could be put down to experimental error, in analysing the char.

##### *Size Effects*

As one might expect, the amount of Solids tended to increase with an increase in particle size. However, as mentioned earlier, it was not always possible to know whether the particle was truly a solid char, or a coal particle that was just slow in beginning to vesiculate. With Kromdraai, the largest size fraction contained the highest number of solids, although the difference with the other sizes was noticeably small.

Kellingley appeared to exhibit little variation in the size fractions over different temperatures, but the 180-212 fraction generally contained more solids, which is probably related to the delay in vesiculation due to the increase in bulk volume.

The greatest difference between the Tower size fractions is between 106-125 and the 180-212 sample at 1150°C. This is perhaps because there is a threshold at this temperature where the smaller sizes are able to plasticize readily, after experiencing a sufficient degree

of heating, whereas the 180-212 fraction was not heated to a temperature whereby physical morphological changes could take place. One can see that at the higher temperatures all the size fractions contained fewer solids, especially the 180-212 fraction from 81% to 20% solids, hence the difference between the size cuts decreases with increasing temperature.

#### 4.4.3 Automated Char Analysis

The method of distance transform char analysis is detailed in Chapter 3 of the thesis. The results for the Automated Char Analysis (ACA) has been presented in 3 ways.

{3} - simply the percentage of the material that was found to exist in the first 3 contours or erosions.

{5} - the same as {3} but 2 contours further down the process.

{95%} - the counts required to disintegrate 95% of the visible material.

The results for these parameters are found in Table 4.4.5 for the 3% oxygen runs and Table 4.4.6 for the 0% oxygen runs. The results are discussed below.

##### 4.4.3.1 Temperature Effects

Kromdraai shows a consistent if not small rise of 10% in the {3} and {5} counts indicating only a small decrease in the overall bulk presence of the char sample with temperature. The 180-212 micron fraction was slightly more obvious with a difference of 20% between 1000°C and 1400°C. This in some way agrees with the manual char results for Spheres % which gave a consistent value despite increasing temperature, and this was related to the low rank vitrinite being able to vesiculate i.e. all the different temperatures used in the study. The {95%} value was also noticeably unchanged by the temperature effects.

Kellingley shows a gradual increase in the {3} counts as temperature increases but only of the order of 10%. The {5} count results show less of an effect and are, in most cases, very high. The {95%} values are lower for the 1300°C and 1400°C runs, than for the 1000°C and 1150°C samples.

Tower shows more evidence of the effect of temperature on the bulk appearance of the char material. All three size ranges show an increase in the {3} and {5} counts, as well as the {95%} value which dropped from 78 to 19 counts. It is clear that an increase in temperature caused even the largest of the anthracite particles to plasticize, to some extent, and so form open networks and spheres. The 180-212 fraction at 1000°C 3% had values of 18% and 26% for the 3 and 5 counts, whereas with the 1400°C runs, values of 50% and 67% were obtained, showing a considerable rise as a result of an increase in temperature.

#### 4.4.3.2 Particle Size Effects

In virtually all cases, the bulk presence of the largest size fraction is greater than that of the other two i.e. the values for {3} and {5} are lower for the 180-212 micron fraction. The relationship between the 53-75 and 106-125 fractions is not quite as straightforward with the 106-125 fraction having higher values for {3} and {5} in certain samples e.g. Tower 1300°C 3%.

Kromdraai - the 1300°C 3% and 1400°C 3% as might be expected, have the highest values. Also noticeable with both temperatures are that all three sizes are virtually the same - showing that high temperatures can cause the same amount of vesiculation to occur in all three size fractions. The 1000°C, 0% and 3% results for the 180-212 fraction show the lowest values and also the greatest difference between the size fractions - one would expect this since, as discussed earlier, the largest size has a much larger total volume and hence is slower in heating up. 1300°C appears to be a sufficient temperature to devolatilise and plasticize the largest sized particles. The lines in-between show an almost linear change with the value for {3} and {5} and the three particle sizes.

Kellingley - two features are most apparent from the graph. Firstly, the similarity of all the different conditions i.e. almost all of the lines are within  $\pm 5\%$  of each other. The 1300, 0% and 3% lines are the clear leaders. The difference between the Kellingley size fractions is most apparent with the {5} values. Both the 106-125 and 53-75 fractions have similar values but the 180-212 fraction is noticeably lower in all cases (even the 1400°C 3%). This, as before, can be related to the lag in vesiculation and plasticization that results from the increased volume of the largest size fraction.

Tower - the 1400°C, 3% results are clear at the top and the 1000°C 0% and 3% at the bottom are the most apparent features of the table. There is, however, generally only 20% difference between the 180-212 fraction and the 53-75 fraction, and the difference is virtually linear with the 1400°C 3% data set. As with Kellingley, the difference between the 180-212 fraction and the other fractions is most apparent with the {5} results. With 1000°C and 1150°C there is a great drop between the percentage values for the {5} counts. With all conditions, one can see little variation in the percentage values for the two smallest sizes, although the 53-75 micron range is a slightly higher in most cases.

#### 4.4.3.3 Oxygen Content Effects

The greatest difference between the oxygen content and the values for {3} and {5} in all coals appears with the 53-75 fraction. Although there may be a reason for this, it probably is not important since the differences are generally low. As mentioned earlier, the main purpose of the presence of oxygen was accepted to be the production of clean, discrete particles with a high level of integrity.

## 4.5 Conclusions For Chapter Four

### 4.5.1 Temperature Effects

An increase in temperature generally increased the R factor value, and also the percentage of thin walled or spherical chars formed by all three size fractions. This was related to the ability of a particle to plasticize and devolatilise, which in turn is related to particle temperatures (during combustion), heating rates and volatile content.

Temperature appeared to be the greatest influence on the char morphology with all three coals. Higher temperatures in the DTF tended to produce larger amounts of void space, if not thinner walled char species as well. Maceral effects did begin to show, when the DTF conditions were set above 1300°C. Tower, which contained more than 90% vitrinite, formed more vesiculated chars than the Kromdraai sample as seen in Table 4.4.5. Rank effects appeared to give way to maceral effects allowing an anthracite to produce more open char (with anisotropy) than the lower ranked South African coal, with its large percentage of high reflectance inertinite.

Temperature appeared to affect the {3} and {5} results obtained from the Automated Char Analysis tests, although the reactive fractions of the coal (namely low reflectance material), particularly in the smaller size fractions, formed open chars whether at 1000°C or 1400°C.

Temperature appeared to have more of an affect on the char types formed than the actual char 'bulk' appearance i.e. the coal fraction most likely to vesiculate formed open chars, whether networks or spheres, and even though the proportion of each changed over the range of temperatures - the ACA results did not change proportionally. Tower, however, genuinely formed more open char types with increasing temperature, although this may have been in the form of networks or spheres. What was measured, however, was an increase in the {3} and {5} values and a decrease in the {95%} values - all indicating an increase in plasticity and deformation with increasing temperature.

#### 4.5.2 Particle Size Effects

Particle size affected the release of volatiles, the R factor value and the morphology of char produced. The difference between the 106-125 range and the 53-75 range was minimal relative to the difference between the 106-125 and 180-212 range. Particle size did have a significant effect on these parameters, but in most cases this difference decreased with increasing temperature.

Particle size relationships seem to show that the 106-125 size was as able, if not better in most cases, to devolatilise and vesiculate as the 53-75 micron sizes, at all temperatures. Despite the 106-125 fraction being theoretically 6 times larger than the 53-75 fraction, temperature settings did not effect the type of char produced i.e. both were able to give similar results for all the char types. There was however, a far more noticeable change in the char types formed by the 106-125 and the 180-212 fractions.

With Automated Char Analysis, {3} and {5} results indicated that particles in the 180-212 fraction were more reluctant to form open chars. The higher temperatures for Kromdraai, Kellingley and Tower reduced this difference, probably because the degree of heating had been sufficient to cause extensive devolatilisation in all sizes. Tower, however, as the least 'susceptible' coal type, was still giving thicker chars in the 180-212 micron range with 1400°C and 3% oxygen, although the difference somewhat less than with the 1000°C runs. At these lower temperatures, minimal amounts of morphological change had occurred.

#### 4.5.3 A Comparison of Manual Char Analysis and Automated Char Analysis (ACA)

This has already been discussed to some extent in section 4.4.2 of this chapter, but it is worth re-iterating that manual analysis is useful qualitatively in terms of char morphology, and quantitatively as far as the number of each char type is concerned. *BUT* as far as an overall quantitative view is concerned, manual results are limited. Since particle size was not introduced to the manual char analysis (on purpose), one cannot make an overall estimate as to the 'amount' of material in a given char group, relative to other types of

char. This is compounded by the use of only one wall thickness criterion, namely  $\pm 5$  micron. The presence of more wall thickness criteria would have perhaps clarified manual results more, but as in the case of particle size, its introduction would have made the whole process even more subjective. There may, theoretically, come a point whereby any test undertaken becomes too subjective for the results to be of any value.

One should note that this ACA program is based on the total number of pixels present in the total number of images analysed. Therefore one solid particle of 200 microns across could be more than 100 times as significant to carbon in ash levels as a thin walled cenosphere. For this reason alone, it is possible to appreciate the difficulty in correlating the results from 500 manual counts with the absolute measurement of at least 50 images, each containing more than 10 particles, making measurements based on only size, thickness and percentage presence (bulk).

In short - the limitation of the manual method is that a solid from manual analysis would only represent 0.2% of the total analyses set, with ACA this solid may represent 2%. Therefore, the ACA program should theoretically represent the more accurate and meaningful method for the analysis of char. However, the work carried in Chapter 5 includes both forms of char analysis, since it is intellectually interesting, if not totally useful, to have a description of the general morphological features of the samples produced in the DTF

#### 4.5.4 Drop Tube Furnace Operating Conditions

A temperature of 1300°C or above should be used for future DTF runs, since temperatures below 1300°C did not satisfactorily devolatilise the largest size fraction (180-212µm). A temperature of 1400°C would have been preferable, but it was accepted that the operating life of the DTF equipment was decreased considerably at 1400°C.

An oxygen content of >0% was necessary to ensure a clean product was produced, with the highest level of collection efficiency possible.

A residence time of 200 milliseconds was possible, but 100 milliseconds was closer to actual devolatilisation times discussed in the literature (Bengtsson, 1984) and 100 milliseconds also allowed satisfactory devolatilisation in most of the samples. 100 milliseconds also resulted in higher collection efficiencies than with 200 milliseconds.

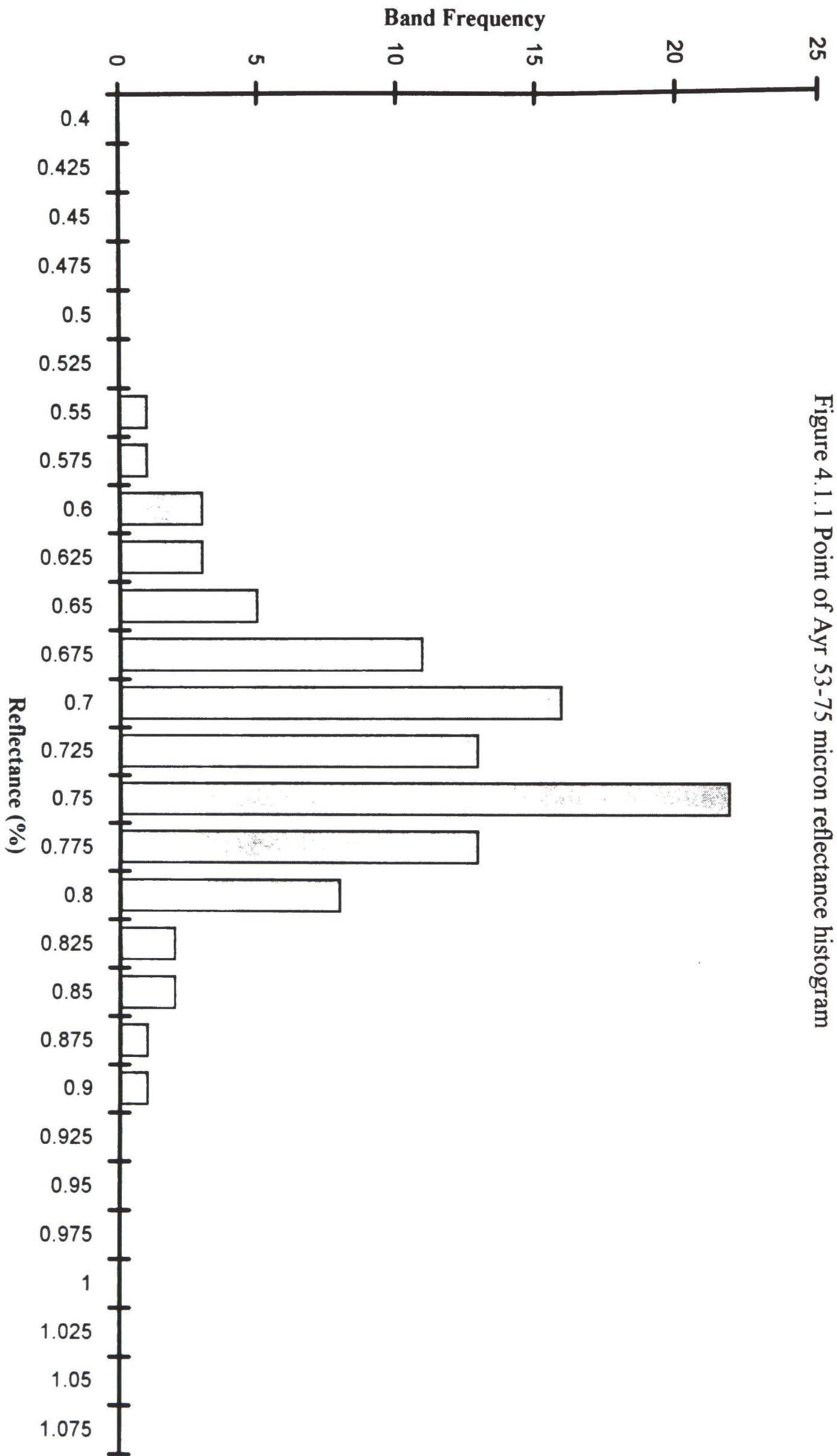


Figure 4.1.1 Point of Ayr 53-75 micron reflectance histogram

Figure 4.1.2 A graph showing volatile content repeatability for Point of Ayr chars

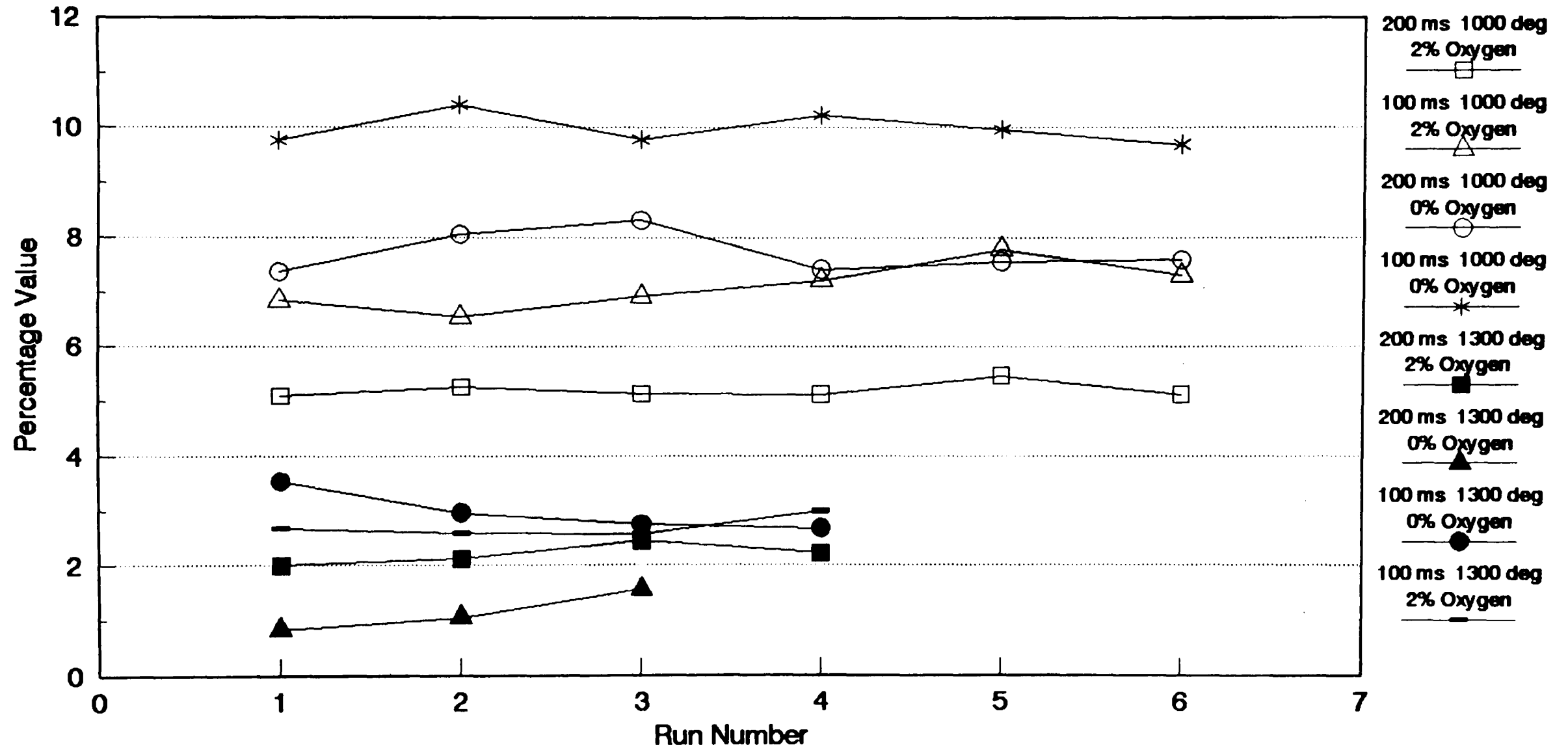


Figure 4.4.1 Particle Size Effects:  
The volatile content of Kellingley chars

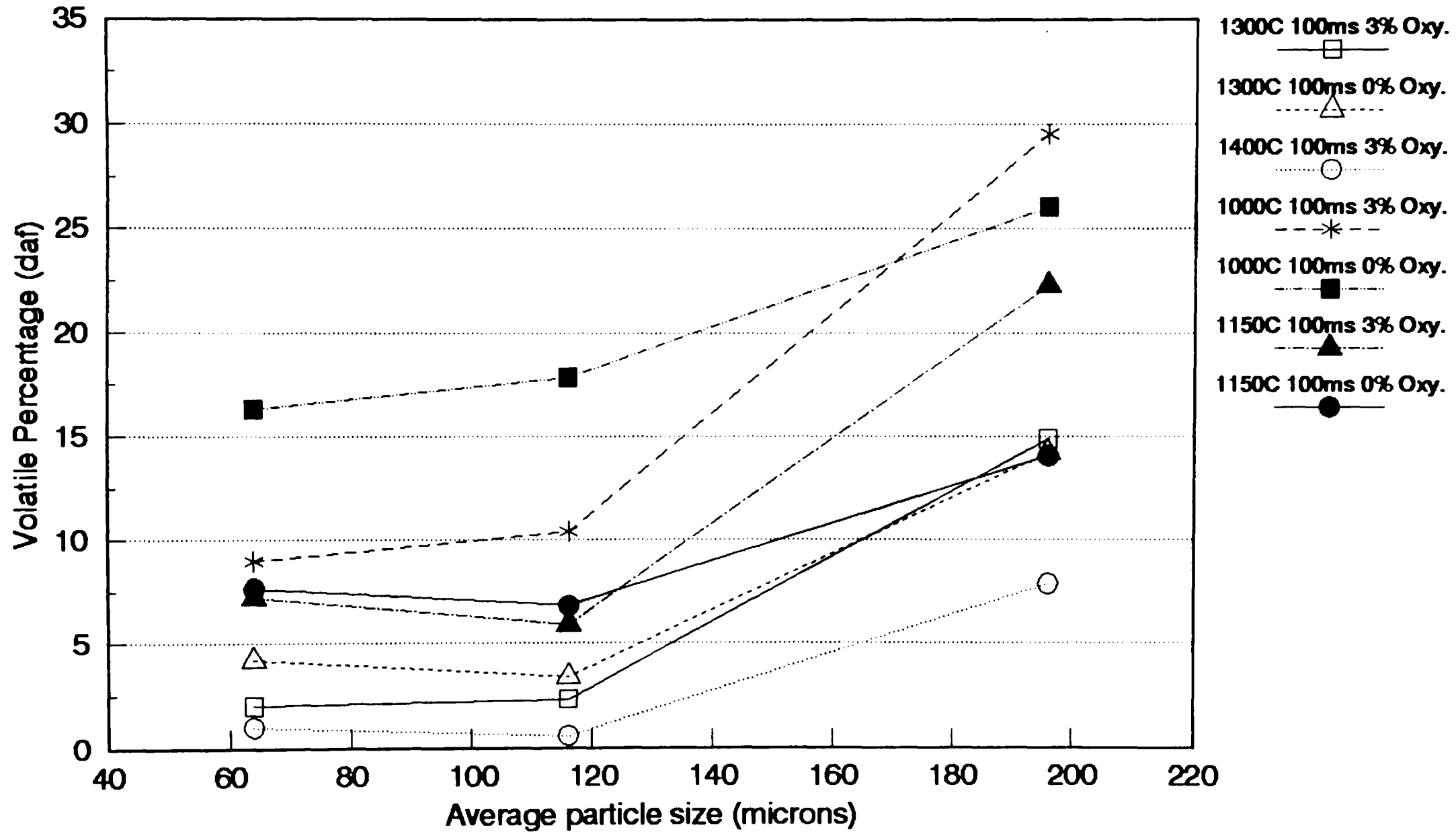


Figure 4.4.2 Particle Size Effects:  
The volatile content of Kromdraai chars

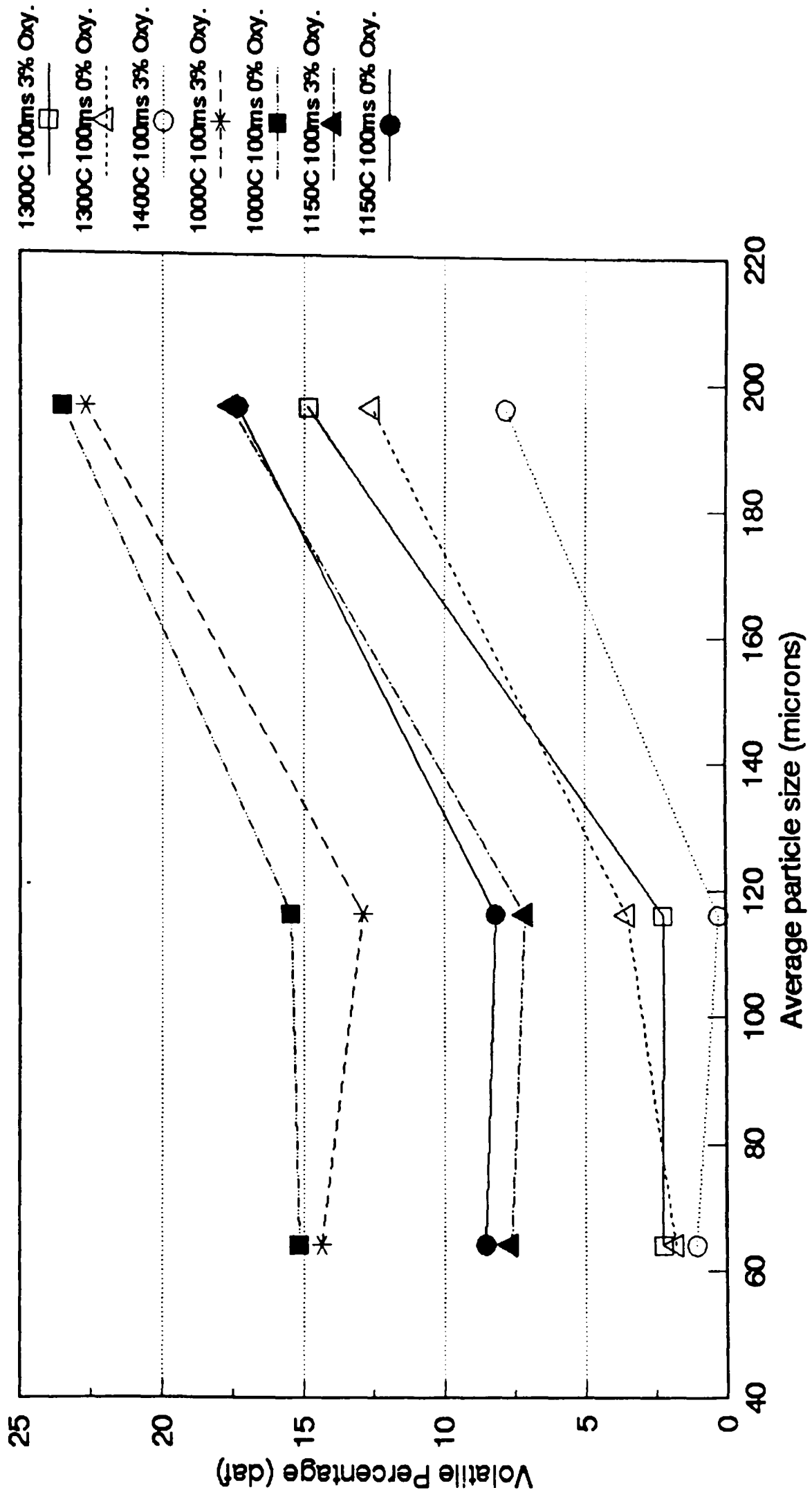


Figure 4.4.3 Particle Size Effects:  
The volatile content of Tower chars

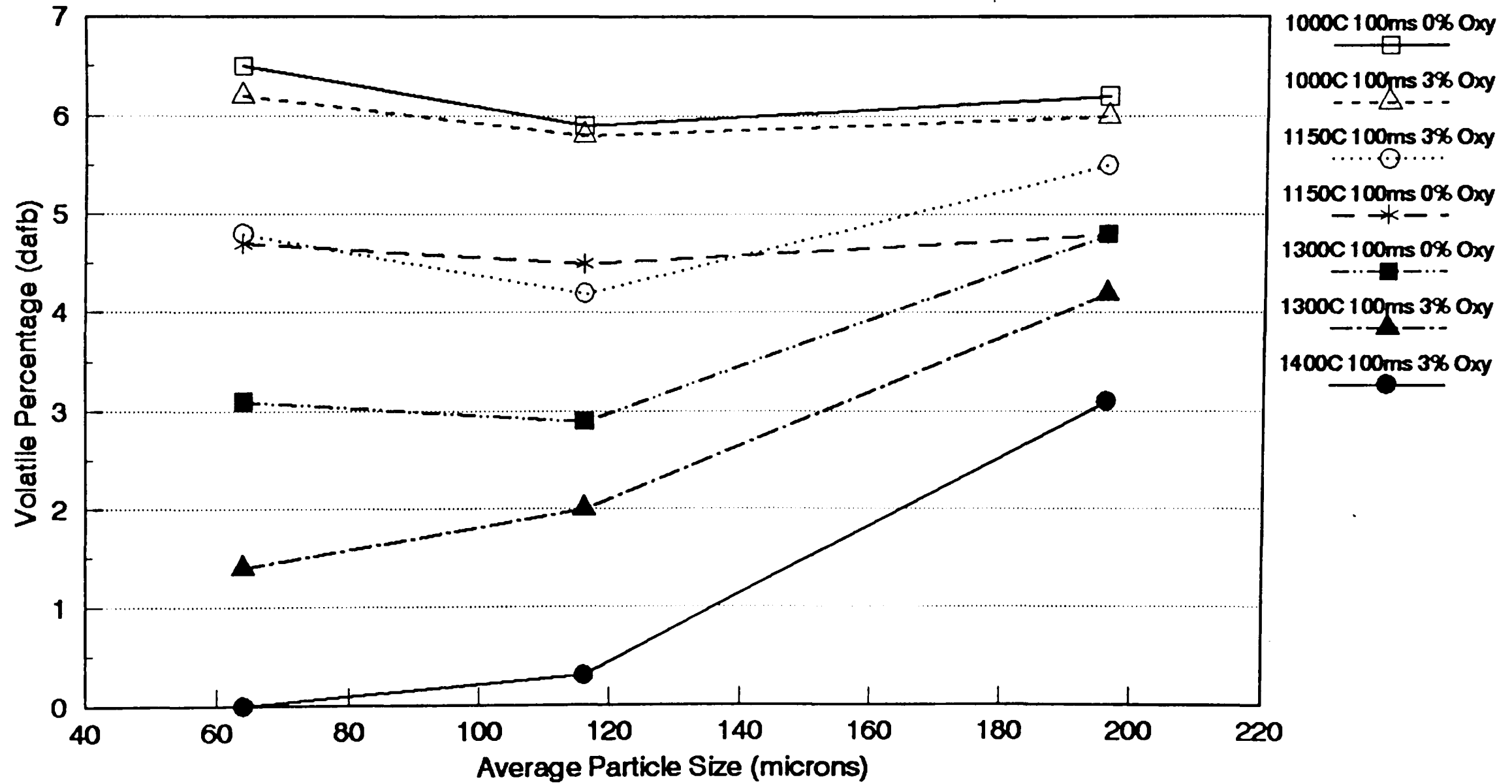


Figure 4.4.4 Temperature Effects: The volatile content of Kellingley chars

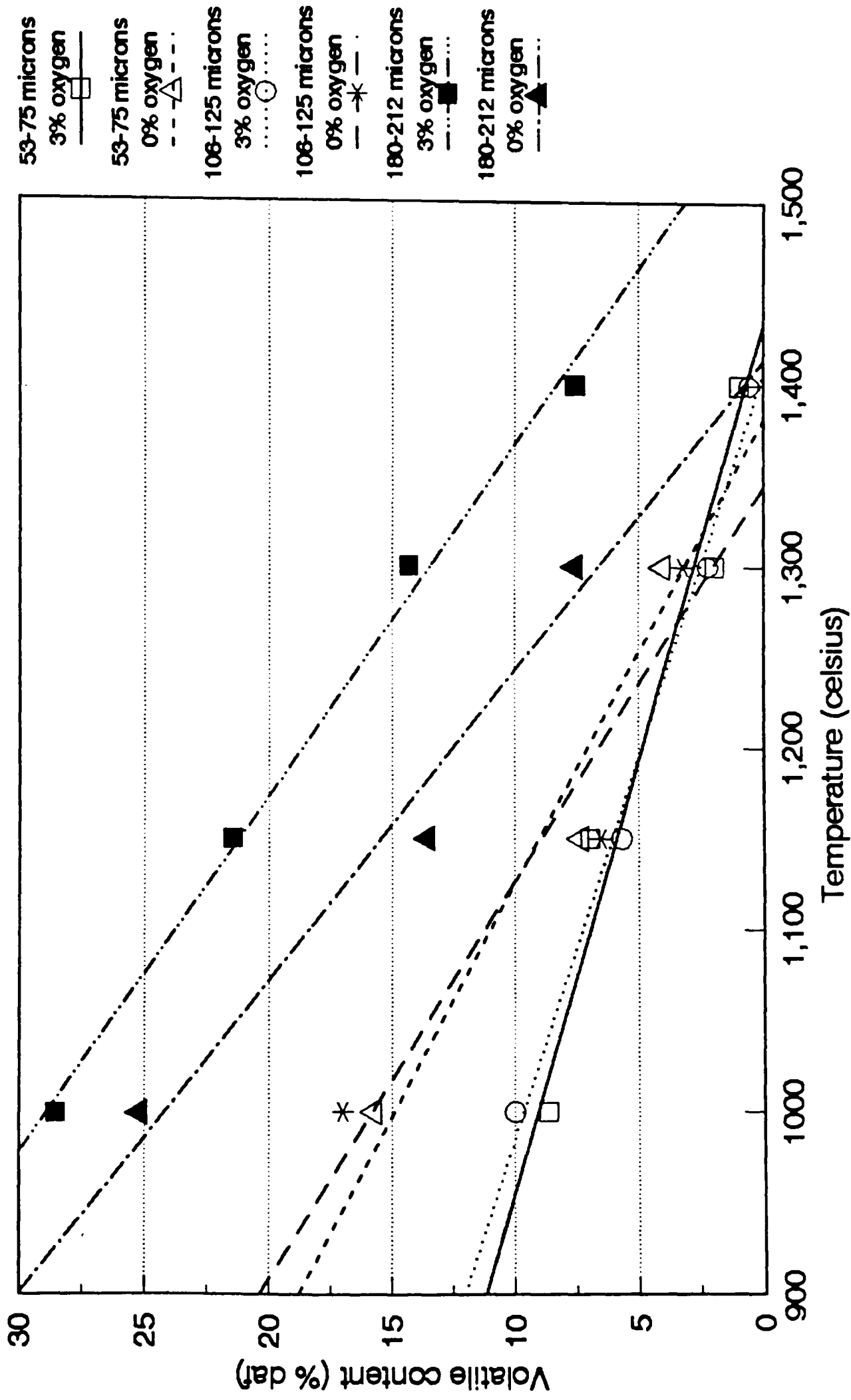


Figure 4.4.5 Temperature Effects: The volatile content of Kromdraai chars

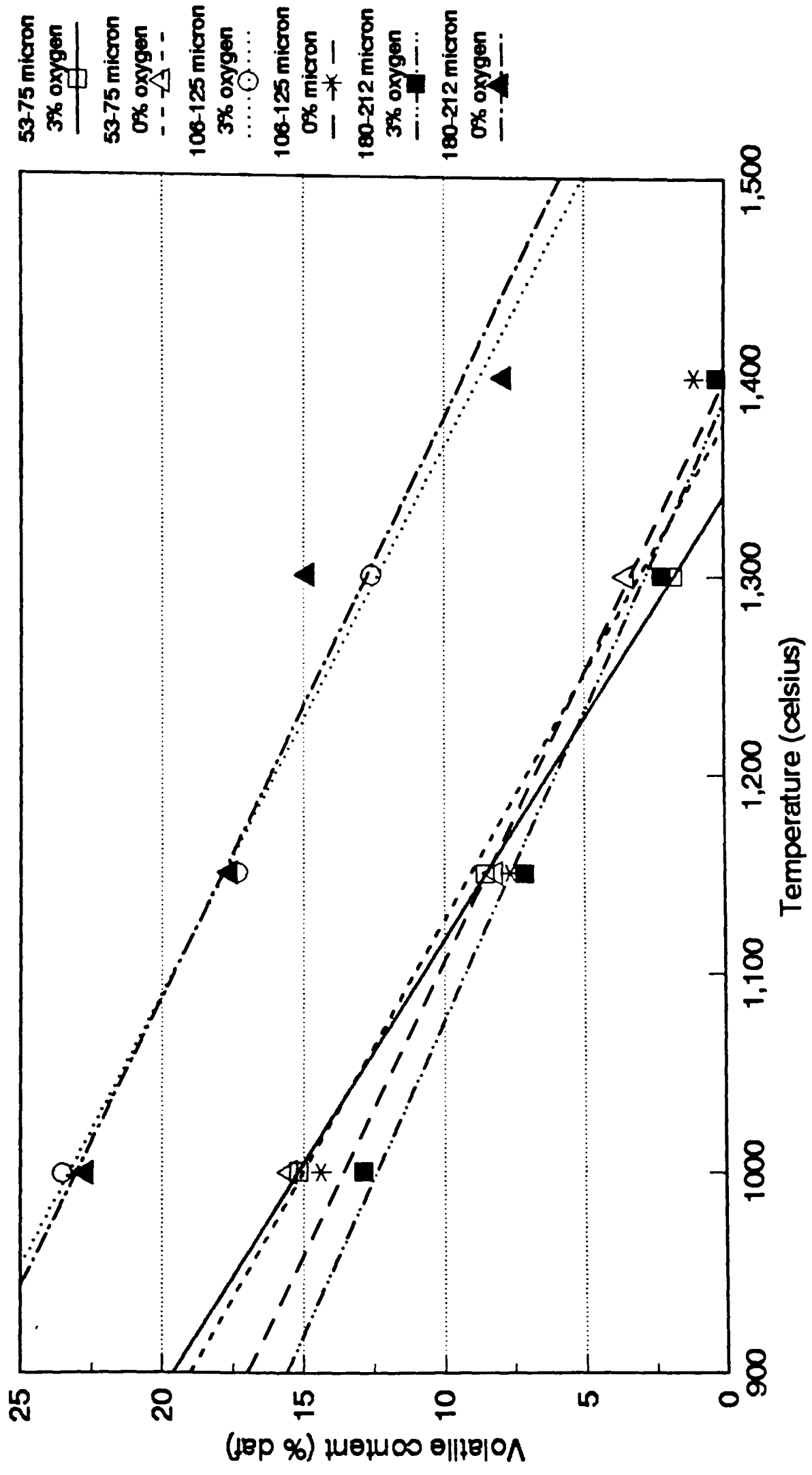


Figure 4.4.6 Temperature Effects:  
The volatile content of Tower chars

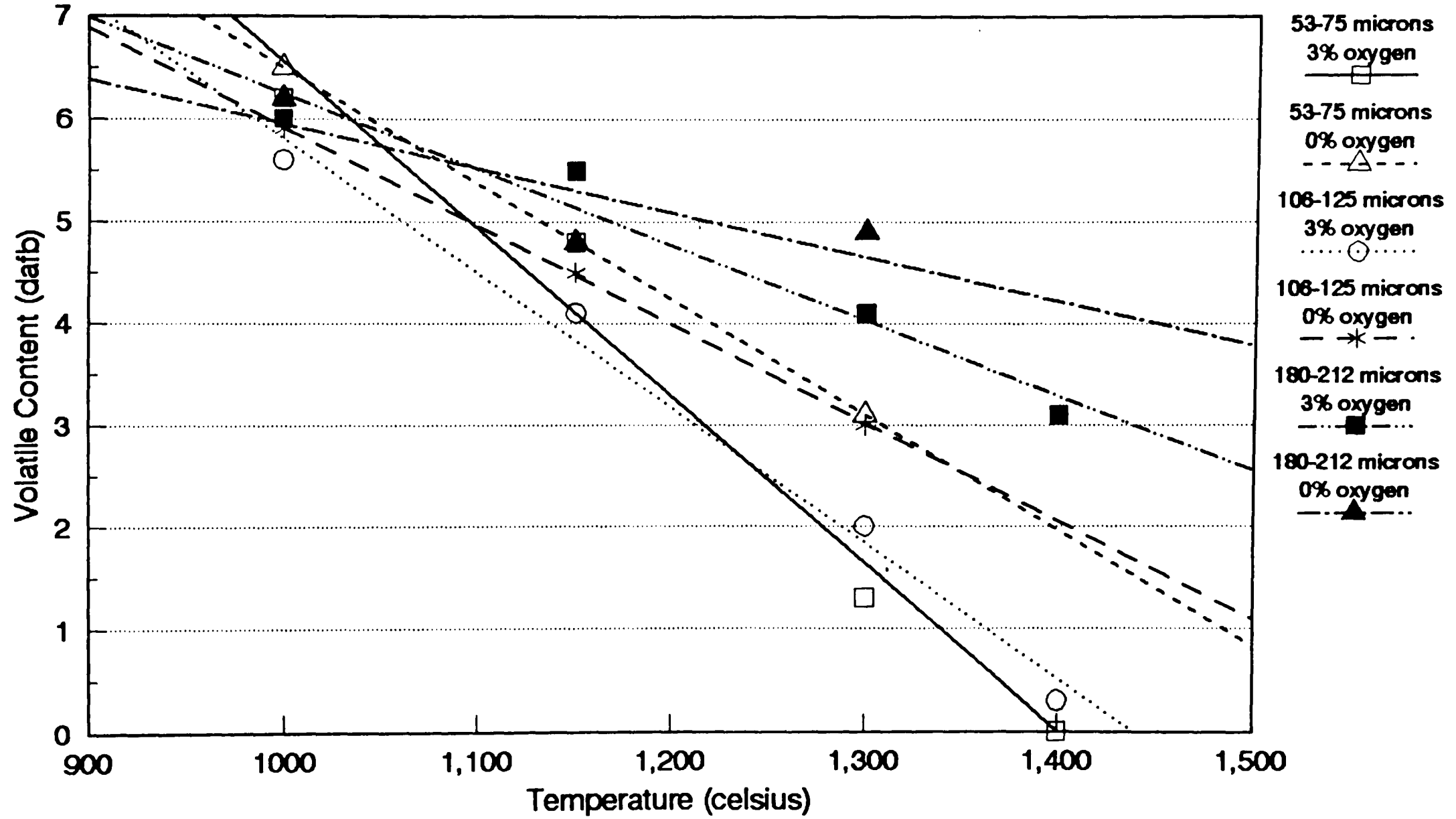


Figure 4.4.7 - The effect of temperature on the R factor values for Kromdraai chars

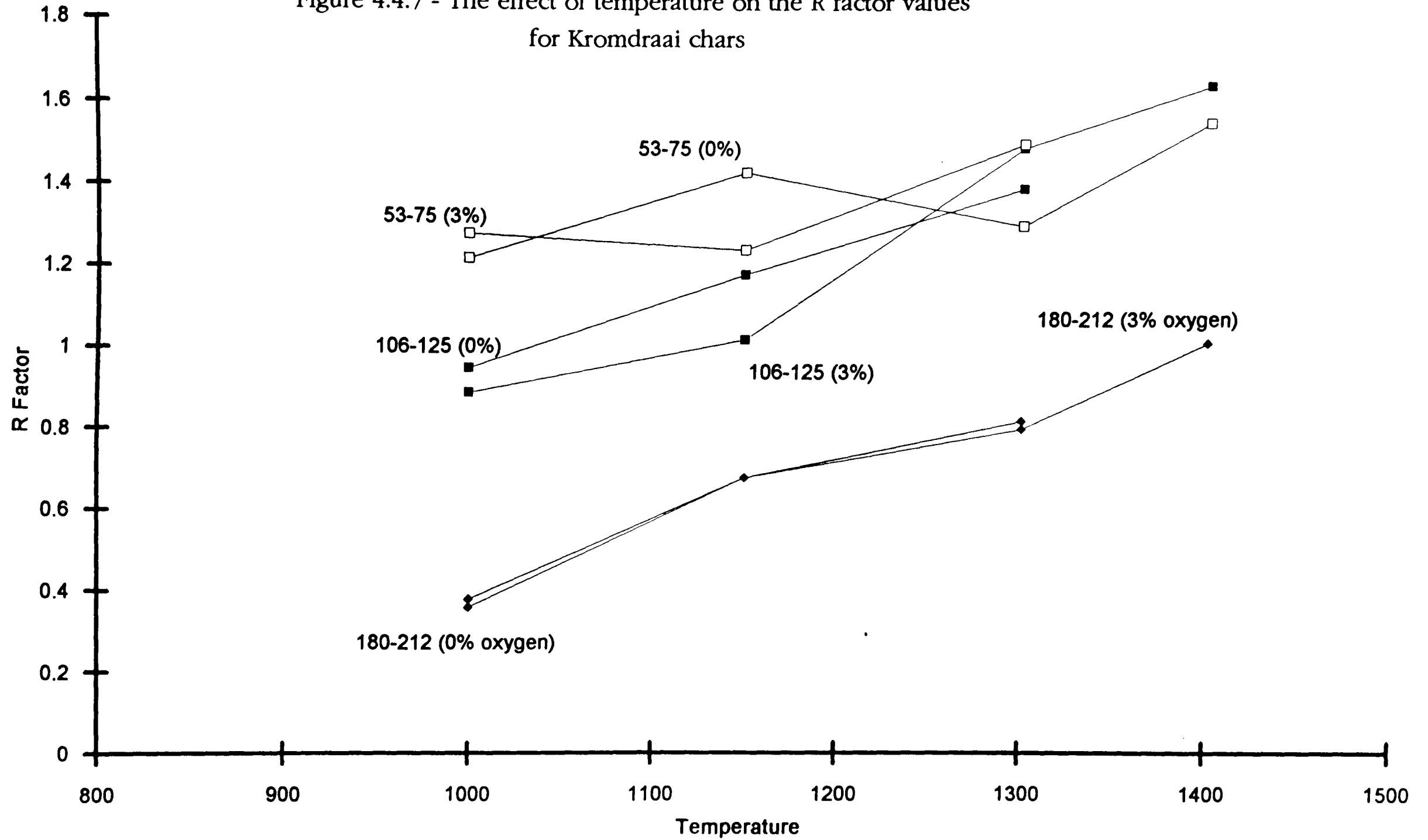
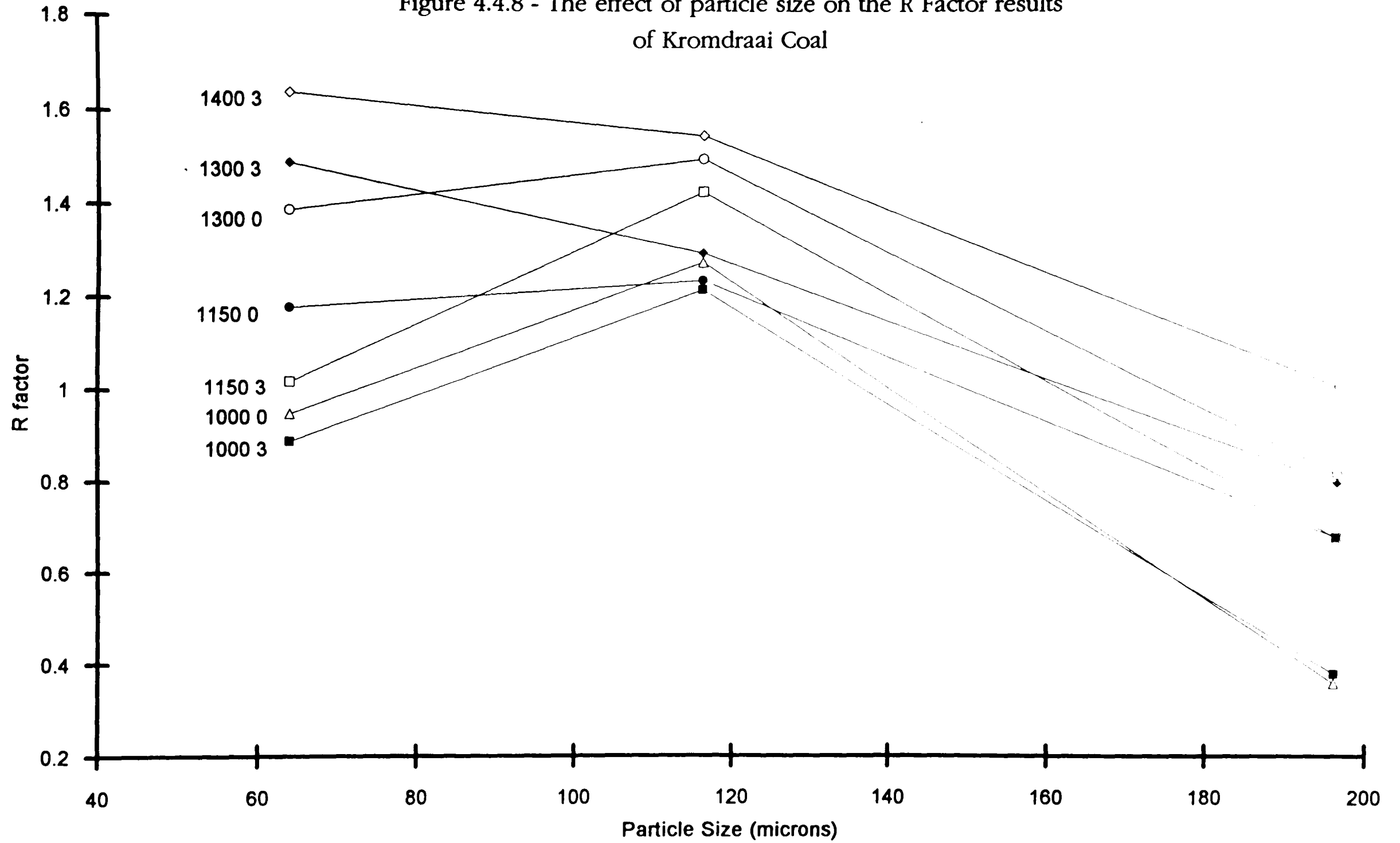


Figure 4.4.8 - The effect of particle size on the R Factor results of Kromdraai Coal



**Table 4.1.1 - The Proximate Analysis for the 53-75  $\mu\text{m}$  fraction of Point of Ayr Coal**

		Dry basis	Dry, Ash Free Basis
Moisture	1.6	--	--
Volatile Content	31.4	31.9	36.7
Fixed Carbon	54.1	55.0	63.3
Ash	12.9	13.1	--
<b>Total</b>	<b>100.0</b>	<b>100.0</b>	<b>100.0</b>

Table 4.1.2 - The maceral analysis results for the 53-75  $\mu\text{m}$  fraction of Point of Ayr Coal.

Maceral Type		Mineral Matter Free
Vitrinite	83.6	85.5
Liptinite	6.1	6.2
Inertinite	8.1	8.3
Mineral	1.4	--
Pyrite	0.8	--
Total	100.0	100.0

Table 4.1.3 - The Ultimate Analysis for the 53-75  $\mu\text{m}$  fraction of Point of Ayr Coal

Element	Percent Presence
Carbon (dmmf)	87.20
Hydrogen (dmmf)	5.80
Oxygen (dmmf)	4.60
Nitrogen (dmmf)	1.60
Sulphate	
Organic (db)	0.63
Sulphate (db)	0.03
Pyrite (db)	1.03
Chlorine (db)	0.15
CO <sub>2</sub> (db)	0.48
Mineral Matter (db)	11.90

Table 4.2.1 - The R factor and Collection Efficiency results for Point of Ayr Experiments

**R Factor Results**

Run Number	1000 degrees				1300 degrees			
	A	B	C	D	E	F	G	H
1	1.39	0.46	1.42	1.27	1.46	1.62	1.69	1.60
2	0.92	0.98	1.42	1.46	1.51	1.42	1.47	1.79
3	1.07	1.02	1.21	1.46	1.46	1.62	1.55	1.97
4	0.99	1.02	1.18	1.38	1.64	***	1.60	1.77
5	0.41	0.14	1.53	1.25	***	***	***	***
6	1.26	1.19	1.05	1.55	***	***	***	***

**Collection Efficiency**

Run Number	1000 degrees				1300 degrees			
	A	B	C	D	E	F	G	H
1	0.78	0.56	0.59	0.77	0.21	0.55	0.27	0.87
2	0.44	0.68	0.75	0.91	0.24	0.53	0.65	0.95
3	0.67	0.70	0.60	0.85	0.36	0.30	0.70	1.13
4	0.65	0.66	0.57	0.82	0.45		0.91	0.84
5	0.49	0.51	0.76	0.81				
6	0.69	0.74	0.57	0.95				

A - 2% OXYGEN & 200 MILLISECONDS  
 B - 2% OXYGEN & 100 MILLISECONDS  
 C - 0% OXYGEN & 200 MILLISECONDS  
 D - 0% OXYGEN & 100 MILLISECONDS

E - 2% OXYGEN & 200 MILLISECONDS  
 F - 0% OXYGEN & 200 MILLISECONDS  
 G - 0% OXYGEN & 100 MILLISECONDS  
 H - 2% OXYGEN & 100 MILLISECONDS

Table 4.3.1 The Proximate Analyses of Kromdraai, Kellingley and Tower

Tower	53-75 micron				106-125 micron				180-212 micron			
		db		dafb		db		dafb		db		dafb
Tower	Moisture	0.3			Moisture	0.4			Moisture	0.1		
	Volatiles	7.0	7.0	7.4	Volatiles	6.7	6.7	7.1	Volatiles	5.8	5.8	6.1
	Carbon	87.6	87.8	92.7	Carbon	87.0	87.3	92.9	Carbon	88.9	89.0	93.9
	Ash	5.2			Ash	6.0			Ash	5.2		
Kromdraai		53-75 micron			106-125 micron			180-212 micron				
		db		dafb	db		dafb	db		dafb		
	Moisture	2.3			Moisture	2.4			Moisture	2.6		
	Volatiles	22.1	22.7	26.1	Volatiles	23.4	24.0	27.2	Volatiles	24.1	24.7	27.9
Carbon	62.6	64.0	73.9	Carbon	62.7	64.2	72.8	Carbon	62.4	64.0	72.1	
Ash	13.0		13.3	Ash	11.5		11.8	Ash	10.9		11.2	
Kellingley		53-75 micron			106-125 micron			180-212 micron				
		db		dafb	db		dafb	db		dafb		
	Moisture	1.4			Moisture	1.7			Moisture	1.7		
	Volatiles	28.8	29.2	35.2	Volatiles	29.9	30.4	36.9	Volatiles	31.9	32.5	36.9
Carbon	53.1	53.8	64.8	Carbon	51.1	52.0	63.1	Carbon	54.5	55.4	63.1	
Ash	16.7		17.0	Ash	17.3		17.6	Ash	11.9		12.1	

Table 4.4.1 R Factor and Collection Efficiency results for the 3 coal types at different DTF conditions

**Kellingley**

	53- 75micron		106- 125micron		180- 212 micron	
	Coll. Eff.	R Fac.	Coll. Eff.	R Fac	Coll. Eff.	R Fac
1000 3%	42.0	-0.24	44.0	-0.42	52.0	0.16
1000 0%	36.0	-1.64	38.0	-2.16	44.0	-0.73
1150 3%	39.0	-1.17	61.0	0.78	62.0	0.9
1150 0%	66.0	0.75	49.0	0.06	52.0	0.64
1300 3%	78.0	1.55	53.0	0.84	41.0	0.56
1300 0%	60.0	1.4	45.0	0.68	40.0	0.68
1400 3%	94.0	1.97	51.0	0.54	48.0	0.92

**Kromdraai**

	53- 75micron		106- 125micron		180- 212 micron	
	Coll. Eff.	R Fac.	Coll. Eff.	R Fac	Coll. Eff.	R Fac
1000 3%	80.0	0.89	72.0	1.22	63.0	0.38
1000 0%	86.0	0.95	98.0	1.28	68.0	-0.36
1150 3%	80.0	1.02	89.0	1.43	65.0	0.68
1150 0%	86.0	1.18	88.0	1.24	68.0	0.68
1300 3%	84.0	1.49	77.0	1.3	59.0	0.8
1300 0%	74.0	1.39	82.0	1.5	57.0	0.82
1400 3%	82.0	1.64	78.0	1.55	61.0	1.01

**Tower**

	53- 75micron		106- 125micron		180- 212 micron	
	Coll. Eff.	R Fac.	Coll. Eff.	R Fac	Coll. Eff.	R Fac
1000 3%	99.0	1.87	71.0	-0.98	99.0	1.87
1000 0%	89.0	-0.15	69.0	-4.7	89.0	-0.15
1150 3%	63.0	-6.21	78.0	-1.83	63.0	-6.21
1150 0%	83.0	-0.56	66.0	-4.72	83.0	-0.56
1300 3%	89.0	1.15	68.0	-2.51	56.0	-2.16
1300 0%	92.0	2.16	55.0	-6.88	64.0	0.18
1400 3%	100.0	3.77	111.0	4.11	98.0	6.57

Coll Eff. - Collection Efficiency  
R fac. - R Factor

Table 4.4.2 Tenui Chars % results.

Oxygen Content	Temp. (deg.)	Kromdraai			Kellingley			Tower		
		53-75	106-125	180-212	53-75	106-125	180-212	53-75	106-125	180-212
3% Oxy	1000	38.4	9.6	9.9	69.2	45.6	25.2	4.0	11.6	9.6
	1150	37.2	35.0	19.3	68.0	45.3	29.0	33.7	25.0	15.9
	1300	32.8	35.6	23.6	59.4	54.2	37.8	60.9	49.6	25.2
	1400	52.4	38.4	20.4	82.5	23.7	19.5	80.3	76.7	40.1
0% oxy	1000	26.8	22.9	14.0	65.3	53.9	26.4	5.5	8.3	24.4
	1150	43.3	30.4	24.6	64.6	52.7	33.2	50.4	49.8	28.8
	1300	50.5	38.7	19.5	72.0	52.1	21.7	57.3	44.7	30.9

Table 4.4.3 Spheres % results

Oxygen Content	Temp. (deg.)	Kromdraai			Kellingley			Tower		
		53-75	106-125	180-212	53-75	106-125	180-212	53-75	106-125	180-212
3% Oxy	1000	43.2	29.1	24.6	68.4	70.8	48.1	15.9	4.0	0.8
	1150	39.7	40.3	20.8	88.7	80.5	72.9	51.9	34.9	1.5
	1300	48.8	50.8	25.2	76.0	76.1	64.3	25.3	3.2	0.0
	1400	36.6	38.6	36.7	91.5	88.9	87.6	5.3	7.0	3.7
0% oxy	1000	43.7	32.6	13.5	91.6	85.2	55.7	22.8	12.3	17.8
	1150	53.0	42.0	36.7	86.4	79.8	67.1	63.5	31.3	6.1
	1300	51.3	48.1	27.6	83.8	83.8	67.4	59.3	12.1	0.7

Table 4.4.4 Solids % results

Oxygen Content	Temp. (deg.)	Kromdraai			Kellingley			Tower		
		53-75	106-125	180-212	53-75	106-125	180-212	53-75	106-125	180-212
3% Oxy	1000	19.4	13.9	19.7	3.0	4.3	9.2	68.0	55.8	81.3
	1150	14.1	12.3	24.1	3.3	1.8	10.0	10.1	8.2	56.4
	1300	17.6	16.4	20.8	3.9	3.2	6.8	12.6	8.4	35.6
	1400	10.8	11.0	10.1	2.1	1.8	1.8	4.1	5.7	19.7
0% oxy	1000	28.0	37.1	32.7	6.0	6.4	18.5	74.9	60.0	71.9
	1150	13.8	15.6	18.1	3.9	2.7	15.3	9.2	10.3	43.7
	1300	13.5	10.5	13.3	3.3	3.6	12.2	7.3	9.0	29.7

Table 4.4.5 - Automated Char Analysis : 3% oxygen results

Temp. Oxy Cont.	Particle Size	Kromdraai			Kellingley			Tower		
		3	5	95%	3	5	95%	3	5	95%
1000 3%	53-75	58.2	77.0	11	76.9	91.6	7	37.8	54.9	19
	106-125	57.1	75.4	13	70.6	87.8	8	36.0	51.0	31
	180-212	47.4	65.9	16	67.3	83.7	11	18.3	26.4	78
1150 3%	53-75	68.5	85.7	10	79.6	93.0	7	70.2	86.5	9
	106-125	57.3	76.1	12	70.4	88.5	9	61.5	77.2	16
	180-212	54.7	73.0	15	63.9	83.1	11	28.7	40.0	59
1300 3%	53-75	71.0	86.0	10	84.8	95.1	5	59.9	78.2	12
	106-125	70.8	85.9	15	82.0	94.9	6	66.3	82.3	12
	180-212	67.9	84.3	16	70.0	87.4	8	41.2	55.5	39
1400 3%	53-75	68.2	84.5	11	81.4	93.1	6	80.4	92.1	7
	106-125	68.6	84.0	12	82.0	90.4	7	68.9	83.7	11
	180-212	67.0	84.4	10	75.5	86.3	9	50.8	67.4	19

Table 4.4.6 - Automated Char Analysis : 0% oxygen results

Temp. Oxy Cont.	Particle Size	Kromdraai			Kellingley			Tower		
		3	5	95%	3	5	95%	3	5	95%
1000 0%	53-75	63.7	81.2	10	77.5	91.1	6	37.4	53.5	20
	106-125	60.2	78.1	12	73.2	89.0	7	41.7	56.0	29
	180-212	47.3	64.7	17	64.5	82.3	8	19.9	28.8	63
1150 0%	53-75	67.8	84.4	9	77.5	92.0	7	70.6	85.6	10
	106-125	62.3	80.6	9	73.2	89.8	7	61.1	78.5	13
	180-212	57.9	76.1	13	64.5	82.7	10	29.0	39.9	57
1300 0%	53-75	65.1	81.6	10	85.4	95.2	6	68.8	83.8	11
	106-125	60.4	78.2	13	78.3	93.3	7	58.8	74.9	17
	180-212	55.8	74.2	17	69.1	86.3	10	45.3	61.2	37

# CHAPTER 5 CHARACTERISATION OF COALS FOR COMBUSTION

## 5.1 Introduction

The aim of this part of the project was to collate various image analysis techniques developed over the period of research. One of the Image Analysis programs was specifically written with the intention of predicting behaviour of the coal in the DTF, whereas others were to be used in order to characterise the products, in order to relate these products to the initial predictions.

Eleven coals were selected on the basis of their varying maceral composition and general coal rank. The three coals, Kromdraai, Kellingley and Tower, featured in Chapter 4 were included.

The aim of the work was to investigate:

- Particle Size Effects - whether or not particle size affects the char morphology over a wide range of coals.
- Maceral Effects - not only the proportion of each maceral, but also the respective reflectance of each maceral.
- The use of the Reactivity Assessment Program to give a rapid prediction of the combustion behaviour of a range of coals.

## 5.2 Drop Tube Furnace Conditions

Only one set of conditions were used in the DTF for these experiments. These conditions were based on the results and conclusions from Chapter 4.

*1300°C* - to allow extensive devolatilisation in all the size ranges including the 180-212 micron cut. Temperatures lower than 1300°C tended to leave a large proportion of the feed sample relatively unchanged.

*100 milliseconds* - this should, in conjunction with the high temperature, allow reasonable levels of devolatilisation whilst also maximising the collection efficiency of the char sample.

*2% oxygen* - a small amount of oxygen was considered important to avoid gaseous tars recondensing on the surface of the chars. The near burner zone is not thought to contain large oxygen levels until the latter stages of the combustion process, some time after pyrolysis.

Each DTF run was performed in duplicate which enabled the repeatability of the system to be tested further, as well as providing more data with which to observe any emerging trends.

### 5.3 Analysis of the 11 Coals

As mentioned in section 5.1, part of the aims of the study was to investigate the effect of particle size on char morphology. In order to do this, 3 size fractions of each coal were used. These were the same as in Chapter 4 i.e. 53-75, 106-125 and 180-212 micron

#### 5.3.1 Proximate Analysis of Sized Coal Fractions

The proximate analyses of the 11 coals and their size fractions are given in Appendix E. It can be seen that small changes occur in the volatile content and ash content between the size fractions.

### 5.3.2 Maceral and Rank (Vitrinite reflectance) Analysis

Table 5.3.1 shows the Rank results for the different coal samples. It can be seen that there is a tendency for the smaller size fraction to have higher Rank values, compared with the two larger size fractions. This is not uncommon, and has been observed by other workers (Kaegi, 1985).

Appendix F contains the results of the maceral analyses of all 33 samples. Table 5.3.2 lists each coal used in the following chapter with a brief description of their petrographic nature. Unlike ash and Rank values, the proportion of each maceral type does not follow a definite pattern with particle size. Inertinite does not always concentrate in the smallest fraction, since its behaviour during grinding can often depend on the grinding method (Stach et al., 1982). In Appendix F there are no real trends for inertinite as displayed by all the coals. Liptinite, however, showed a tendency to concentrate in the largest size fraction of 180-212 microns, and was occasionally more than double the amount found in the 53-75 micron fraction. This liptinite fractionation has been observed in other coals (Thompson et al., 1993).

### 5.3.3 Image Analysis Of The Coal Samples

The Reflectance/Fluorescence plots for each coal fraction is given in Appendix G. The liptinite fraction has been given as a single block at the bottom of the grey scale axis, since liptinite is the darkest of the macerals present. It can be seen that all 11 coal samples have distinctive profiles. The maceral analysis results for the reflectance/fluorescence tests can be seen in Table 5.3.3. All size cuts are also shown in Appendix G and it is possible to see that the cuts are similar but not identical. The most noticeable variations on each coal is the size of the liptinite block, at the bottom end of the grey scale.

## 5.4 Char Results

In this section, emphasis is given to discussing the affects of particle size on the results from all the different types of analysis. However, a few other related subjects are also discussed in the general assessment of the DTF products.

### 5.4.1 Volatile Release

#### 5.4.1.1 Proximate Volatile Content

The proximate analysis results for the chars from the 11 coals in three size fractions are given in Appendix H.

Figure 5.4.1 shows the relationship of volatile content (dafb) to particle size. The use of a three point graph is not 'presented' to derive any mathematical relationship of particle size to volatile content, but simply to show the similarity of the 53-75 and the 106-125 fractions, and the disproportionate increase in the volatile content of the largest size fraction (180-212 micron).

#### 5.4.1.2 Collection Efficiency

Collection efficiency results for each run are given in Table 5.4.1.

The decrease in collection efficiency that occurs with increasing particle size can be seen in Table 5.4.1. This may have been caused by the behaviour of these particles inside the work tube i.e. not undergoing laminar flow conditions. It is not possible to say exactly why the collection efficiency is lower for larger particles, but it is probably related to the way larger particles behave inside the Drop Tube Furnace before reaching the collector probe.

The 53-75 fraction exhibited the best collection efficiency values and in some cases, exceeded 100%, as did the 106-125 fraction. This phenomena is not uncommon

(Thompson et al., 1993), and often results from low ash percentages in the initial coal, which will also lead to inaccuracies in the R factor calculations.

#### 5.4.1.3 R Factor

The R factor values for each sample are given in Table 5.4.2.

As with collection efficiency, the R factor values varied as a function of ash content, especially when the ash content of the initial sample was around 5% or less. Island Creek, El Cerrejon and Tower, either gave negative values or showed large variations between repeat samples.

R factors tended to decrease with increasing particle size. Kellingley and Kaltim Prima did not follow this pattern. Kaltim Prima did contain low ash levels, hence could be expected to give inaccurate R factors, but Kellingley 180-212 contained ash levels greater than 10% hence there is no real explanation why it gave odd results. The ash content of McQuarie samples was greater than 5%, and hence can be taken as more accurate than the coals like Kaltim Prima. With McQuarie, the 53-75 range gave an R factor of 1.90 compared with that of the 180-212 range gave only 1.09.

Most of the coal samples contained more volatile matter than was detected in the proximate analysis, although the underestimation is hard to calculate since, in these experiments, oxygen was used to clean the samples. Theoretically, the presence of oxygen should have increased the values of the R factor by oxidising some carbon as well as volatile matter. However, it is apparent from these results that a coal that experiences high temperatures and high heating rates, emits more volatile matter than was originally measured by proximate analysis, and this agrees with the findings of other workers (Thompson et al., 1993; Badzioch et al., 1968; Gibbins et al., 1991).

## 5.4.2 Manual Char Analysis Results

All the samples were analysed using the Appendix A nomenclature for char identification. As with Chapter 4, the results have been simplified somewhat by using 3 basic groups of char types, namely Tenui-chars %, Spheres %, and Solids %. These results are found in Table 5.4.3 to 5.4.5. The individual detailed analyses can be found in Appendix I.

### 5.4.2.1 Tenui-Chars %

Kromdraai, Bentinck, China SSM and Drummond all showed a decrease in the percentage of Tenui-chars with particle size. Particular to these coals, there was no sudden change between the size fractions. The percentage of thin walled chars changed proportionally as particle size increased. With all four coals, increasing particle size correlated clearly with fewer thin walled chars.

Kellingley showed a good correlation between the duplicate samples, both produced thicker walled chars in the larger sizes. Quite a difference existed between the 53-75 and 106-125 sizes, which is not the same as the results obtained in Chapter 4. In the previous chapter the 106-125 fraction gave similar char results to the 53-75 fraction. It was noted at the time of analysis that the difference between the two fractions was small, in terms of wall thickness, but the lowest size cut was slightly smaller, and definitely below 5 micron. In cases like this, optical char analysis can become more subjective than objective. El Cerrejon, Island Creek and McQuarie chars all showed this same trend of sudden change with the 106-125 micron fraction, producing disproportionately less thin walled chars.

With Tower, the 53-75 fraction produced approximately twice as many Tenui-chars as the 180-212 fraction, but only 7-10% more than the 106-125 micron range. Although Kellingley was of a lower Rank, Tower apparently produced more thin walled char particles. The visible difference between the chars produced by the two coal types was the degree of anisotropy shown by the Tower samples. Island Creek also showed a similar tendency to form anisotropic chars. A photograph of a Tower char showing this anisotropy is included in Appendix A. This characteristic is common in higher ranked coals

(Bailey, 1990) and is known to affect the burnout propensity of a coal (Bend, 1992). The difference between tenui and crassi walls is sometimes difficult to judge, and the objective of Table 5.4.3 was really only to make general comparisons of size effects, and possibly coal types. Kaltim Prima was like Tower, showing a noticeable change in thin walled chars with the largest fraction. The 106-125 range for this coal was as able as the 53-75 fraction in achieving plasticity. The percentage of Tenui-Chars may or may not be higher than recorded, because at the time of analysis, it was noted that char walls were close to the 5  $\mu\text{m}$  border. For best comparisons, the ACA program evaluates both particle size and char type.

Pinang was an odd coal, relative to the others, because all three size ranges formed similar amounts of thin walled chars. Also, unlike the chars from other coals, these Tenui-Chars were *sponge-like*. This description was derived from the physical appearance of the chars, since the network walls were extremely thin and the number of pores were much greater than the other examples of networks.

#### 5.4.2.2 Spheres %

The 106-125 and 53-75 chars for Kromdraai were similar, indicating that at this condition, the reactive fraction in both was able to vesiculate equally well. A 10% gap existed between the 106-125 and 180-212 fraction - as with Tenui-Chars this difference was almost certainly a result of slower vesiculation. Spheres % may not be the best parameter to draw conclusions from since in this case, the 180-212 Kromdraai samples formed large amounts of Crassi-Networks and hence did, to some extent, plasticize. Kaltim Prima's largest size fraction also showed the same tendency to form Crassi-Networks instead of spheres.

Kellingley, Bentinck, Island Creek and McQuarie chars tended to form spheres rather than Networks or Solids. With all four, particle size did not appear to affect the production of spheres. e.g. with Bentinck the 106-125 and 53-75 fractions both formed the same amount of spheres. Wall thickness was the major difference between each size. Approximately 50% of the 106-125 range had a wall thickness above 5 micron.

Tower produced small amounts of spheres in most cases, although the 53-75 micron fraction was most able to produce single cavity chars, and in one sample 13 times that seen in the 180-212 size.

El Cerrejón showed a slight increase in the number of spheres formed by the two lowest sizes, but this was small relative to the value of Spheres % for the 180-212 fraction, which preferentially formed Crassi-Networks.

Pinang chars contained low levels of spheres, since all fractions formed the unusual 'sponge' type chars. It is possible to relate the unusual behaviour of the coal to its exceptionally low Rank, although not with total certainty. However, it has been documented that low ranked coals do preferentially form Networks chars (Clove & Lester, 1994).

China SSM had a noticeable variation between duplicate runs, but this could be experimental error. Also noticeable is the similar amounts of spheres formed by all three size ranges, with the middle size range showing the greatest tendency to form spheres.

#### 5.4.2.3 Solids %

The two smallest size fractions of Kromdraai char contained more Solids, whereas the 180-212 fraction tended to form more Crassi-Spheres. One should note that Solids % is a combination of Fusinoids and Solid chars, and with the 106-125 and 53-75 fraction, the Fusinoid chars make up the majority of the Solids %. In the case of the 180-212 fraction, a considerable amount of particles were identified as Crassi-Networks, which in practice was the broadest description for a char particle, since its walls could be any thickness above 5 microns and contain above two vacuoles. Therefore, provided that the majority of a char particle was not Solid, and the shape of the vacuoles were not Fusinoid-like, the particle could be classed as Crassi-Network. With hindsight, a further class of particle that divided up the Crassi-Network group, would have been useful. Therefore, one should be careful when attempting to interpret manual char analyses.

The high levels of Solids present in the Tower char samples were comparable<sup>to</sup> Kromdraai although, unlike Kromdraai, the majority of Solids came from the Solid char species rather than the fusinoid group. It was decided that at 1300°C and 2% oxygen, Solid chars were likely to remain solid (or reasonably 'closed') throughout the combustion process, and hence were not classed as unaltered coal particles.

El Cerrejon, Drummond, Pinang, China SSM, McQuarie, Kaltim Prima and Kellingley all contained low levels of Solids, showing that no real correlation existed between size and the production of Solid chars.

Island Creek chars contained similar levels of Solids for all three size fractions, which were higher than with the bituminous samples. Although Island Creek tended to form crassiwalled spheres, there was no criterion after crassiwalled spheres with which to gauge wall thickness, which in most cases, were much thicker than 5 microns. The differences that occur within a single char species will lead to some confusion in interpretation of results. Whether or not one should really make any definite conclusions from manual analyses could be a source of much contention.

#### 5.4.3 Automated Char Analysis (ACA).

The results for the automated char analysis of the samples are given in Table 5.4.6. At this stage it is only possible to compare size fractions for a particular coal since at this stage the characterisation of the coals has not been discussed. Automated Char Analysis results are related to coal type, however, in section 5.6.

The results show consistent trends of decreasing {3} and {5} and increasing {95%} with increasing particle size. These changes can be seen in Figures 5.4.2 (for {3}) and 5.4.3 (for {5}). In some cases, these differences are quite large. Pinang, was unusual, and gave high values for all three size fractions for all ACA parameters. This was consistent with the manual analysis where all three size fractions gave similar amounts of thin walled chars and only trace amounts of Solids. Pinang and Kromdraai were the only two coals not to follow

the trend of decreasing {5} and {3} with increasing particle size. It is possible that this may have been caused by the maceral fractionation described in section 1.6.1. The other 9 coals, however, all showed a relatively stable decrease in the values for {3} and {5}.

The {95%} values in Figure 5.4.4 show a tendency to increase with increasing size. This agrees with manual analyses which indicated that the 180-212 fraction tended to form thicker walled chars. Pinang, as in Figures 5.4.2 and 5.4.3, contradicts the trend of the other 10 coals and shows a lower {95%} for the 180-212 fraction than with the 106-125 fraction. However, the rest show increasing {95%} results with increasing particle size. Tower, in particular, shows a large increase for the {95%} value of the 180-212 fraction - perhaps because the anthracite particles required more time, and a higher temperature before extensive plasticity could be achieved. Overall, it can be seen that there was a distinct tendency for the smaller particles to form thinner walled chars.

#### 5.4.4 TGA Intrinsic reactivity Measurements

Due to time limitations only one of the two samples for each fraction were tested for Intrinsic Reactivity. The results for all three size cuts of each char are shown in Table 5.4.7.

##### 5.4.4.1 Peak Temperature

Unusual results emerged for Peak Temperature i.e. no distinct pattern existed with particle size. It is not really possible to say why the Peak Temperature value for the 106-125 fractions were in some cases much higher than the other two fractions, but 6 of the 11 coals showed the 106-125 range to have the highest Peak Temperature. However, all three fractions followed a similar order between coal types i.e. Tower always had the highest Peak Temperature, and Pinang the lowest. The order between these two varied a little, with El Cerrejon giving an oddly high value and this is discussed in section 6.2. The majority of the 180-212 chars (bar Kromdraai, Island Creek and Tower) had similar values ranging between 613°C and 617°C.

#### 5.4.4.2 Burnout Temperature

Burnout Temperature results were similar to those of Peak Temperature where the 106-125 range gave the highest temperatures. The order between coals within a particular size range followed a rough order with Tower and Island Creek having the highest two temperatures. Pinang and Bentinck are at the opposite end, having the two lowest values consistently. The spread of results is, on the whole, smaller than with Peak Temperature - with the majority of values falling within 20°C of each other, indicating that the burnout of the most inert fraction of char within any char sample, occurs at a similar temperature. Intrinsic Reactivity, at this stage, was studied qualitatively. Any conclusions concerning anomalous results were speculative at the time of this project and further work was necessary. Section 6.5.1 discusses future work pending, related to a more detailed investigation into Intrinsic Reactivity.

### 5.5 Prediction Systems

As discussed in Chapter 1, there are several ways of predicting the way a coal, or coal fraction, will behave during rapid heating, devolatilisation and combustion. In order to compare the results for char analysis and the intrinsic reactivity of the chars produced in the DTF, three of these classical prediction systems were adopted in order to compare them with the predictions made by the new Reactivity Assessment Program (RAP) program. The parameters for this prediction are as follows:

- **RANK** - or vitrinite reflectance. As mentioned in Chapter 1, workers have found Rank to be one of the most reliable means of predicting the combustion characteristics of a coal.
- **REACTIVE MACERALS** - a classical definition for the Reactive Macerals in a coal was adopted i.e. all liptinite, all vitrinite and a third of semi-fusinite (Furimsky, 1990). All values were calculated from the manual point count results (on a mineral matter free basis) contained in Appendix I.

- **REACTIVE NUMBER** - this corresponds to the cumulative percentage of the coal that falls below the 130 grey scale mark in the reflectance/fluorescence runs shown in section 5.3.3. The value of 130 was taken because it falls within the semi-fusinite band for most bituminous coals. The boundary between reactive and unreactive macerals is thought to exist within this maceral sub-group, as discussed in section 1.3.1. This same cut-off value was used for all the different coals in order to develop the relative proportions of reactive macerals in each group.
- **AVERAGE REACTIVE NUMBER** - was the average of the sum of the grey scale range (0-255) weighted by the percentage frequency of each grey scale. A low Average Reactive Number corresponds to reactive coal sample. A high Average Reactive Number indicates that the coal is unreactive.
- **FUEL RATIO** - simply the ratio of Fixed Carbon to Volatile Matter, both on a dry ash free basis. This is possibly the simplest criterion for prediction, but its use is common in industry.

The results for all five parameters can be seen in Table 5.5.1. If all five parameters predict combustion behaviour then they should correlate with each other, regardless of the fact that the parameters are based on different aspects in the coal. On this basis it should be possible to correlate all 33 samples from the 11 coals, independently of size, since the parameters for each, should reflect that particular size range. All 5 prediction parameters are correlated with each other, and the results are represented in the form of Figures 5.5.1 to 5.5.10. It can be seen that there is not always a linear relationship between all the different parameters. Certain parameters appear to have absolutely no correlation at all with the others. In section 5.6 the correlation of the 5 prediction parameters with char results is discussed. In order to do this, correlation with a single size range was necessary, since size affected char morphology.

#### 5.5.1 Reactive Macerals with Rank

Coals with Rank values  $< 1.0$  appear to have a zero order relationship with Reactive Macerals. However, if all the points are considered, then there is no correlation between Reactive Macerals and Rank.

### 5.5.2 Reactive Macerals with Reactive Number

Reactive Number appear to have no correlation.

### 5.5.3 Reactive Macerals with Average Reactive Number

Similar to Reactive Number but inverted, and again showing a large amount of scatter.

### 5.5.4 Reactive Macerals with Fuel Ratio

If the coals with Fuel Ratio s below 3.0 are considered there appears to small trend of decreasing Fuel Ratio with increasing Reactive Macerals. The whole picture, however, shows a poor correlation.

### 5.5.5 Rank with Reactive Number

Most points indicate an acceptable correlation between Rank and Reactive Number. Unfortunately outliers occur around the 50% mark for Reactive Macerals. These correspond to the South African Coal called Kromdraai, which, despite having a low vitrinite reflectance, had an overall low Reactivity Number caused by a large proportion of high reflectance inertinite in the coal. Any number of outliers could be added to the figure by including coals examined in several other studies, but for commercial reasons these cannot be included. These coals would further emphasise the limitations of Rank as a prediction parameter, since in these coals, as with Kromdraai, vitrinite is not the 'dominant' maceral in the coal. When vitrinite exists in proportions greater than 70%, the correlation between Rank and Reactive Number is reasonable. If vitrinite is less than 70% of the coal, then it is possible that anomalous results are produced.

### 5.5.6 Rank with Average Reactive Number

Similar to Reactive Number, showing a linear trend for most results, except the same coals that were outliers with Reactive Number. Coals with high levels of inertinite cause problems. These coals are not always best represented by Rank values.

### 5.5.7 Rank with Fuel Ratio

The non linear relationship of Rank with Fuel Ratio appears to increase, almost exponentially at the end, with some degree of scatter with the highest values. This corresponds to minimal changes in volatile content between the three anthracite size fractions, but since the value for Fuel Ratio is a fraction - any differences are exaggerated. Kromdraai again, stands clear as a coal that doesn't fit the pattern, simply because Rank is not the best parameter to consider when considering world coals.

### 5.5.8 Reactive Number with Fuel Ratio

Up to a Fuel Ratio of 6, the relationship is roughly linear, although the actual differences become very small above a Reactive Number of 85. The anthracite coal samples resident on the Y axis gives the relationship a curve.

### 5.5.9 Reactive Number with Average Reactive Number

Reactive Number with Average Reactive Number appear to correlate reasonably well. But this would be expected, since both parameters are similar ways of interpreting the same data.

### 5.5.10 Average Reactive Number with Fuel Ratio

A reverse of Fuel Ratio to Reactive Number, in that an increase in Average Reactive Number (lower Reactive Number) corresponds to a higher Fuel Ratio. The relationship between the two is roughly linear until the anthracite samples at the top end, which

produces an exponential type increase in Fuel Ratio. In order to validate this exponential plot, one would need more coals in between the anthracite and the rest of the coals, as well as perhaps a meta-anthracite, to show an even higher Fuel Ratio value (although meta-anthracite would probably damage the camera attached to the image analyser).

## 5.6 Prediction Comparison

In this section the five prediction parameters are compared with the characteristics of the chars obtained in the various analysis techniques. The correlations between the prediction parameters are considered again, but in more detail, and only within a specific size fraction. The eight char parameters considered are listed below.

- Tenui-chars %
- Spheres %
- Solids %
- ACA {3}
- ACA {5}
- ACA {95%}
- TGA Peak Temperature
- TGA Burnout Temperature

The correlation results gave a means of relative comparison of the different parameters, and was more practical than providing a multitude of graphs, with no statistical means of determining which parameter was the best.

The correlation data for each size fraction is given in Tables 5.6.1 to 5.6.3 and any interesting results from each column are discussed here.

Correlations with:

### 5.6.1 Reactive Number

With all three size fractions, Reactive Macerals and Reactive Number bear no relationship whatsoever.

Rank has a varying correlation with Reactive Number over the three size ranges. The largest size has the best correlation value, and the 106-125 fraction has the lowest - hence there appears to be no definite pattern of size dependency. The reason for this anomaly is not clear. as mentioned before Rank can be a misleading parameter if the vitrinite does not 'reflect' the rest of the macerals in the coal. For this reason the correlation between Reactive Number and Rank, although quite good, should be interpreted carefully.

Average Reactive Number and Reactive Number, as explained earlier, are two ways of interpreting the same experimental data, hence it no surprise that they correlate well with all three size ranges. It is worth noting that Reactive Number is not exactly the same as Average Reactive Number i.e. a correlation coefficient of 1 would mean that the 'results' were relatively the same, even though the physical number produced was different.

Fuel Ratio and Reactive Number, when viewed graphically, appear to have an exponential relationship (see 5.5.8). The two higher ranked coals gave a non-linear increase. This is partly why the correlation coefficient for Fuel Ratio and Reactive Number was not good with any of the size fractions.

All three size fractions gave a poor correlation between Reactive Number and any of the three manual char indices. The 180-212 fraction did give a slightly better result with Solids % - showing perhaps the tendency for less reactive large particles to form unvesiculated char types.

Particle size had a significant effect on the relationship between Reactive Number and the parameters from the Automated Char Analysis (ACA), namely {3}, {5} and {95%}. The

53-75 micron range gave poor results for all three ACA parameters, due to the high ranked coals Tower and Island Creek. Even though both were deemed to be unreactive - at this small particle size they were able to plasticize and form thin walled chars. This agrees with the results from the previous chapter, where Tower was able to change between Solids and crassi-walled chars at lower temperatures, to form thinner, more vesiculated chars at 1300°C. At this small size, with high heating rates and high temperatures even these 'unreactive' coals vesiculated. See Figures 5.6.1 to 5.6.3 for a graphical representation of the results for ACA parameters against Reactive Number. The degree of anisotropy shown by Tower and Island Creek chars was the one distinguishing feature. Their lower reactivity (section 5.4.4) was also noticeable. The 106-125 and 180-212 fractions showed an improvement between the ACA parameters and Reactive Number. This can be related to the changes seen in the two higher ranked coals. As discussed above, the smallest size cuts of these unreactive coals were able to deform during rapid heating which gave rise to a poor correlation coefficient. These larger particles, however, were apparently less able to plasticize, probably due to their increased volume. This is perhaps why the 180-212 fraction gave the best correlation values because the least reactive coals were too large to undergo significant transformations which would produce open char structures. The 180-212 fraction gave a poor result for {3} and Reactive Number, probably due to the nature of the char particles. As is clear from the manual char results, the largest size range generally produced thicker walled chars - hence with {3} there probably isn't a significant difference between the chars formed by any of the 11 coals. This would explain why {5} showed a better correlation, and why {95%} gave the best results. This 'burnout' parameter ({95%}) is possibly the most meaningful way of interpreting ACA analyses, since it disregards particle size and does not assume a definite number of contours to be representative of combustion times. {95%} simply gives the relative number of contours required to cover 95% of all char material seen in each analysis.

The reason for the good correlation between Reactive Number with Peak Temperature and Burnout Temperature with all three size ranges, is perhaps due to the large difference between the two unreactive coals, in terms of both Intrinsic Reactivity and Reactive Number. These two points on the graph are so far down the scale, that it tends to minimise

any variations between the rest of the samples. However, it is reasonable to assume that there is a relationship between 'unreactive' coals and 'unreactive' chars.

### 5.6.2 Reactive Macerals

All three size fractions gave similar results. There appears to be no correlation between any prediction parameter or char parameter with Reactive Macerals.

### 5.6.3 Rank

The 53-75 and 180-212 fractions both showed that Rank can relate to other prediction parameters. This is partly due to the scale of the Rank results i.e. two coals with a Rank value of > 1.3%, the rest between about 0.5% and 0.9% - hence the two highest samples decrease the effect of any scatter in the main cluster of coals. The other reason for Rank correlating with other parameters is perhaps genuine in that Rank does, in many cases, allude to petrographic composition, especially with Northern Hemisphere coals. As explained previously, the relationship breaks down with many Gondwala coals.

### 5.6.4 Average Reactive Number

Average Reactive Number appears to relate well to Fuel Ratio, despite the non-linear nature of Fuel Ratio. This may be caused by the method used to calculate Average Reactive Number, which gives a slightly different interpretation of the reflectance & fluorescence plots compared with Reactive Number.

The relationship between Average Reactive Number and ACA parameters are similar to those of Reactive Number in section 5.6.1, but not quite as close.

### 5.6.5 Fuel Ratio

Not a very good set of results with any of the three size ranges. The Solids % correlation may be a result of the two high ranked coals, again minimising the differences between the lower ranked coals.

### 5.6.6 Tenui-Chars %

Tenui-Chars % do not really relate to any of the remaining parameters.

### 5.6.7 Spheres %

All three size ranges show little correlation between Spheres % and ACA and TGA results:

### 5.6.8 Solids %

The Solids % results for all three size ranges show correlation with different ACA parameters, depending on their size. The Solids % in the 53-75 micron fraction relates best to the {3} and {5} results. This is a peculiarity of this smallest size range. The presence of Solids would result in a lower {3} and {5}, but in the long term i.e. the {95%} value, chars such as Crassi-Networks and Crassi-Spheres would have as much an effect as the Solid chars. This might be due to the relative importance of thicker walled chars in the smaller sizes. If the relative value of Solids to crassi-walled chars does change with size then one should see the correlation results change as particle size increases. In reality this is seen with the 106-125 and 180-212 fractions. With an ACA value of {3}, the effect of Solid chars is unclear since all char types have thicker walls in these larger sizes, so Solids would probably not emerge as a problem until after several more contours. One can see the correlation between Solids % and {5} and {95%} improve, especially with the 180-212 fraction, which doesn't even relate too well to {5}, again because of the increased wall thickness of all the types.

### 5.6.9 {3} ACA Values

Poor {3} results with the two smallest fractions caused poor {5} and {95%} values. However, this isn't the case with the 180-212 fraction where a char with a poor {3} value could have a good or bad {95%} value. It confirms the point made in section 5.6.8.

### 5.6.10 {5} ACA Values

Smaller char particles give the best correlation between {5} and {95%} results. A fall off in agreement can be seen the larger fractions.

### 5.6.11 {95%} ACA Values

Correlated badly with the TGA parameters of Peak Temperature and Burnout Temperature, in all three size ranges.

### 5.6.12 Peak Temperature

As with 5.6.5, the two higher ranked coals affect any correlation. Over a large scale however, there may be some correlation between 'unreactive' coals and 'unreactive' chars.

### 5.6.13 General Conclusions From The Correlation Data.

Virtually no correlation existed between any prediction parameter and manual Tenui-Chars % and Spheres %.

The Reactive Number index generally gave the best correlation between the different combustion parameters - especially Solids %, {5} and Peak Temperature. The Average Reactive Number and Reactive Number correlated well with all three sizes, but did not give identical interpretations of the reactivity of each coal.

Particle size affected the correlation of the different ACA parameters with manual results i.e. the correlation coefficient between Solids % and the {3} and {5} and {95%} values depended on the size of char particle. Thicker walled chars in the smaller sizes resulted in lower {3} and {5} values but not necessarily a high {95%} value. With large particles, however, the correlation of the {3} was much poorer than with the {5}, because the non-Solid chars were much thicker.

#### 5.6.14 Prediction Parameter Conclusions

It can be seen that there is no definite correlation between any one prediction system and any one combustion parameter; whether it is a measure of Intrinsic Reactivity, or a measurement of the type of chars formed. There appears to be an exception from each prediction system which invalidates the correlation.

The correlation between the prediction systems might have improved somewhat if one had only considered a small range of coals i.e. with a Rank of less than 1.3%. The Tower anthracite and Island Creek coal were included in the work in order to widen the range of results for the Reactivity Assessment Program, but realistically were never likely to be considered for combustion on a large scale.

Only the smallest size fraction of the two unreactive coals were able to form relatively open chars. This was probably because of the high temperature used to prepare the char. Had a lower temperature been used, of say 1000°C, then denser Solid chars would probably have been produced by these two coals. However, since temperatures of 1000°C are probably not representative of real combustion conditions, it would have been harder to justify any conclusions from reactivity studies had this condition been used. The chars produced by these two coals were open, and therefore similar to the chars from other coals, *but* (as discussed earlier) the optical texture of the chars was distinctly different. Significant levels of anisotropy was only evident in the chars from these two coals, which agrees with the findings of other workers (Bailey et al., 1990). It is therefore possible that this degree of anisotropy, which is linked with low Intrinsic Reactivity, caused the high values for Peak Temperature and Burnout Temperature as seen in Table 5.4.7.

Unfortunately, it is not possible to begin modelling char burnout, without comprehensive studies on reaction mechanisms of char combustion inside a pulverised fuel burner. If one did have the information with which to combine the reactivity of the chars with their morphological characteristics, then it would be possible to prove the validity of the Reactivity Assessment Program. As it is, this is not possible.

The aim of the project was to develop a rapid means of characterising coals by comparing these results with chars produced in a Drop-Tube. It appears inadequate just to compare the morphological nature of the chars with the Reactive Number, since the nature of the chars can be totally different, both in terms of optical texturing and Intrinsic Reactivity. For this reason, the two anomalous coals were removed from further discussions in order to only consider chars of similar isotropic nature, and so effectively lower the range of coal ranks considered. Section 5.7 looks specifically at the remaining 9 coals, and the correlation between the prediction parameters and the characteristics of the chars.

## 5.7 Coals Below 1% Reflectance

Tables 5.7.1 to 5.7.3 show the correlation data for the various char and coal parameters, without Tower and Island Creek. One can see quite clearly that there are distinct differences between all the results, when the two higher ranked samples are excluded.

### 5.7.1 Reactive Number

The relationship between Reactive Number and Rank has been discussed at great length, as well as why Rank does not necessarily best represent the coal. The relationship between Reactive Number and Reactive Macerals is slightly different. From Table 5.7.1, a good correlation of Reactive Macerals and Reactive Number can be seen. The inclusion of coals with high inertinite levels of low reflectance, which is common with coals from Australia (Shibaoka et al., 1989c, Phong-Anant et al., 1989a, Thomas et al., 1989a), would change the correlation of Reactive Number to Reactive Macerals. This kind of coal would have a low Reactive Macerals value, but would have a high Reactive Number. Therefore one

cannot simply relate Reactive Number to Reactive Macerals, since the model would not work with certain coals from the Southern Hemisphere. The fact that the 11 coals generally did not have significant amounts of low reflectance inertinite meant that Reactive Macerals gave good agreement with Reactive Number.

Without the two extreme Rank values from the Tower and Island Creek coals, there is no real correlation of Rank with Reactive Number. The Kromdraai sample, in some ways, contributed to the lack of agreement between the two parameters.

Without the two low 'reactive' coals, the relationship of Reactive Number with Average Reactive Number is still good, as one might expect (section 5.6.1).

There is considerable improvement between Fuel Ratio and Reactive Number with only the 9 coals, because of the linear range of Fuel Ratio (5.6.1). All three sizes show the same improvement.

A significant improvement between Reactive Number and Solids % with the smallest size, although the largest fraction has lost any correlation perhaps due to the smaller 'range' of results and the thicker walls of this largest size fraction.

The Reactive Number of all three sizes relate to different ACA parameters; {3}, {5} and {95%}. The smallest two sizes correlated well with {3}, {5} and {95%}, whereas the 180-212 fraction correlates best with {95%} probably for the same reasons as discussed in section 5.6.8. Figures 5.7.1 to 5.7.3 represent the correlation data for the ACA parameters with Reactive Number.

With a much smaller range of Reactive Numbers there appears to be a poor correlation with TGA results.

### 5.7.2 Reactive Macerals

All three size ranges show a similar poor correlation to Rank, although values for Reactive Macerals with Average Reactive Number are better. The relationship between Fuel Ratio and Reactive Macerals is improved somewhat with the removal of the two higher ranked coals.

The rest of the parameters show similar trends as with Reactive Number but generally with poorer correlations.

### 5.7.3 Rank

Rank shows a similar relationship to char parameters, the same as Reactive Macerals did in section 5.7.2 i.e. very little since some coals do not necessarily behave as the reflectance of its tellocollinite suggests.

### 5.7.4 Average Reactive Number

The correlation value for Average Reactive Number and Fuel Ratio shows that, over this small range, 'unreactive' samples also have high Fuel Ratios.

The amount of Solids % does appear to reflect the coals Average Reactive Number, although the largest size fraction is the least dependant. This largest size however does correlate much better with the ACA parameters, especially {95%}. This could be related to the objective nature of the Image Analysis tests as compared with the more subjective nature of manual analysis, which faced problems with char type identification (section 5.6.1).

### 5.7.5 Fuel Ratio

The Fuel Ratio results reflect those of Average Reactive Number i.e. Fuel Ratio correlates to certain manual char analyses and ACA parameters, but the largest size range only shows

a significant trend with {95%} - where the difference between the chars produced becomes clearer. Since all the chars produced by all the different coal types had thick walls, ACA parameters like {3} are not able to differentiate char types.

#### 5.7.6 Tenui-Chars %

A dramatic change of correlation results with Tenui-Chars %, with the removal of the two higher ranked coals. The chars in the 53-75 micron range show some connection between {3} and thin walled chars - which could be expected since good {3} values would require plenty of thin walled chars. Another feature of this size range is the correlation of Tenui-Chars % and {95%}. It is not possible to give a definite reason for this except that on a relative scale Tenui-Chars are probably more statistically important than in the largest size fractions. Hence the relationship is lost somewhat in the 180-212 cut.

#### 5.7.7 Spheres %

From the Spheres % results, it is apparent that the type of char that is formed by different coals could be spheres or networks. For this reason Spheres % correlates badly with the remaining char parameters.

#### 5.7.8 Solids %

{3} appears to relate well with all ACA parameters, although the relationship appears to be dependant somewhat on size. All the ACA values for the two smallest sizes appear to be affected by the amount of Solids % present in the sample. The opposite is seen in the 180-212 micron samples where Solids % did not correlate well with the {95%} results. This may be due to errors during manual char analysis and mis-identification of Crassi-Networks, or may relate to the changing relative affect of thick walled chars on the overall analysis i.e. it is possible that thick walled larger particles are relatively more important in the larger particle sizes.

### 5.7.9 {3} ACA values

Size appears to affect correlations between {3}, {5} and {95%}. With 53-75 and 106-125 fractions poor {3} means poor {5} and {95%} values but with 180-212, the connection between {3} and {95%} is not seen i.e. the distinction between poor char blocks cannot necessarily be related to the initial 'burnout' parameter of {3}.

### 5.7.10 {5} ACA Values

A different set of results compared to section 5.7.9 in that a poor {5} value means a poor {95%} value, including the largest size fraction where it appears that the link between 'burnoff' ({5}) and 'burnout' ({95%}) in a range of coals is clearer than with {3} and {95%}.

### 5.7.11 {95%} ACA Values

This ACA parameter does not correlate with either TGA parameter in any size, although one should note that the TGA range of Peak Temperature and Burnout Temperature with these 11 coals is small and hence not the best situation to establish a relationship.

### 5.7.12 Peak Temperature

Similar results and explanation as in 5.7.11, can be seen between Peak Temperature and Burnout Temperature.

## 5.8 Overall Conclusions On The Prediction Parameters

1. The Reactive Number parameter gave best correlations to ACA parameters. The Reactive Number also appears to be the best way of interpreting the reflectance data obtained from the Reactivity Assessment Program. The use of a threshold (Reactive Number) instead of an average (Average Reactive Number) over the whole grey scale, was also simpler, involving less calculations.

2. There appeared to be no definite relationship between Peak Temperature, Burnout Temperature with anything else. The range of Rank values is so small, it was difficult to really know whether Rank did correlate to Intrinsic Reactivity measurements.
3. The percentage of Tenui-Chars% affected {3} values with the smallest size range. The larger particle size cuts gave thicker chars, and hence the correlation was lost.
4. Average Reactive Number appeared to give the best correlation with Fuel Ratio.
5. Rank gave very poor correlation to anything.
6. The {3} and {5} ACA values for 180-212 micron char fraction did not differentiate between the chars formed by the various coals. This is probably because of the thickness of the char walls in the largest size fraction. With the largest particle size, only the {95%} ACA results was able to show distinct differences between char samples.
7. Tenui-Chars % corresponded to {3} values more than {5} - which is logical since early burn-off should result from thin walled chars.
8. Spheres % did not really correlate to anything. The tendency of a coal to form networks or spheres may have depended, to some extent, on the Rank of the vitrinite, but the thickness of the chars from vitrinite seemed to be more dependant on the size of the initial coal particle.
9. Big particles produced relatively thick walls chars as well as increasing the proportion of Solids in a char sample.
10. The correlation of Reactive Number with Automated Char Analysis parameters were much improved with the smaller range of coals. This was because the degree of anisotropy exhibited in the char samples was minimal, hence all the chars were of a similar Intrinsic Reactivity, hence was not a factor in need of consideration.

All these coals would be considered for combustion based on their proximate analyses and one can see that the Reactivity Assessment or Reactive Number calculated for each one does correlate with the morphology of chars produced at 1300°C. The actual figure for morphology i.e. {3}, {5} or {95%} with which the Reactive Number correlates appeared to be a function of particle size. All the ACA parameters of the smaller char particles correlate to the Reactive Number for their respective coals. However, the largest size

gives good agreement only with {95%} values - since the difference between the char types is not clear at {3} or {5}.

**Figure 5.4.1 Particle Size Effects : The volatile content of the chars from the 11 coals**

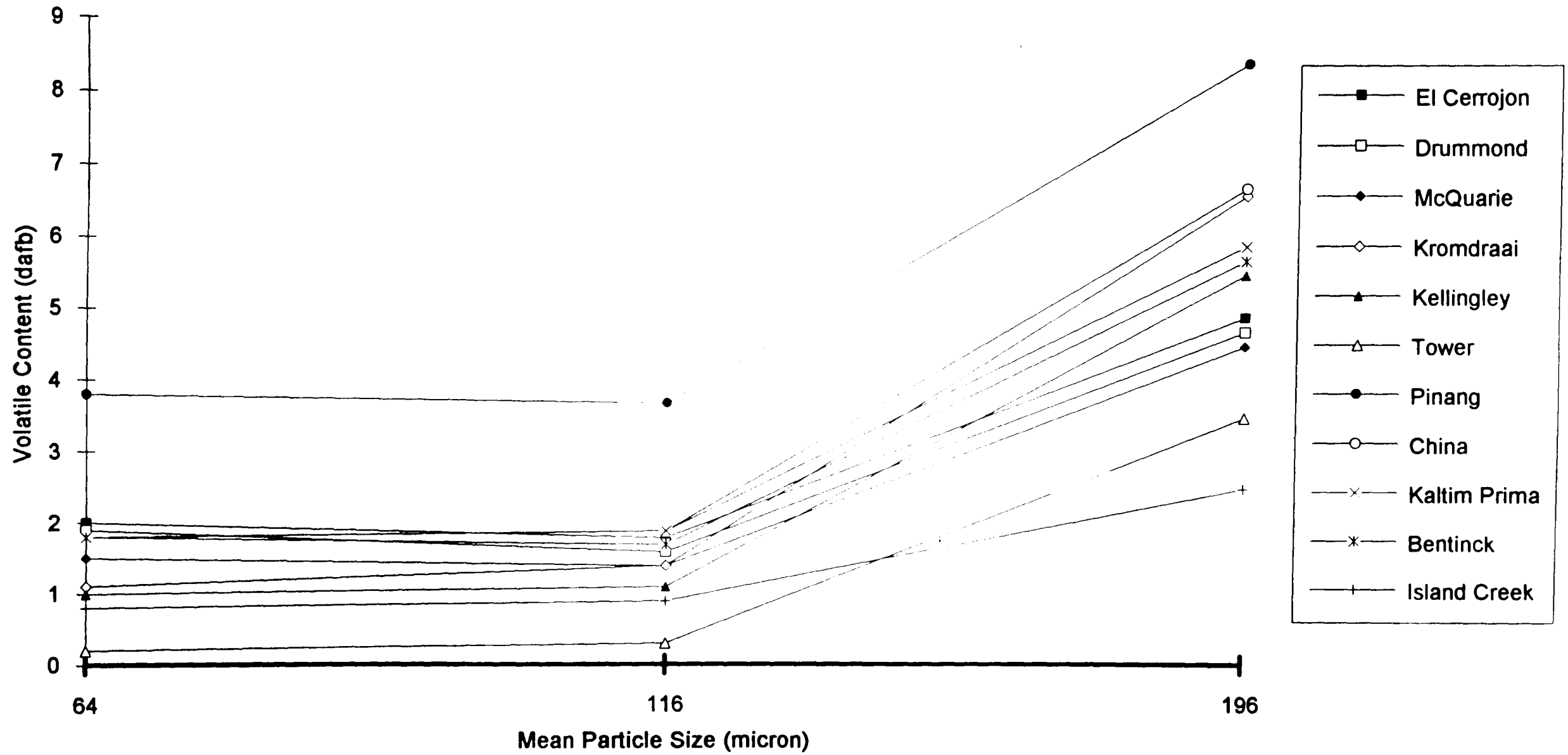


Figure 5.4.2 Particle Size Effects: ACA {3} values for the 11 coals

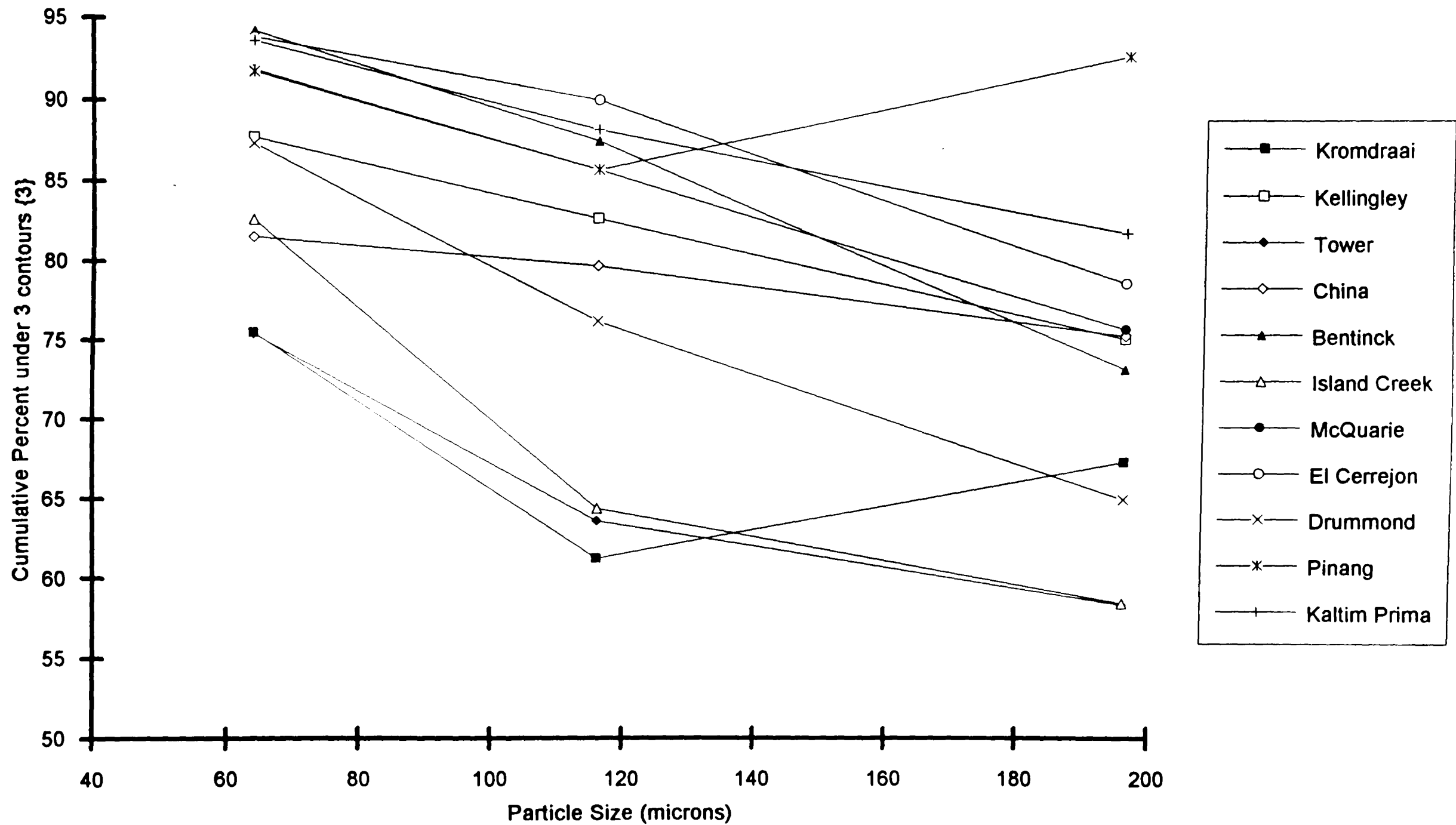


Figure 5.4.3 : Particle Size Effects : ACA {5} values for the 11 coals

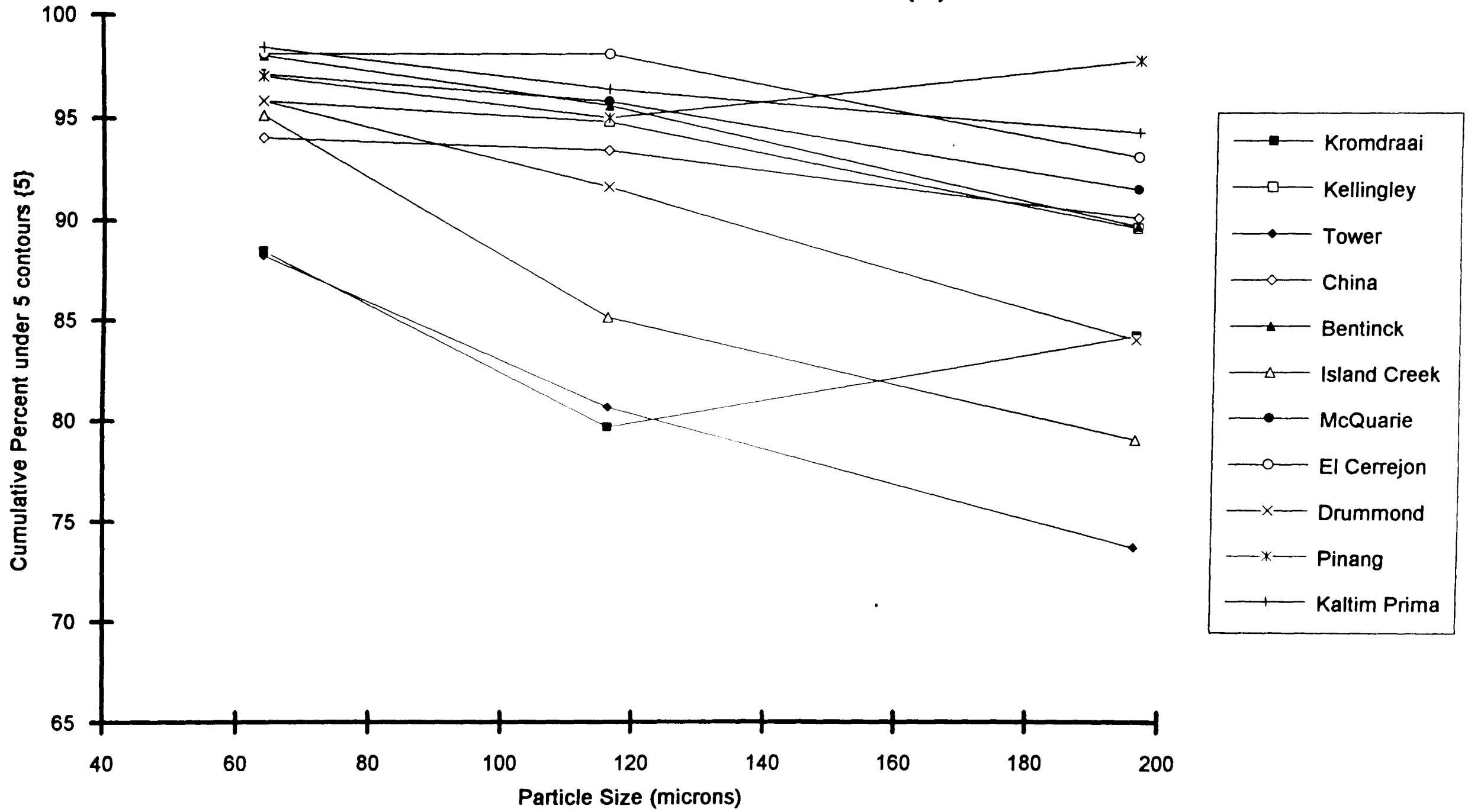


Figure 5.4.4 : Particle Size Effects: ACA {95%} values for the 11 coals

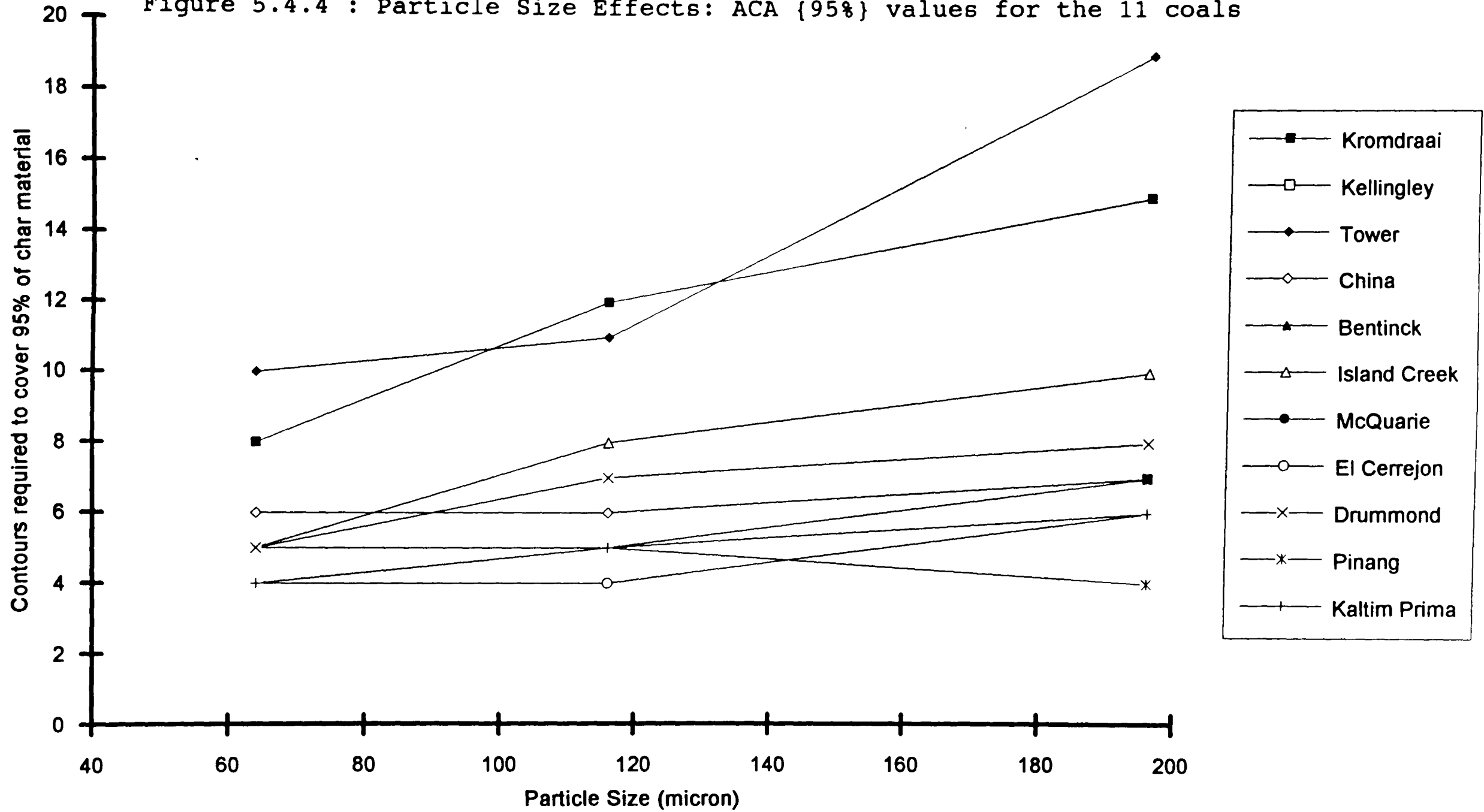


Figure 5.5.1 Rank against Reactive Macerals

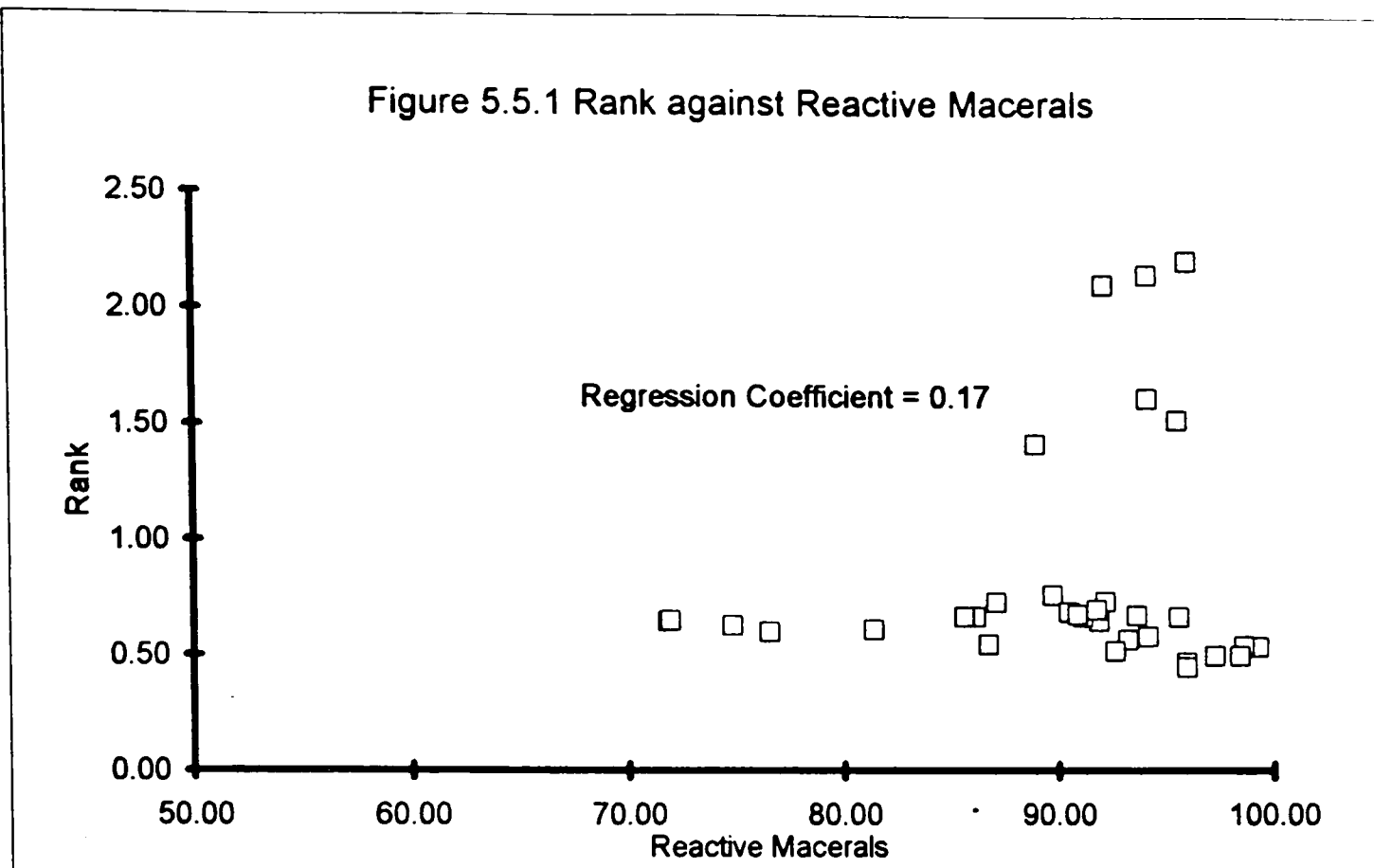


Figure 5.5.2 Reactive Macerals against Reactive Number

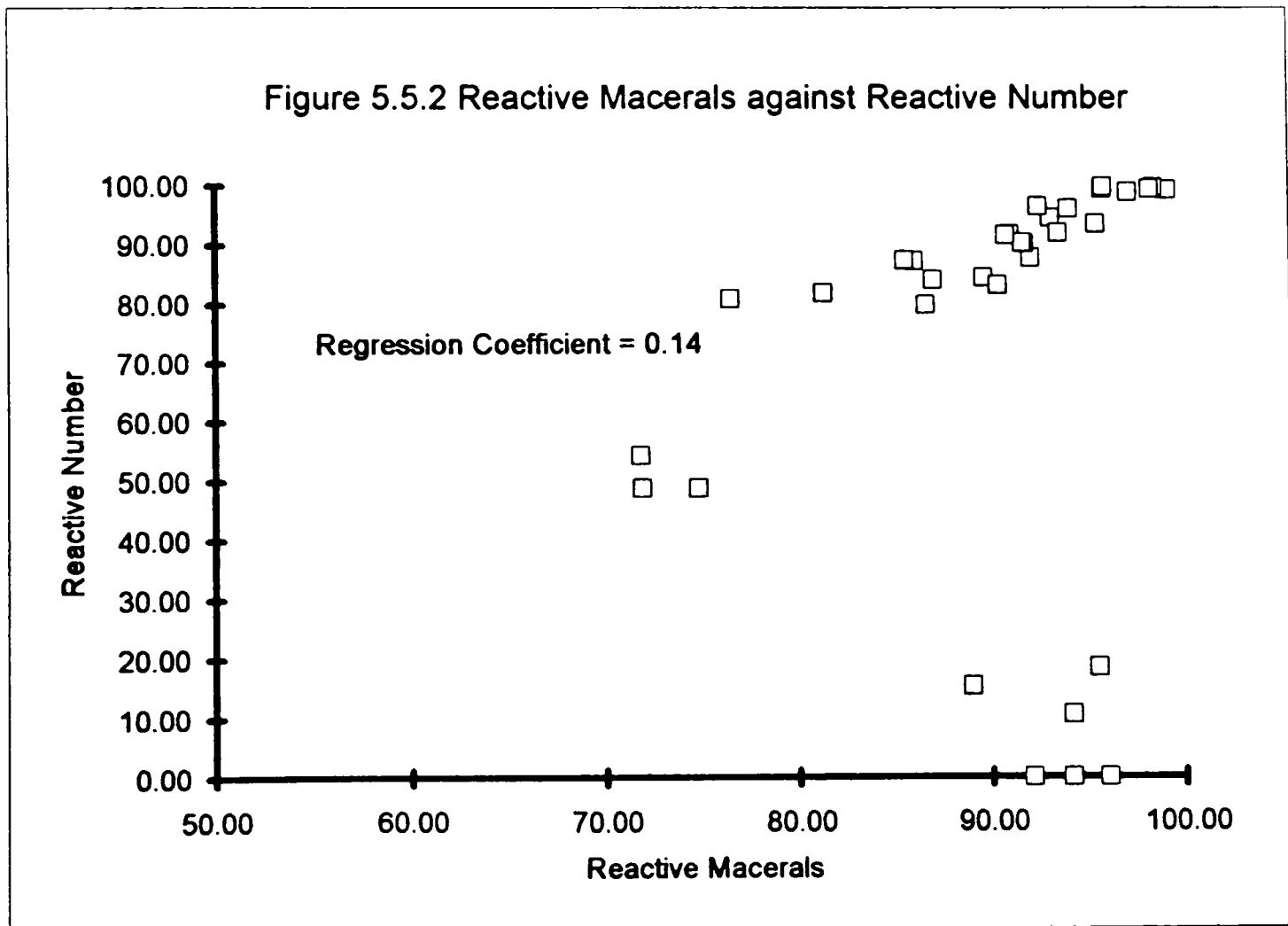


Figure 5.5.3 Average Reactive Number against Reactive Macerals

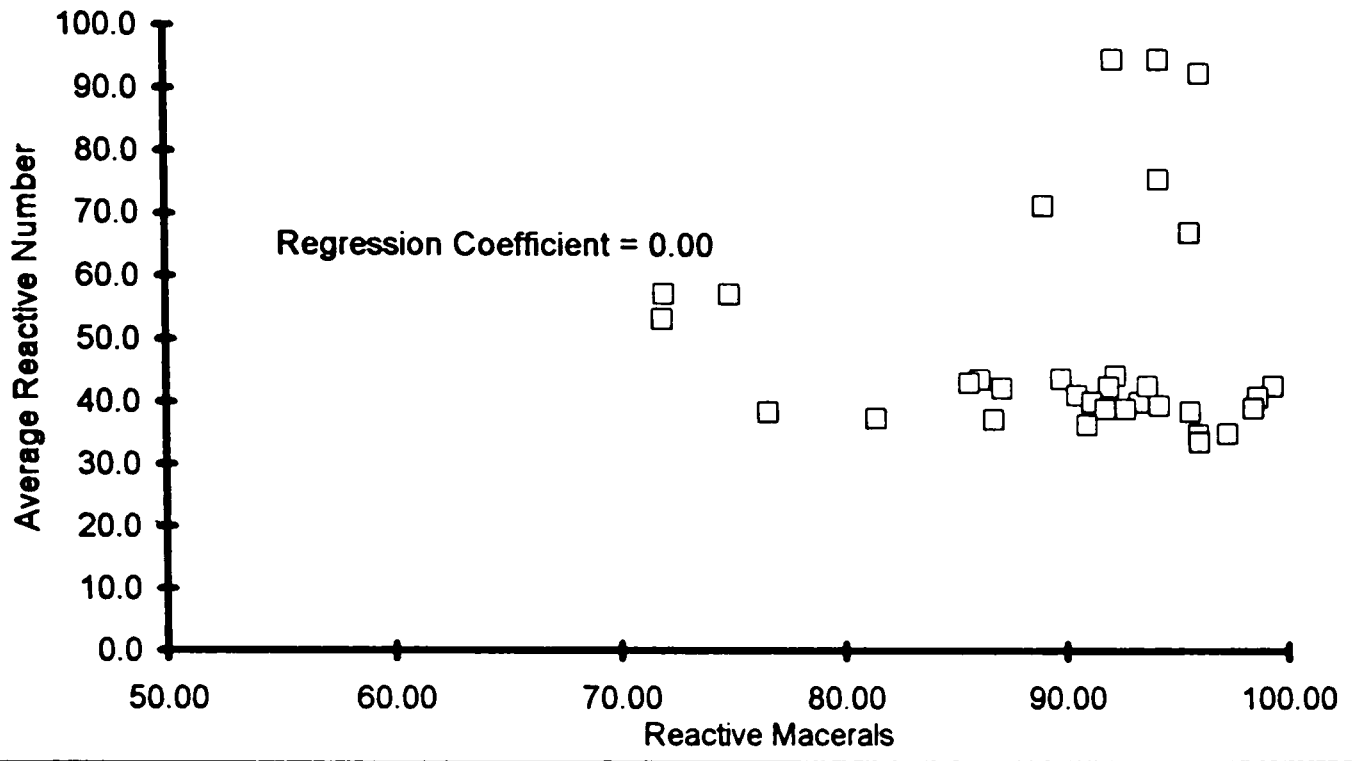


Figure 5.5.4 Fuel Ratio against Reactive Macerals

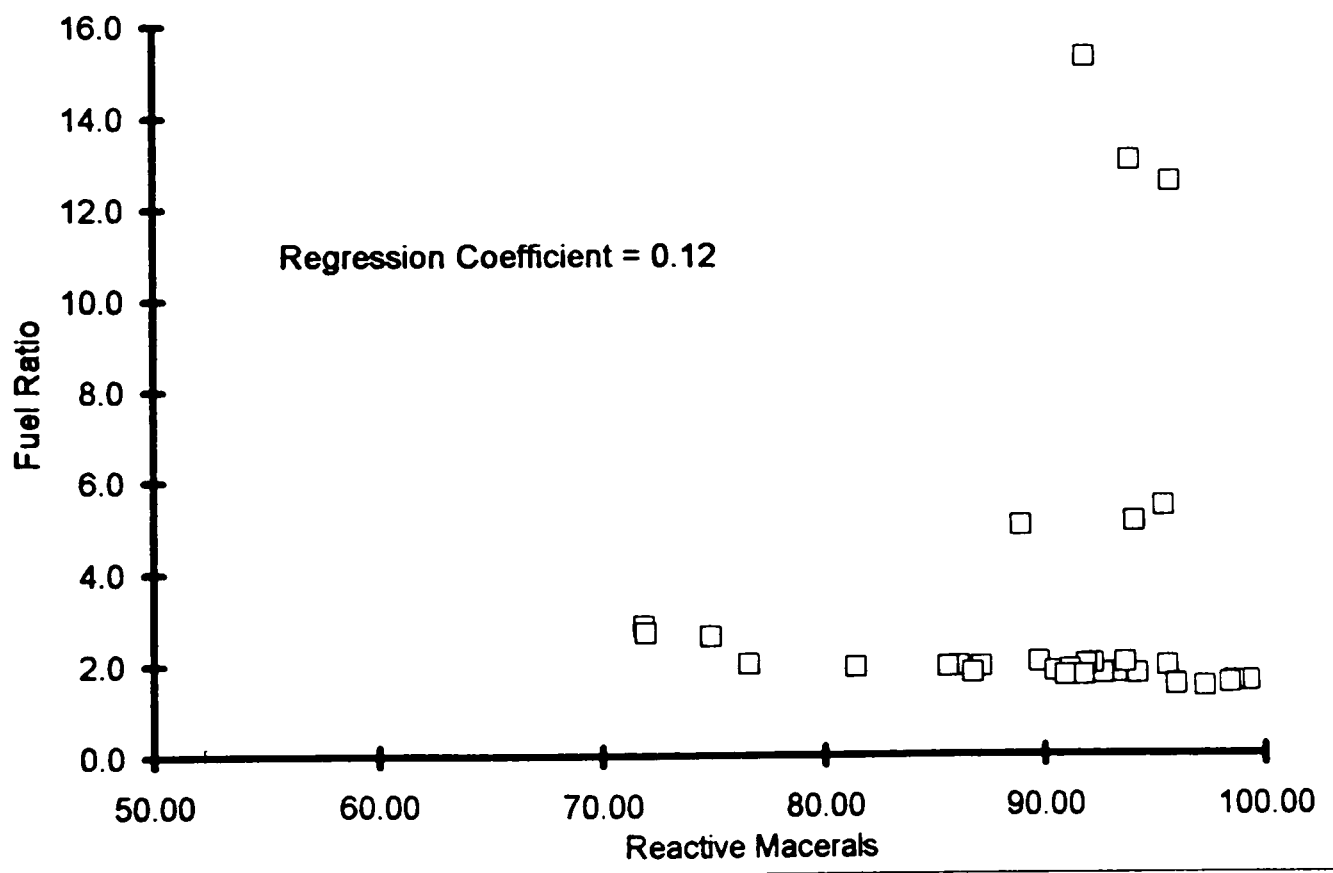


Figure 5.5.5 Rank against Reactive Number

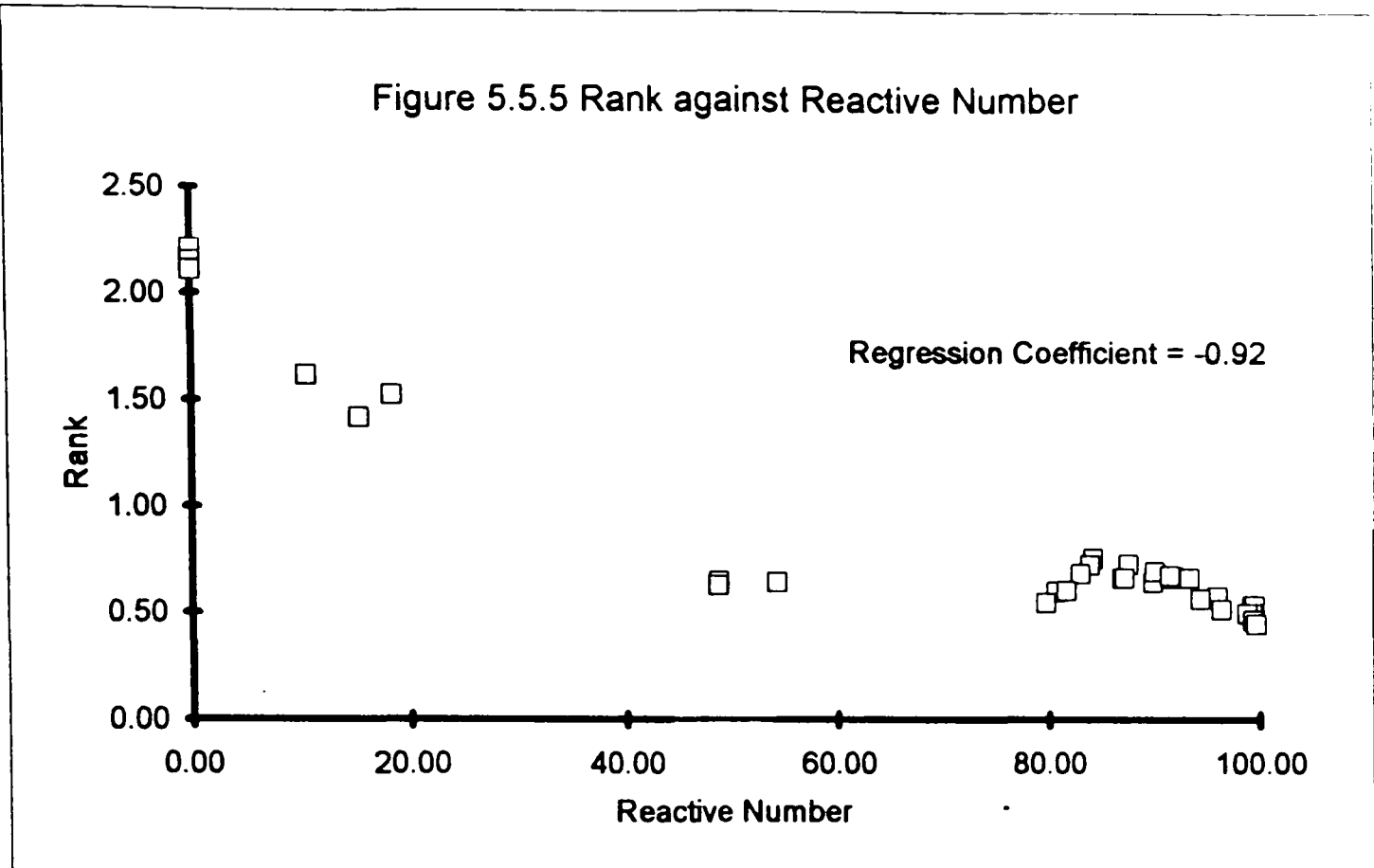


Figure 5.5.6 Average Reactive Number against Rank

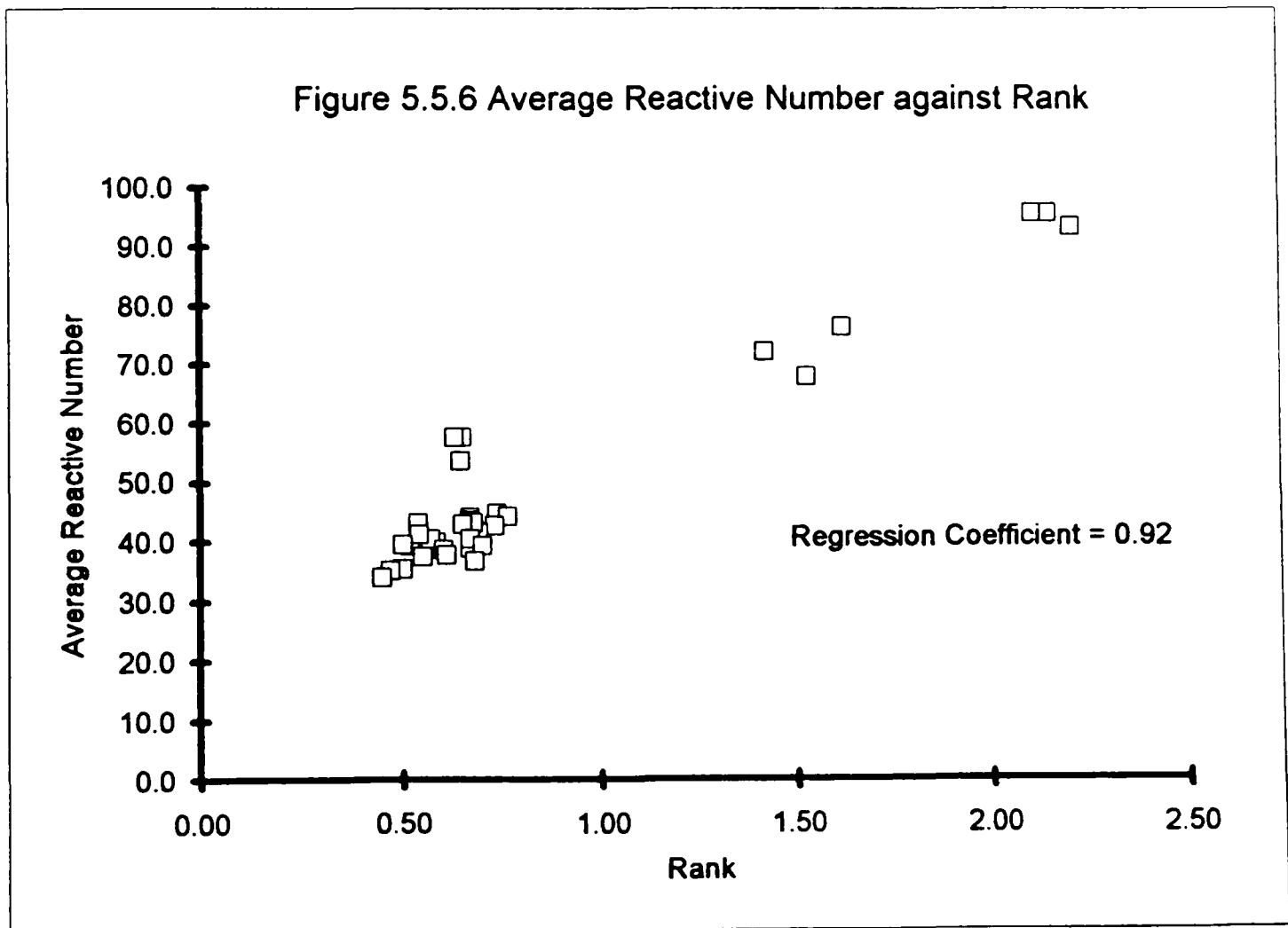


Figure 5.5.7 Fuel Ratio against Rank

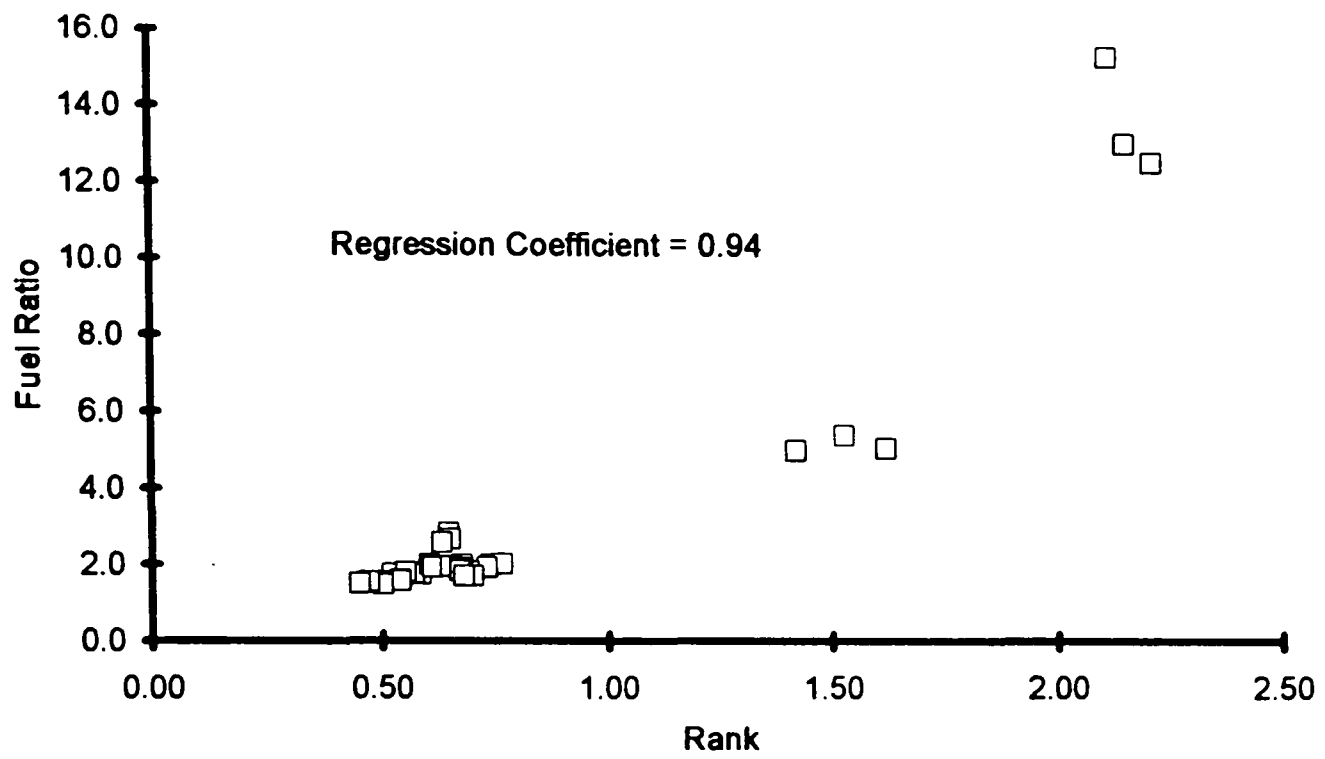


Figure 5.5.8 Fuel Ratio against Reactive Number

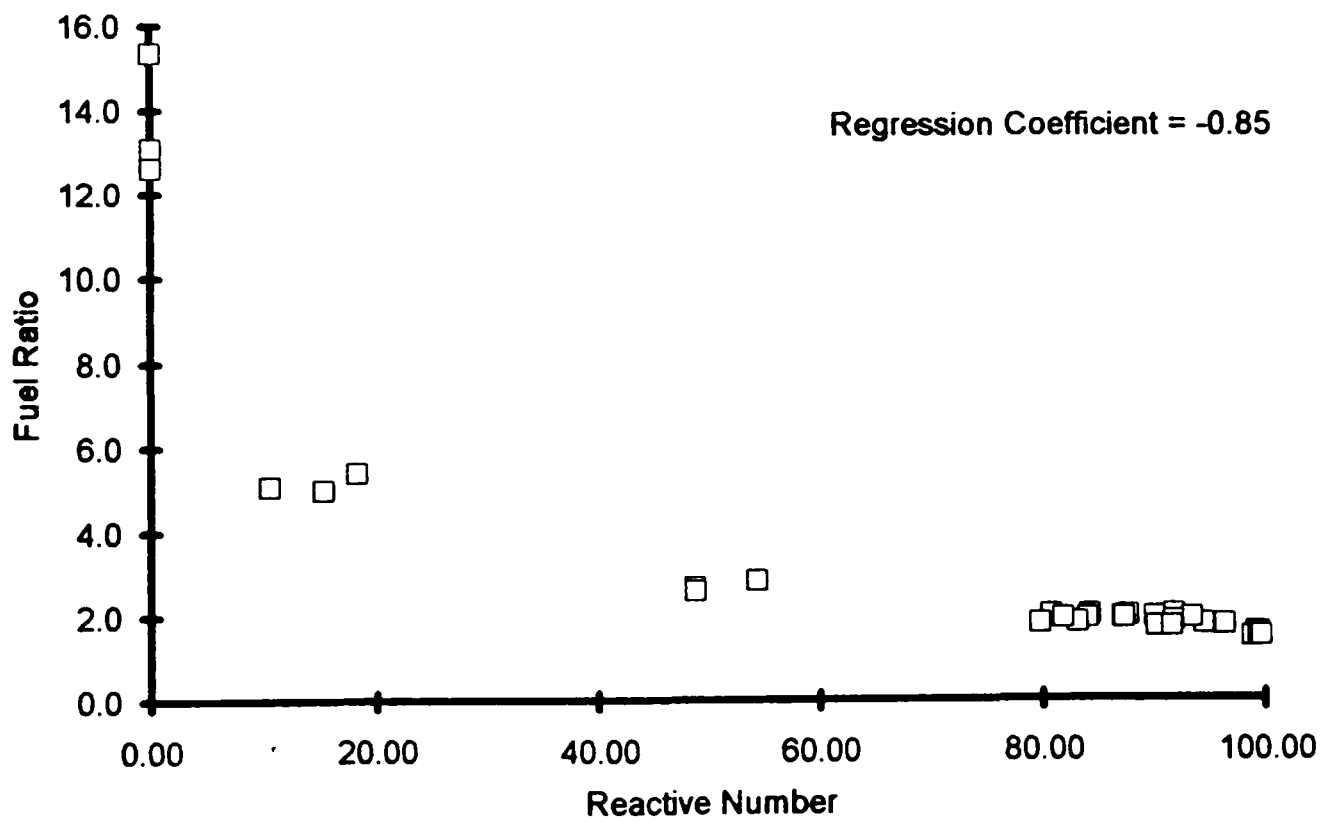




Figure 5.6.1 The correlation of Reactive Number and ACA {3}

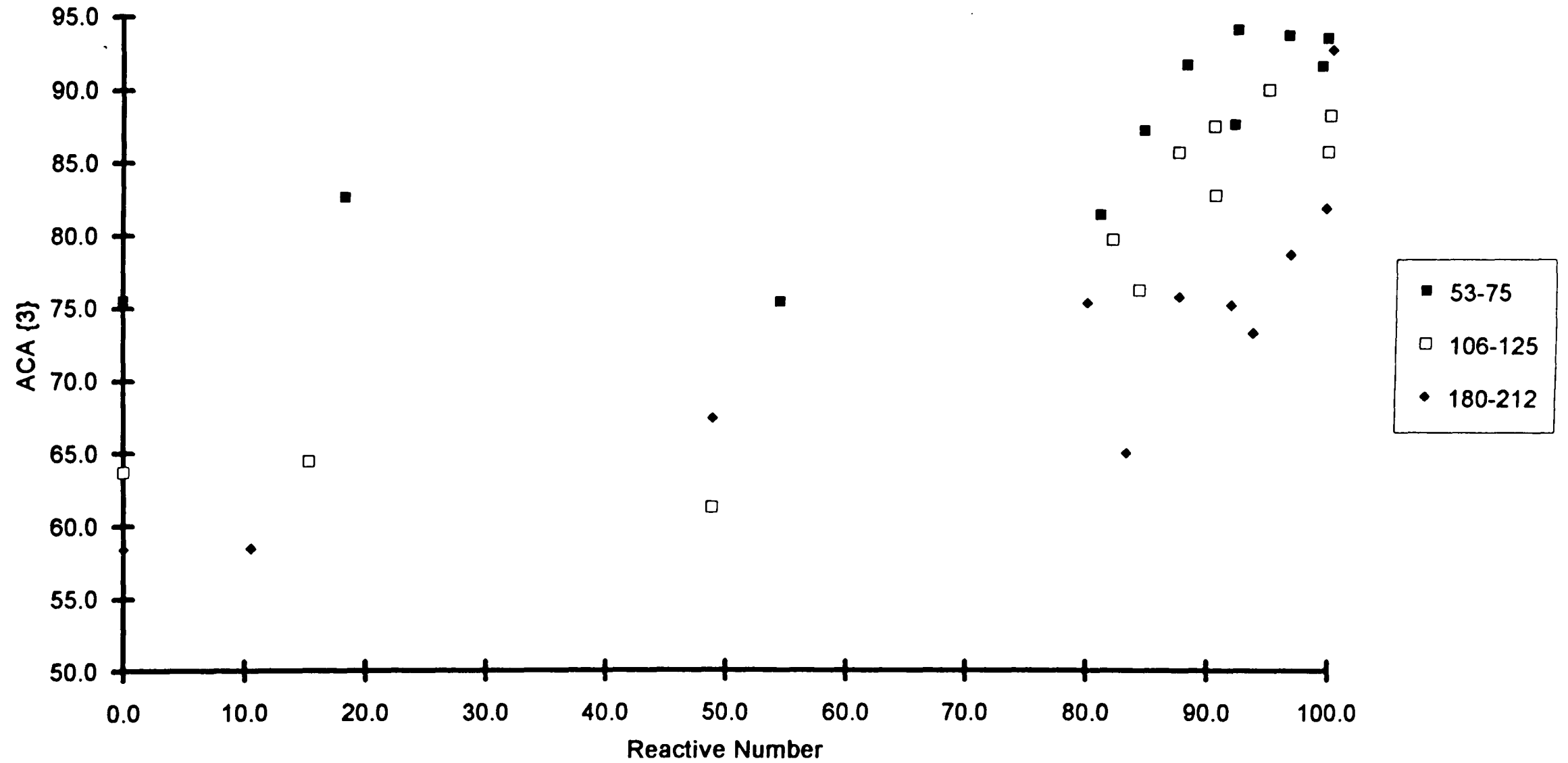


Figure 5.6.2 - The correlation of Reactive Number with ACA {5}

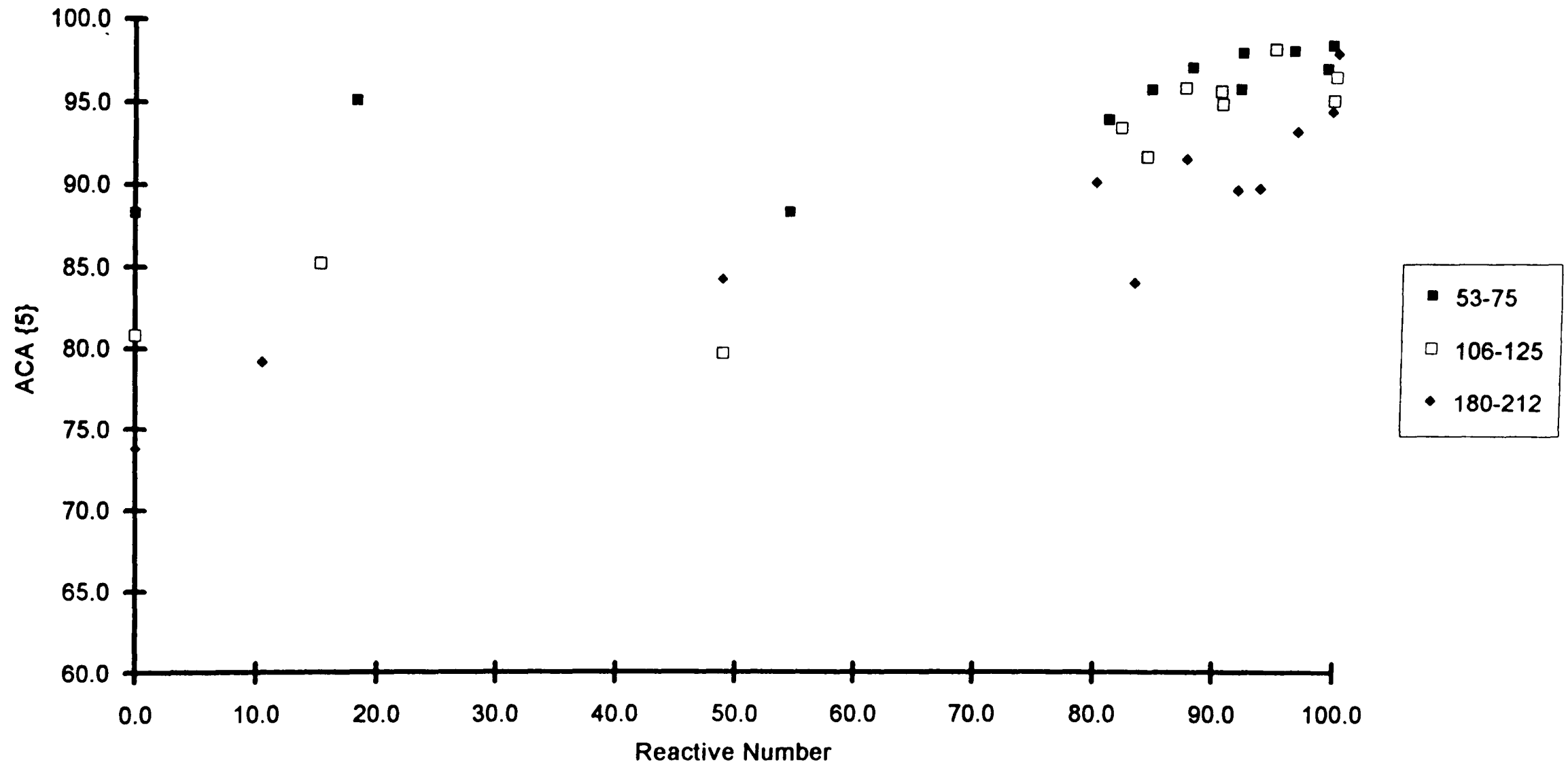


Figure 5.6.2 - The correlation of Reactive Number with ACA {95%}

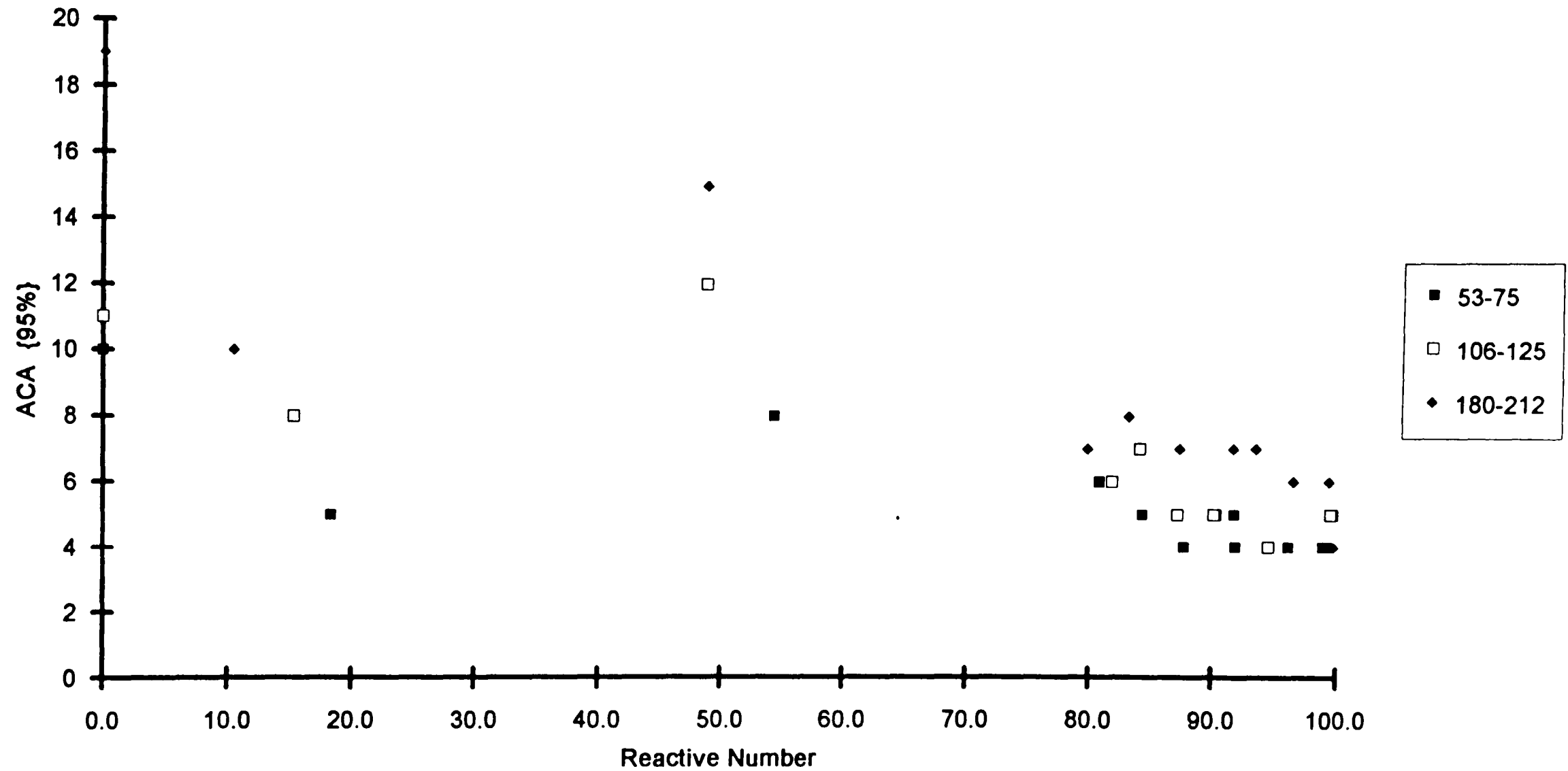


Figure 5.7.1 9 Coals : The correlation of Reactive Number and ACA {3}

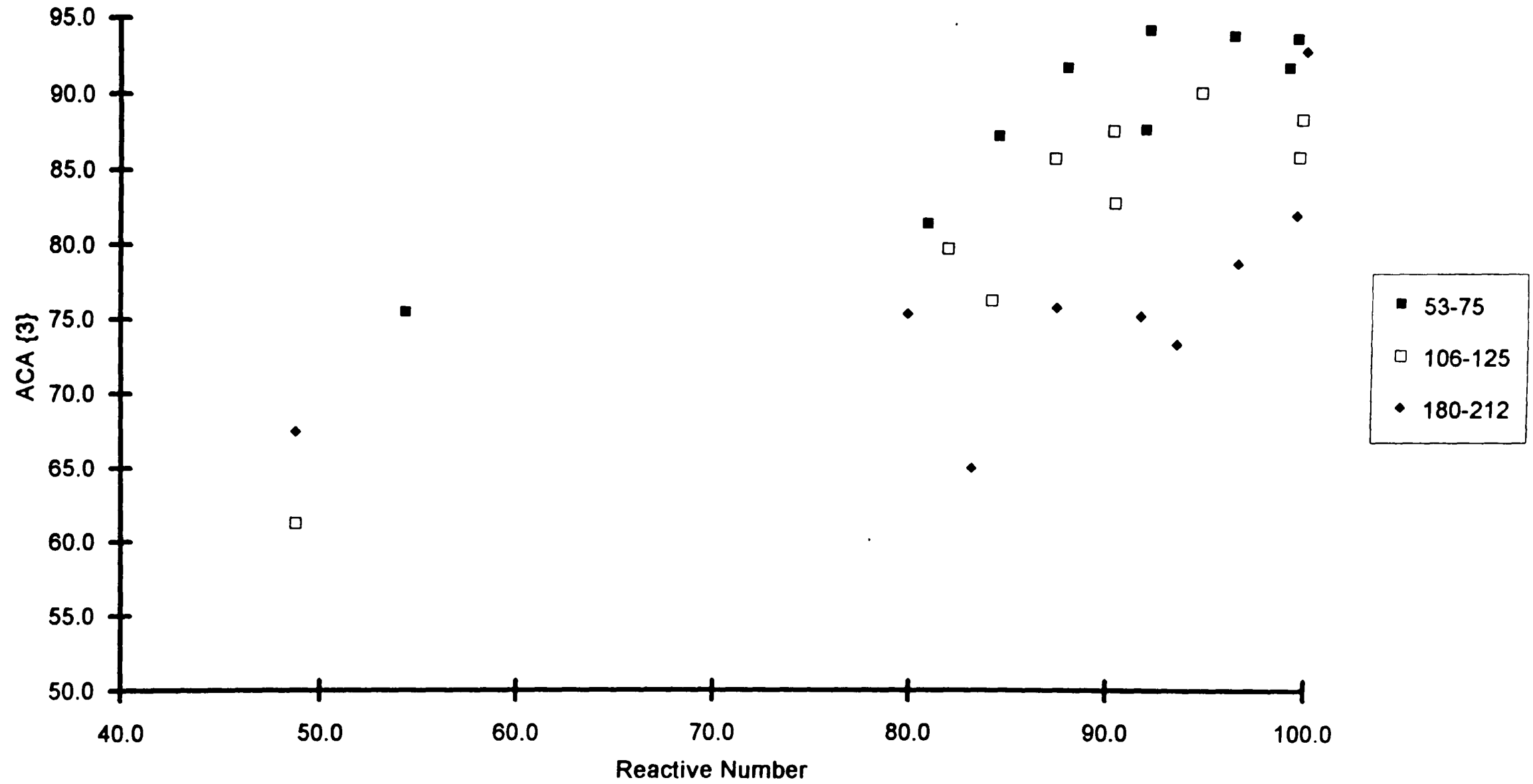


Figure 5.7.2 9 Coals : the correlation of Reactive Number with ACA {5}

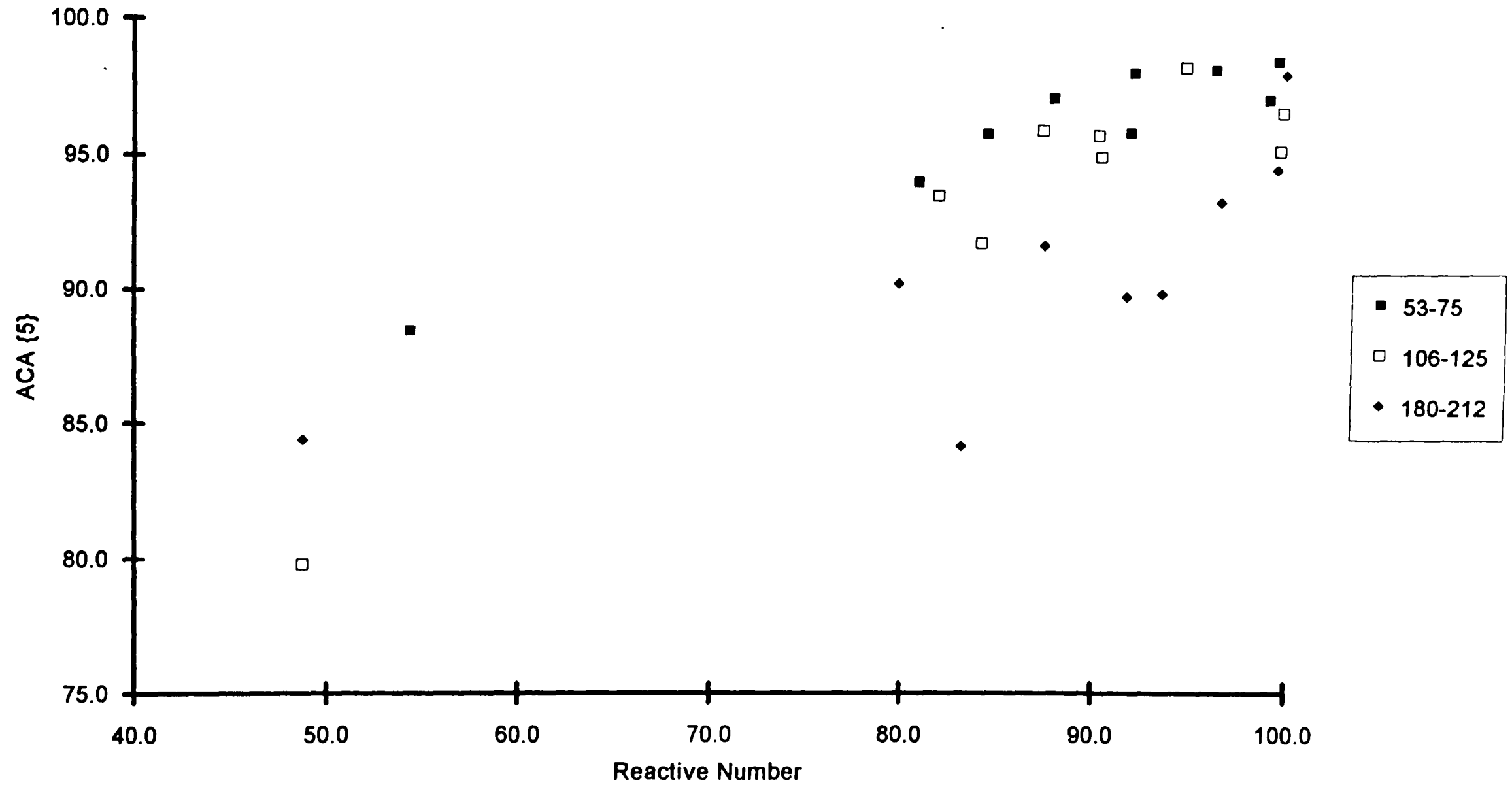


Figure 5.7.3 9 Coals : The correlation of Reactive Number with ACA {95%}

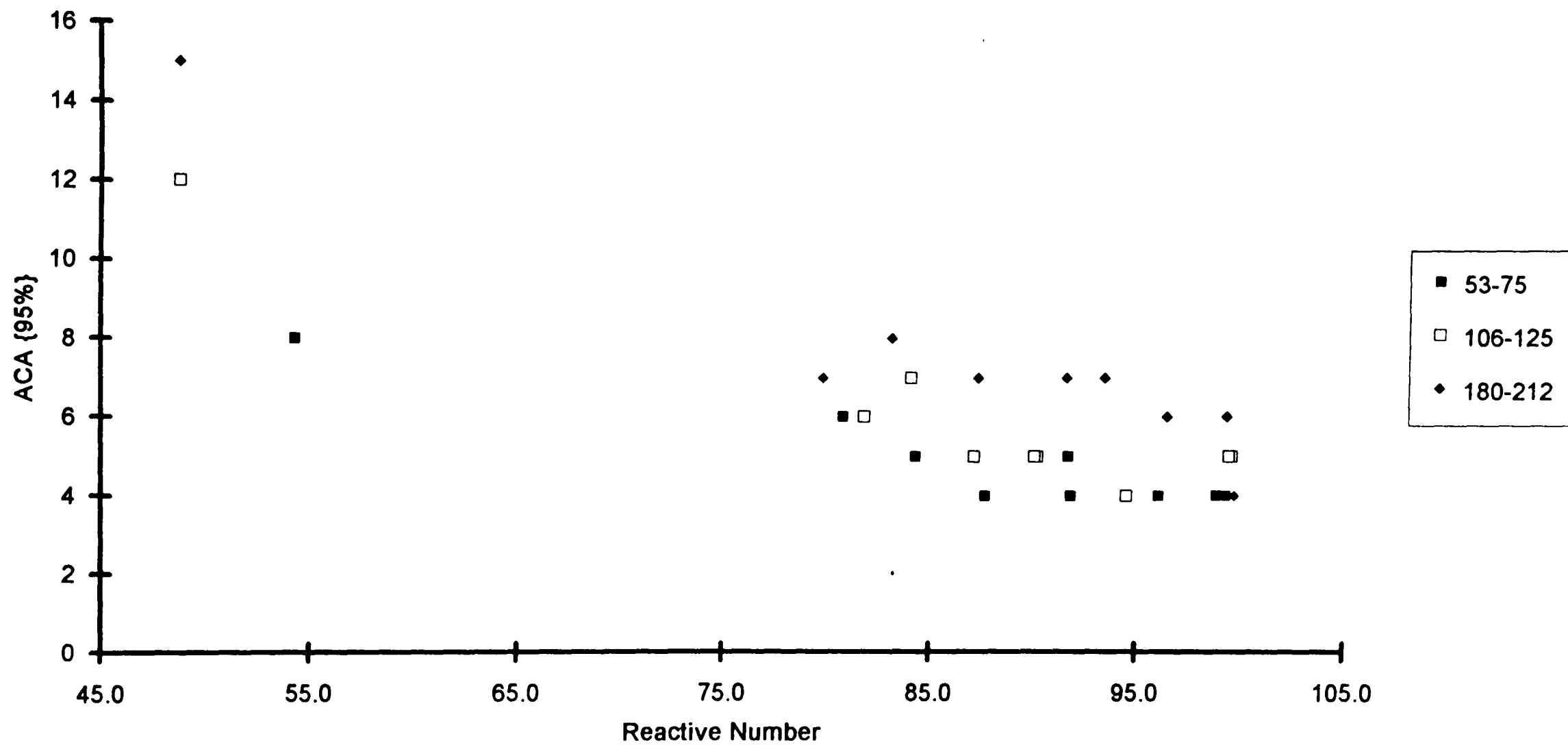


Table 5.3.1 The Rank results for the 11 coals

	<b>Bentinck</b>	<b>st. dev.</b>	<b>Drummond</b>	<b>st. dev.</b>	<b>El Cerrojon</b>	<b>st. dev.</b>	<b>China SSM</b>	<b>st. dev.</b>
53-75	0.68	0.05	0.76	0.07	0.58	0.07	0.60	0.06
106-125	0.65	0.07	0.73	0.09	0.57	0.04	0.61	0.05
180-212	0.67	0.06	0.69	0.09	0.52	0.06	0.55	0.06
	<b>McQuarie</b>	<b>st. dev.</b>	<b>Kaltim Prima</b>	<b>st. dev.</b>	<b>Kellingley</b>	<b>st. dev.</b>	<b>Pinang</b>	<b>st. dev.</b>
53-75	0.74	0.07	0.54	0.05	0.67	0.09	0.50	0.07
106-125	0.67	0.09	0.54	0.06	0.70	0.07	0.47	0.09
180-212	0.67	0.08	0.50	0.05	0.68	0.08	0.45	0.03
	<b>Kromdraai</b>	<b>st. dev.</b>	<b>Island Creek</b>	<b>st. dev.</b>	<b>Tower</b>	<b>st. dev.</b>		
53-75	0.65	0.10	1.53	0.13	2.21	0.25		
106-125	0.65	0.10	1.42	0.13	2.15	0.17		
180-212	0.63	0.06	1.62	0.10	2.11	0.24		

Table 5.3.2 Description of the Coals Used in Chapter 5.

Coal Name	Description
Kromdraai	Contains a large amount of inertinite most of which has a high reflectance
Drummond	Similar to British coals like Kellingley but with a higher inertinite content
Island Creek	A low volatile, high Ranked American coal which has a high vitrinite percentage
McQuarie	An Australian coal and it is mainly vitrinite with a similar Rank to some British coals.
El Cerrejon	Similar vitrinite content to McQuarie but with a lower Rank value
Bentinck	A good British coal with typical maceral content for a British coal.
Kellingley	Similar to Bentinck but with a higher liptinite percentage
Pinang	A low Ranked, low ash Indonesian coal.
Kaltim Prima	Very high vitrinite levels, like in Pinang, but with a slightly higher Rank
China SSM	A coal with high inertinite although a higher proportion of this maceral group is low reflectance semi fusinite
Tower	A Welsh anthracite

Table 5.3.3 Maceral Analysis Results for all 11 coals in 3 size fraction as determined by Image Analysis Methods

53-75 fraction

	Bentinck	Drummond	El Cerrejon	Island Creek	Kaltim Prima	McQuarie	Pinang	China SSM	Kellingley	Kromdraai	Tower
Liptinite	3.7	3.9	0.7	0.3	1.9	3.1	1.6	6.6	7.3	5.9	0.2
Vitrinite	90.7	85.8	94.8	95.7	97.4	89.8	96.5	62.1	86.6	62.1	93.9
Inertinite	5.6	10.3	4.5	4.0	0.7	7.1	1.9	31.3	6.1	31.9	6.0
Total	100.0	100.0	100.0	100.0	100.0	100.0	100.0	100.0	100.0	100.0	100.0

106-125 fraction

	Bentinck	Drummond	El Cerrejon	Island Creek	Kaltim Prima	McQuarie	Pinang	China SSM	Kellingley	Kromdraai	Tower
Liptinite	6.8	7.6	2.2	0.1	1.7	4.4	1.8	9.9	8.3	2.8	0.1
Vitrinite	84.0	77.7	89.9	87.9	97.0	77.9	93.8	65.2	83.7	57.3	90.6
Inertinite	9.2	14.7	7.9	12.0	1.3	17.7	4.4	24.9	8.0	39.9	9.3
Total	100.0	100.0	100.0	100.0	100.0	100.0	100.0	100.0	100.0	100.0	100.0

180-212 fraction

	Bentinck	Drummond	El Cerrejon	Island Creek	Kaltim Prima	McQuarie	Pinang	China SSM	Kellingley	Kromdraai	Tower
Liptinite	12.5	9.9	2.1	0.0	3.7	6.9	3.7	14.1	12.2	5.2	0.1
Vitrinite	83.0	76.1	88.9	92.1	96.1	78.6	94.6	67.8	76.4	54.0	92.1
Inertinite	4.5	14.0	9.0	7.9	0.2	14.5	1.7	18.1	11.4	40.8	7.8
Total	100.0	100.0	100.0	100.0	100.0	100.0	100.0	100.0	100.0	100.0	100.0

Table 5.4.1 The Collection Efficiency Results for all Chars

Char Type	Size	A	B
Kromdraai	53-75	93.0	90.3
	106-125	107.9	82.5
	180-212	75.7	50.0
Kellingley	53-75	99.7	89.9
	106-125	58.6	46.3
	180-212	59.5	50.3
Tower	53-75	105.9	93.8
	106-125	111.2	90.7
	180-212	58.3	56.6
McQuarie	53-75	96.6	87.6
	106-125	93.9	78.0
	180-212	62.7	63.2
El Cerrejon	53-75	89.4	104.9
	106-125	71.4	64.0
	180-212	43.9	35.8
Drummond	53-75	85.5	84.7
	106-125	77.2	73.4
	180-212	54.5	52.3
China SSM	53-75	95.9	92.9
	106-125	71.9	89.5
	180-212	67.8	69.0
Bentinck	53-75	99.3	85.8
	106-125	91.6	94.2
	180-212	36.4	26.0
Island Creek	53-75	75.2	84.3
	106-125	71.5	61.7
	180-212	35.5	35.5
Pinang	53-75	65.4	63.4
	106-125	58.2	61.3
	180-212	60.2	61.4
Kaltim Prima	53-75	53.1	72.0
	106-125	43.2	61.0
	180-212	57.0	52.6

Table 5.4.2 - The R factor results from all the chars

Size	Bentinck		Island Creek*		McQuarie		Kromdraai		Kellingley	
53-75	1.89	1.59	0.65	1.66	1.90	1.76	1.66	1.59	1.79	1.66
106-125	1.65	1.78	0.29	-0.24	1.71	1.37	1.97	1.49	0.57	0.37
180-212	-0.33	-1.76	-4.51	-3.03	1.09	1.10	1.46	1.06	0.99	1.24
	Drummond		China		Pinang*		El Cerrejon*		Tower*	
53-75	1.60	1.58	1.84	1.74	1.49	1.37	1.63	1.85	3.13	1.08
106-125	1.41	1.34	1.32	1.61	1.16	1.30	1.18	1.00	4.17	2.66
180-212	1.28	0.98	1.25	1.29	1.31	1.26	0.42	-0.18	1.50	2.16
	Kaltim Prima*									
53-75	0.95	0.93								
106-125	0.51	0.73								
180-212	1.12	0.63								

\* indicates coals and chars with values around or below 5%

Table 5.4.3 The Tenui-Char % Results

Coal Type	53-75 micron		106-125 micron		180-212 micron	
	A	B	A	B	A	B
Kromdraai	35.5	32.2	20.3	23.2	11.5	12.9
China SSM	41.7	43.8	26.6	25.6	16.9	14.8
McQuarie	63.2	78.0	23.6	23.9	5.4	6.7
Pinang	91.4	88.5	94.0	96.3	88.6	86.4
Kellingley	51.1	50.4	13.8	13.0	7.2	8.5
Bentinck	88.6	91.1	44.7	40.0	22.2	19.2
El Cerrejon	70.4	71.8	49.1	35.3	4.5	2.7
Kaltim Prima	66.8	61.8	61.6	65.6	32.8	33.6
Tower	65.6	69.7	54.7	62.8	29.8	27.3
Island Creek	50.2	60.5	18.9	11.3	4.0	3.9
Drummond	68.6	68.0	24.0	16.0	12.7	3.3

Table 5.4.4 The Spheres % Results

Coal Type	53-75 micron		106-125 micron		180-212 micron	
	A	B	A	B	A	B
Kromdraai	25.3	32.0	32.2	33.9	18.6	19.5
China SSM	79.4	71.8	71.4	71.3	49.9	47.1
McQuarie	75.1	68.1	86.3	81.3	77.2	72.8
Pinang	11.6	10.7	6.5	2.8	11.4	7.2
Kellingley	78.5	79.8	85.0	79.3	74.6	76.9
Bentinck	81.3	73.8	82.2	75.8	55.9	51.4
El Cerrejon	92.7	94.0	80.8	81.3	53.5	48.6
Kaltim Prima	86.1	92.4	87.9	86.9	29.3	26.7
Tower	11.2	13.0	6.3	5.1	3.0	0.8
Island Creek	83.8	82.2	74.3	73.9	75.7	71.3
Drummond	83.6	87.2	80.3	77.4	57.2	56.6

Table 5.4.5 The Solids % Results

Coal Type	53-75 micron		106-125 micron		180-212 micron	
	A	B	A	B	A	B
Kromdraai	9.2	11.6	15.7	13.5	3.7	7.8
China SSM	2.6	3.8	4.5	2.7	1.5	2.5
McQuarie	3.5	3.1	2.3	2.5	3.9	2.7
Pinang	0.2	0.5	0.3	0.8	0.7	0.7
Kellingley	2.1	1.7	0.5	1.4	2.1	2.7
Bentinck	2.5	2.0	1.4	0.7	7.0	1.2
El Cerrejon	0.7	3.1	0.2	2.0	2.3	4.5
Kaltim Prima	0.7	0.2	0.5	0.7	0.5	0.7
Tower	6.7	5.3	7.0	5.9	15.9	15.0
Island Creek	5.8	2.7	3.9	3.5	4.6	5.6
Drummond	5.7	1.6	2.0	4.0	1.3	2.8

Table 5.4.6 ACA Char Analysis results for all the chars in Chapter 5

Size Fraction	ACA	Kromdraal	Kellingley	Tower	China	Bentinck	Island Creek	McQuarie	El Cerrejon	Drummond	Pinang	Kaltim Prima
53-75	{3}	75.6	87.8	75.5	81.6	94.3	82.7	91.9	93.9	87.4	91.8	93.7
	{5}	88.5	95.9	88.3	94.1	98.1	95.2	97.2	98.2	95.9	97.1	98.5
	95%	8	5	10	6	4	5	4	4	5	4	4
106-125	{3}	61.3	82.9	63.7	79.9	87.7	64.5	85.9	90.2	76.4	85.9	88.4
	{5}	79.8	95.0	80.8	93.6	95.8	85.3	96.0	98.3	91.8	95.2	96.6
	95%	12	5	11	6	5	8	5	4	7	5	5
180-212	{3}	67.5	75.3	58.4	75.5	73.4	58.5	75.9	78.8	65.1	92.9	82.0
	{5}	84.4	89.8	73.8	90.3	89.9	79.2	91.7	93.3	84.2	98.0	94.5
	95%	15	7	19	7	7	10	7	6	8	4	6

Table 5.4.7 A Results for the Intrinsic Reactivity Measurements of the Size Fractionated Char Samples

		Kromdraai	Tower	Pinang	Drummond	Kellingley	Island Creek	Kaltim Prima	China	McQuarie	El Cerrojon	Bentinck
53-75 micron	Peak Temperature	547	581	497	528	523	565	514	529	507	529	513
	Burnout Point	625	690	599	614	606	673	617	606	608	628	605
106-125 micron	Peak Temperature	597	658	510	554	558	644	580	557	542	606	557
	Burnout Point	632	698	556	624	628	682	625	627	619	629	610
180-212 micron	Peak Temperature	604	677	510	534	540	627	542	557	539	554	557
	Burnout Point	632	696	595	614	613	665	617	609	615	616	603

Table 5.5.1 The Prediction Parameter Results

Size	El Cerrejon	McQuarie	Drummond	China SSM	Kaltim Prima	Island Creek	Bentinck	Pinang	Kromdraai	Kellingley	Tower
<b>Fraction</b>	<b>REACTIVE MACERALS</b>										
53-75	94.2	92.2	89.8	76.5	99.3	95.5	93.7	97.3	71.8	91.2	96.0
106-125	93.3	86.1	87.1	81.4	98.6	89.0	91.9	96.0	71.9	91.8	94.1
180-212	92.7	85.6	90.5	86.7	98.5	94.2	95.6	96.0	74.8	90.9	92.1
	<b>RANK</b>										
53-75	0.58	0.74	0.76	0.60	0.54	1.53	0.68	0.50	0.65	0.67	2.21
106-125	0.57	0.67	0.73	0.61	0.54	1.42	0.65	0.47	0.65	0.70	2.15
180-212	0.52	0.67	0.69	0.55	0.50	1.62	0.67	0.45	0.63	0.68	2.11
	<b>REACTIVE NUMBER</b>										
53-75	96.1	87.7	84.3	80.8	99.3	18.3	91.9	98.9	54.3	91.7	0.0
106-125	94.5	87.1	84.0	81.8	99.6	15.3	90.1	99.4	48.8	90.2	0.0
180-212	96.4	87.3	83.1	79.8	99.3	10.5	93.4	99.7	48.7	91.6	0.0
	<b>AVERAGE REACTIVE NUMBER</b>										
53-75	39.9	44.7	44.2	43.1	38.6	67.6	43.1	35.4	53.5	40.4	93.1
106-125	40.4	44.0	42.6	41.2	37.7	71.9	42.9	35.2	57.5	39.3	95.3
180-212	39.3	43.5	41.5	39.5	37.5	76.1	38.9	34.0	57.5	36.7	95.4
	<b>FUEL RATIO</b>										
53-75	1.8	2.0	2.0	2.0	1.6	5.4	2.0	1.5	2.8	1.8	12.6
106-125	1.8	1.9	1.9	1.9	1.6	5.0	2.0	1.5	2.7	1.7	13.1
180-212	1.8	1.9	1.8	1.8	1.5	5.1	1.9	1.5	2.6	1.7	15.4

Table 5.6.1 The correlation data between all prediction parameters and char analysis results for the 53-75 micron chars

	Reac.Mac.	Rank	Av. Re.Num.	Fuel Ratio	TenuiChars%	Spheres%	Solid%	{3}	{5}	{95%}	Peak Temp	Burn. Temp
Reac. Num.	0.05	-0.93	-0.97	-0.90	0.31	0.41	-0.63	0.80	0.75	-0.78	-0.94	-0.93
Reac. Mac.		0.25	0.06	0.17	0.74	0.12	-0.68	0.57	0.54	-0.40	-0.14	0.21
Rank			0.97	0.97	-0.04	-0.36	0.37	-0.60	-0.59	0.69	0.86	0.93
Av. Re. Num.				0.97	-0.18	-0.44	0.56	-0.73	-0.74	0.81	0.91	0.93
Fuel Ratio					-0.05	-0.50	0.42	-0.65	-0.69	0.80	0.84	0.90
TenuiChar						-0.07	-0.61	0.68	0.56	-0.46	-0.45	-0.16
Sphere							-0.41	0.51	0.65	-0.62	-0.23	-0.25
Solids								-0.83	-0.87	0.76	0.65	0.43
{3}									0.96	-0.91	-0.81	-0.60
{5}										-0.97	-0.75	-0.57
{95%}											0.80	0.64
Peak T.												0.92

Table 5.6.2 - The correlation data between all prediction parameters and char analysis results for the 106-125 micron chars

	Reac.Mac.	Rank	Av. Re.Num.	Fuel Ratio	TenuiChars	Spheres	Solid	{3}	{5}	{95%}	Peak T.	Burnout. T.
Reac. Num.	0.21	-0.85	-0.97	-0.86	0.18	0.45	-0.57	0.89	0.89	-0.81	-0.84	-0.93
Reac. Mac.		0.03	-0.08	0.13	0.61	0.03	-0.79	0.53	0.49	-0.54	-0.02	0.02
Rank			0.78	0.63	-0.27	-0.10	0.17	-0.67	-0.59	0.45	0.75	0.86
Av. Re. Num.				0.94	-0.07	-0.49	0.50	-0.81	-0.83	0.78	0.84	0.93
Fuel Ratio					0.13	-0.56	0.32	-0.63	-0.69	0.65	0.74	0.87
TenuiChar						-0.58	-0.29	0.32	0.19	-0.17	-0.20	-0.19
Sphere							-0.43	0.47	0.57	-0.57	-0.14	-0.26
Solids								-0.80	-0.85	0.90	0.41	0.34
{3}									0.98	-0.95	-0.65	-0.73
{5}										-0.98	-0.66	-0.71
{95%}											0.60	0.63
Peak T.												0.92

Table 5.6.3 - The correlation data between all prediction parameters and char analysis results for the 180-212 micron chars

	Reac.Mac.	Rank	Av. Re.Num.	Fuel Ratio	TenuiChars	Spheres	Solid	{3}	{5}	{95%}	Peak T.	Burnout. T.
Reac. Num.	0.20	-0.92	-0.98	-0.82	0.22	0.22	-0.82	0.83	0.92	-0.85	-0.87	-0.76
Reac. Mac.		0.11	-0.12	0.05	0.37	0.00	-0.15	0.27	0.22	-0.43	-0.05	0.23
Rank			0.96	0.92	-0.15	-0.17	0.87	-0.77	-0.88	0.76	0.83	0.89
Av. Re. Num.				0.91	-0.17	-0.29	0.90	-0.79	-0.91	0.88	0.89	0.85
Fuel Ratio					0.01	-0.45	0.95	-0.62	-0.79	0.83	0.84	0.82
TenuiChar						-0.64	-0.13	0.63	0.41	-0.23	0.21	-0.13
Sphere							-0.40	-0.14	0.10	-0.43	-0.57	-0.15
Solids								-0.68	-0.82	0.91	0.82	0.77
{3}									0.96	-0.76	-0.50	-0.64
{5}										-0.87	-0.70	-0.74
{95%}											0.78	0.65
Peak T.												0.70



Table 5.7.2 - 9 Coals: The correlation data between all prediction parameters and char analysis results for the 106-125 micron chars

	Reac.Mac.	Rank	Av. Re.Num.	Fuel Ratio	TenuiChars	Spheres	Solid	{3}	{5}	{95%}	Peak T.	Burnout. T.
Reac. Num.	0.95	-0.43	-0.96	-0.97	0.54	0.26	-0.98	0.94	0.95	-0.95	-0.40	-0.49
Reac. Mac.		-0.46	-0.88	-0.92	0.61	0.20	-0.89	0.88	0.84	-0.84	-0.27	-0.47
Rank			0.45	0.46	-0.91	0.52	0.26	-0.39	-0.29	0.29	0.15	0.46
Av. Re. Num.				0.99	-0.54	-0.14	0.94	-0.84	-0.88	0.89	0.49	0.47
Fuel Ratio					-0.55	-0.18	0.94	-0.86	-0.89	0.89	0.44	0.44
TenuiChar						-0.55	-0.38	0.44	0.34	-0.34	-0.38	-0.72
Sphere							-0.37	0.38	0.45	-0.41	0.37	0.48
Solids								-0.94	-0.97	0.97	0.42	0.45
{3}									0.98	-0.98	-0.24	-0.42
{5}										-1.00	-0.28	-0.35
{95%}											0.32	0.38
Peak T.												0.80

Table 5.7.3 - 9 Coals: The correlation data between all prediction parameters and char analysis results for the 180-212 micron chars

	Reac.Num.	Reac. Mac.	Rank	Av. Re.Num.	Fuel Ratio	TenuiChars	Spheres	Solid	{3}	{5}	{95%}	Peak T.	Burnout. T.
Reac. Num.	0.94		-0.37	-0.94	-0.93	0.36	0.17	-0.70	0.65	0.75	-0.96	-0.48	0.21
Reac. Mac.			-0.39	-0.90	-0.89	0.42	-0.02	-0.72	0.58	0.66	-0.87	-0.40	0.19
Rank				0.37	0.48	-0.67	0.70	0.53	-0.81	-0.77	0.44	-0.39	0.27
Av. Re. Num.					0.97	-0.42	-0.14	0.80	-0.64	-0.69	0.96	0.43	0.06
Fuel Ratio						-0.45	-0.06	0.91	-0.68	-0.73	0.96	0.44	0.00
TenuiChar							-0.68	-0.55	0.82	0.68	-0.45	0.51	-0.19
Sphere								0.14	-0.42	-0.26	-0.15	-0.78	0.21
Solids									-0.62	-0.61	0.78	0.33	0.11
{3}										0.97	-0.70	0.25	-0.11
{5}											-0.78	0.07	-0.04
{95%}												0.41	0.03
Peak T.													-0.30

# CHAPTER 6 CONCLUSIONS AND RECOMMENDATIONS FOR FURTHER WORK

## 6.1 Particle Size

The most apparent effect of particle size is that the largest particles, from 180 to 212 microns, have the poorest performance out of the three size ranges. The main reason for the higher volatile content, lower R factor and thicker char walls is probably linked to the rate of heating in larger particles. The volume ratio of 180-212 to the 106-125 particles is approximately 5 and to 53-75 particles it is 28. It is reasonable to assume that these bigger particles will be slower to heat up simply due to their increased volume. If the same size ranges were heated with the same high temperature conditions except with a much longer residence time of say 20 seconds, it is possible that all three size ranges would form similar char types. All the DTF experiments in Chapter 5 used 100 milliseconds residence time, and this shows distinct differences between the largest size range with the other two. The differences between the 106-125 and 53-75 in some cases were small but the smallest fraction generally showed some tendency to form the thinner more vesiculated chars.

Particle size affected char types formed from the different maceral types and in some ways masked the effect of maceral type. Only the high reflectance inertinite, common in Northern Hemisphere coals, did not really vesiculate in any size. The presence of large particles could mask the effect of macerals, which is why tight size bands were used in all experiments.

It is not clear what kinetics determine char combustion i.e. mass transfer or chemical reactivity, but it is clear that the amount of material present in the flame will be an important factor in determining the time required for combustion. As mentioned previously, the larger particles may eventually form vesiculated chars similar to smaller particles, but this may take longer than is available in the furnace. This is possibly why some workers have successfully

linked particle size with burnout performance (Shibaoka, 1986, 1989c, 1985, Williamson & Cooke, 1991).

## 6.2 Intrinsic Reactivity

The results from the intrinsic reactivity tests were less conclusive than expected. However coals with low Reactive Numbers did form unreactive chars. El Cerrejon gave an unpredictably unreactive char in some of the tests and this may be a reason for its apparent poor combustion performance in certain small scale rig tests (Vleeskens et al., 1993). Some of the chars which gave the most open structures also gave high peak temperatures and burnout temperatures. At this stage it is not possible to say whether chars with similar intrinsic reactivities will burn better, without further investigations.

## 6.3 Prediction Systems

### 6.3.1 Rank

Rank has been the best combustion parameter to date with Northern Hemisphere coals, since the reflectance of vitrinite does roughly correlate to its combustion behaviour. Since vitrinite is the major maceral type, and the inertinite generally has a high reflectance, the rank of these coals tends to be the most important petrographic factor.

Problems arise with Rank, as a prediction system, when analysing geologically unusual or different coals, predominantly from the Southern Hemisphere. The proportions of the macerals as well as the relationship of the semi-fusinite to the vitrinite is not straightforward. A prediction parameter based on only half the constituents of the coal, which may or may not relate to the other half, will tend to generate poor results.

### 6.3.2. Reactive Macerals

Results using the classical definition of what is and isn't reactive were very poor, especially over the full range of 11 coals. The limitation of relating Reactive Macerals to combustion is the same as with Rank. The problems with the system are as follows;

- The range of vitrinite - the use of Reactive Macerals would be restricted to groups of coals which shared a similar Rank value.
- The type of vitrinite - Pseudovitrinite is vitrinite but certainly not reactive.
- Inertinite can be up to 90% reactive (Thomas et al., 1991a), hence assuming that only 30% of semi-fusinite is reactive can give rise to anomalous results, especially if the sample contains 40-50% inertinite, as do some Australian coals.
- The subjective and costly nature of the maceral analysis also makes Reactive Macerals a doubtful proposition for a prediction parameter.

### 6.3.3 Fuel Ratio

The use of Fuel Ratio is not particularly useful when a coal contains a fraction of inert material which does not significantly alter its proximate analysis. In practice, a high volatile coal could be mixed with a low volatile coal to produce an apparently favourable Fuel Ratio. 'Designer Coals', which have been tailor made to fit a required proximate specification, would be difficult to detect using Fuel Ratio. A good example of this is an American coal used in burner trials in Sweden which, despite containing large quantities of Pseudovitrinite, was not detected as a problem using proximate analysis (Bengtsson, 1987).

If the integrity of a coal supply could be guaranteed, then it may be possible to use Fuel Ratio as a means of predicting combustion behaviour for a range of similar coals.

#### 6.3.4 Average Reactive Number

Average Reactive Number correlated reasonably well with the char results discussed in section 5.7. However, it was felt that Average Reactive Number did not provide the best means of interpreting the reflectance/fluorescence results, since the differences between coals like Kromdraai and Kellingley were minimised by the way that Average Reactive Number was calculated. i.e. for Average Reactive Number, Kromdraai gave 54, and Kellingley gave 40. With Reactive Number, Kromdraai gave 50% and Kellingley gave 90%.

#### 6.3.5 Reactive Number

Reactive Number gave the best correlation with the results from Automated Char Analysis, especially when considering isotropic chars. The Reactive Number was possibly the best prediction parameter for a number of reasons.

- *The speed of the analysis.* The analysis of a sample required less than 20 minutes, from receiving a polished coal block. This rapid analysis would be extremely useful in industry.
- *The objective nature of the analysis.* The method requires no subjective interpretation. Producing results is simple since the analysis begins with the calibration of the equipment using a light standard, making the threshold the same every time.
- *The simplicity of the analysis.* The method does not require a skilled operator to run the experiment. The software is user friendly and the procedure is relatively simple. For these reasons, the cost to perform this kind of analysis would be much lower than when contracting to a manual petrographer.
- *The ability to detect blends.* The method would detect contamination, oxidation or blending quite easily. The need to monitor supplies for consistency of a bulk order is imperative if one is to avoid costly mistakes.

For the reasons above, using the Reactive Number from the Reactivity Assessment Program, is one of the better means of characterising coals for combustion.

## 6.4 Image Analysis in Industry

This would depend, to some extent, on the changes occurring not only in the imported coal market, but also on the utilisation of coal in power generation. The current trend appears to be towards gas fired power stations, mainly due to cost. Despite the uncertainty that currently exists in Britain, the use of coal in power generation world wide is not really in any doubt. The use of image analysis to predict reactivity would probably not be important if a power station could guarantee the continuity and integrity of their coal supply. But if this is not possible, then image analysis could become a useful quality control tool, as well as a powerful means of characterising different coals for combustion. As mentioned in section 6.3, the image analyser has several assets when considering its use in an industrial environment i.e. speed, accuracy and operating cost.

The other benefits of Reactivity Assessment Program are the simplicity of interpreting the results, and its objectivity. Maceral Analysis has been considered a 'black art' for a long time, producing useful but inaccessible results. The petrographic nature of a coal may be incorporated in discussion in the power industry if results were more straightforward. In essence, petrography must become more accessible to coal users, if it is to be incorporated in the day to day management of a power station.

## 6.5 Directions for Future Research

### 6.5.1 Intrinsic Reactivity

Little is known about temperatures in a pulverised fuel boiler flame. It is not clear whether char combustion is controlled by mass transfer or chemical kinetics in the char combustion stage.

As shown in Chapter 5, there are large differences in Intrinsic Reactivity results for different chars, especially when they exhibit anisotropic properties. This may or may not have some effect on the successful burnout of certain char types.

A project due to start in October 1994 at Nottingham, aims to investigate the affect of temperatures inside the furnace on the intrinsic reactivity of the char, as well as the changes that occur from the initial coal sample to the pyrolysed char to the final combustible material present in the fly ash. Work on this 'to-date' has provided results which indicate that a number of interesting reactions probably occur in the latter stages of combustion.

### 6.5.2 Combustion Macro

From the results in this thesis and from other private contracts, several parameters appeared to be most important, when assessing a coal for combustion.

1. Particle size - the distribution of particle size. In theory 75% of the pulverised fuel should be below 75 microns. In practice this isn't always true, and it is possible that poor burnout is related to particle size problems i.e. insufficient grinding of the coals. The El Cerrejon anomaly may well be due to an excess of large particles (Vleeskens et al., 1993).
2. The 'reactivity' of the sample - the reflectance of the semi-fusinite, the rank of the vitrinite and the amount of liptinite will all have some effect on burnout.
3. The mineral matter content of the initial sample - as discussed in Chapter 1, the presence of certain cations affects char types (Kleesattel et al., 1987) and their reactivities.

A Combustion Macro, using similar methods to the Electrical Power Research Institute, would hopefully include all these parameters in order to predict the overall combustion performance of a coal. The Macro would weight the more important parameters, such as particle size, as well as acknowledging the effect of certain mineral types on combustion kinetics.

### 6.5.3 1 MW Furnace

One of the ways in which intrinsic reactivity effects and the combustion macro can be investigated is with the use of the new 1MW furnace at Ratcliffe-on-Soar. The system enables sampling at different positions inside the furnace and hence any changes in char morphology, reactivity etc. with different coals can be monitored closely.

The DTF is a reasonable approximation of combustion conditions, in terms of heating rates and temperatures, but the 1MW furnace can produce large quantities of sample from a system which models the whole combustion process.

### 6.5.4 Interpretation of the Reactivity Results

The Reactive Number and Average Reactive Number are two simple ways of interpreting the reflectance/fluorescence plot i.e. a simple threshold or a weighted average of the grey scale. The results were encouraging but it may be necessary to revise this approach, and use a more comprehensive means of interpretation, in order to improve correlation's between initial predictions and burnout. One such revision includes the position of the vitrinite peak. As shown in Chapter 5, even the high ranked vitrinite samples produced thin walled networks. Relating char morphology to Reactive Number, over a wide range of coal types, is clearly inadequate. In order to do this, weight must be given to the position of the vitrinite peak - as well as the semi-fusinite and fusinite peaks.

If the combustion behaviour is dependant, to some extent, on intrinsic reactivity, then this revision of interpretation may not be necessary, because at present the threshold method appears to break down with coals with a Rank greater than 1%. The difference between chars from these coals and other chars is the degree of anisotropy. Coals with a rank value less than 1% do not appear to produce significant quantities of anisotropic chars - which no doubt affects the intrinsic reactivity of the sample.

It will be necessary to examine the results from the 1MW furnace in order to determine whether the interpretation of reflectance/fluorescence plots should be revised.

#### 6.5.5 Artificial Intelligence

The use of expert systems in coal petrography has been limited to only a few workers (Prado, 1992), although it is possible that in the future, computers will be used to provide a more detailed analysis of coal particle 'structure', as well as the maceral make-up of the different maceral species.

To tie in size and shape analysis with '*reactivity*' analysis would allow a more detailed and perhaps more useful prediction to be made for combustion performance. This type of shape evaluation is possible with basic image analysis systems, and one such program has been written to do this on the IBAS at Nottingham. However, relating more complicated associations with this kind of size analysis would be much quicker with a system using artificial intelligence.

#### 6.5.6 Single Particle Analysis

Many workers have used laser microreactors to investigate the combustion behaviour of single macerals and microlithotypes and coal particles in general (Thomas et al., 1989b, Shibaoka et al., 1989a). The one distinct advantage of this method over others is the direct link between a specific coal maceral/microlithotype to a specific char type. Since heating rates and flame temperatures are similar to real combustion, the times required for pyrolysis and combustion can be measured as well as the type of char particle formed.

For this reason the laser microreactor provides an absolute means of determining the nature of certain particles in a combustion flame. The results are captured on a high speed film and so the step-by-step behaviour of the particle in the flame can be observed. Drop-Tube Furnaces, Heated Wire Meshes and Entrained Flow Reactors all have the same problem in relating

certain char types to the original feed material. With coals like Drummond one can not be certain whether a dense char may have originated from pseudovitrinite, fusinite or desmocolinite.

Future work in this area would hopefully involve the collaboration of workers with a laser microreactor and the Coal Technology Research Group, using all the various techniques which could characterise single coal particles and comparing them with the chars produced.

Since the chars produced in the laser flame can be combusted through to ash, this may provide another means of determining the affect of intrinsic reactivity on combustion rates, as well as providing a definite means of linking coal macerals with char types.

## References

**Allen J., Gehring K. (1989)**

*Evaluation of the Petrographic controls on coal quality and thermal reactivity.*

Advances in Western Canadian Coal Geoscience- Forum Proceedings.

**Allen, M., Cloke, M., Lester, E., Miles N.J., (1994)**

*Repeatability of maceral analysis using image analysis systems*

accepted for publication in Fuel, September, 1994.

**Badzioch S., Sainsbury R.B., Hawksley P.G.W. (1968).**

*Thermal decomposition of pulverised-fuel particles Part 2 analysis of experimental data.*

BCURA report 340, March 1968. Leatherhead, Surrey.

**Bailey J.G. (1989a).**

*Sampling and testing of maceral concentrates for P.F. combustion.*

Proc. Macerals Symposium 10-11 May, 1989. 11pp. CSIRO, NSW.

**Bailey J., Tate A., Wall T. (1989b).**

*Maceral concentrates and coal in PF combustion.*

Extended. Abstracts: Joint Int. Conf. Aus/NZ/Jap. Combustion Institute, 115-117, 1989.

NSW.

**Bailey J., Tate A., Diessel C., Wall T. (1989c).**

*A char morphology system with application to coal combustion.*

Extended. Abstracts: Joint Int. Conf. Aus/NZ/Jap. Combustion Institute, 109-111, 1989.

NSW.

**Bailey J.G. (1990).**

*Image analysis of char from pyrolysed lithotype concentrates- advances in the study of the Sydney basin.*

Publication no. 344. p174-181 University of Newcastle (NSW).

**Bailey J.G., Tate A., Diessel C.F.K., Wall T.F. (1990).**

*A char morphology system with applications to coal combustion.*

Fuel 69, 225-239.

**Bend S.L., Edwards I.A.S., Marsh H. (1989).**

*Petrographic characterization of coals to relate to combustion efficiency.*

Int. Conf. Coal Sci. IEA 1989, 437-440. Tokyo, NEDO.

**Bend S.L., Edwards I.A.S., Marsh H. (1992).**

*The influence of rank upon char morphology and combustion.*

Fuel 71, 493-501.

**Benedict L.G., Thompson R.R., Shigo J.J., Aikman R.P. (1968).**

*Pseudovitrinite in Appalachian coking coals.*

Fuel 47, 125-143.

**Bengtsson M. (1984).**

*Petrographic structures in an American and a Polish coal, and their change during combustion.*

Commun. Serv. Geol. Portugal. (1984) 70 fasc. 2, 277-284.

**Bengtsson M. (1986).**

*Combustion behaviour for a range of coals of various origins and petrographic composition.*

Thesis Diss. (Mar) 1986. Royal Inst. Technol., Dept. of Heat & Transfer. 64pp.

**Bengtsson M. (1987a).**

*Combustion behaviour for a coal containing a high proportion of pseudovitrinite.*

Fuel Process. & Technol. 15 201-212.

**Bengtsson M. (1987b).**

*Combustion behaviour for a range of coals of various origins and petrographic compositions.*

Inter. Conf. Coal Sci. 1987, 893-896 (Ed. J. Moulijn). Elsevier.

**Bouska V. (1981).**

*Geochemistry of Coal.*

Coal Science & Technology 1. Elsevier 284pp.

**British Standard 1016 Part 3 (1965).**

*Methods for the analysis and testing of coal and coke: Part 3 - Proximate analysis of coal*

British Standards Institute, London.

**British Standard 6127 Part 1 (1981).**

*Glossary of Terms relating to the petrographic analysis of bituminous coal and anthracite.*

8 pages, 1981, Milton Keynes.

**British Standard 6127 Part 2 (1982).**

*Method of preparing coal samples for petrographic analysis.*

12 pages, 1981, Milton Keynes.

**British Standard 6127 Part 4 (1990).**

*Method of determining microlithotypes, carbominerites and minerite composition.*

12 pages, 1990, Milton Keynes.

**Bustin R.M., Cameron A.R., Grieve D.A., Kalkreuth W.D. (1983).**

*Coal Petrology, Its principles, methods and applications.*

Short Course Notes Vol. 3 Victoria 1983, Geol. Assoc. of Canada.

**Carpenter A. (1988).**

*Coal Classification.*

IEA Coal Research, London 104pp.

**Chao E., Minkin J., Thompson C. (1982a).**

*Recommended procedures and techniques for the petrographic description of bituminous coals.*

Int. J. Coal Geol. 2, 151-179.

**Chao E., Minkin J., Thompson C. (1982b).**

*Application of automated image analysis to coal petrography.*

Int. J. Coal Geol. 2, 113-150.

**Chapparro L.F. (1987).**

*Automated microscopy methods for measuring pyritic sulphur content of coal and determining degree of liberation of pyrite in coal.*

Final Report. DOE/PC/916565-2, 66 pages, Dept. of Electrical Engineering Pittsburgh University for the Department of Energy.

**Ciuryla V., Weimer R.F., Bivans D., Motika S. (1979).**

*Ambient pressure thermogravimetric characterization of four different coals and their chars.*

Fuel 58, 748-754.

**Coal Research Establishment (1993).**

*The CRE Coal sample bank: A users Handbook*

compiled by P Burchill and D.S. Way, Feb. 1993. British Coal Corporation.

**Coin C., Hall K. (1989).**

*Rapid laser micropyrolysis of coal to assess the fusibility characteristics of the inertinite group of macerals.*

Proc. Macerals Symposium 10-11 May, 1989. 11pp. CSIRO, NSW.

**Crelling J.C. (1982).**

*Automated Petrographic characterisation of coal lithotypes.*

Int. J. of Coal Geol. 1, 347-359.

**Crelling J.C., Skorupska N., Marsh H. (1988).**

*Reactivity of coal macerals and lithotypes.*

Fuel 67, 781-785.

**Crelling J.C., Hippo E.J., Woerner B., West D. (1992).**

*Combustion characteristics of selected whole coals and macerals.*

Fuel 71, 151-158.

**Denton G.H., Bayer J.L., Hassel R.E. (1967).**

*Progress and problems in routine petrographic evaluation of coals for coke plant use.*

J. of Metals 19 (May), 88-92.

**Diessel C.F.K., Wolff-Fischer E. (1987a).**

*On the relationship between reflectance, fluorescence and fusibility of inertinite in Ruhr coals.*

Int. Conf. Coal Sci. 1987, 901-907. Maastricht (Ed. J. Moulijn et al.), Elsevier.

**Diessel C.F.K. Wolff-Fischer E. (1987b).**

*Coal and coke petrographic investigations into the fusibility of Carboniferous and Permian coking coals.*

Int. J. Coal Geol. **9**, 87-108.

**Essenhigh R. (1981).**

*Fundamentals of Coal Combustion*

Chemistry of Coal Utilisation (2nd Vol.) 1153-1312. Ed. M. Elliot. Wiley Press NY.

**Fermont W.J.J., Chermin H.A.G., Joziasse J., Nater K.A. (1989).**

*The concentration of coal macerals on a kilogram scale from three carboniferous hardcoals.*

Int. Conf. Coal Sci. IEA 1989, 113-116. Tokyo, NEDO.

**Finch J.A., Gomez C.O. (1989).**

*Technical Note: seperability curves from image analysis data.*

Minerals Engng, **2**, 565-568.

**Furimsky E., Palmer A.D., Kalkreuth W.D., Cameron A.R., Kovacik G. (1990).**

*Prediction of Coal Reactivity during combustion and gasification by petrographic data.*

Fuel Process. & Technol. **25**, 135-151.

**Galehouse J.S. (1971).**

*Point Counting.*

Proc. Sed. Petr., 384-407 (Eds R.E. Carver), John Wiley, New York.

**Gibb W.H. (1992)**

*Ratcliffe Power Station Unit 2: Results of 3rd Slagging trial firing Dawmill coal.*

**PowerGen Report Ref no. PT/92/220077/M, 12-15 May 1992.**

**Gibbins J., Man C.K., Pendlebury K.J. (1991).**

*Determination Of Rapid Heating Volatile Matter Contents As A Routine Test.*

Taken from the preprints of the paper presented at the 1st Int. Conf. on Combustion Technologies for a clean environment at Vilamora, Portugal, 3-6th September, 1991. 12 pp.

**Goodarzi F., Murchison D.G. (1978).**

*Influence of heating rate variation on the anisotropy of carbonized vitrinites.*

Fuel 57, 273-284.

**Gromulski J., Sieurin J. (1983).**

*Combustion and burnout studies for two different coals in a 4MW furnace compared with results from a DTF.*

IFRF Conf. 1983, 34pp.

**Haley E., Thomas K.M., Marsh H., Edwards L.A.S. (1991).**

*Coal char reactivity and burn-off.*

Int. Conf. Coal Sci. IEA 1991, 275-278. Newcastle Upon Tyne, Butterworth Heinemann.

**Hower J., Esterle J., Wild G., Pollock J. (1990).**

*Perspectives of coal lithotype analysis.*

J. of Coal Qual. 9 (2) 48-52.

**ISO Standard 7404:2 (1985).**

*Methods for the petrographic analysis of bituminous coal and anthracite - method of preparing coal samples.*

**Jamaluddin A.S. (1992).**

*Estimation of Kinetic parameters for char oxidation.*

Fuel 71, 311-317.

**Jenkins R.G., Nandi S.P., Walker P.L. (1973).**

*Reactivity of heat treated coals in air at 500°C.*

Fuel **53**, 288-293.

**Jones M.L. McCollor D.P., Weber B.J. (1987).**

*Combustion behaviour of ion exchanged coal chars.*

Extended. Abstracts: Joint Int. Conf. Aus/NZ/Jap. Combustion Institute, 116-118, 1987. NSW.

**Jones R.B., McCourt C., Morley C., King K. (1985a).**

*Maceral and Rank influence on the morphology of coal char.*

Fuel **64**, 1460-1467.

**Jones R.B., Morley C., McCourt C.B. (1985b).**

*Maceral Effects on the morphology and combustion of coal char.*

Int. Conf. Coal Sci. 1985 Sydney, 669-672. Pergamon.

**Kaegi D. (1985).**

*On the identification and origin of Pseudovitrinite.*

Int. J. of Coal Geol. **4**, 309-319.

**Kleesattel D., Benson S.A., Jones M.L., McCollor D.P. (1987).**

*A petrographic examination of chars produced by the rapid pyrolysis of low rank coals.*

Extended. Abstracts: Joint Int. Conf. Aus/NZ/Jap. Combustion Institute, 27-34, 1987. NSW.

**Kojima K. (1976).**

*Automatic System for evaluating coking coals.*

Iron and Steel Int. **46**, 435-436.

**Kopp O., Harris L. (1984).**

*Initial volatilization temperatures and average volatilization rates of coal- their relation to coal rank and other characteristics.*

Int. J. Coal Geol. **3**, 333-348.

**Kosina M., Hrnčir J. (1983).**

*The properties of macerals in Czechoslovakian coals rich in inertinite.*

Int. J. Coal Geol. **3**, 145-156.

**Krevelan E. Van (1961).**

*Coal Typology, Chemistry, Physics and Constitution,*

Elsevier, Amsterdam.

**Kuili J., Jian X., Duoho H. (1988).**

*The use of automated coal petrography in determining maceral group composition and the reflectance of vitrinite.*

Int. Journ. Coal Geol. **9** 385-395.

**Lee G.K., Whaley H. (1983).**

*Modifications of combustion and fly-ash characteristics by coal blending.*

J. Inst. Energy 1983 (Dec.), 190-197.

**Lester, E., Allen, M., Cloke, M., Miles, N.J. (1994a).**

*An automated image-analysis system for major maceral group analysis in coals.*

awaiting publication in Fuel, September, 1994.

**Lester E., Allen M., Cloke M. (1994b).**

*The characterisation of char particles using automated image analysis,*

under preparation for publication in Energy and Fuels.

**Lester, E., Allen, M., Cloke, M., Miles, N.J., (1994c)**

*An automated image-analysis system for major maceral group analysis in coals.* awaiting publication in Fuel, September, 1994.

**Lightman P., Street P.J. (1968).**

*Microscopic Examination of heat treated pulverized coal particles.*

Fuel 47, 7-28.

**Littlejohn R.F. (1966).**

*Mineral matter and ash distribution in 'As-fired' samples of pulverised fuel samples.*

J. Inst. Fuel 39, 59-67.

**Mahajan O., Walker P. (1979).**

*Effect of inorganic matter removal from coals and chars on their surface areas.*

Fuel 58, 333-337.

**Morgan M., Roberts P.A. (1987).**

*Coal Combustion characteristics studies at the International Flame Research Foundation.*

Fuel Process. Technol. 15, 173-187.

**Nandi B.N., Brown T.D., Lee G.K. (1977).**

*Inert coal macerals in combustion.*

Fuel 56, 125-130.

**Neill P., Given P., Weldon D. (1987).**

*A search for synthetic relationships between aromaticity and rank of high sulphur coals*

Fuel 66, 92-95.

**Oka N., Murayama T., Matsuoka H., Yamada S., Yamada T., Shinozaki S., Shibaoka M., Thomas C. (1987).**

*The influence of rank and maceral composition on ignition and char burnout of pulverized coal.*

Fuel Process. & Technol. 15, 213-224.

**Ottaway M.R. (1982).**

*Use of thermogravimetry for proximate analysis of coals and cokes.*

Fuel 61, 713-716.

**Patrick J.W., Shaw F.H. (1972).**

*Influence of Sodium Carbonate on coke reactivity.*

Fuel 51, 69-75.

**Phong-Anant P., Salehi M., Thomas C., Baker J., Conroy A. (1989a).**

*Burnout and reactivity of coal macerals.*

Int. Conf. Coal Sci. IEA 1989, 253-256. Tokyo, NEDO.

**Pitt G.L., Dawson K.M. (1979).**

*Some considerations involved in the automation of reflectance measurement on coal.*

J. of Microscopy 116, 321-328.

**Prado J. (1992).**

*A small report in the Minutes of the ICCP meeting held in Greece, September 1992.*

**Pratt K.C. (1989).**

*Particle size distribution in coal and its contribution to results obtained through automated systems.*

Advances in Western Canadian Geoscience 1989 - Forum Proceedings.

**Radovic L.R., Walker P.L., Jenkins R.G. (1983a).**

*Effect of lignite pyrolysis conditions on calcium oxide dispersion and subbituminous reactivity.*

Fuel **62**, 209-212.

**Rentel K. (1987).**

*The combined maceral-microlithotype analysis for the characterization of reactive inertinites.*

Int. J. Coal Geol. **9**, 77-86.

**Riepe W., Steller M. (1984).**

*Characterisation of coal and coal blends by automatic image analysis.*

Fuel **63**, 313-317.

**Roberts F., Young J.Z. (1952).**

*Flying Spot Microscope.*

Proc. Inst. Elec. Engng. (London) **99**, 747-760.

**Sakurovs R., Lynch L., Webster D., Maher T. (1991).**

*The fusibility of Australian coals: relationships between results from NMR measurements and Gieseler plastometry.*

J. Coal Qual. **10** (1), 37-41.

**Schapiro N., Gray R., Eusner G. (1961).**

*Recent developments in coal petrography. Blast Furnace, Coke Ovens and Raw Materials*

Proceed. A.I.M.E. **20**, 89-112.

**Schobert H. (1987).**

*Coal: the energy source of the past and future.*

Am. Chem. Soc. D.C. 298pp.

**Shibaoka M. (1969).**

*Combustion of coal in thin sections.*

Fuel 47, 285-295.

**Shibaoka M., Thomas C.G., Young B.C., Oka N., Matsuoka H., Tamara K., Murayama T. (1985a).**

*The influence of rank and maceral composition of pulverized coal.*

Int. Conf. Coal Sci. 1985, Sydney, 665-668. Pergamon.

**Shibaoka M. (1985b).**

*Microscopic investigation of unburnt char in fly-ash.*

Fuel 64, 263-269.

**Shibaoka M. (1986).**

*Carbon content of fly ash and size distribution of unburnt char particles in fly ash.*

Fuel 65, 449-450.

**Shibaoka M., Thomas C.G., Heng S., Mackay G.H. (1987).**

*Significance of morphological features of macerals in coal utilization research.*

Proc. Int. Conf. Coal Sci. (J. Moulijn), 105-110.

**Shibaoka M., Thomas C.G., Gawronski E., Young B.C. (1989a).**

*A new concept in the microscopic classification of PF char.*

Int. Conf. Coal Sci. IEA 1989, 1123-1126. Tokyo, NEDO.

**Shibaoka M., Gawronski E. (1989b).**

*Colouring of macerals by thin film coating.*

Int. Conf. Coal Sci. IEA 1989, 117-120. Tokyo, NEDO.

**Shiboaka M., Thomas C.G., Gawronski E. (1989c).**

*Microscopic investigations of combustion residues of inertinite rich coals from laboratory and power station samples.*

Proc. Macerals Symposium 10-11 May, 1989. 18pp. CSIRO, NSW.

**Skorupska N.M. (1987)**

PhD Thesis, Newcastle upon Tyne University, 1987.

**Skorupska N.M., Sanyal A., Hesselman G., Crelling J.C., Edwards Marsh H. (1987).**

*The use of an entrained flow reactor to assess the reactivity of coals of high inertinite content.*

Int. Conf. Coal Sci., Maastricht, 1987. 827-831. (eds Moulijn J.A. et al.), Elsevier.

**Skorupska N.M., Haley E., Marsh H., Edwards L.A.S. (1989).**

*An assessment of the properties which control the reactivity of coal chars.*

Proc. Int. Conf. Coal Sci. IEA, 439-432.

**Skorupska N.M., Marsh H. (1989).**

*The importance of petrographic characterization of coal for combustion processes.*

Applied Energy Research: Proceed. Inst. Energy Conf. at Swansea 1989.

**Speight J.G. (1983).**

*The chemistry and technology of coal.*

M. Dekker inc. USA. 528pp.

**Stach E., Machowsky M., Teichmuller M., Taylor G., Chandra D., Teichmuller R. (1982).**

*Textbook of Coal Petrology.*

3rd Ed. Gebruder Borntraeger.

**Stanmore B. (1989).**

*Reactivity of low volatile coals by DTG analysis.*

Extn. Abstr. Joint Int. Conf. Aus/NZ/Jap. 103-105. Combustion Institute.

**Steller M., Kalkreuth W., Wiesenkamper I. (1991).**

*Effect of vitrinite and inertinite fluorescence properties and combustion and hydrogenation reactivities of coals.*

Int. Conf. Coal Sci. IEA 1991, 90-93. Newcastle Upon Tyne,. Butterworth Heinemann.

**Steyn J., Smith W. (1977).**

*Coal Petrography in the evaluation of South African coals.*

Coal, Gold and Base Minerals of S.A. 109-114.

**Street P.J., Weight R.P., Lightman P. (1969).**

*Further investigations of structural changes occurring in pulverized coal.*

Fuel **48**, 343-365.

**Suarez-Ruiz I., Crelling J.C., Bensley D.F. (1991).**

*Petrographic characterisation of Spanish bituminous coals from the Central Teverga Basins.*

Int. Conf. Coal Sci. IEA 1991, 119-121. Newcastle Upon Tyne,. Butterworth Heinemann.

**Tate A., Wall T.F., Bailey J.G. (1987).**

*Burnout of pulverized coal experiments and modelling of laboratory and industrial scale furnace.*

Extended Abstracts: Joint Conf. Western States and Jap. Sect. Combustion Institute. 1987, 110-112.

**Taylor G., Liu S., Diessel C.F. (1989).**

*The cold climate origin of inertinite rich Gondwala coals.*

Int. J. Coal Geol. **11**, 1-22.

**Taylor G., Liu S.Y. (1989).**

*Micrinite- its nature, origin and significance.*

Int. J. Coal Geol. 14, 29-46.

**Thomas C.G., Holcombe D., Shibaoka M., Young B.C., Brunckhorst L.F., Gawronski E. (1989a).**

*Determination of the effect of coal rank and maceral composition on PF combustion reactivity.*

Int. Conf. Coal Sci. IEA 1989, 257-260. Tokyo, NEDO.

**Thomas C.G., Shibaoka M., Gawronski E., Gosnell M.E., Phong-Anant D., Brunckhorst L.F., Salehi M.R. (1989b).**

*Swelling and plasticity of inertinite in PF combustion.*

Int. Conf. Coal Sci. IEA 1989, 213-216. Tokyo, NEDO.

**Thomas C.G., Shibaoka M., Gawronski E., Gosnell M.E., Brunckhorst L.F. (1989c),**

*Macerals fusion behaviour in thermal coals.*

Proc. Macerals Symposium 10-11 May, 1989. 35pp. CSIRO, NSW.

**Thomas C.G., Shibaoka M., Phong-Anant D., Gawronski E., Gosnell M.E. (1991a).**

*Determination of percentage reactives under PF combustion conditions.*

Int. Conf. Coal Sci. IEA 1991, 48-51. Newcastle Upon Tyne, Butterworth Heinemann.

**Thomas C.G., Shibaoka M., Gosnell M.E., Gawronski E., Phong-Anant D. (1991b).**

*Coal combustion studied with a laser microreactor- a video.*

Int. Conf. Coal Sci. IEA 1991, 424-427. Newcastle Upon Tyne, Butterworth Heinemann.

**Thompson A.W., Stainsby R.E., Simpson B. (1993).**

*Collaborative program on Nox research: Drop Tube Studies*

International Combustion Report No. 25717, July 1993.

**Tsai C.Y. (1985).**

*PhD Thesis.*

Penn State University. ~250pp.

**Tsai C.Y., Scaroni A.W. (1987).**

*Pyrolysis and combustion of bituminous coal fractions in an entrained flow reactor.*

Energy & Fuels 1, 263-269.

**Unsworth J.F., Barratt D.J., Roberts P.T. (1991).**

*Coal Quality and combustion performance - an international perspective.*

Coal Science and Technology Series 19, 1991. Elsevier, Netherlands. 638pp.

**Vleeskens J.M., Bos P., Kos C.H., Ross M. (1985)**

*Pyrite association and coal cleaning, an optical image analysis study.*

Fuel 64, 343-347.

**Vleeskens J.M., Nandi B.N. (1986).**

*Burnout of coals:- comparative bench-scale experiments on pulverized fuel and fluidised bed combustion.*

Fuel 65, 797-802.

**Vleeskens J.M., Roos C.M. (1993).**

*Final Stages of combustion in technical burners - effect of coal type.*

ECSC Report No. ECN-C-93-083, December 1993.

**Wall T.F., Tate A., Bailey J. (1989a).**

*The temperatures attained by burning coal char particles.*

Extn. Abstr. Joint Int. Conf. Aus/NZ/Jap Sections Combustion Institute, 1989. 97-99. NSW.

**Ward C.R. (1984),**

*Coal geology and coal technology.*

Blackwell Publish. 345pp.

**White A., Davies M.R., Jones S.D. (1989)**

*Reactivity and characterisation of coal maceral concentrates.*

Fuel **68**, 511-519.

**White D. (1994),**

*at the meeting of the Coal Characterisation Division,*

Churchill College, Cambridge, April 1994.

**Williamson J., Beeley T., Cooke S., Gibbins J., McCann K. (1991).**

*Fundamentals of Char burnout - origin of carbon in pulverised fuel ash from utility boilers.*

Annual BCURA report, research Grant B17 July 1991-June 1992.

**Young B.C., Smith L.W. (1986).**

*Effect of Coal Rank and Pyrolysis conditions.*

Coal Combustion, 91-100. (Ed. J. Feng).

**Young B.C., Thomas C.G., Hamor R.J., Banas E., Shibaoka M. (1987).**

*The effects of maceral composition and rank in coal combustion.*

Extended Abstr.: Joint Conf. Western States and Jap. Sect. Combustion Institute, 119-121.

NSW.

**Zhang. C., Huang X., Xu X. (1986).**

*Experimental study on the microstructure of pulverized coal particles in combustion processes.*

Coal Combustion, 109-120. (Ed. J. Feng).

# Glossary

*ACA* - Automated Char Analysis. Refers to the distance transform method for contouring char particles.

*ACA {3}* - refers to the cumulative percentage of pixels that fall under 3 contours in the ACA program.

*ACA {5}* - refers to the cumulative percentage of pixels that fall below 5 contours in the ACA program.

*ACA {95%}* - is the number of contours required to cover 95% of all the char walls analysed in a scan. Thick walls have higher ACA 95% numbers.

*Aniso-crassisphere* - a particle with >75% of its walls with a thickness  $> 5\text{mm}$  and optical anisotropy.

*Aniso-temuinetwork* - a particle containing several internal spheres with >75% of its walls with a thickness  $< 5\text{mm}$ , and optical anisotropy.

*Aniso-temuisphere* - a particle with >75% of its walls with a thickness  $< 5\text{mm}$  and optical anisotropy.

*Anisotropy* - a substance possessing different physical properties in different directions.

*Aromaticity* - the degree to which a cyclic organic compound containing double bonds within the molecular structure, exhibits the high stability, and specific reactivity of benzene and its derivatives.

*Ash* - the non-volatile inorganic residue remaining after the ignition of organic material (i.e. coal).

*Average Reactive Number* - an average of grey scale and frequency for any coal measured using the *Reactivity Assessment Program*.

*Bireflectance* - an expression of the increasing degree of order achieved by the aromatic lamellae within a given particle of vitrinite, determined by %  $R_{ort\ min}$  and %  $R_{ort\ max}$ . Graphite is an example of a substance with high bireflectance (17.8 %)

*Bituminous coal* - a coal of medium rank, where  $R_{ort}$  is between 0.49% and 1.9%. Long flame coals, containing a high proportion of volatile hydrocarbons.

*Burnout Temperature* - the point on the derivative TGA plot where the combustion rate falls below 1% per minute.

*Char* - the residual solid matter after pyrolysis of a natural or man-made organic material, which may or may not yield further volatiles if heat is applied.

*Clarain* - the term clarain designates very finely stratified coal layers with a thickness of at least several millimetres, having a lustre between that of vitrain and durain.

*Clarite* - a microlithotype composed of 95% vitrinite and liptinite, and >5% of each.

*Coal rank* - the degree of coalification.

*Combustion* - a chemical reaction, or series of reactions, during which oxygen reacts with a substance to form a flame emitting heat and light.

*Correlation Coefficient* - see Excel Help menu for details.

*DAFB* - dry ash free basis

*DB* - dry basis

*Durain* - can be black or grey. Black durain has a faintly greasy lustre. Hard. Can be confused with carbonaceous shale. Composed mainly of inertinites and exinitic species.

*Durite* - a microlithotype composed of 95% inertinite and liptinite, and >5% of each.

*Exinite/Liptite* - a microlithotype composed of no less than 95% alginite, cutinite, liptodetrinite, resinite or sporinite.

*Fixed Carbon* - the difference between initial mass and the sum of volatiles present, ash & moisture content.

*Fly ash* - particles of less than 10mm in size that result from incombustible mineral matter within a coal.

*Fuel Ratio* - simply the ratio of Fixed Carbon to Volatile Content, both calculated on a Dry, Ash Free Basis.

*Fusain* - a dull coal, like charcoal with a silky lustre.

*I.C.C.P.* - International Committee for Coal Petrology.

*Inertinite* - the name for the maceral group containing , fusinite, inertodetrinite, macrinite, micrinite, sclerotinite, semifusinite.

*Inertite* - a microlithotype composed of 95% inertinite.

*Intrinsic Reactivity* - refers to the chemical reactivity of the chars, as determined by TGA methods. Specifically *Burnout Temperature* and *Peak Temperature*.

*Iso-crassisphere* - a particle with >75% of its walls with a thickness  $> 5^{\mu}$ m and optical isotropy.

*Iso-temuinetwork* - a particle containing several internal spheres with >75% of its walls with a thickness < 5mm, and optical isotropy.

*Iso-temuisphere* - a particle with >75% of its walls with a thickness < 5mm and optical isotropy.

*Isotropic* - describes the optical texturing of a substance where there is no visible order.

*Liptinite* - the new term for exinite.

*Liptite* - see Exinite.

*Lithotype* - occur on the macroscale (3 to 10 millimetres), and describe the subject by appearance, namely colour and texture.

*Maceral* - describes both the shape and nature of the microscop-ically recognizable units of the coal.

*Microlithotype* - describes the association of sub-macerals within a particle with a diameter no less than 50mm in size.

*Mineral Matter* - the inorganic fraction of the coal, with is both within the coal (epigenetic) and incorporated in the macerals themselves (syngeneic).

*Mixed Dense Char* - a particle with > 50% of its surface area present as a solid.

*Mixed Porous Char* - a particle with > 50% of its area as an open void.

*Moisture Content* - the amount of water which is released at temperatures between 105 and 130°C.

*Morphology* - the physical structuring of a material.

*Near Burner Zone* - the area close to the inlet of coal feed material. Associated with pyrolysis and early char combustion stages.

*Open Solid* - a char particle with 'slits' or cracks in its structuring.

*Oxidation* - the addition of oxygen to a compound. More generally, any reaction involving the loss of electrons from an atom.

*Peak Temperature* - is the temperature that marks the peak of the DTA curve.

*Petrography* - the scientific description of the composition and formation of rocks.

*Point Counter* - a statistical tool used in petrographic studies, enabling a petrographer to record what falls under the cross hairs of the microscope after the sample is a fixed distance each time.

*Proximate Analysis* - an analytical technique in which a coal sample is exposed to various temperatures and atmospheres enabling moisture content, volatile matter, fixed carbon and ash to be determined.

*Pseudovitrinite* - can be differentiated from vitrinite by its higher reflectance, angular edging, slitted surface and visible cell structure.

*Pyrolysis* - the destructive distillation of coal in the absence of air.

*Rank* - indicates the degree of coalification occurred. In this thesis *Rank* refers to the value for Mean Random Vitrinite Reflectance.

*RAP* - refers to the *Reactivity Assessment Program*, which assesses a coal on the basis of its grey scale histogram, including liptinite detected using fluorescence. The use of the term *Reactivity Assessment Program* was preferable to *Coal Reactivity Assessment Program* due to its unfortunate acronym.

*Reactive Number* - the cumulative percentage of a coal which falls below 130 grey scale units, as measured under with the *Reactivity Assessment Program*.

*Reflectance* - the ratio which the luminous flux reflected from a surface bears to that falling on it.

*Solid* - a char particle which appears to be without structural deformation or opening.

*Thermogravimetry* - a technique in which a sample is heated during which any change in weight is monitored.

*Thermoplastic* - any material which becomes plastic/softens on heating, but will solidify on cooling.

*Ultimate Analysis* - provides the levels of Carbon, Hydrogen, Nitrogen, Sulphur and Oxygen present in a sample of coal, as well as the mineral content.

*Unfused Solid* - A char particle which has not undergone any pyrolysis, and remains structurally unaltered from its time of initial exposure to heat to the point at which its begins to combust.

*Vitrain* - a lithotype, with bright/vitreous lustre with high levels of the maceral vitrinite.

*Vitrinite* - a maceral group containing Tellinite, Collinite, Pseudovitrinite and various other submacerals.

*Vitrinite* - a microlithotype composed of at least 95% vitrinite.

*Volatile Matter* - is the name for the material lost during proximate analysis at high temperatures (around 900°C), and can be calculated indirectly by subtracting fixed carbon, moisture content and ash content from 100 percent.

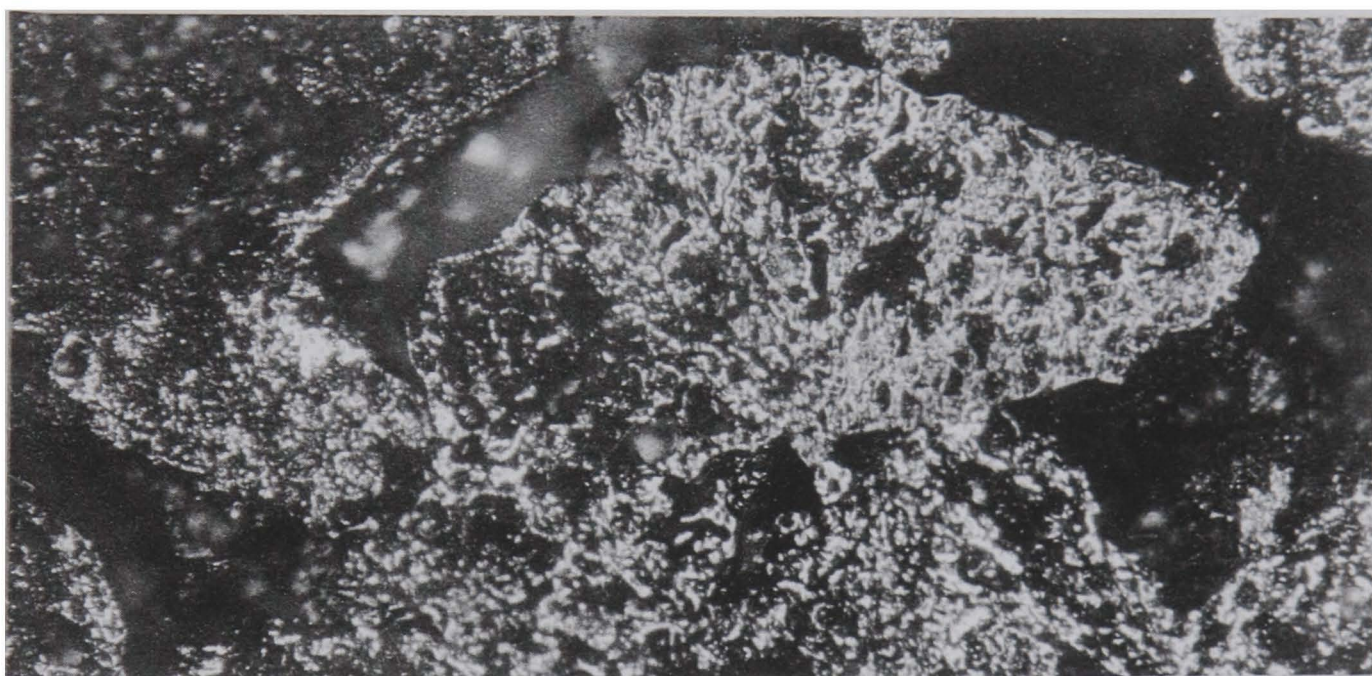
*Volatiles* - primary gaseous decomposition products some of which will be solids or liquids at ambient pressure and temperature.

*Yoda* - a Jedi Knight Instructor.

APPENDIX A - Char Nomenclature Photographs



Anisotropic Crassi-Network Char (from an Anthracite)

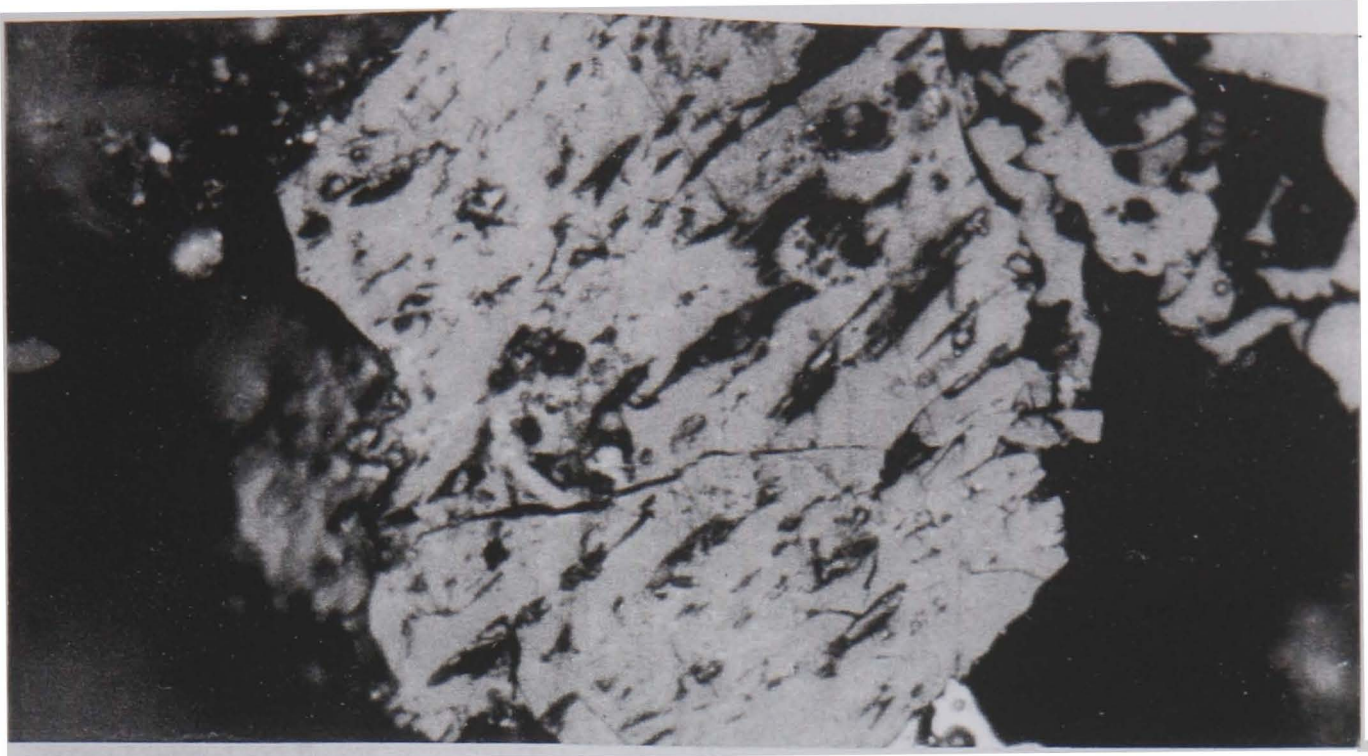


Sponge Char

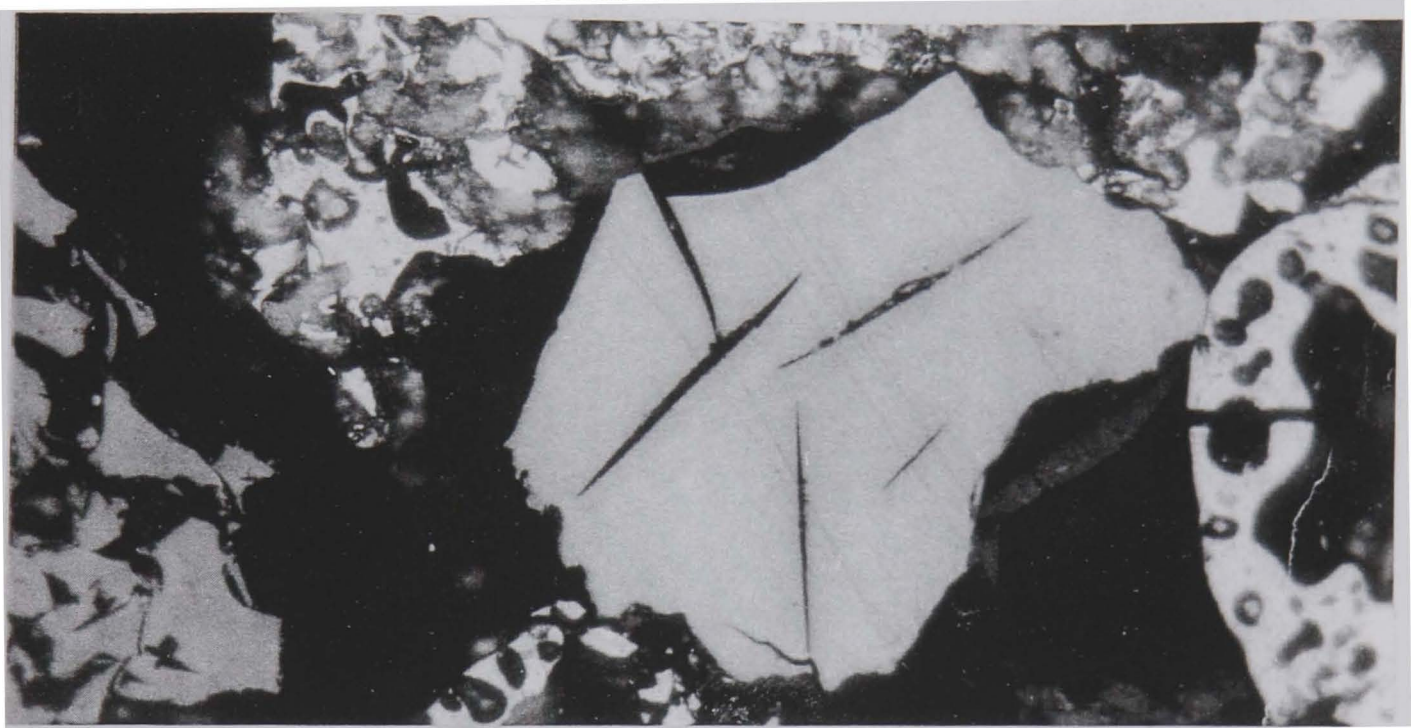


Crassi-Sphere

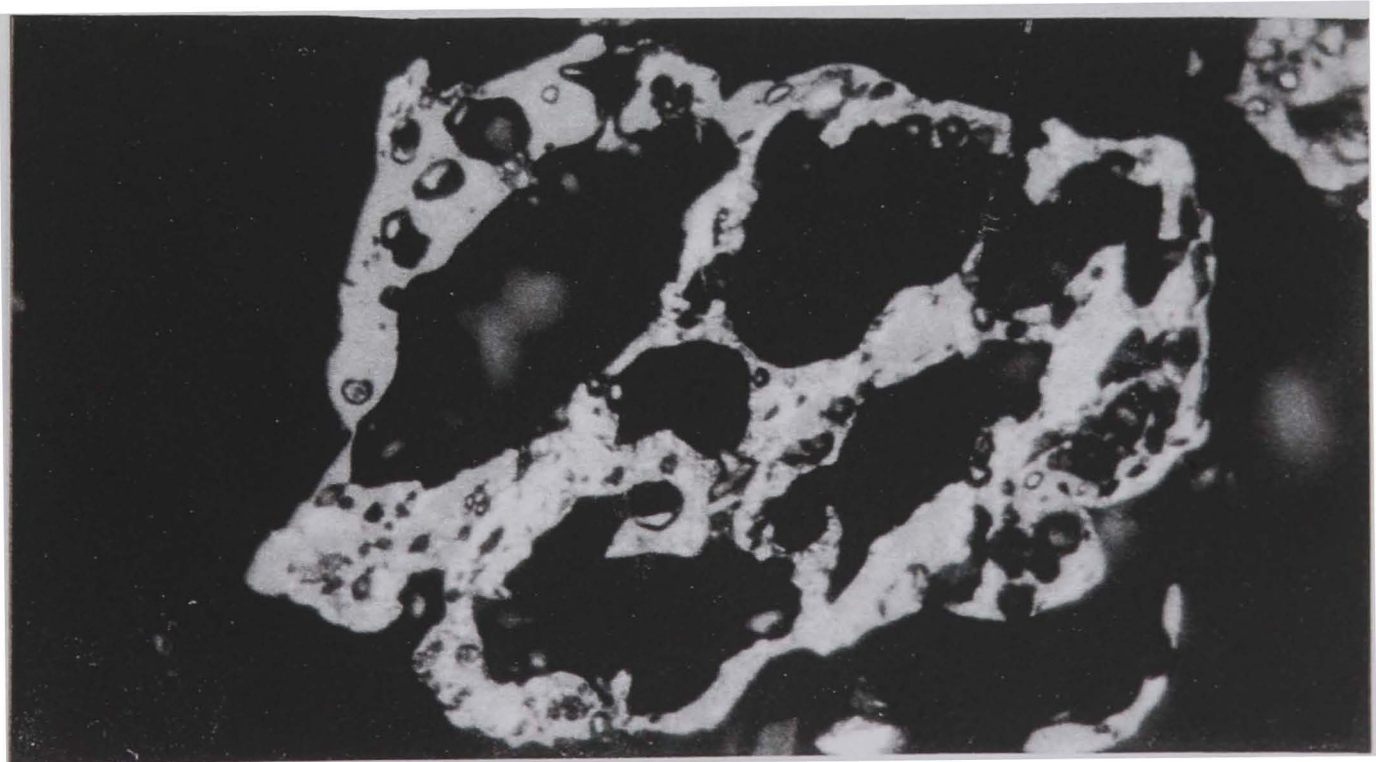
APPENDIX A - Char Nomenclature Photographs



Fusinoid Char



Solid Char - typical of pseudovitrinite chars with tears and splits

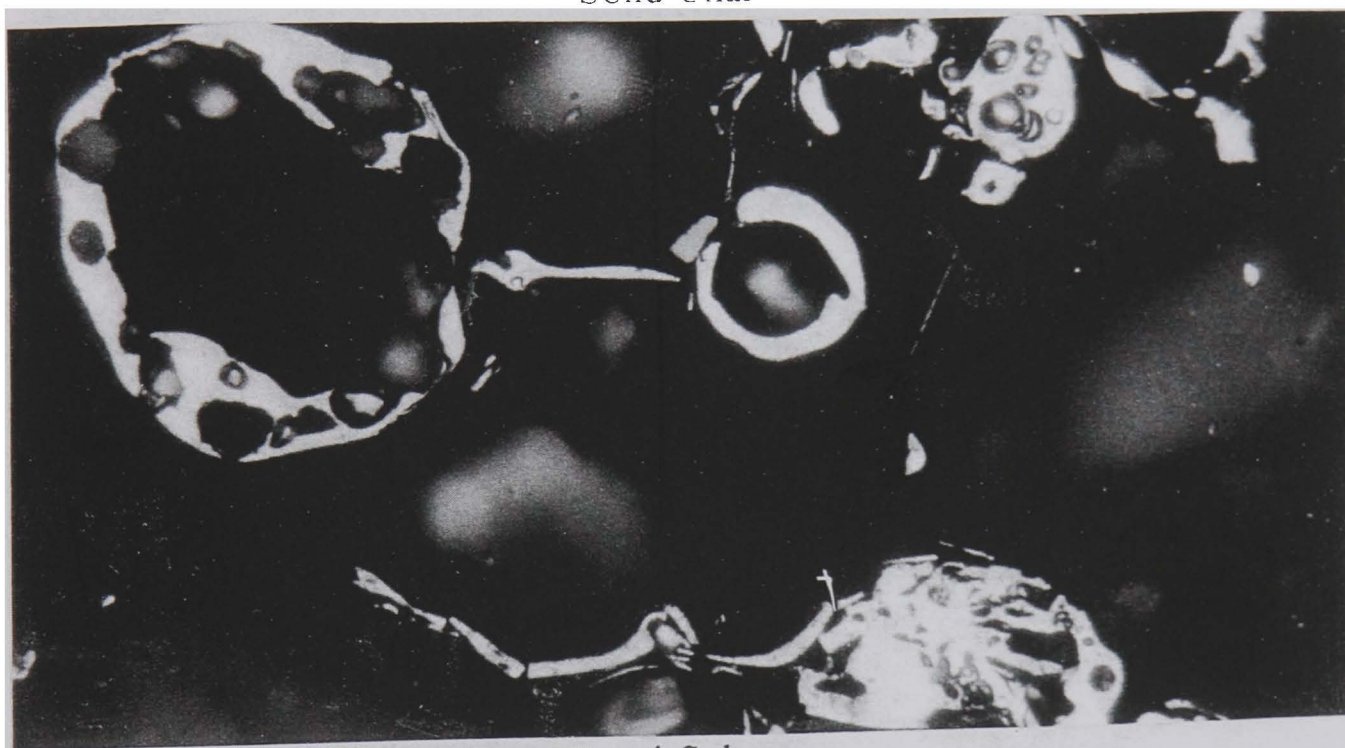


Crassi-Network

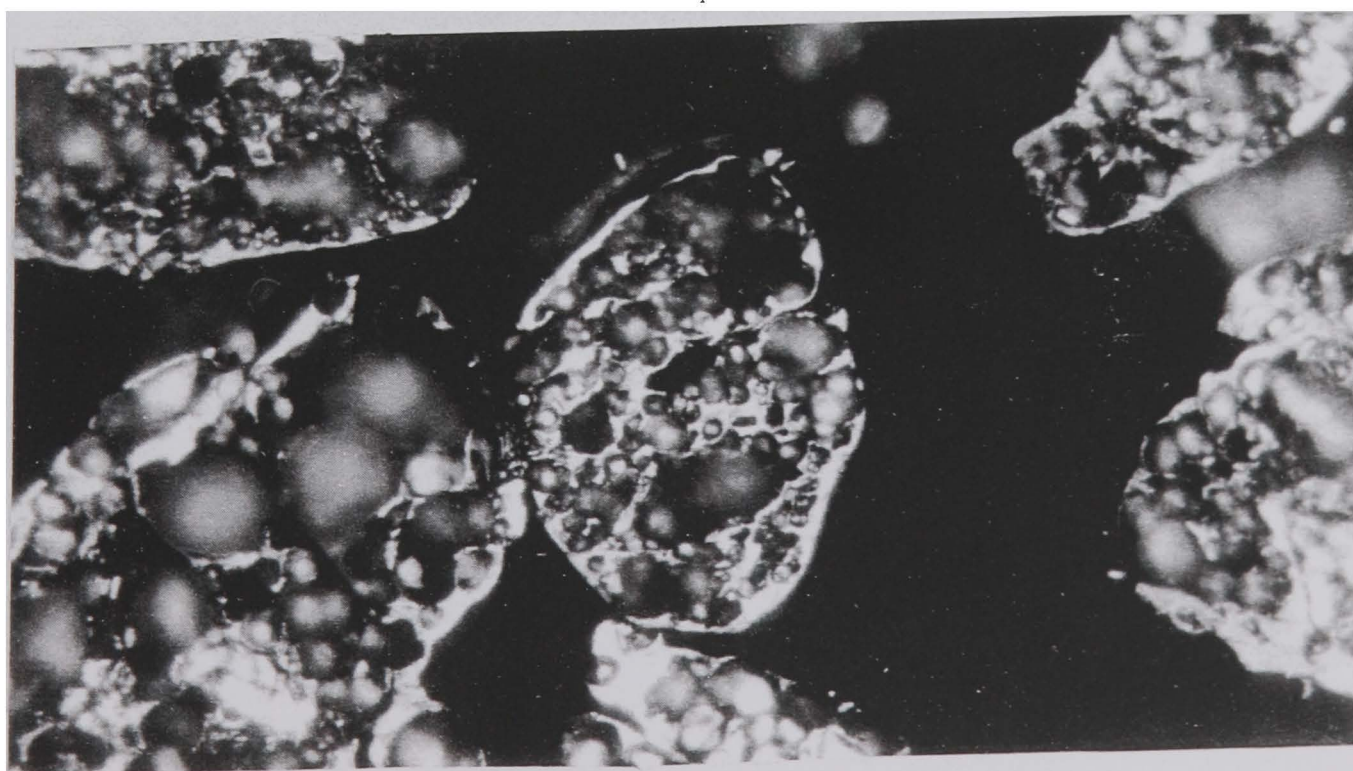
APPENDIX A - Char Nomenclature Photographs



Solid Char



Tenui-Sphere



Tenui-Network

APPENDIX B - Proximate Analysis of Point of AYT Chars

200 milliseconds 2% oxygen and 1000 degrees

Sample 1	dry basis	dafb	Sample 2	dry basis	dafb
Moisture	4.33		Moisture	4.47	
Volatiles	1.88	6.55	Volatiles	5.02	6.39
Fixed Carbon	69.72	93.45	Fixed Carbon	73.56	93.61
Ash	21.07	22.02	Ash	16.95	17.75
Total	100.00	100.00	Total	100.00	100.00

Sample 3	dry basis	dafb	Sample 4	dry basis	dafb
Moisture	4.51		Moisture	4.02	
Volatiles	4.91	6.34	Volatiles	4.95	6.27
Fixed Carbon	72.58	93.66	Fixed Carbon	73.66	93.73
Ash	18.00	18.85	Ash	17.39	18.12
Total	100.00	100.00	Total	100.00	100.00

Sample 5	dry basis	dafb	Sample 6	dry basis	dafb
Moisture	4.85		Moisture	4.95	
Volatiles	5.20	6.42	Volatiles	4.87	6.46
Fixed Carbon	75.85	93.58	Fixed Carbon	70.56	93.54
Ash	14.10	11.82	Ash	19.63	20.65
Total	100.00	100.00	Total	100.00	100.00

200 milliseconds 2% oxygen and 1000 degrees

Sample 1	dry basis			dafb	Sample 2	dry basis			dafb
Moisture	4.33				Moisture	4.47			
Volatiles	4.88	5.10	6.55		Volatiles	5.02	5.26	6.39	
Fixed Carbon	69.72	72.88	93.45		Fixed Carbon	73.56	76.99	93.61	
Ash	21.07	22.02			Ash	16.95	17.75		
Total	100.00	100.00	100.00		Total	100.00	100.00	100.00	

Sample 3	dry basis			dafb	Sample 4	dry basis			dafb
Moisture	4.51				Moisture	4.02			
Volatiles	4.91	5.14	6.34		Volatiles	4.93	5.13	6.27	
Fixed Carbon	72.58	76.01	93.66		Fixed Carbon	73.66	76.74	93.73	
Ash	18.00	18.85			Ash	17.39	18.12		
Total	100.00	100.00	100.00		Total	100.00	100.00	100.00	

Sample 5	dry basis			dafb	Sample 6	dry basis			dafb
Moisture	4.85				Moisture	4.93			
Volatiles	5.20	5.47	6.42		Volatiles	4.87	5.13	6.46	
Fixed Carbon	75.85	79.72	93.58		Fixed Carbon	70.56	74.22	93.54	
Ash	14.10	14.82			Ash	19.63	20.65		
Total	100.00	100.00	100.00		Total	100.00	100.00	100.00	

200 milliseconds 2% oxygen and 1000 degrees

Sample 1	dry basis			dafb	Sample 2	dry basis			dafb
Moisture	4.33				Moisture	4.47			
Volatiles	4.88	5.10	6.55		Volatiles	5.02	5.26	6.39	
Fixed Carbon	69.72	72.88	93.45		Fixed Carbon	73.56	76.99	93.61	
Ash	21.07	22.02			Ash	16.95	17.75		
Total	100.00	100.00	100.00		Total	100.00	100.00	100.00	

Sample 3	dry basis			dafb	Sample 4	dry basis			dafb
Moisture	4.51				Moisture	4.02			
Volatiles	4.91	5.14	6.34		Volatiles	4.93	5.13	6.27	
Fixed Carbon	72.58	76.01	93.66		Fixed Carbon	73.66	76.74	93.73	
Ash	18.00	18.85			Ash	17.39	18.12		
Total	100.00	100.00	100.00		Total	100.00	100.00	100.00	

Sample 5	dry basis			dafb	Sample 6	dry basis			dafb
Moisture	4.85				Moisture	4.93			
Volatiles	5.20	5.47	6.42		Volatiles	4.87	5.13	6.46	
Fixed Carbon	75.85	79.72	93.58		Fixed Carbon	70.56	74.22	93.54	
Ash	14.10	11.82			Ash	19.63	20.65		
Total	100.00	100.00	100.00		Total	100.00	100.00	100.00	

100 milliseconds 2% oxygen and 1000 degrees

Sample 1	dry basis			dafb	Sample 2	dry basis			dafb
Moisture	4.71				Moisture	4.36			
Volatiles	6.52	6.85	8.06		Volatiles	6.25	6.54	7.98	
Fixed Carbon	74.44	78.12	91.94		Fixed Carbon	72.07	75.36	92.02	
Ash	14.33	15.03			Ash	17.32	18.11		
Total	100.00	100.00	100.00		Total	100.00	100.00	100.00	

Sample 3	dry basis			dafb	Sample 4	dry basis			dafb
Moisture	1.58				Moisture	5.25			
Volatiles	6.60	6.92	8.50		Volatiles	6.85	7.22	8.88	
Fixed Carbon	71.14	74.55	91.50		Fixed Carbon	70.25	74.14	91.12	
Ash	17.67	18.52			Ash	17.65	18.63		
Total	100.00	100.00	100.00		Total	100.00	100.00	100.00	

Sample 5	dry basis			dafb	Sample 6	dry basis			dafb
Moisture	4.73				Moisture	4.61			
Volatiles	7.41	7.78	9.01		Volatiles	6.97	7.31	9.13	
Fixed Carbon	74.85	78.57	90.99		Fixed Carbon	69.38	72.76	90.87	
Ash	13.01	13.65			Ash	19.01	19.93		
Total	100.00	100.00	100.00		Total	100.00	100.00	100.00	

200 milliseconds 0% oxygen and 1000 degrees

Sample 1	dry basis			dafb	Sample 2	dry basis			dafb
Moisture	3.92				Moisture	4.10			
Volatiles	7.08	7.37	9.47		Volatiles	7.72	8.05	10.35	
Fixed Carbon	67.69	70.45	90.53		Fixed Carbon	66.81	69.67	89.65	
Ash	21.30	22.17			Ash	21.37	22.28		
Total	100.00	100.00	100.00		Total	100.00	100.00	100.00	

Sample 3	dry basis			dafb	Sample 4	dry basis			dafb
Moisture	4.58				Moisture	3.80			
Volatiles	6.60	6.92	8.50		Volatiles	8.00	8.31	10.39	
Fixed Carbon	71.14	74.55	91.50		Fixed Carbon	68.99	71.71	89.61	
Ash	17.67	18.52			Ash	19.22	19.98		
Total	100.00	100.00	100.00		Total	100.00	100.00	100.00	

Sample 5	dry basis			dafb	Sample 6	dry basis			dafb
Moisture	3.88				Moisture	3.87			
Volatiles	7.13	7.42	9.23		Volatiles	7.27	7.56	9.90	
Fixed Carbon	70.09	72.92	90.77		Fixed Carbon	66.20	68.87	90.10	
Ash	18.90	19.66			Ash	22.65	23.56		
Total	100.00	100.00	100.00		Total	100.00	100.00	100.00	

100 milliseconds 0% oxygen and 1000 degrees

Sample 1	dry basis			dafb	Sample 2	dry basis			dafb
Moisture	3.57				Moisture	3.57			
Volatiles	9.11	9.76	12.28		Volatiles	10.04	10.41	13.45	
Fixed Carbon	67.22	69.71	87.72		Fixed Carbon	64.59	66.98	86.55	
Ash	19.80	20.53			Ash	21.80	22.61		
Total	100.00	100.00	100.00		Total	100.00	100.00	100.00	

Sample 3	dry basis			dafb	Sample 4	dry basis			dafb
Moisture	3.49				Moisture	3.71			
Volatiles	9.44	9.78	12.64		Volatiles	9.84	10.22	13.05	
Fixed Carbon	65.22	67.58	87.36		Fixed Carbon	65.55	68.07	86.95	
Ash	21.85	22.64			Ash	20.91	21.71		
Total	100.00	100.00	100.00		Total	100.00	100.00	100.00	

Sample 5	dry basis			dafb	Sample 6	dry basis			dafb
Moisture	3.67				Moisture	3.46			
Volatiles	9.69	9.96	12.63		Volatiles	9.35	9.69	12.71	
Fixed Carbon	67.04	68.87	87.37		Fixed Carbon	64.23	66.53	87.29	
Ash	19.60	20.14			Ash	22.96	23.79		
Total	100.00	98.97	100.00		Total	100.00	100.00	100.00	

200 milliseconds 0% oxygen and 1300 degrees

Sample 1	dry basis		dafb	Sample 2	dry basis		dafb
Moisture	0.23			Moisture	1.33		
Volatiles	0.83	0.83	1.09	Volatiles	1.04	1.05	1.34
Fixed Carbon	74.95	75.12	98.91	Fixed Carbon	76.27	77.30	98.66
Ash	24.00	24.05		Ash	21.36	21.65	
Total	100.00	100.00	100.00	Total	100.00	100.00	100.00

Sample 3	dry basis		dafb
Moisture	2.24		
Volatiles	1.52	1.56	2.06
Fixed Carbon	72.23	73.89	97.94
Ash	24.00	24.55	
Total	100.00	100.00	100.00

200 milliseconds 2% oxygen and 1300 degrees

Sample 1	dry basis		dafb	Sample 2	dry basis		dafb
Moisture	2.39			Moisture	3.12		
Volatiles	1.96	2.00	2.58	Volatiles	2.05	2.12	2.75
Fixed Carbon	73.84	75.65	97.42	Fixed Carbon	72.44	74.77	97.25
Ash	21.81	22.35		Ash	22.39	23.11	
Total	100.00	100.00	100.00	Total	100.00	100.00	100.00

Sample 3	dry basis		dafb	Sample 4	dry basis		dafb
Moisture	3.30			Moisture	3.37		
Volatiles	2.36	2.44	3.15	Volatiles	2.14	2.22	2.96
Fixed Carbon	72.50	74.97	96.85	Fixed Carbon	70.20	72.65	97.04
Ash	21.85	22.59		Ash	24.29	25.14	
Total	100.00	100.00	100.00	Total	100.00	100.00	100.00

100 milliseconds 0% oxygen and 1300 degrees

Sample 1	dry basis		dafb	Sample 2	dry basis		dafb
Moisture	2.31			Moisture	1.59		
Volatiles	3.45	3.53	4.75	Volatiles	2.91	2.96	2.96
Fixed Carbon	69.14	70.77	95.25	Fixed Carbon	73.50	74.69	74.69
Ash	25.11	25.70		Ash	22.00	22.35	
Total	100.00	100.00	100.00	Total	100.00	100.00	77.65

Sample 3	dry basis		dafb	Sample 4	dry basis		dafb
Moisture	1.65			Moisture	1.74		
Volatiles	2.70	2.75	3.58	Volatiles	2.64	2.68	3.54
Fixed Carbon	72.68	73.90	96.42	Fixed Carbon	71.91	73.18	96.46
Ash	22.97	23.35		Ash	23.72	24.14	
Total	100.00	100.00	100.00	Total	100.00	100.00	100.00

100 milliseconds 2% oxygen and 1300 degrees

Sample 1	dry basis		dafb	Sample 2	dry basis		dafb
Moisture	1.67			Moisture	1.64		
Volatiles	2.64	2.68	3.54	Volatiles	2.55	2.59	3.56
Fixed Carbon	71.96	73.18	96.46	Fixed Carbon	69.06	70.21	96.44
Ash	23.73	24.14		Ash	26.75	27.19	
Total	100.00	100.00	100.00	Total	100.00	100.00	100.00

Sample 3	dry basis		dafb	Sample 4	dry basis		dafb
Moisture	1.80			Moisture	3.38		
Volatiles	2.52	2.57	3.74	Volatiles	2.89	2.99	4.11
Fixed Carbon	64.84	66.03	96.26	Fixed Carbon	67.33	69.68	95.89
Ash	30.84	31.40		Ash	26.40	27.33	
Total	100.00	100.00	100.00	Total	100.00	100.00	100.00

1000 degrees 100 milliseconds 3% oxygen

	53-75 micron			106-125 micron			180-212 micron			
		dry basis	dafb		dry basis	dafb		dry basis	dafb	
Kromdraai	Moisture	2.32		2.32		0.47				
	Volatiles	11.27	11.54	13.84	11.27	11.54	13.84	5.55	5.58	5.96
	Fixed Carbon	70.14	71.81	86.16	70.14	71.81	86.16	87.53	87.94	94.04
	Ash	16.27	16.66		16.27	16.66		6.45	6.48	
	Total	100.00	100.00	100.00	100.00	100.00	100.00	100.00	100.00	100.00

	53-75 micron			106-125 micron			180-212 micron			
		dry basis	dafb		dry basis	dafb		dry basis	dafb	
Kellingley	Moisture	2.65		2.02		1.08				
	Volatiles	7.24	7.44	8.64	8.27	8.44	10.00	24.75	25.02	28.53
	Fixed Carbon	76.52	78.60	91.36	74.39	75.92	90.00	62.00	62.68	71.47
	Ash	13.59	13.96		15.32	15.64		12.17	12.30	
	Total	100.00	100.00	100.00	100.00	100.00	100.00	100.00	100.00	100.00

	53-75 micron			106-125 micron			180-212 micron			
		dry basis	dafb		dry basis	dafb		dry basis	dafb	
Tower	Moisture	0.15		0.60		0.47				
	Volatiles	5.78	5.79	6.13	5.24	5.27	5.60	5.55	5.58	5.96
	Fixed Carbon	88.48	88.61	93.87	88.38	88.91	94.40	87.53	87.94	94.04
	Ash	5.59	5.60		5.78	5.81		6.45	6.48	
	Total	100.00	100.00	100.00	100.00	100.00	100.00	100.00	100.00	100.00

1150 degrees 100 milliseconds 3% oxygen

	53-75 micron			106-125 micron			180-212 micron			
		dry basis	dafb		dry basis	dafb		dry basis	dafb	
Kromdraai	Moisture	2.75		3.04		0.56				
	Volatiles	5.91	6.08	7.35	5.45	5.62	6.85	5.12	5.15	5.42
	Fixed Carbon	74.50	76.61	92.65	74.15	76.47	93.15	89.27	89.77	94.58
	Ash	16.84	17.32		17.36	17.90		5.05	5.08	
	Total	100.00	100.00	100.00	100.00	100.00	100.00	100.00	100.00	100.00

	53-75 micron			106-125 micron			180-212 micron			
		dry basis	dafb		dry basis	dafb		dry basis	dafb	
Kellingley	Moisture	2.35		1.97		0.98				
	Volatiles	6.05	6.20	6.97	4.28	4.37	5.68	17.73	17.91	21.45
	Fixed Carbon	80.72	82.66	93.03	71.07	72.50	94.32	64.91	65.55	78.55
	Ash	10.88	11.14		22.68	23.14		16.38	16.54	
	Total	100.00	100.00	100.00	100.00	100.00	100.00	100.00	100.00	100.00

	53-75 micron			106-125 micron			180-212 micron			
		dry basis	dafb		dry basis	dafb		dry basis	dafb	
Tower	Moisture	1.09		0.93		0.56				
	Volatiles	4.58	4.63	4.79	3.89	3.93	4.16	5.12	5.15	5.42
	Fixed Carbon	90.94	91.94	95.21	89.71	90.55	95.84	89.27	89.77	94.58
	Ash	3.39	3.43		5.47	5.52		5.05	5.08	
	Total	100.00	100.00	100.00	100.00	100.00	100.00	100.00	100.00	100.00

1300 degrees 100 milliseconds 3% oxygen

	53-75 micron		106-125 micron		180-212 micron	
	dry basis	dafb	dry basis	dafb	dry basis	dafb
<b>Kromdraai</b>						
Moisture	2.82		3.03		1.75	
Volatiles	1.67	1.72	2.15	1.71	1.76	2.13
Fixed Carbon	76.00	78.21	97.85	78.68	81.14	97.87
Ash	19.51	20.08		16.58	17.10	
<b>Total</b>	<b>100.00</b>	<b>100.00</b>	<b>100.00</b>	<b>100.00</b>	<b>100.00</b>	<b>100.00</b>

	53-75 micron		106-125 micron		180-212 micron	
	dry basis	dafb	dry basis	dafb	dry basis	dafb
<b>Kellingley</b>						
Moisture	1.72		2.35		1.75	
Volatiles	1.38	1.40	1.93	2.48	2.54	3.22
Fixed Carbon	70.06	71.29	98.07	74.45	76.24	96.78
Ash	26.84	27.31		20.72	21.22	
<b>Total</b>	<b>100.00</b>	<b>100.00</b>	<b>100.00</b>	<b>100.00</b>	<b>100.00</b>	<b>100.00</b>

	53-75 micron		106-125 micron		180-212 micron	
	dry basis	dafb	dry basis	dafb	dry basis	dafb
<b>Tower</b>						
Moisture	1.11		0.91		0.48	
Volatiles	1.20	1.21	1.28	1.84	1.86	1.96
Fixed Carbon	92.45	93.49	98.72	91.99	92.83	98.04
Ash	5.24	5.30		5.26	5.31	
<b>Total</b>	<b>100.00</b>	<b>100.00</b>	<b>100.00</b>	<b>100.00</b>	<b>100.00</b>	<b>100.00</b>

1400 degrees 100 milliseconds 3% oxygen

	53-75 micron			106-125 micron			180-212 micron		
	dry basis	dafb		dry basis	dafb		dry basis	dafb	
<b>Kromdraai</b>									
Moisture	2.06			3.14			2.44		
Volatiles	0.78	0.80	1.01	0.97	1.00	1.23	6.06	6.21	7.52
Fixed Carbon	76.43	78.04	98.99	77.73	80.25	98.77	74.50	76.36	92.48
Ash	20.73	21.17		18.16	18.75		17.00	17.43	
<b>Total</b>	<b>100.00</b>	<b>100.00</b>	<b>100.00</b>	<b>100.00</b>	<b>100.00</b>	<b>100.00</b>	<b>100.00</b>	<b>100.00</b>	<b>100.00</b>

	53-75 micron			106-125 micron			180-212 micron		
	dry basis	dafb		dry basis	dafb		dry basis	dafb	
<b>Kellingley</b>									
Moisture	0.76			0.50			1.94		
Volatiles	0.60	0.60	0.93	0.43	0.43	0.54	6.06	6.18	7.58
Fixed Carbon	63.77	64.26	99.07	78.98	79.38	99.46	73.90	75.36	92.42
Ash	34.87	35.14		20.09	20.19		18.10	18.46	
<b>Total</b>	<b>100.00</b>	<b>100.00</b>	<b>100.00</b>	<b>100.00</b>	<b>100.00</b>	<b>100.00</b>	<b>100.00</b>	<b>100.00</b>	<b>100.00</b>

	53-75 micron			106-125 micron			180-212 micron		
	dry basis	dafb		dry basis	dafb		dry basis	dafb	
<b>Tower</b>									
Moisture	0.00			0.21			0.77		
Volatiles	0.00	0.00	0.00	0.26	0.26	0.28	2.78	2.80	3.06
Fixed Carbon	93.42	93.42	100.00	91.02	91.21	99.72	88.04	88.72	96.94
Ash	6.58	6.58		8.51	8.53		8.41	8.48	
<b>Total</b>	<b>100.00</b>	<b>100.00</b>	<b>100.00</b>	<b>100.00</b>	<b>100.00</b>	<b>100.00</b>	<b>100.00</b>	<b>100.00</b>	<b>100.00</b>

1000 degrees 100 milliseconds 0% oxygen

	53-75 micron			106-125 micron			180-212 micron			
		dry basis	dafb		dry basis	dafb		dry basis	dafb	
Kromdraai	Moisture	2.42		2.60		0.45				
	Volatiles	6.55	6.71	8.20	6.35	6.52	7.83	4.47	4.49	4.76
	Fixed Carbon	73.32	75.14	91.80	74.72	76.71	92.17	89.35	89.75	95.24
	Ash	17.71	18.15		16.33	16.77		5.73	5.76	
	Total	100.00	100.00	100.00	100.00	100.00	100.00	100.00	100.00	100.00

	53-75 micron			106-125 micron			180-212 micron			
		dry basis	dafb		dry basis	dafb		dry basis	dafb	
Kellingley	Moisture	1.54		1.95		1.16				
	Volatiles	13.94	14.16	15.75	14.90	15.20	17.01	22.54	22.80	25.17
	Fixed Carbon	74.55	75.72	84.25	72.71	74.16	82.99	67.00	67.79	74.83
	Ash	9.97	10.13		10.44	10.65		9.30	9.41	
	Total	100.00	100.00	100.00	100.00	100.00	100.00	100.00	100.00	100.00

	53-75 micron			106-125 micron			180-212 micron			
		dry basis	dafb		dry basis	dafb		dry basis	dafb	
Tower	Moisture	0.91		0.91		0.45				
	Volatiles	4.47	4.51	4.73	4.16	4.20	4.41	4.47	4.49	4.76
	Fixed Carbon	89.96	90.79	95.27	90.26	91.09	95.59	89.35	89.75	95.24
	Ash	4.66	4.70		4.67	4.71		5.73	5.76	
	Total	100.00	100.00	100.00	100.00	100.00	100.00	100.00	100.00	100.00

1150 degrees 100 milliseconds 0% oxygen

	53-75 micron			106-125 micron			180-212 micron			
		dry basis	dafb		dry basis	dafb		dry basis	dafb	
Kromdraai	Moisture	2.09		2.09		0.45				
	Volatiles	11.88	12.13	14.62	11.88	12.13	14.62	5.92	5.95	6.26
	Fixed Carbon	69.40	70.88	85.38	69.40	70.88	85.38	88.71	89.11	93.74
	Ash	16.63	16.98		16.63	16.98		4.92	4.94	
	Total	100.00	100.00	100.00	100.00	100.00	100.00	100.00	100.00	100.00

	53-75 micron			106-125 micron			180-212 micron			
		dry basis	dafb		dry basis	dafb		dry basis	dafb	
Kellingley	Moisture	2.03		2.17		1.18				
	Volatiles	5.83	5.95	7.36	5.30	5.42	6.55	11.42	11.56	13.55
	Fixed Carbon	73.36	74.88	92.64	75.59	77.27	93.45	72.83	73.70	86.45
	Ash	18.78	19.17		16.94	17.32		14.57	14.74	
	Total	100.00	100.00	100.00	100.00	100.00	100.00	100.00	100.00	100.00

	53-75 micron			106-125 micron			180-212 micron			
		dry basis	dafb		dry basis	dafb		dry basis	dafb	
Tower	Moisture	0.06		0.37		0.45				
	Volatiles	6.13	6.13	6.45	5.57	5.59	5.87	5.92	5.95	6.26
	Fixed Carbon	88.98	89.03	93.55	89.36	89.69	94.13	88.71	89.11	93.74
	Ash	4.83	4.83		4.70	4.72		4.92	4.94	
	Total	100.00	100.00	100.00	100.00	100.00	100.00	100.00	100.00	100.00

1300 degrees 100 milliseconds 0% oxygen

	53-75 micron			106-125 micron			180-212 micron			
		dry basis	dafb		dry basis	dafb		dry basis	dafb	
Kromdraai	Moisture	3.96		3.10		2.07				
	Volatiles	3.16	3.29	4.08	2.65	2.73	3.35	9.98	10.19	12.12
	Fixed Carbon	74.24	77.30	95.92	76.46	78.91	96.65	72.35	73.88	87.88
	Ash	18.64	19.41		17.79	18.36		15.60	15.93	
	Total	100.00	100.00	100.00	100.00	100.00	100.00	100.00	100.00	100.00

	53-75 micron			106-125 micron			180-212 micron			
		dry basis	dafb		dry basis	dafb		dry basis	dafb	
Kellingley	Moisture	2.73		2.35		1.94				
	Volatiles	2.91	2.99	4.01	2.48	2.54	3.22	11.19	11.41	13.69
	Fixed Carbon	69.73	71.69	95.99	74.45	76.24	96.78	70.57	71.97	86.31
	Ash	24.63	25.32		20.72	21.22		16.30	16.62	
	Total	100.00	100.00	100.00	100.00	100.00	100.00	100.00	100.00	100.00

	53-75 micron			106-125 micron			180-212 micron			
		dry basis	dafb		dry basis	dafb		dry basis	dafb	
Tower	Moisture	1.89		1.71		0.80				
	Volatiles	2.86	2.92	3.09	2.76	2.81	2.93	4.45	4.49	4.74
	Fixed Carbon	89.63	91.36	96.91	91.34	92.93	97.07	89.49	90.21	95.26
	Ash	5.62	5.73		4.19	4.26		5.26	5.30	
	Total	100.00	100.00	100.00	100.00	100.00	100.00	100.00	100.00	100.00















<b>Drummond</b>	53-75 micron				106-125 micron			180-212 micron				
	Moisture	2.19			Moisture	2.11		Moisture	1.88			
	Volatiles	29.08	29.73	33.22	Volatiles	29.67	30.31	34.21	Volatiles	30.55	31.14	35.48
	Carbon	58.45	59.76	66.78	Carbon	57.05	58.28	65.79	Carbon	55.56	56.62	64.52
	Ash	10.28	10.51		Ash	11.18	11.42		Ash	12.01	12.24	
<b>McQuarie</b>	53-75 micron				106-125 micron			180-212 micron				
	Moisture	2.11			Moisture	1.87		Moisture	1.92			
	Volatiles	27.97	28.58	33.50	Volatiles	28.20	28.74	34.10	Volatiles	27.48	28.02	34.22
	Carbon	55.54	56.74	66.51	Carbon	54.51	55.55	65.91	Carbon	52.83	53.87	65.78
	Ash	14.38	14.69		Ash	15.41	15.71		Ash	17.76	18.11	
<b>Island Creek</b>	53-75 micron				106-125 micron			180-212 micron				
	Moisture	0.29			Moisture	0.05		Moisture	0.25			
	Volatiles	14.96	15.00	15.58	Volatiles	15.73	15.73	16.64	Volatiles	14.97	15.00	16.43
	Carbon	81.05	81.29	84.42	Carbon	78.80	78.84	83.36	Carbon	76.14	76.33	83.57
	Ash	3.70	3.71		Ash	5.43	5.43		Ash	8.64	8.66	

<b>Pinang</b>	53-75 micron				106-125 micron			180-212 micron		
	Moisture	6.91			Moisture	7.10		Moisture	6.79	
	Volatiles	36.14	38.83	40.35	Volatiles	35.33	38.03	39.43	Volatiles	36.51
	Carbon	53.44	57.41	59.66	Carbon	54.26	58.41	60.57	Carbon	54.73
	Ash	3.51	3.77		Ash	3.31	3.56		Ash	1.97
<b>Kaltim Prima</b>	53-75 micron				106-125 micron			180-212 micron		
	Moisture	3.84			Moisture	3.95		Moisture	4.07	
	Volatiles	35.89	37.32	38.64	Volatiles	36.45	37.94	38.78	Volatiles	36.47
	Carbon	56.99	59.27	61.36	Carbon	57.54	59.90	61.22	Carbon	56.48
	Ash	3.28	3.41		Ash	2.07	2.15		Ash	2.98
<b>China SSM</b>	53-75 micron				106-125 micron			180-212 micron		
	Moisture	2.78			Moisture	2.72		Moisture	2.66	
	Volatiles	28.07	28.87	33.38	Volatiles	27.98	28.76	34.26	Volatiles	30.00
	Carbon	56.02	57.62	66.62	Carbon	53.69	55.19	65.74	Carbon	53.74
	Ash	13.14	13.52		Ash	15.61	16.05		Ash	13.60

<b>Bentinck</b>	53-75 micron				106-125 micron			180-212 micron				
	Moisture	2.62			Moisture	2.73		Moisture	3.22			
	Volatiles	28.12	28.88	33.37	Volatiles	27.95	28.73	33.89	Volatiles	28.35	29.29	34.28
	Carbon	56.15	57.66	66.63	Carbon	54.52	56.05	66.12	Carbon	54.35	56.15	65.72
	Ash	13.11	13.46		Ash	14.80	15.22		Ash	14.09	14.55	
<b>El Cerrejon</b>	53-75 micron				106-125 micron			180-212 micron				
	Moisture	3.70			Moisture	3.34		Moisture	3.49			
	Volatiles	31.95	33.18	36.31	Volatiles	32.91	34.05	36.14	Volatiles	33.15	34.35	36.27
	Carbon	56.05	58.21	63.70	Carbon	58.14	60.15	63.85	Carbon	58.24	60.35	63.73
	Ash	8.30	8.62		Ash	5.60	5.79		Ash	5.11	5.30	
<b>Tower</b>	53-75 micron				106-125 micron			180-212 micron				
	Moisture	0.28			Moisture	0.36		Moisture	0.11			
	Volatiles	6.95	6.97	7.35	Volatiles	6.65	6.68	7.10	Volatiles	5.79	5.79	6.11
	Carbon	87.60	87.84	92.65	Carbon	87.03	87.35	92.89	Carbon	88.86	88.96	93.89
	Ash	5.17	5.19		Ash	5.95	5.97		Ash	5.24	5.25	

<b>Kromdraai</b>	53-75 micron				106-125 micron			180-212 micron				
	Moisture	2.29			Moisture	2.41		Moisture	2.56			
	Volatiles	22.13	22.65	26.13	Volatiles	23.42	24.00	27.20	Volatiles	24.09	24.73	27.85
	Carbon	62.57	64.03	73.87	Carbon	62.69	64.23	72.80	Carbon	62.41	64.05	72.15
	Ash	13.01	13.31		Ash	11.48	11.77		Ash	10.94	11.23	
<b>Kellingley</b>	53-75 micron				106-125 micron			180-212 micron				
	Moisture	1.43			Moisture	1.73		Moisture	1.66			
	Volatiles	28.78	29.19	35.17	Volatiles	29.86	30.38	36.89	Volatiles	31.92	32.45	36.93
	Carbon	53.05	53.82	64.83	Carbon	51.08	51.98	63.11	Carbon	54.50	55.42	63.07
	Ash	16.74	16.98		Ash	17.34	17.64		Ash	11.92	12.12	

53-75 micron analyses for 11 coal samples used in the  
drop-tube experiments

El Cerrojon			McQuarie			Drummond		
	mmf			mmf			mmf	
Vitrinite	91.40	92.51	Vitrinite	85.20	87.30	Vitrinite	81.60	82.42
Liptinite	0.40	0.40	Liptinite	3.00	3.07	Liptinite	4.80	4.85
Semi-Fusinite	3.80	3.85	Semi-Fusinite	5.40	5.53	Semi-Fusinite	7.40	7.47
Fusinite	3.20	3.24	Fusinite	4.00	4.10	Fusinite	5.20	5.25
Mineral	1.20		Mineral	2.40		Mineral	1.00	
Pyrite	0.00		Pyrite	0.00		Pyrite	0.00	
Total	100	100	Total	100	100	Total	100	100

China SSM			Kaltim Prima			Island Creek		
	mmf			mmf			mmf	
Vitrinite	61.20	61.69	Vitrinite	96.40	96.79	Vitrinite	94.60	94.60
Liptinite	7.40	7.46	Liptinite	2.20	2.21	Liptinite	0.20	0.20
Semi-Fusinite	22.00	22.18	Semi-Fusinite	1.00	1.00	Semi-Fusinite	2.20	2.20
Fusinite	8.60	8.67	Fusinite	0.00	0.00	Fusinite	3.00	3.00
Mineral	0.80		Mineral	0.20		Mineral	0.00	
Pyrite	0.00		Pyrite	0.20		Pyrite	0.00	
Total	100	100	Total	100	100	Total	100	100

53-75 micron analyses for 11 coal samples used in the  
drop-tube experiments

Bentinck			Pinang			Kromdraai		
	mmf			mmf			mmf	
Vitrinite	82.40	88.03	Vitrinite	92.40	94.09	Vitrinite	56.00	57.26
Liptinite	3.80	4.06	Liptinite	2.20	2.24	Liptinite	6.80	6.95
Semi-Fusinite	4.40	4.70	Semi-Fusinite	2.80	2.85	Semi-Fusinite	22.40	22.90
Fusinite	3.00	3.21	Fusinite	0.80	0.81	Fusinite	12.60	12.88
Mineral	5.40		Mineral	1.80		Mineral	2.20	
Pyrite	1.00		Pyrite	0.00		Pyrite	0.00	
Total	100	100	Total	100	100	Total	100	100

Kellingley			Tower		
	mmf			mmf	
Vitrinite	77.40	80.79	Vitrinite	93.60	95.12
Liptinite	7.80	8.14	Liptinite	0.00	0.00
Semi-Fusinite	6.40	6.68	Semi-Fusinite	2.60	2.64
Fusinite	4.20	4.38	Fusinite	2.20	2.24
Mineral	4.00		Mineral	1.20	
Pyrite	0.20		Pyrite	0.40	
Total	100	100	Total	100	100

106-125 micron analyses for 11 coal samples used in the  
drop-tube experiments

Bentinck			Pinang			Kromdraai		
	mmf			mmf			mmf	
Vitrinite	75.00	83.33	Vitrinite	91.00	91.55	Vitrinite	60.00	60.85
Liptinite	6.00	6.67	Liptinite	3.00	3.02	Liptinite	4.40	4.46
Semi-Fusinite	5.20	5.78	Semi-Fusinite	4.20	4.23	Semi-Fusinite	19.60	19.88
Fusinite	3.80	4.22	Fusinite	1.20	1.21	Fusinite	14.60	14.81
Mineral	9.80		Mineral	0.60		Mineral	1.40	
Pyrite	0.20		Pyrite	0.00		Pyrite	0.00	
<b>Total</b>	<b>100</b>	<b>100</b>	<b>Total</b>	<b>100</b>	<b>100</b>	<b>Total</b>	<b>100</b>	<b>100</b>

Kellingley			Tower		
	mmf			mmf	
Vitrinite	75.60	77.62	Vitrinite	90.80	92.65
Liptinite	12.20	12.53	Liptinite	0.00	0.00
Semi-Fusinite	4.80	4.93	Semi-Fusinite	4.40	4.49
Fusinite	4.80	4.93	Fusinite	2.80	2.86
Mineral	2.00		Mineral	1.80	
Pyrite	0.60		Pyrite	0.20	
<b>Total</b>	<b>100</b>	<b>100</b>	<b>Total</b>	<b>100</b>	<b>100</b>

106-125 micron analyses for 11 coal samples used in the  
drop-tube experiments

El Cerrojon			McQuarie			Drummond		
	mmf			mmf			mmf	
Vitrinite	88.60	90.22	Vitrinite	75.20	79.49	Vitrinite	72.20	73.98
Liptinite	2.00	2.04	Liptinite	4.00	4.23	Liptinite	9.00	9.22
Semi-Fusinite	3.00	3.05	Semi-Fusinite	6.80	7.19	Semi-Fusinite	11.40	11.68
Fusinite	4.60	4.68	Fusinite	8.60	9.09	Fusinite	5.00	5.12
Mineral	1.60		Mineral	5.40		Mineral	2.20	
Pyrite	0.20		Pyrite	0.00		Pyrite	0.20	
Total	100	100	Total	100	100	Total	100	100

China SSM			Kaltim Prima			Island Creek		
	mmf			mmf			mmf	
Vitrinite	62.20	63.08	Vitrinite	94.20	95.93	Vitrinite	85.60	86.29
Liptinite	11.20	11.36	Liptinite	2.20	2.24	Liptinite	0.40	0.40
Semi-Fusinite	20.60	20.89	Semi-Fusinite	1.40	1.43	Semi-Fusinite	6.80	6.85
Fusinite	4.60	4.67	Fusinite	0.40	0.41	Fusinite	6.40	6.45
Mineral	1.40		Mineral	1.80		Mineral	0.80	
Pyrite	0.00		Pyrite	0.00		Pyrite	0.00	
Total	100	100	Total	100	100	Total	100	100

180-212 micron analyses for 11 coal samples used in the  
drop-tube experiments

El Cerrojon			McQuarie			Drummond		
	mmf			mmf			mmf	
Vitrinite	88.00	89.61	Vitrinite	73.40	77.26	Vitrinite	72.40	74.79
Liptinite	1.20	1.22	Liptinite	5.40	5.68	Liptinite	12.40	12.81
Semi-Fusinite	5.40	5.50	Semi-Fusinite	7.60	8.00	Semi-Fusinite	8.40	8.68
Fusinite	3.60	3.67	Fusinite	8.60	9.05	Fusinite	3.60	3.72
Mineral	1.80		Mineral	5.00		Mineral	3.20	
Pyrite	0.00		Pyrite	0.00		Pyrite	0.00	
Total	100	100	Total	100	100	Total	100	100

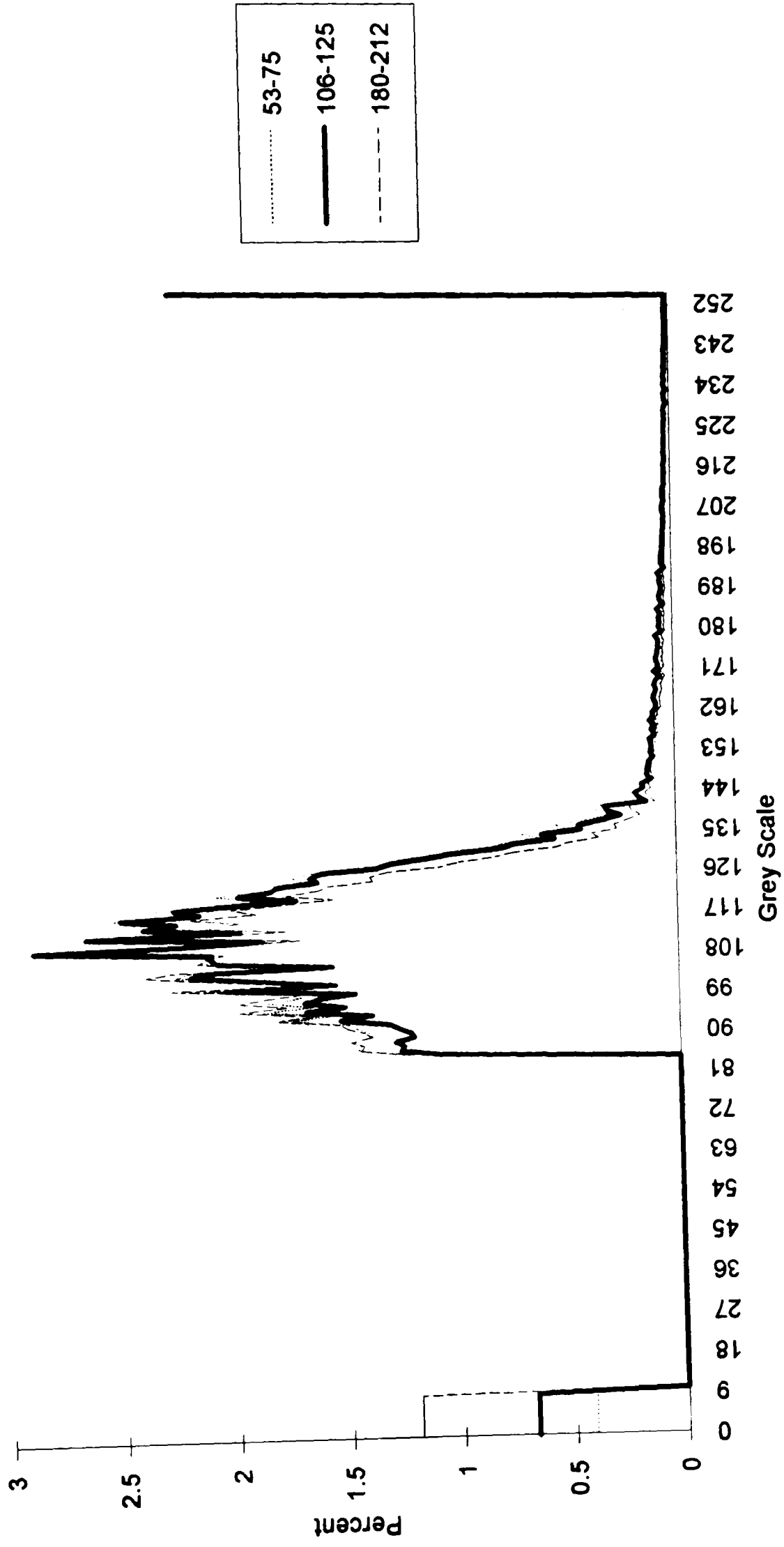
China SSM			Kaltim Prima			Island Creek		
	mmf			mmf			mmf	
Vitrinite	65.20	65.99	Vitrinite	95.00	95.96	Vitrinite	92.20	92.76
Liptinite	16.20	16.40	Liptinite	2.00	2.02	Liptinite	0.00	0.00
Semi-Fusinite	12.80	12.96	Semi-Fusinite	1.40	1.41	Semi-Fusinite	4.20	4.23
Fusinite	4.60	4.66	Fusinite	0.60	0.61	Fusinite	3.00	3.02
Mineral	1.20		Mineral	1.00		Mineral	0.40	
Pyrite	0.00		Pyrite	0.00		Pyrite	0.20	
Total	100	100	Total	100	100	Total	100	100

180-212 micron analyses for 11 coal samples used in the  
drop-tube experiments

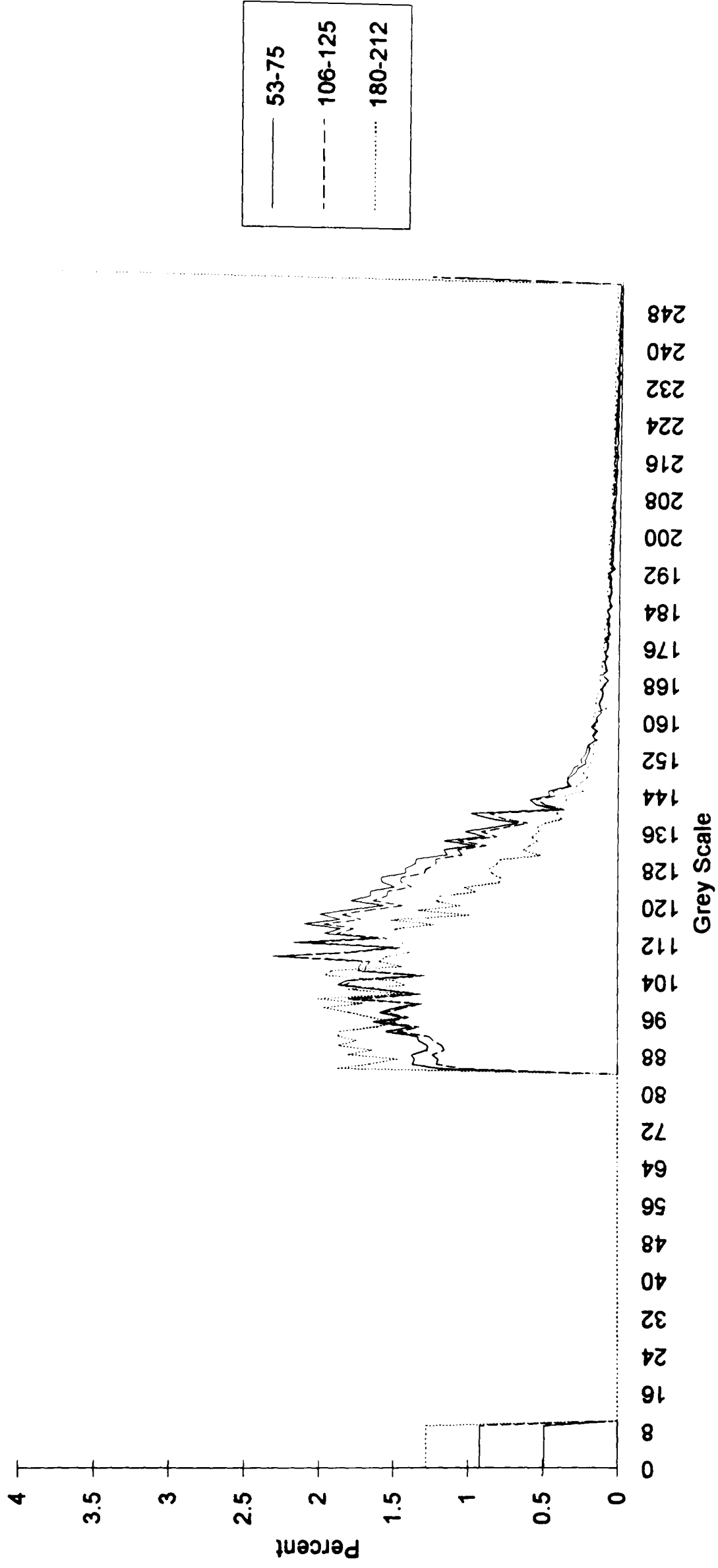
Bentinck			Pinang			Kromdraai		
	mmf			mmf			mmf	
Vitrinite	77.80	82.77	Vitrinite	90.60	92.07	Vitrinite	61.80	62.55
Liptinite	11.20	11.91	Liptinite	2.60	2.64	Liptinite	7.00	7.09
Semi-Fusinite	2.60	2.77	Semi-Fusinite	3.80	3.86	Semi-Fusinite	15.40	15.59
Fusinite	2.40	2.55	Fusinite	1.40	1.42	Fusinite	14.60	14.78
Mineral	5.60		Mineral	1.60		Mineral	1.20	
Pyrite	0.40		Pyrite	0.00		Pyrite	0.00	
<b>Total</b>	<b>100</b>	<b>100</b>	<b>Total</b>	<b>100</b>	<b>100</b>	<b>Total</b>	<b>100</b>	<b>100</b>

Kellingley			Tower		
	mmf			mmf	
Vitrinite	68.60	72.36	Vitrinite	88.20	89.82
Liptinite	15.60	16.46	Liptinite	0.00	0.00
Semi-Fusinite	6.00	6.33	Semi-Fusinite	6.80	6.92
Fusinite	4.60	4.85	Fusinite	3.20	3.26
Mineral	3.60		Mineral	1.60	
Pyrite	1.60		Pyrite	0.20	
<b>Total</b>	<b>100</b>	<b>100</b>	<b>Total</b>	<b>100</b>	<b>100</b>

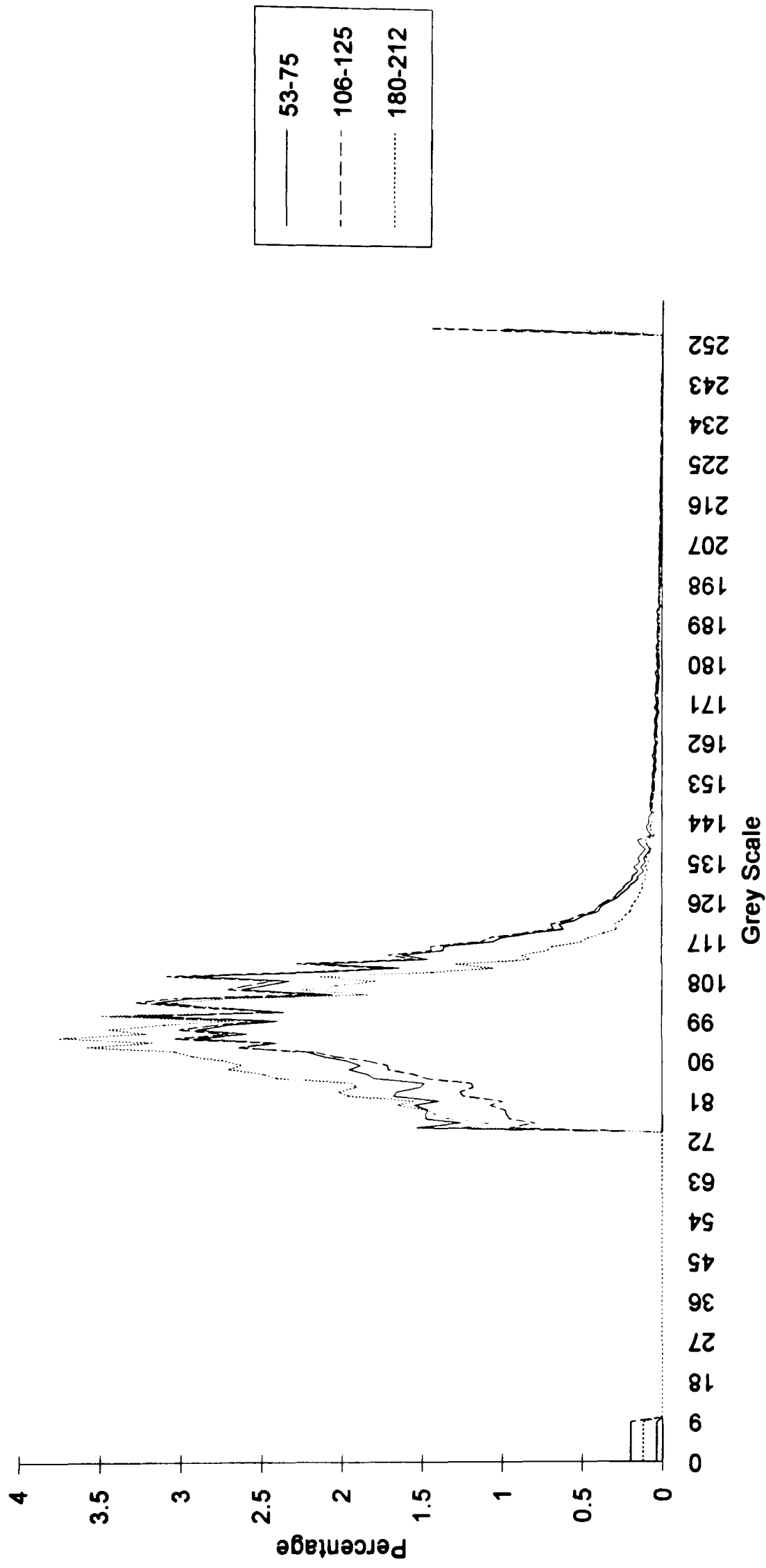
# Bentinck Coal Fractions



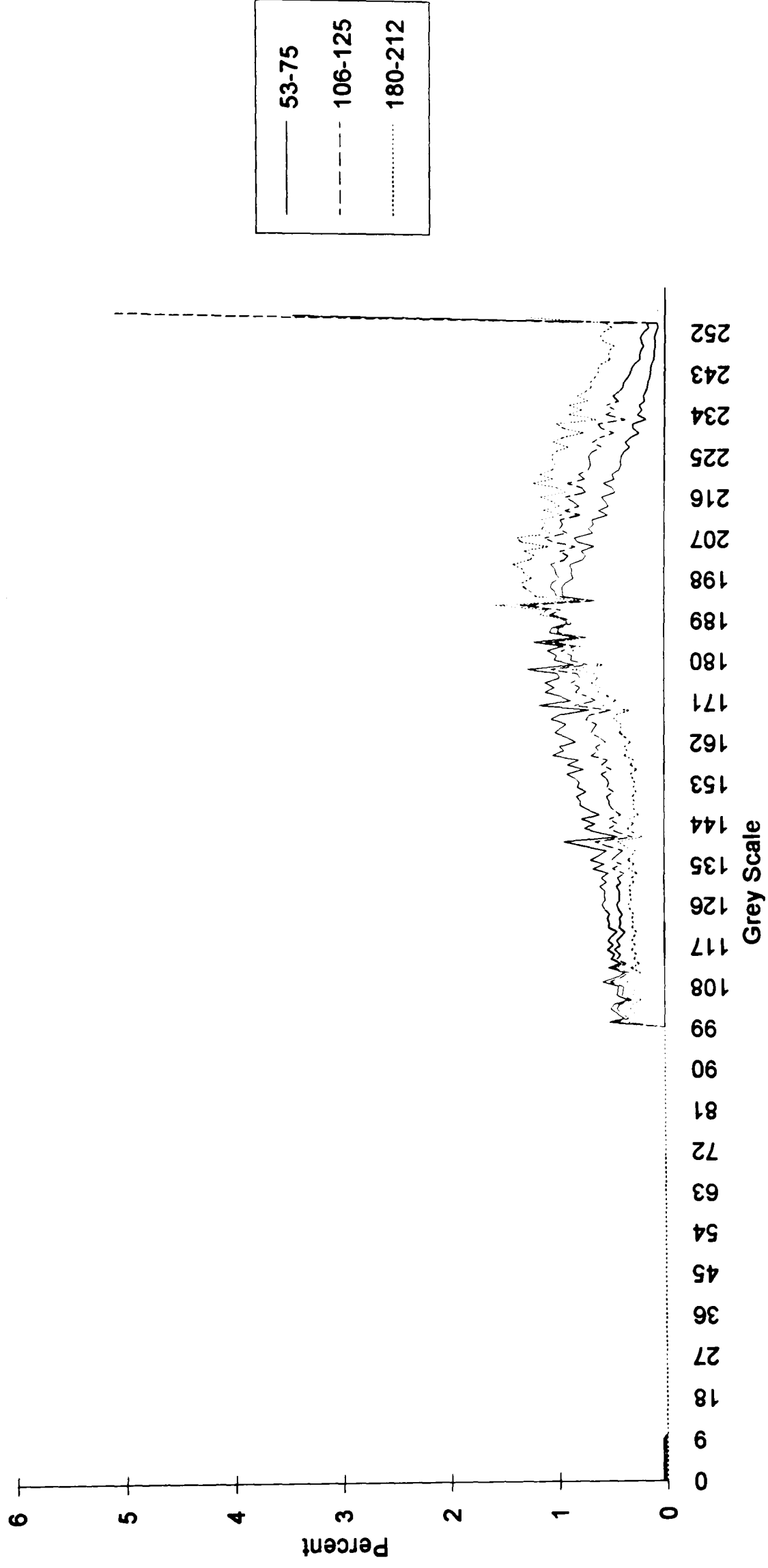
# Drummond Coal Fractions



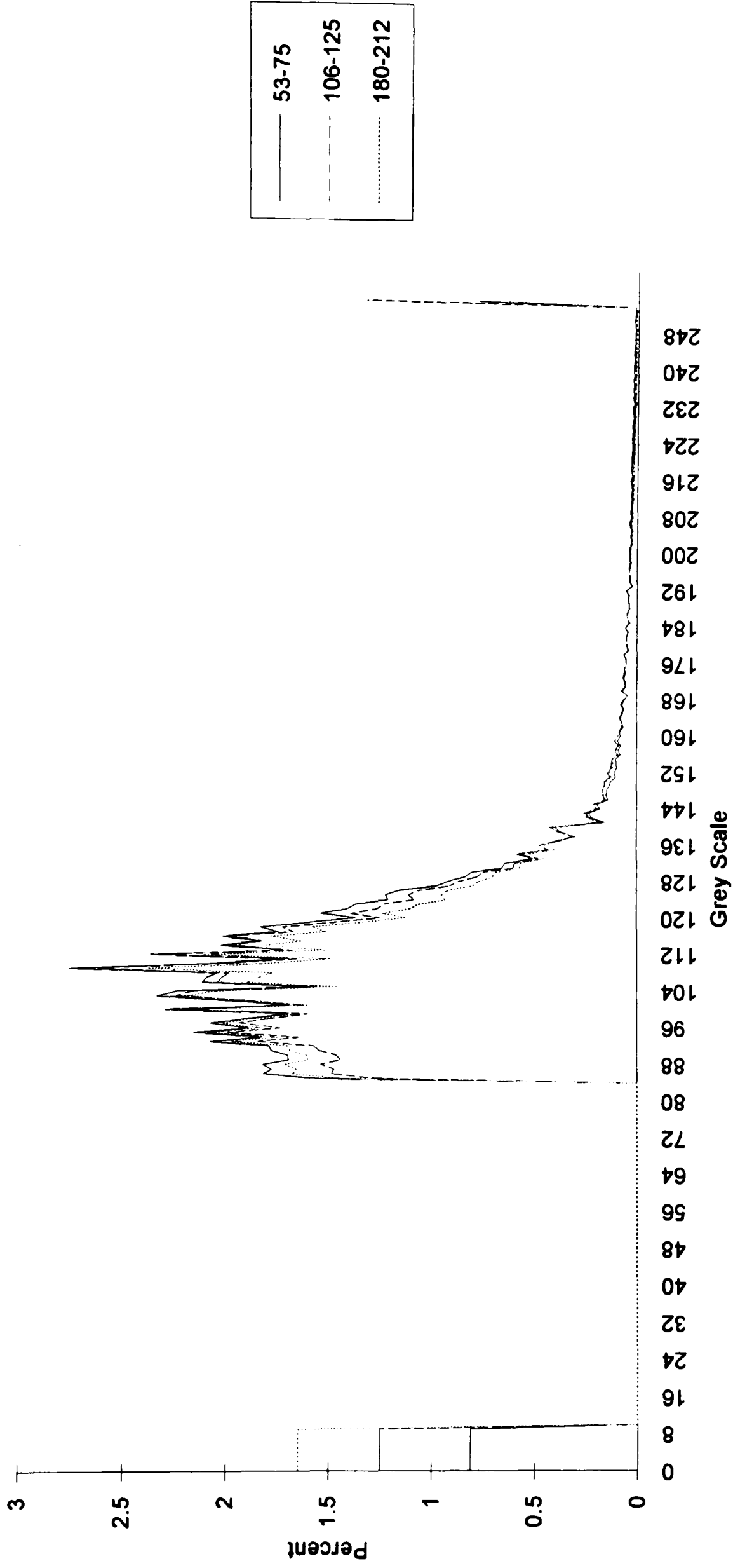
### El Cerrejon Coal Fractions



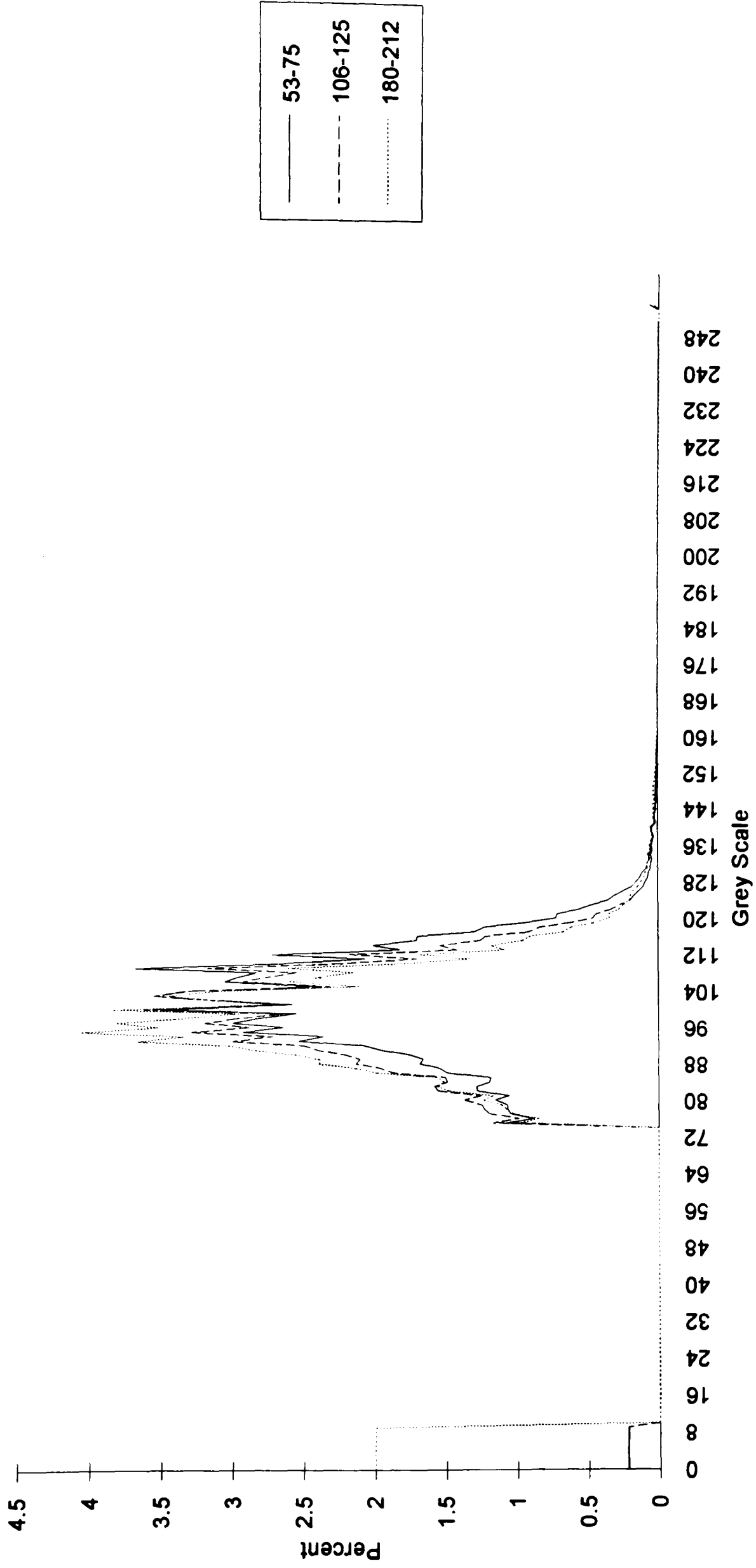
# Island Creek



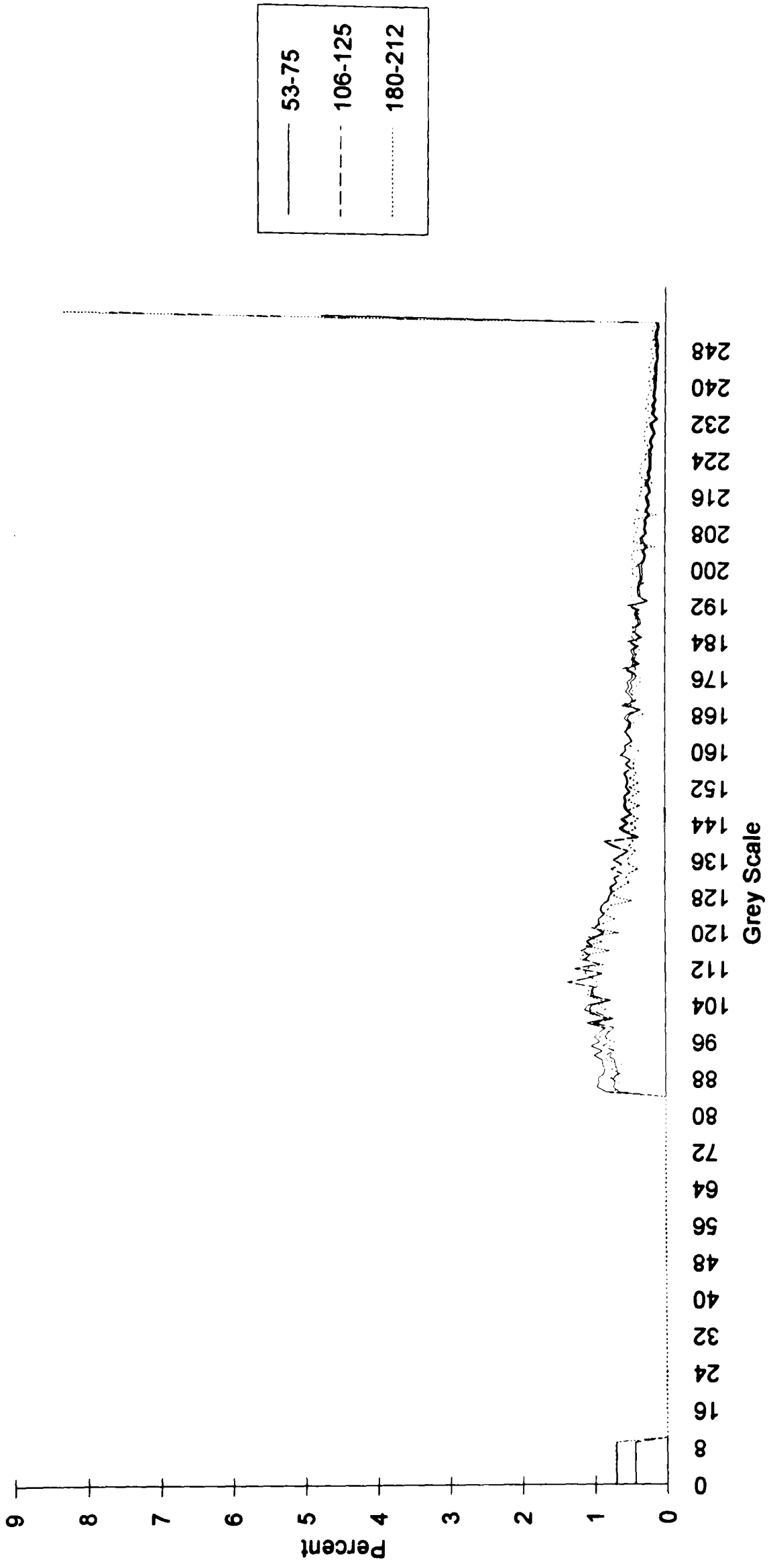
# Kellingley Coal Fractions



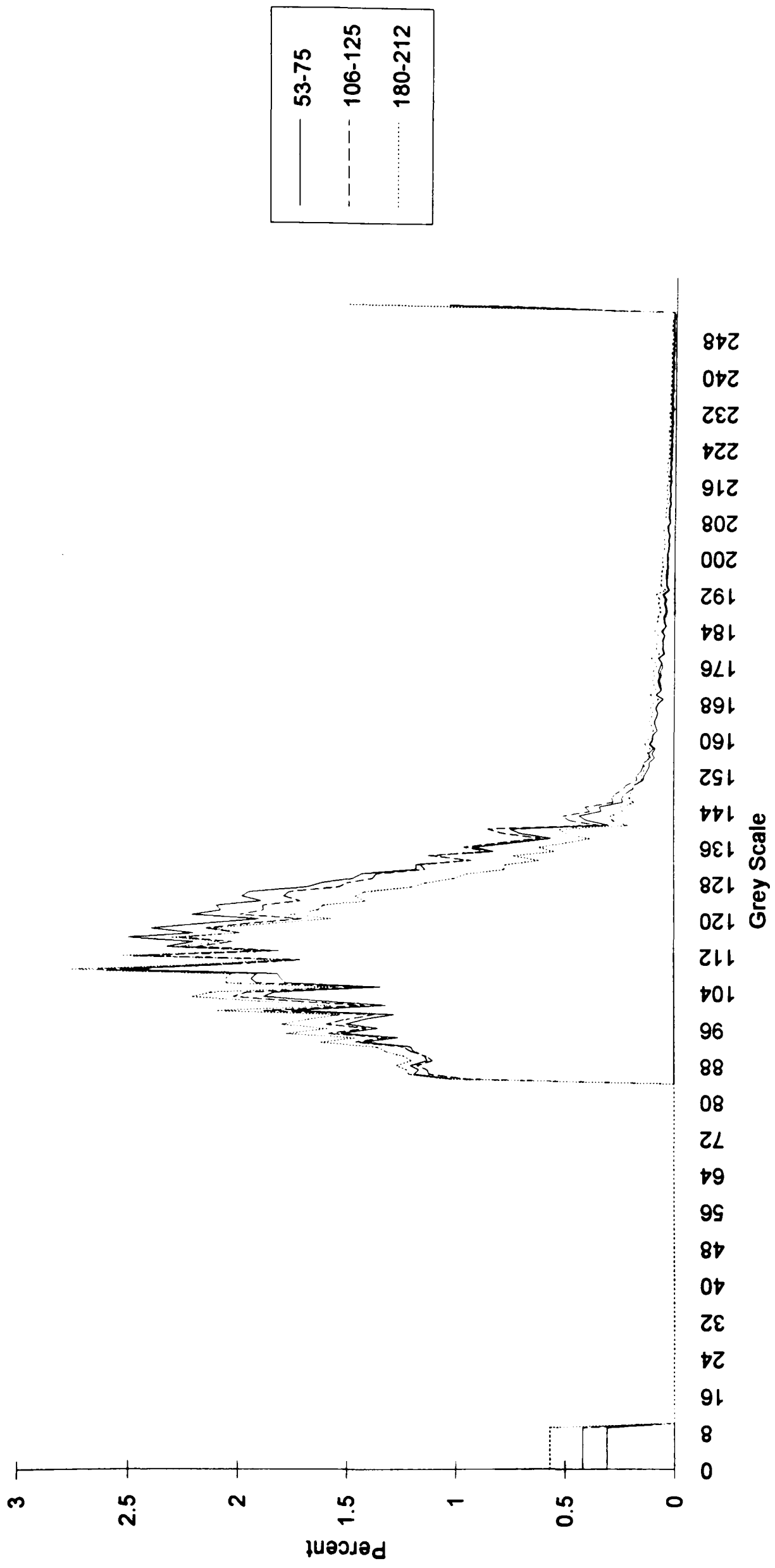
# Kaltim Prima Coal Fractions



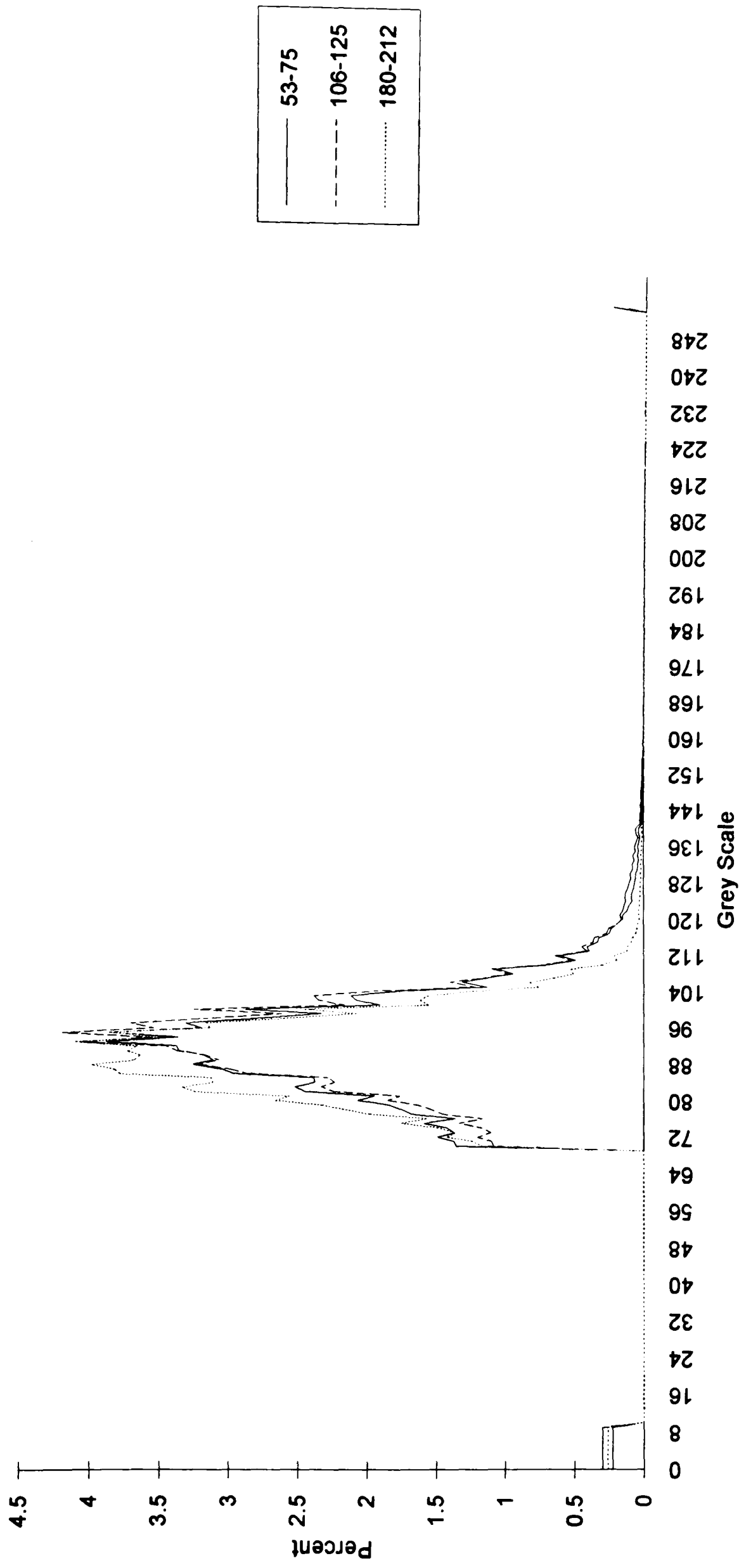
# Kromdraai Coal Fractions



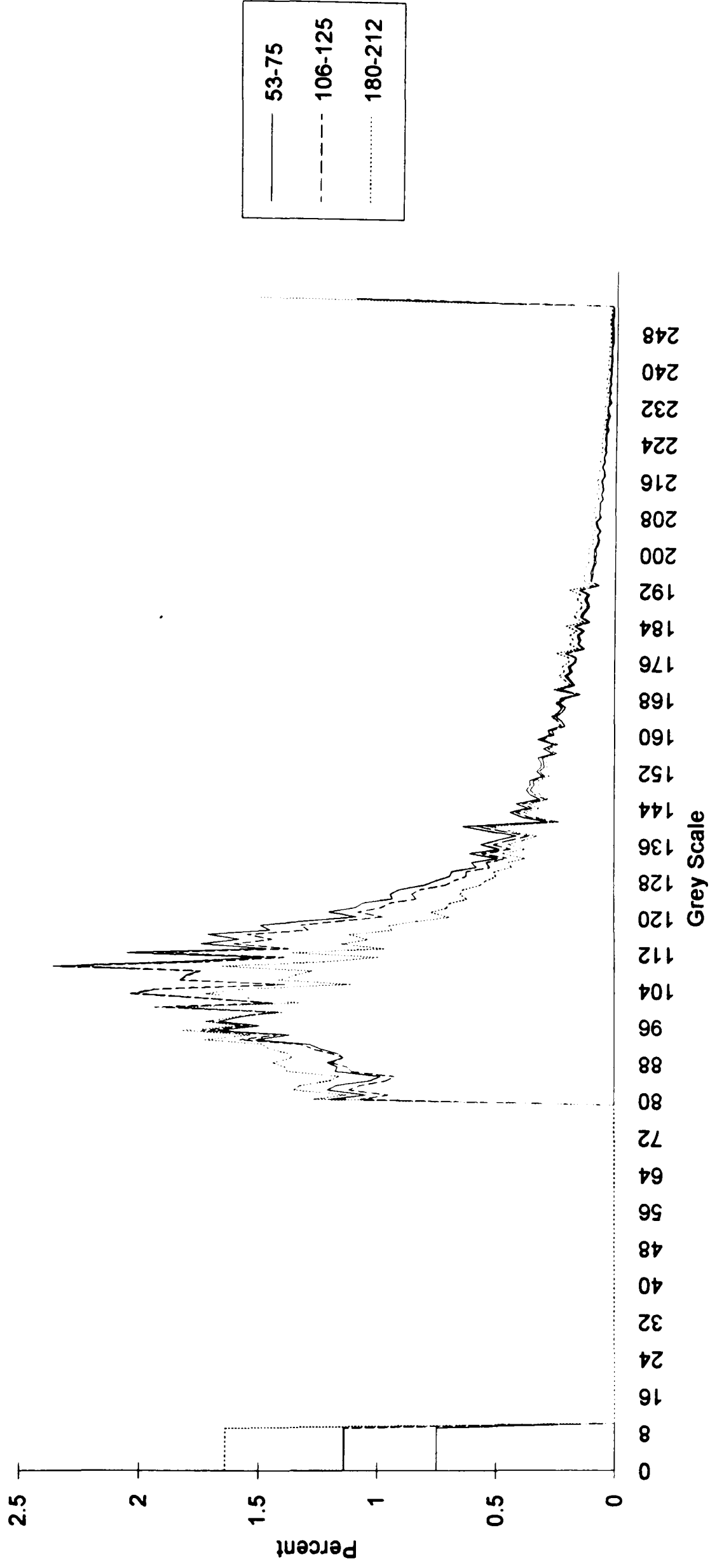
# McQuarie Coal Fractions



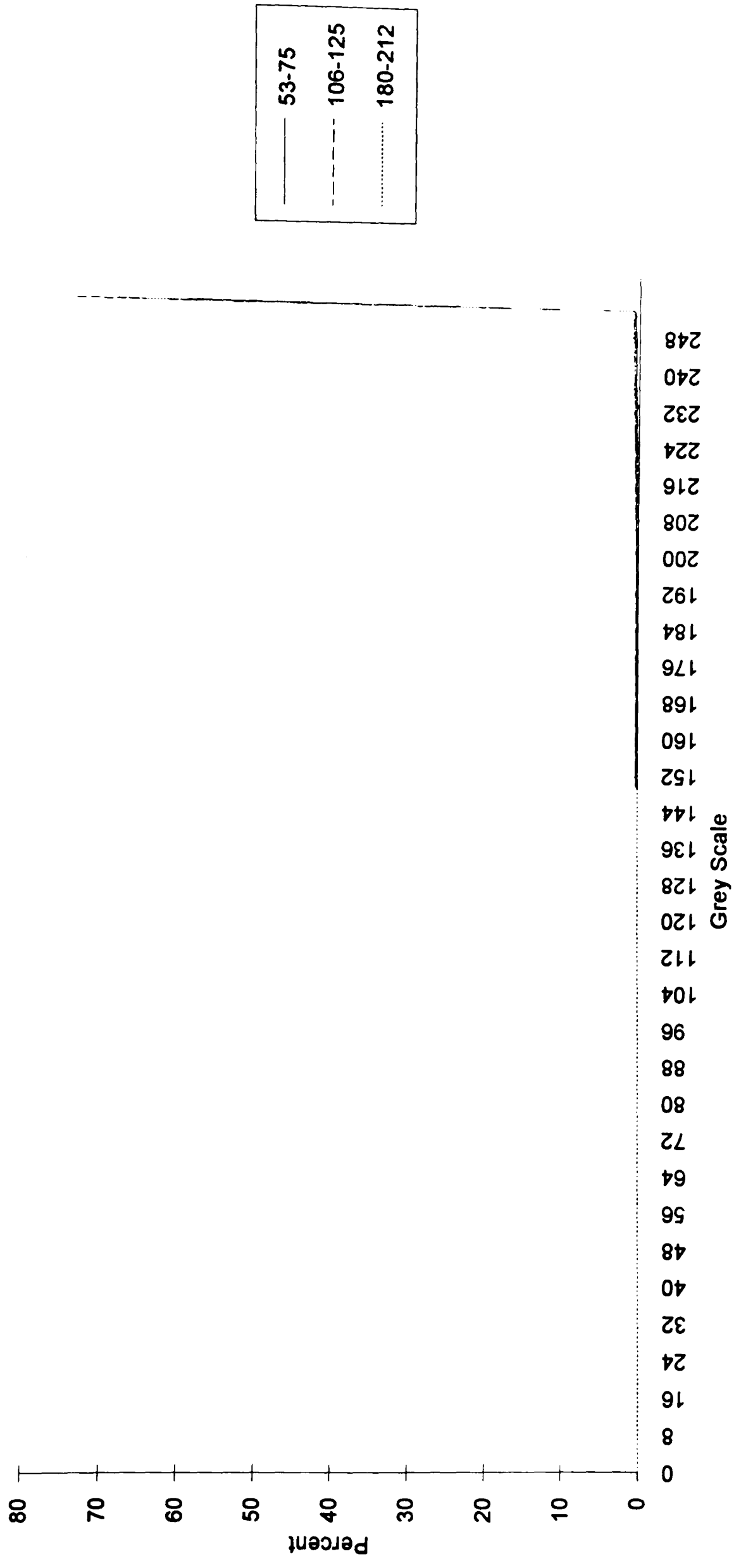
# Pinang Coal Fractions



# China SSM Coal Fractions



# Tower Coal Fractions



**BENTINCK**

<b>53-75</b>				db	dafb	<b>53-75</b>				db	dafb
Moisture	2.41					Moisture	1.91				
Volatiles	1.37	1.40	1.99			Volatiles	1.11	1.13	1.51		
Carbon	67.28	68.94	98.00			Carbon	72.52	73.93	98.49		
Ash	28.95	29.66				Ash	24.46	24.93			
Total	100.00	100.00	100.00			Total	100.00	100.00	99.99		
<b>106-125</b>				db	dafb	<b>106-125</b>				db	dafb
Moisture	2.25					Moisture	1.52				
Volatiles	0.80	0.82	1.15			Volatiles	1.22	1.24	1.80		
Carbon	68.73	70.31	98.85			Carbon	66.52	67.54	98.20		
Ash	28.22	28.87				Ash	30.74	31.22			
Total	100.00	100.00	100.00			Total	100.00	100.00	100.00		
<b>180-212</b>				db	dafb	<b>180-212</b>				db	dafb
Moisture	2.64					Moisture	2.37				
Volatiles	4.46	4.58	5.28			Volatiles	5.32	5.45	6.03		
Carbon	79.98	82.15	94.72			Carbon	82.95	84.96	93.97		
Ash	12.92	13.27				Ash	9.36	9.59			
Total	100.00	100.00	100.00			Total	100.00	100.00	100.00		

**KELLINGLEY**

<b>53-75</b>				db	dafb	<b>53-75</b>				db	dafb
Moisture	1.03					Moisture	1.19				
Volatiles	0.72	0.73	1.13			Volatiles	0.56	0.56	0.84		
Carbon	63.10	63.76	98.87			Carbon	65.66	66.45	99.16		
Ash	35.15	35.51				Ash	32.59	32.99			
Total	100.00	100.00	100.00			Total	100.00	100.00	100.00		
<b>106-125</b>				db	dafb	<b>106-125</b>				db	dafb
Moisture	1.15					Moisture	1.68				
Volatiles	1.01	1.02	1.30			Volatiles	0.65	0.66	0.83		
Carbon	76.73	77.62	98.70			Carbon	78.14	79.48	99.18		
Ash	21.12	21.36				Ash	19.53	19.86			
Total	100.00	100.00	100.00			Total	100.00	100.00	100.00		
<b>180-212</b>				db	dafb	<b>180-212</b>				db	dafb
Moisture	2.02					Moisture	1.83				
Volatiles	5.44	5.56	6.76			Volatiles	3.24	3.30	4.14		
Carbon	75.06	76.61	93.24			Carbon	75.02	76.42	95.86		
Ash	17.47	17.83				Ash	19.91	20.28			
Total	100.00	100.00	100.00			Total	100.00	100.00	100.00		

**KALTIM PRIMA**

<b>53-75</b>		<b>db</b>	<b>dafb</b>	<b>53-75</b>		<b>db</b>	<b>dafb</b>
Moisture	4.74			Moisture	4.39		
Volatiles	1.66	1.74	1.84	Volatiles	1.43	1.49	1.62
Carbon	88.57	92.98	98.16	Carbon	86.92	90.91	98.39
Ash	5.03	5.28		Ash	7.26	7.60	
<b>Total</b>	<b>100.00</b>	<b>100.00</b>	<b>100.00</b>	<b>Total</b>	<b>100.00</b>	<b>100.00</b>	<b>100.00</b>
<b>106-125</b>		<b>db</b>	<b>dafb</b>	<b>106-125</b>		<b>db</b>	<b>dafb</b>
Moisture	4.54			Moisture	4.33		
Volatiles	1.77	1.86	1.91	Volatiles	1.75	1.83	1.90
Carbon	91.14	95.48	98.09	Carbon	90.32	94.41	98.09
Ash	2.54	2.66		Ash	3.60	3.76	
<b>Total</b>	<b>100.00</b>	<b>100.00</b>	<b>99.99</b>	<b>Total</b>	<b>100.00</b>	<b>100.00</b>	<b>99.99</b>
<b>180-212</b>		<b>db</b>	<b>dafb</b>	<b>180-212</b>		<b>db</b>	<b>dafb</b>
Moisture	3.86			Moisture	3.93		
Volatiles	4.92	5.12	5.41	Volatiles	4.79	4.99	5.24
Carbon	86.00	89.46	94.58	Carbon	86.68	90.23	94.77
Ash	5.21	5.42		Ash	4.60	4.79	
<b>Total</b>	<b>100.00</b>	<b>100.00</b>	<b>100.00</b>	<b>Total</b>	<b>100.00</b>	<b>100.00</b>	<b>100.00</b>

**TOWER**

<b>53-75</b>		<b>db</b>	<b>dafb</b>	<b>53-75</b>		<b>db</b>	<b>dafb</b>
Moisture	0.30			Moisture	0.14		
Volatiles	0.14	0.14	0.15	Volatiles	0.34	0.34	0.36
Carbon	92.94	93.22	99.85	Carbon	93.42	93.55	99.64
Ash	6.61	6.63		Ash	6.10	6.11	
<b>Total</b>	<b>100.00</b>	<b>100.00</b>	<b>100.00</b>	<b>Total</b>	<b>100.00</b>	<b>100.00</b>	<b>100.00</b>
<b>106-125</b>		<b>db</b>	<b>dafb</b>	<b>106-125</b>		<b>db</b>	<b>dafb</b>
Moisture	0.46			Moisture	0.20		
Volatiles	0.44	0.44	0.48	Volatiles	0.23	0.23	0.25
Carbon	90.86	91.28	99.52	Carbon	92.32	92.50	99.75
Ash	8.24	8.28		Ash	7.25	7.27	
<b>Total</b>	<b>100.00</b>	<b>100.00</b>	<b>100.00</b>	<b>Total</b>	<b>100.00</b>	<b>100.00</b>	<b>100.00</b>
<b>180-212</b>		<b>db</b>	<b>dafb</b>	<b>180-212</b>		<b>db</b>	<b>dafb</b>
Moisture	0.83			Moisture	0.92		
Volatiles	3.23	3.26	3.46	Volatiles	3.56	3.59	3.82
Carbon	90.24	90.99	96.54	Carbon	89.57	90.41	96.18
Ash	5.70	5.75		Ash	5.94	6.00	
<b>Total</b>	<b>100.00</b>	<b>100.00</b>	<b>100.00</b>	<b>Total</b>	<b>100.00</b>	<b>100.00</b>	<b>100.00</b>

**ISLAND CREEK**

<b>53-75</b>		<b>db</b>	<b>dafb</b>	<b>53-75</b>		<b>db</b>	<b>dafb</b>
Moisture	1.00			Moisture	1.13		
Volatiles	0.61	0.62	0.64	Volatiles	0.60	0.61	0.64
Carbon	94.32	95.27	99.35	Carbon	93.38	94.45	99.35
Ash	4.07	4.11		Ash	4.89	4.94	
<b>Total</b>	<b>100.00</b>	<b>100.00</b>	<b>99.99</b>	<b>Total</b>	<b>100.00</b>	<b>100.00</b>	<b>99.99</b>
<b>106-125</b>		<b>db</b>	<b>dafb</b>	<b>106-125</b>		<b>db</b>	<b>dafb</b>
Moisture	1.00			Moisture	1.28		
Volatiles	0.57	0.58	0.61	Volatiles	0.52	0.53	0.56
Carbon	92.79	93.73	99.39	Carbon	93.04	94.25	99.45
Ash	5.64	5.69		Ash	5.16	5.23	
<b>Total</b>	<b>100.00</b>	<b>100.00</b>	<b>100.00</b>	<b>Total</b>	<b>100.00</b>	<b>100.00</b>	<b>100.00</b>
<b>180-212</b>		<b>db</b>	<b>dafb</b>	<b>180-212</b>		<b>db</b>	<b>dafb</b>
Moisture	1.34			Moisture	1.35		
Volatiles	2.29	2.32	2.45	Volatiles	2.57	2.60	2.77
Carbon	91.27	92.51	97.55	Carbon	90.21	91.44	97.24
Ash	5.09	5.16		Ash	5.87	5.96	
<b>Total</b>	<b>100.00</b>	<b>100.00</b>	<b>99.99</b>	<b>Total</b>	<b>100.00</b>	<b>100.00</b>	<b>100.01</b>

**DRUMMOND**

<b>53-75</b>		<b>db</b>	<b>dafb</b>	<b>53-75</b>		<b>db</b>	<b>dafb</b>
Moisture	2.59			Moisture	2.52		
Volatiles	1.54	1.58	1.97	Volatiles	1.39	1.42	1.77
Carbon	76.36	78.39	98.03	Carbon	76.79	78.78	98.22
Ash	19.52	20.04		Ash	19.29	19.79	
<b>Total</b>	<b>100.00</b>	<b>100.00</b>	<b>100.01</b>	<b>Total</b>	<b>100.00</b>	<b>100.00</b>	<b>99.99</b>
<b>106-125</b>		<b>db</b>	<b>dafb</b>	<b>106-125</b>		<b>db</b>	<b>dafb</b>
Moisture	3.00			Moisture	2.68		
Volatiles	1.16	1.19	1.49	Volatiles	1.28	1.31	1.63
Carbon	76.46	78.83	98.51	Carbon	77.35	79.48	98.38
Ash	19.38	19.98		Ash	18.70	19.21	
<b>Total</b>	<b>100.00</b>	<b>100.00</b>	<b>100.00</b>	<b>Total</b>	<b>100.00</b>	<b>100.00</b>	<b>100.00</b>
<b>180-212</b>		<b>db</b>	<b>dafb</b>	<b>180-212</b>		<b>db</b>	<b>dafb</b>
Moisture	2.35			Moisture	2.21		
Volatiles	3.23	3.30	4.15	Volatiles	4.26	4.36	5.29
Carbon	74.51	76.31	95.85	Carbon	76.33	78.05	94.71
Ash	19.91	20.39		Ash	17.20	17.59	
<b>Total</b>	<b>100.00</b>	<b>100.00</b>	<b>100.00</b>	<b>Total</b>	<b>100.00</b>	<b>100.00</b>	<b>100.00</b>

**EL CERROJON**

<b>53-75</b>		db	dafb	<b>53-75</b>		db	dafb
Moisture	2.90			Moisture	2.83		
Volatiles	1.58	1.63	2.00	Volatiles	1.55	1.59	2.05
Carbon	77.27	79.58	97.99	Carbon	73.95	76.10	97.94
Ash	18.25	18.79		Ash	21.67	22.30	
Total	100.00	100.00	99.99	Total	100.00	100.00	99.99
<b>106-125</b>		db	dafb	<b>106-125</b>		db	dafb
Moisture	2.76			Moisture	3.02		
Volatiles	1.49	1.53	1.70	Volatiles	1.53	1.58	1.73
Carbon	86.33	88.78	98.29	Carbon	86.93	89.63	98.26
Ash	9.42	9.68		Ash	8.52	8.78	
Total	100.00	100.00	99.99	Total	100.00	100.00	99.99
<b>180-212</b>		db	dafb	<b>180-212</b>		db	dafb
Moisture	2.90			Moisture	2.67		
Volatiles	4.16	4.28	4.57	Volatiles	4.83	4.97	5.23
Carbon	86.92	89.52	95.43	Carbon	87.64	90.04	94.77
Ash	6.02	6.20		Ash	4.85	4.99	
Total	100.00	100.00	100.00	Total	100.00	100.00	100.00

**PINANG**

<b>53-75</b>		db	dafb	<b>53-75</b>		db	dafb
Moisture	6.20			Moisture	6.21		
Volatiles	3.08	3.28	3.61	Volatiles	3.29	3.51	3.81
Carbon	82.32	87.76	96.39	Carbon	82.97	88.47	96.19
Ash	8.41	8.96		Ash	7.53	8.03	
Total	100.00	100.00	100.00	Total	100.00	100.00	100.00
<b>106-125</b>		db	dafb	<b>106-125</b>		db	dafb
Moisture	6.55			Moisture	5.97		
Volatiles	3.11	3.33	3.55	Volatiles	2.96	3.15	3.39
Carbon	84.38	90.30	96.45	Carbon	84.44	89.81	96.61
Ash	5.96	6.38		Ash	6.62	7.04	
Total	100.00	100.00	100.01	Total	100.00	100.00	100.00
<b>180-212</b>		db	dafb	<b>180-212</b>		db	dafb
Moisture	4.74			Moisture	5.28		
Volatiles	8.45	8.87	9.27	Volatiles	7.35	7.76	8.10
Carbon	82.69	86.80	90.73	Carbon	83.40	88.05	91.90
Ash	4.13	4.33		Ash	3.97	4.19	
Total	100.00	100.01	100.00	Total	100.00	100.00	100.00

**KROMDRAAI**

<b>53-75</b>		db	dafb	<b>53-75</b>		db	dafb
Moisture	1.28			Moisture	1.64		
Volatiles	0.78	0.79	1.01	Volatiles	0.98	0.99	1.26
Carbon	76.60	77.59	98.99	Carbon	76.95	78.23	98.74
Ash	21.35	21.62		Ash	20.44	20.78	
Total	100.00	100.00	100.00	Total	100.00	100.00	100.00
<b>106-125</b>		db	dafb	<b>106-125</b>		db	dafb
Moisture	1.27			Moisture	1.88		
Volatiles	1.07	1.08	1.40	Volatiles	0.99	1.01	1.24
Carbon	75.59	76.56	98.60	Carbon	79.16	80.68	98.76
Ash	22.07	22.36		Ash	17.97	18.31	
Total	100.00	100.00	100.00	Total	100.00	100.00	100.00
<b>180-212</b>		db	dafb	<b>180-212</b>		db	dafb
Moisture	2.35			Moisture	1.88		
Volatiles	4.58	4.69	5.69	Volatiles	6.23	6.35	7.49
Carbon	75.92	77.74	94.31	Carbon	76.95	78.43	92.51
Ash	17.15	17.56		Ash	14.94	15.22	
Total	100.00	100.00	100.00	Total	100.00	100.00	100.00

**McQUARIE**

<b>53-75</b>		db	dafb	<b>53-75</b>		db	dafb
Moisture	2.52			Moisture	2.47		
Volatiles	0.83	0.85	1.26	Volatiles	1.19	1.22	1.73
Carbon	65.29	66.97	98.74	Carbon	67.55	69.26	98.28
Ash	31.36	32.17		Ash	28.79	29.52	
Total	100.00	100.00	99.99	Total	100.00	100.00	100.01
<b>106-125</b>		db	dafb	<b>106-125</b>		db	dafb
Moisture	2.24			Moisture	2.49		
Volatiles	0.59	0.60	0.87	Volatiles	1.23	1.26	1.70
Carbon	66.99	68.52	99.13	Carbon	71.00	72.81	98.29
Ash	30.19	30.88		Ash	25.28	25.92	
Total	100.00	100.00	100.00	Total	100.00	100.00	99.99
<b>180-212</b>		db	dafb	<b>180-212</b>		db	dafb
Moisture	2.59			Moisture	2.29		
Volatiles	3.71	3.81	5.16	Volatiles	2.77	2.84	3.84
Carbon	68.29	70.10	94.83	Carbon	69.36	70.98	96.16
Ash	25.41	26.08		Ash	25.58	26.18	
Total	100.00	100.00	99.99	Total	100.00	100.00	100.00

## CHINA SSM

<b>53-75</b>		<b>db</b>		<b>dafb</b>		<b>53-75</b>		<b>db</b>		<b>dafb</b>	
Moisture	0.70					Moisture	2.68				
Volatiles	1.07	1.08		1.51		Volatiles	1.32	1.36		1.87	
Carbon	69.63	70.12		98.49		Carbon	69.60	71.52		98.13	
Ash	28.60	28.80				Ash	26.39	27.12			
<b>Total</b>	<b>100.00</b>	<b>100.00</b>		<b>100.00</b>		<b>Total</b>	<b>100.00</b>	<b>100.00</b>		<b>100.00</b>	
<b>106-125</b>		<b>db</b>		<b>dafb</b>		<b>106-125</b>		<b>db</b>		<b>dafb</b>	
Moisture	1.54					Moisture	2.29				
Volatiles	1.00	1.02		1.38		Volatiles	1.49	1.53		2.17	
Carbon	71.93	73.06		98.62		Carbon	67.07	68.64		97.82	
Ash	25.52	25.92				Ash	29.15	29.83			
<b>Total</b>	<b>100.00</b>	<b>100.00</b>		<b>100.00</b>		<b>Total</b>	<b>100.00</b>	<b>100.00</b>		<b>99.99</b>	
<b>180-212</b>		<b>db</b>		<b>dafb</b>		<b>180-212</b>		<b>db</b>		<b>dafb</b>	
Moisture	2.20					Moisture	2.39				
Volatiles	5.00	5.11		6.62		Volatiles	5.00	5.12		6.66	
Carbon	70.53	72.12		93.38		Carbon	70.00	71.72		93.35	
Ash	22.27	22.77				Ash	22.61	23.17			
<b>Total</b>	<b>100.00</b>	<b>100.00</b>		<b>100.00</b>		<b>Total</b>	<b>100.00</b>	<b>100.00</b>		<b>100.01</b>	

Kromdraai			53-75			106-125			180-212		
TenuiSphere	8.5	8.5	TenuiSphere	8.0	8.1	TenuiSphere	2.2	2.2			
CrassiSphere	16.8	16.8	CrassiSphere	23.7	24.1	CrassiSphere	16.4	16.4			
TenuiNetwork	27.0	27.0	TenuiNetwork	12.0	12.2	TenuiNetwork	8.6	8.6			
CrassiNetwork	38.5	38.5	CrassiNetwork	39.4	40.0	CrassiNetwork	68.5	68.5			
Fused	5.0	5.0	Fused	10.0	10.1	Fused	3.2	3.2			
Solid	4.2	4.2	Solid	5.5	5.6	Solid	0.5	0.5			
Sponge	0.0	0.0	Sponge	0.0	0.0	Sponge	0.7	0.7			
Coal	0.0		Coal	0.0		Coal	0.0				
Mineral	0.0		Mineral	1.5		Mineral	0.0				
Total	100.0	100.0	Total	100.0	100.0	Total	100.0	100.0			

Kromdraai			53-75			106-125			180-212		
TenuiSphere	11.0	11.1	TenuiSphere	6.7	6.7	TenuiSphere	1.2	1.2			
CrassiSphere	20.8	20.9	CrassiSphere	27.0	27.2	CrassiSphere	18.2	18.3			
TenuiNetwork	21.0	21.2	TenuiNetwork	16.4	16.5	TenuiNetwork	11.6	11.7			
CrassiNetwork	35.0	35.3	CrassiNetwork	36.0	36.1	CrassiNetwork	60.8	61.0			
Fused	7.8	7.8	Fused	9.7	9.7	Fused	5.6	5.6			
Solid	3.8	3.8	Solid	3.7	3.7	Solid	2.1	2.1			
Sponge	0.0	0.0	Sponge	0.0	0.0	Sponge	0.0	0.0			
Coal	0.5		Coal	0.0		Coal	0.0				
Mineral	0.3		Mineral	0.5		Mineral	0.5				
Total	100.0	100.0	Total	100.0	100.0	Total	100.0	100.0			

China SSM			53-75			106-125			180-212		
TenuiSphere	32.8	32.9	TenuiSphere	16.0	16.0	TenuiSphere	2.3	2.3			
CrassiSphere	46.2	46.4	CrassiSphere	55.1	55.4	CrassiSphere	47.3	47.6			
TenuiNetwork	8.7	8.8	TenuiNetwork	10.5	10.5	TenuiNetwork	14.3	14.4			
CrassiNetwork	9.2	9.2	CrassiNetwork	13.5	13.5	CrassiNetwork	33.7	34.0			
Fused	0.5	0.5	Fused	3.7	3.8	Fused	1.0	1.0			
Solid	2.1	2.1	Solid	0.7	0.8	Solid	0.5	0.5			
Sponge	0.0	0.0	Sponge	0.0	0.0	Sponge	0.3	0.3			
Coal	0.0		Coal	0.0		Coal	0.0				
Mineral	0.5		Mineral	0.5		Mineral	0.8				
Total	100.0	100.0	Total	100.0	100.0	Total	100.0	100.0			

China SSM			53-75			106-125			180-212		
TenuiSphere	30.7	31.0	TenuiSphere	15.8	16.0	TenuiSphere	1.5	1.5			
CrassiSphere	40.4	40.8	CrassiSphere	54.7	55.3	CrassiSphere	44.8	45.6			
TenuiNetwork	12.7	12.8	TenuiNetwork	9.5	9.6	TenuiNetwork	13.1	13.3			
CrassiNetwork	11.5	11.6	CrassiNetwork	16.3	16.5	CrassiNetwork	36.4	37.0			
Fused	2.5	2.5	Fused	1.9	2.0	Fused	1.7	1.8			
Solid	1.2	1.3	Solid	0.7	0.7	Solid	0.7	0.8			
Sponge	0.0	0.0	Sponge	0.0	0.0	Sponge	0.0	0.0			
Coal	0.0		Coal	0.0		Coal	0.2				
Mineral	1.0		Mineral	1.0		Mineral	1.5				
Total	100.0	100.0	Total	100.0	100.0	Total	100.0	100.0			

McQuarie			53-75			106-125			180-212		
TenuiSphere	50.5	50.9	TenuiSphere	17.8	18.0	TenuiSphere	2.1	2.3			
CrassiSphere	24.0	24.2	CrassiSphere	67.5	68.3	CrassiSphere	73.6	74.9			
TenuiNetwork	12.3	12.3	TenuiNetwork	5.5	5.6	TenuiNetwork	3.1	3.1			
CrassiNetwork	9.0	9.1	CrassiNetwork	5.8	5.8	CrassiNetwork	14.3	14.4			
Fused	0.3	0.3	Fused	1.3	1.3	Fused	1.2	1.2			
Solid	3.3	3.3	Solid	1.0	1.0	Solid	2.6	2.7			
Sponge	0.0	0.0	Sponge	0.0	0.0	Sponge	1.4	1.4			
Coal	0.0		Coal	0.0		Coal	0.0				
Mineral	0.8		Mineral	1.3		Mineral	1.7				
Total	100.0	100.0	Total	100.0	100.0	Total	100.0	100.0			

McQuarie			53-75			106-125			180-212		
TenuiSphere	55.5	55.5	TenuiSphere	13.1	13.2	TenuiSphere	1.7	1.7			
CrassiSphere	12.6	12.6	CrassiSphere	67.6	68.1	CrassiSphere	71.1	71.1			
TenuiNetwork	22.5	22.5	TenuiNetwork	8.4	8.5	TenuiNetwork	4.9	4.9			
CrassiNetwork	6.3	6.3	CrassiNetwork	5.4	5.5	CrassiNetwork	19.5	19.5			
Fused	1.4	1.4	Fused	1.5	1.5	Fused	2.2	2.2			
Solid	1.7	1.7	Solid	1.0	1.0	Solid	0.5	0.5			
Sponge	0.0	0.0	Sponge	2.2	2.2	Sponge	0.0	0.0			
Coal	0.0		Coal	0.0		Coal	0.0				
Mineral	0.0		Mineral	0.7		Mineral	0.0				
Total	100.0	100.0	Total	100.0	100.0	Total	100.0	100.0			

Pinang			53-75			106-125			180-212		
TenuiSphere	3.5	3.5	TenuiSphere	1.8	1.8	TenuiSphere	5.3	5.3			
CrassiSphere	8.1	8.1	CrassiSphere	4.8	4.8	CrassiSphere	6.0	6.1			
TenuiNetwork	2.4	2.4	TenuiNetwork	6.5	6.5	TenuiNetwork	7.2	7.3			
CrassiNetwork	0.2	0.2	CrassiNetwork	1.0	1.0	CrassiNetwork	4.6	4.6			
Fused	0.0	0.0	Fused	0.0	0.0	Fused	0.0	0.0			
Solid	0.2	0.2	Solid	0.3	0.3	Solid	0.7	0.7			
Sponge	85.5	85.5	Sponge	85.8	85.8	Sponge	75.8	76.0			
Coal	0.0		Coal	0.0		Coal	0.2				
Mineral	0.0		Mineral	0.0		Mineral	0.0				
Total	100.0	100.0	Total	100.0	100.0	Total	100.0	100.0			

Pinang			53-75			106-125			180-212		
TenuiSphere	2.0	2.0	TenuiSphere	0.8	0.8	TenuiSphere	4.0	4.0			
CrassiSphere	8.7	8.7	CrassiSphere	2.0	2.0	CrassiSphere	3.2	3.2			
TenuiNetwork	5.2	5.2	TenuiNetwork	6.0	6.0	TenuiNetwork	11.1	11.1			
CrassiNetwork	2.2	2.2	CrassiNetwork	1.0	1.0	CrassiNetwork	9.7	9.7			
Fused	0.2	0.2	Fused	0.0	0.0	Fused	0.2	0.2			
Solid	0.2	0.2	Solid	0.8	0.8	Solid	0.5	0.5			
Sponge	80.9	81.3	Sponge	89.5	89.5	Sponge	71.4	71.4			
Coal	0.0		Coal	0.0		Coal	0.0				
Mineral	0.5		Mineral	0.0		Mineral	0.0				
Total	100.0	100.0	Total	100.0	100.0	Total	100.0	100.0			

Kellingley			53-75			106-125			180-212		
TenuiSphere	36.0	38.3	TenuiSphere	7.5	7.6	TenuiSphere	3.5	3.6			
CrassiSphere	37.8	40.2	CrassiSphere	75.7	77.3	CrassiSphere	69.1	71.0			
TenuiNetwork	12.0	12.8	TenuiNetwork	6.1	6.2	TenuiNetwork	3.0	3.1			
CrassiNetwork	6.3	6.6	CrassiNetwork	8.2	8.4	CrassiNetwork	19.2	19.7			
Fused	0.5	0.5	Fused	0.0	0.0	Fused	1.7	1.8			
Solid	1.5	1.6	Solid	0.5	0.5	Solid	0.2	0.3			
Sponge	0.0	0.0	Sponge	0.0	0.0	Sponge	0.5	0.5			
Coal	0.0		Coal	0.0		Coal	2.5				
Mineral	6.0		Mineral	2.1		Mineral	0.2				
Total	100.0	100.0	Total	100.0	100.0	Total	100.0	100.0			

Kellingley			53-75			106-125			180-212		
TenuiSphere	33.0	38.5	TenuiSphere	5.2	5.4	TenuiSphere	5.5	6.0			
CrassiSphere	35.5	41.3	CrassiSphere	71.4	73.9	CrassiSphere	65.5	70.9			
TenuiNetwork	10.3	12.0	TenuiNetwork	7.4	7.7	TenuiNetwork	2.3	2.5			
CrassiNetwork	5.6	6.6	CrassiNetwork	11.2	11.6	CrassiNetwork	16.5	17.9			
Fused	1.2	1.4	Fused	1.4	1.4	Fused	2.0	2.2			
Solid	0.2	0.3	Solid	0.0	0.0	Solid	0.5	0.5			
Sponge	0.0	0.0	Sponge	0.0	0.0	Sponge	0.0	0.0			
Coal	0.0		Coal	0.0		Coal	1.5				
Mineral	14.2		Mineral	3.4		Mineral	6.3				
Total	100.0	100.0	Total	100.0	100.0	Total	100.0	100.0			

Bentinck			53-75			106-125			180-212		
TenuiSphere	71.0	74.4	TenuiSphere	32.7	34.2	TenuiSphere	5.7	5.9			
CrassiSphere	6.6	6.9	CrassiSphere	45.8	48.0	CrassiSphere	47.9	50.0			
TenuiNetwork	13.6	14.2	TenuiNetwork	9.8	10.3	TenuiNetwork	15.6	16.2			
CrassiNetwork	1.9	2.0	CrassiNetwork	5.6	5.9	CrassiNetwork	20.0	20.9			
Fused	0.5	0.5	Fused	0.0	0.0	Fused	3.7	3.9			
Solid	1.9	2.0	Solid	1.3	1.4	Solid	3.0	3.1			
Sponge	0.0	0.0	Sponge	0.2	0.2	Sponge	0.0	0.0			
Coal	0.0		Coal	0.0		Coal	0.2				
Mineral	4.5		Mineral	4.5		Mineral	4.0				
Total	100.0	100.0	Total	100.0	100.0	Total	100.0	100.0			

Bentinck			53-75			106-125			180-212		
TenuiSphere	68.1	70.0	TenuiSphere	29.0	29.7	TenuiSphere	2.1	2.1			
CrassiSphere	3.7	3.8	CrassiSphere	45.1	46.1	CrassiSphere	49.1	49.3			
TenuiNetwork	20.5	21.1	TenuiNetwork	10.1	10.4	TenuiNetwork	17.0	17.1			
CrassiNetwork	3.0	3.1	CrassiNetwork	12.8	13.1	CrassiNetwork	30.2	30.4			
Fused	1.7	1.8	Fused	0.0	0.0	Fused	0.7	0.7			
Solid	0.2	0.3	Solid	0.7	0.7	Solid	0.5	0.5			
Sponge	0.0	0.0	Sponge	0.0	0.0	Sponge	0.0	0.0			
Coal	0.0		Coal	0.0		Coal	0.0				
Mineral	2.7		Mineral	2.3		Mineral	0.5				
Total	100.0	100.0	Total	100.0	100.0	Total	100.0	100.0			

El Cerrejon			53-75			106-125			180-212		
TenuiSphere	64.8	64.9	TenuiSphere	39.7	39.9	TenuiSphere	2.0	2.0			
CrassiSphere	27.7	27.8	CrassiSphere	40.7	40.9	CrassiSphere	50.7	51.5			
TenuiNetwork	5.5	5.5	TenuiNetwork	9.2	9.2	TenuiNetwork	1.9	1.9			
CrassiNetwork	1.1	1.1	CrassiNetwork	9.7	9.7	CrassiNetwork	41.1	41.7			
Fused	0.5	0.5	Fused	0.0	0.0	Fused	0.3	0.3			
Solid	0.2	0.2	Solid	0.2	0.2	Solid	2.0	2.0			
Sponge	0.0	0.0	Sponge	0.0	0.0	Sponge	0.5	0.5			
Coal	0.0		Coal	0.0		Coal	0.0				
Mineral	0.2		Mineral	0.5		Mineral	1.5				
Total	100.0	100.0	Total	100.0	100.0	Total	100.0	100.0			

El Cerrejon			53-75			106-125			180-212		
TenuiSphere	70.4	70.4	TenuiSphere	34.0	34.0	TenuiSphere	1.2	1.2			
CrassiSphere	23.6	23.6	CrassiSphere	47.3	47.3	CrassiSphere	47.4	47.4			
TenuiNetwork	1.5	1.5	TenuiNetwork	1.3	1.3	TenuiNetwork	1.5	1.5			
CrassiNetwork	1.5	1.5	CrassiNetwork	15.5	15.5	CrassiNetwork	45.4	45.4			
Fused	2.4	2.4	Fused	1.0	1.0	Fused	0.7	0.7			
Solid	0.7	0.7	Solid	1.0	1.0	Solid	3.7	3.7			
Sponge	0.0	0.0	Sponge	0.0	0.0	Sponge	0.0	0.0			
Coal	0.0		Coal	0.0		Coal	0.0				
Mineral	0.0		Mineral	0.0		Mineral	0.0				
Total	100.0	100.0	Total	100.0	100.0	Total	100.0	100.0			

Kaltim Prima			53-75			106-125			180-212		
TenuiSphere	55.3	55.5	TenuiSphere	50.4	50.5	TenuiSphere	2.5	2.5			
CrassiSphere	30.6	30.7	CrassiSphere	37.3	37.4	CrassiSphere	26.7	26.8			
TenuiNetwork	10.1	10.1	TenuiNetwork	10.6	10.6	TenuiNetwork	11.2	11.3			
CrassiNetwork	1.7	1.7	CrassiNetwork	0.5	0.5	CrassiNetwork	39.7	39.8			
Fused	0.0	0.0	Fused	0.5	0.5	Fused	0.0	0.0			
Solid	0.7	0.7	Solid	0.0	0.0	Solid	0.5	0.5			
Sponge	1.2	1.2	Sponge	0.5	0.5	Sponge	19.0	19.0			
Coal	0.0		Coal	0.0		Coal	0.0				
Mineral	0.2		Mineral	0.2		Mineral	0.5				
Total	100.0	100.0	Total	100.0	100.0	Total	100.0	100.0			

Kaltim Prima			53-75			106-125			180-212		
TenuiSphere	54.7	54.7	TenuiSphere	53.5	53.5	TenuiSphere	3.5	3.5			
CrassiSphere	37.7	37.7	CrassiSphere	33.4	33.4	CrassiSphere	23.2	23.2			
TenuiNetwork	7.2	7.2	TenuiNetwork	5.9	5.9	TenuiNetwork	14.1	14.1			
CrassiNetwork	0.2	0.2	CrassiNetwork	0.2	0.2	CrassiNetwork	42.5	42.5			
Fused	0.0	0.0	Fused	0.5	0.5	Fused	0.0	0.0			
Solid	0.2	0.2	Solid	0.2	0.2	Solid	0.7	0.7			
Sponge	0.0	0.0	Sponge	6.2	6.2	Sponge	16.0	16.0			
Coal	0.0		Coal	0.0		Coal	0.0				
Mineral	0.0		Mineral	0.0		Mineral	0.0				
Total	100.0	100.0	Total	100.0	100.0	Total	100.0	100.0			

Tower			53-75			106-125			180-212		
TenuiSphere	4.2	4.2	TenuiSphere	0.8	0.8	TenuiSphere	0.2	0.2			
CrassiSphere	7.0	7.0	CrassiSphere	5.5	5.5	CrassiSphere	2.7	2.7			
TenuiNetwork	61.3	61.3	TenuiNetwork	54.0	54.0	TenuiNetwork	29.6	29.6			
CrassiNetwork	20.7	20.7	CrassiNetwork	32.8	32.8	CrassiNetwork	51.5	51.5			
Fused	4.2	4.2	Fused	2.0	2.0	Fused	4.3	4.3			
Solid	2.5	2.5	Solid	5.0	5.0	Solid	11.6	11.6			
Sponge	0.0	0.0	Sponge	0.0	0.0	Sponge	0.0	0.0			
Coal	0.0		Coal	0.0		Coal	0.0				
Mineral	0.0		Mineral	0.0		Mineral	0.0				
Total	100.0	100.0	Total	100.0	100.0	Total	100.0	100.0			

Tower			53-75			106-125			180-212		
TenuiSphere	4.0	4.0	TenuiSphere	1.7	1.7	TenuiSphere	0.0	0.0			
CrassiSphere	9.0	9.0	CrassiSphere	3.4	3.4	CrassiSphere	0.8	0.8			
TenuiNetwork	65.5	65.7	TenuiNetwork	60.8	61.1	TenuiNetwork	27.3	27.3			
CrassiNetwork	16.0	16.0	CrassiNetwork	27.7	27.9	CrassiNetwork	56.8	56.9			
Fused	2.5	2.5	Fused	3.2	3.2	Fused	6.8	6.8			
Solid	2.8	2.8	Solid	2.7	2.7	Solid	8.3	8.3			
Sponge	0.0	0.0	Sponge	0.0	0.0	Sponge	0.0	0.0			
Coal	0.0		Coal	0.0		Coal	0.0				
Mineral	0.3		Mineral	0.5		Mineral	0.3				
Total	100.0	100.0	Total	100.0	100.0	Total	100.0	100.0			

Island Creek			53-75			106-125			180-212		
TenuiSphere	43.1	43.2	TenuiSphere	10.6	10.6	TenuiSphere	3.0	3.0			
CrassiSphere	40.5	40.6	CrassiSphere	63.7	63.7	CrassiSphere	72.2	72.7			
TenuiNetwork	7.0	7.0	TenuiNetwork	8.3	8.3	TenuiNetwork	1.0	1.0			
CrassiNetwork	3.4	3.4	CrassiNetwork	13.6	13.6	CrassiNetwork	18.6	18.7			
Fused	4.6	4.6	Fused	2.2	2.2	Fused	1.9	1.9			
Solid	1.2	1.2	Solid	1.7	1.7	Solid	2.6	2.7			
Sponge	0.0	0.0	Sponge	0.0	0.0	Sponge	0.0	0.0			
Coal	0.0		Coal	0.0		Coal	0.0				
Mineral	0.2		Mineral	0.0		Mineral	0.7				
Total	100.0	100.0	Total	100.0	100.0	Total	100.0	100.0			

Island Creek			53-75			106-125			180-212		
TenuiSphere	47.8	47.8	TenuiSphere	5.5	5.5	TenuiSphere	2.2	2.2			
CrassiSphere	34.4	34.4	CrassiSphere	68.4	68.4	CrassiSphere	69.1	69.1			
TenuiNetwork	12.7	12.7	TenuiNetwork	5.8	5.8	TenuiNetwork	1.7	1.7			
CrassiNetwork	2.4	2.4	CrassiNetwork	16.8	16.8	CrassiNetwork	21.4	21.4			
Fused	1.2	1.2	Fused	2.0	2.0	Fused	3.4	3.4			
Solid	1.5	1.5	Solid	1.5	1.5	Solid	2.2	2.2			
Sponge	0.0	0.0	Sponge	0.0	0.0	Sponge	0.0	0.0			
Coal	0.0		Coal	0.0		Coal	0.0				
Mineral	0.0		Mineral	0.0		Mineral	0.0				
Total	100.0	100.0	Total	100.0	100.0	Total	100.0	100.0			

Drummond			53-75			106-125			180-212		
TenuiSphere	60.1	60.6	TenuiSphere	14.2	14.3	TenuiSphere	4.8	5.0			
CrassiSphere	22.9	23.0	CrassiSphere	65.7	66.0	CrassiSphere	50.5	52.2			
TenuiNetwork	8.0	8.1	TenuiNetwork	9.7	9.8	TenuiNetwork	5.5	5.7			
CrassiNetwork	2.6	2.6	CrassiNetwork	8.0	8.0	CrassiNetwork	32.7	33.8			
Fused	1.7	1.7	Fused	1.2	1.3	Fused	0.8	0.8			
Solid	4.0	4.0	Solid	0.7	0.8	Solid	0.5	0.5			
Sponge	0.0	0.0	Sponge	0.0	0.0	Sponge	2.0	2.1			
Coal	0.0		Coal	0.0		Coal	0.0				
Mineral	0.7		Mineral	0.5		Mineral	3.3				
Total	100.0	100.0	Total	100.0	100.0	Total	100.0	100.0			

Drummond			53-75			106-125			180-212		
TenuiSphere	62.6	62.9	TenuiSphere	11.4	11.5	TenuiSphere	0.8	0.8			
CrassiSphere	24.2	24.4	CrassiSphere	65.6	66.0	CrassiSphere	55.3	55.8			
TenuiNetwork	5.1	5.1	TenuiNetwork	4.5	4.5	TenuiNetwork	2.5	2.5			
CrassiNetwork	6.0	6.0	CrassiNetwork	14.0	14.1	CrassiNetwork	37.8	38.1			
Fused	0.7	0.7	Fused	1.4	1.4	Fused	2.0	2.0			
Solid	0.9	0.9	Solid	2.6	2.6	Solid	0.8	0.8			
Sponge	0.0	0.0	Sponge	0.0	0.0	Sponge	0.0	0.0			
Coal	0.2		Coal	0.0		Coal	0.0				
Mineral	0.2		Mineral	0.5		Mineral	1.0				
Total	100.0	100.0	Total	100.0	100.0	Total	100.0	100.0			